Technical Report
TR-18-04
March 2019

The last 130000 years in Fennoscandia reconstructed based on a long and fossil-rich sediment sequence preserved at Sokli in northern Finland

New evidence for highly dynamic environmental and climate conditions

Karin F. Helmens

SVENSK KÄRNBRÄNSLEHANTERING AB

SWEDISH NUCLEAR FUEL
AND WASTE MANAGEMENT CO

Box 3091, SE-169 03 Solna
Phone +46 8 459 84 00
skb.se

SVENSK KÄRNBRÄNSLEHANTERING

ISSN 1404-0344
SKB TR-18-04
ID 1688658
March 2019

The last 130 000 years in Fennoscandia reconstructed based on a long and fossil-rich sediment sequence preserved at Sokli in northern Finland

New evidence for highly dynamic environmental and climate conditions

Karin Femke Helmens
Department of Physical Geography, Stockholm University

Keywords: Late Quaternary, Climate variability, Quantitative climate estimates, Continentality, Glacial, Interglacial, Fennoscandian Ice Sheet, Ecosystem dynamics, Multi-proxy analysis, Sokli, Northern Finland.

Preface

The following report constitutes a final report of an extensive multi-proxy paleoclimate study on lacustrine and fluvial sediments spanning the last 130 000 years obtained from the Sokli site in northern Finland. The study was initiated and administrated by Prof. Jens-Ove Näslund (SKB) and Dr. Karin F. Helmens (Stockholm University). Dr. Karin F. Helmens coordinated all scientific work between researchers at Stockholm University, University of Helsinki, University of Nottingham, Natural History Museum, UK, University of Bergen and National Taiwan University. The contributions by individual researchers are summarized in Sections 3.1, 4.1 and 5.1 (Materials and methods).

The results will be used, together with other published scientific information, for constructing future climate scenarios for SKB's work on assessing the long-term safety of nuclear waste repositories in Sweden. The safety assessments performed for the planned repository for spent nuclear fuel in Forsmark, Sweden, focus on a time period of 100 000 years, and cover a total time span of one million years. Since this covers the timescale upon which Quaternary climate and ice-sheet cycles have operated, the effect of future glacial-interglacial conditions upon repository safety needs to be analyzed. In this context, the present study provides important results on the highly varying climate and environmental conditions in Fennoscandia for the Holocene (MIS 1), the Early Weichselian (Brørup Interstadial, MIS 5c, and Herning Stadial, MIS 5d) and the Eemian Interglacial (MIS 5e). Corresponding information from the Middle Weichselian (early MIS 3) (also obtained from the Sokli sediment sequences), and a first comparison of the Last Interglacial-Glacial cycle (MIS 5-2) at Sokli and other northern and central European sites, have been reported by Dr. Karin F. Helmens in previous SKB reports (TR-09-16 and TR-13-02).

The report manuscript was scientifically reviewed by Dr. Normunds Stivrins (University of Latvia) and Prof. Christian Bigler (Umeå University). Input to an earlier version of the manuscript was provided by Jens-Ove Näslund (SKB) and Christina Truedsson (Tintra konsult).

Stockholm, February 2019

Jens-Ove Näslund
Coordinator Climate Research Programme SKB

Summary

The reconstruction of environmental and climate conditions in Fennoscandia during the Late Quaternary is hampered by a highly fragmented sediment record and poor dating control. Here we study an unusual long and fossil-rich sedimentary sequence that spans the last 130 000 years. These sediments have been preserved in deeply weathered rocks of a magma intrusion (Sokli Carbonatite Massif) in the north-eastern Fennoscandian Precambrian Shield. We use multiple abiotic and biotic proxies and novel climate inference methods to reconstruct depositional environments, ecosystem response and dynamics, and quantitative climate parameters. This report focuses on deposits dated to the Last (Eemian; MIS 5e) and present (Holocene; MIS 1) Interglacials in the Sokli basin, as well as deposits dated to the Early Weichselian Brørup (MIS 5c) and Herning (MIS 5d) warm and cold stages respectively. Results on the Middle Weichselian (early MIS 3) sediments at Sokli have been previously published in the SKB report series, whereas the Early Weichselian Odderade (MIS 5a) warm stage is still under study.

The Sokli basin was glaciated during MIS 6, 5b, 4 and (late 3) 2. Our main conclusions are: 1) The Fennoscandian Ice Sheet was highly dynamic during the Weichselian with significantly less extensive ice-sheet cover over Fennoscandia, both in space and time, than previously reconstructed. 2) Boreal forest at Sokli is not only inferred for the warm MIS 5e and MIS 1 interglacials but also during the Early Weichselian MIS 5c and MIS 5a warm stages. This is in sharp contrast to the cold tundra or ice-covered conditions previously reconstructed for Sokli during MIS 5c and MIS 5a, with sub-arctic birch woodland in areas presently covered by mixed boreal forest south of Sokli. 3) Present-day, or higher, summer temperatures inferred for MIS 5e, 5c, 5a, early 3 and the early-Holocene are in concordance with enhanced summer insolation values at high northern latitudes. 4) High climate variability was not only confined to the Weichselian; two centennial/millennial-scale climate events, with cold and dry conditions, intersected Eemian (MIS 5e) warmth. 5) Warm summers and nutrient rich conditions resulted in the development of diverse biota both in the Sokli Ice Lake and along its shores, and trees or open forest on surrounding land, during the various deglaciation phases. 6) The multi-proxy approach allows for comprehensive reconstructions of catchment stability/instability, lake water chemistry, lake infilling and (nearby) terrestrialisation during warm MIS 5e, 5c, 5a and 1; a braided river flanked by steppe-tundra vegetation, pointing to a strong continental climate with possible deep permafrost, is reconstructed in detail for MIS 5d. 7) Our studies show the importance of multi-proxy analysis in reconstructing Late Quaternary environmental and climate changes and indicate that caution should be taken when validating climate model simulations against single proxy climate data.

Sammanfattning

Rekonstruktioner av miljö- och klimatförhållanden under senkvartär tidbegränsas av en mycket fragmenterad sedimenthistorik och osäker kronologi. Vi studerar här en ovanligt lång och fossilrik sedimentsekvens som täcker de senaste 130 000 åren. Sedimenten har bevarats i djupt vittrade bergarter tillhörande en magmaintrusion (’Sokli Carbonatite Massif’) belägen i den nordöstra delen av den Fennoskandiska urbergssköldenskölden. Vi använder en flertal abiotiska och biotiska s k proxy-analyser samt nyligen utvecklade metoder för att studera paleoklimat för att rekonstruera avlagringssmiljöer, ekosystemens respons och dynamik, samt kvantitativa klimatdata. Denna rapport fokuserar på avlagringar i Sokli-bäckenet daterade till den näst senaste (eem; MIS 5e) och nuvarande (holocen; MIS 1) interglaciala perioderna, samt på avlagringar daterade till den varma interstadialen brørup (MIS 5c) och den kalla stadialen herning (MIS 5d) under tidig Weichsel. Motsvarande resultat från mitt-Weichsel (tidig MIS 3) har tidigare publicerats i SKB:s rapportserie, medan studier av interstadialen Odderade (MIS 5a) under tidig Weichsel fortfarande pågår. Soklibäckenet var nedisat under MIS 6, 5b, 4 och (sen 3-) 2. Våra huvudsakliga slutsatser är: 1) Den fennoskandiska inlandsisen hade ett mycket dynamiskt uppträdande under weichselistiden med betydligt mindre isutbredning över Fennoskandia, både rums- och tidsmässigt, jämfört med tidigare rekonstruktioner. 2) Boreal skog rekonstrueras här inte bara för de varma interglacialerna eem (MIS 5e) och holocen (MIS 1) utan även för de varma interstadialerna brørup (MIS 5c) och odderade (MIS 5a) under tidig-Weichsel. Denna rekonstruktion, står i skarp kontrast till de kalla tundraförhållanden, eller istäckta förhållanden, som tidigare rekonstruerats här, med sub-arktisk björkskog i områden nu täckt av blandad boreal skog söder om Sokli, för brørup och odderade. 3) Rekonstruerade sommartemperaturer lika höga eller högre än dagens för perioderna MIS 5e, 5c, 5a, tidig 3 samt för tidig holocen överensstämmer med en ökad insolation under sommaren på höga latituder. 4) En hög variabilitet i klimatet var inte enbart begränsad till Weichsel; två perioder med kallt och torrt klimat avbröt även den varma eem-interglacialen (MIS 5e). 5) Varma somrar och näringsrika förhållanden resulterade i utveckling av ett mångskiftande biota både i Sokli-issjön och längs dess stränder, samt av träd eller öppen skog på de omkringliggande områdena under de olika deglaciationsfaserna. 6) Angreppssättet med många olika proxy-analyser möjliggör omfattande rekonstruktioner av avrinningsområdets stabilitet/instabilitet, lakustrin vattenkemi, sedimentation i sjön, och terrestrialisering av närliggande områden under de varma perioderna eem (MIS 5e), brørup (MIS 5c), odderade (MIS 5a) och holocen (MIS 1). En flätad flodfåra kantad av stäpp-tundravegetation, indikerande ett starkt kontinentalt klimat, med möjlig djup permafrost, har rekonstruerats i detalj för stadialen herning (MIS 5d). 7) Våra studier visar på vikten av att använda multi-proxyanalys vid rekonstruktioner av miljö och klimat under senkvartär, samt att försiktighet behöver vidtas när validering av klimatmodellsimuleringar görs mot klimatdata från enbart en proxyparameter.

Extended Summary

This report presents the results of a detailed study on sediments of the present Holocene Interglacial (last 11 kyr), and sediments of MIS 5c-d age (Early Weichselian ca 90 to 115 kyr ago) and MIS 5e age (Eemian Interglacial between ca 115 and 130 kyr ago) recovered from the small Sokli sedimentary basin in boreal north-eastern Finland. By applying multiple proxies (geochemical data, Loss On Ignition (LOI), Carbon/Nitrogen ratios (C/N), pollen, diatoms, chironomids, macrofossils) and various quantitative climate reconstruction methods (transfer function approach, plant indicator species), a comprehensive reconstruction of environmental (e.g. depositional environments, azonale and zonal vegetation developments) and climate conditions at Sokli during these time-intervals are made. The study exploits the unique *in situ* preservation of Late Quaternary sediments in the Sokli basin as well as the unusual large thickness and fossil-richness of the geological beds. The results from Sokli greatly revise earlier paleo-environmental and paleo-climate reconstructions for Fennoscandia. The earlier paleo-climate reconstructions were based on the long-distance correlation of poorly-dated stratigraphic fragments and correlation with the marine oxygen-isotope record which was used as a proxy for global ice volumes.

Holocene Interglacial climate and environmental conditions (last ca 11 kyr)

A study on the Holocene lake sequence from the Loitsana Lake in the Sokli basin was performed in order to obtain a reference section for the older sediments in the Sokli basin. The Holocene development of the Loitsana Lake is complex, influenced by i) an initial phase of glacial lake evolution; ii) marked changes in fluvial input due to nearby, progressive wetland expansion (terrestrialization); iii) lake infilling; and iv) groundwater flow from a nearby esker chain. A combination of events, as recognized at Loitsana, can be expected to have influenced the Holocene development of many lakes in the formerly glaciated boreal zone of northern Europe.

Our multi-proxy study on the early-Holocene glacio-lacustrine sediments in the Loitsana basin has revealed unexpectedly rich aquatic and wetland assemblages. With the former ice margin of the Fennoscandian Ice Sheet within a distance of 10 km from the coring-site, the fossils reconstruct rich ecosystems both in the glacial lake and along its shores and surrounding birch forests on recently deglaciated land. Rich biota developed due to high nutrient levels during deglaciation and warm summers. It is probable that pioneering *Betula* quickly advanced over the newly-deglaciated terrain in front of the retreating ice margin.

Whereas the quantitative temperature reconstruction for the Holocene based on pollen of terrestrial plant taxa in the Loitsana sediments follows the classical trend of gradually increasing early-Holocene mean July air temperatures in Fennoscandia, with a mid-Holocene maximum July warming between ca 8 and 4 cal. kyr BP, plant macrofossils of telmatic vegetation (aquatics, wetland, shore habitats), and chironomids (aquatic insects), indicate an early onset of the maximum in July air temperatures in the early-Holocene prior to ca 10 cal. kyr BP. The Holocene summer temperature evolution, recently reconstructed by aquatic/wetland taxa at several sites in northern Fennoscandia, follows the gradually decreasing orbitally-forced June insolation at 60 °N since 11 cal. kyr BP. Chironomid-inferred continentality-index suggests a more continental climate regime, with warm summers and cold winters, during the early-Holocene than at present. The low early-Holocene terrestrial pollen-inferred July temperature values are probably driven by local factors as well as a relatively slow response of trees (particularly tree populations), compared to aquatic/wetland taxa (which do not depend on e.g. soil formation), to early-Holocene climate warming.

The results obtained on the Holocene Loitsana Lake sequence furthermore show that the effect of the local carbonate-rich bedrock at Sokli on paleo-temperature reconstructions is neglectable. Furthermore, the fossil assemblages, and successive developments in these assemblages, found in the early-Holocene glacial lake sediments at Loitsana support the inferred glacio-lacustrine depositional environment for the early MIS 3 sediments in the Sokli basin. Characteristically, fossil assemblages in the glacial lake sediments of early-Holocene and MIS 3 age include e.g. distinct representations of pooid phytoliths, reworked Tertiary diatoms, heavily silicified *Aulacoseira* diatom species and the bryozoan *Fredericella indica,* indicating significant wave action and shore erosion along the relatively large glacial lake.

Following the opening of a spillway along the retreating margin of the Fennoscandian Ice Sheet, both deposits record a sudden fall in lake level and further shallowing of the glacial lake, accompanied by rising nutrient levels and local establishments of diverse aquatic and telmatic communities.

Early Weichselian MIS 5c interstadial climate and environmental conditions (ca 90–105 kyr BP)

Another compelling result from the present study is the boreal character of the climate during MIS 5c (the Brørup Interstadial around 95 kyr BP), with mean July air temperatures reaching several degrees higher than today. Earlier reconstructions suggested cold tundra conditions at Sokli during MIS 5c and sub-arctic birch woodland in areas presently covered by mixed boreal forest south of Sokli. In the present study, high summer temperatures are inferred from exceptional rich plant macrofossil assemblages associated with an overall fluvial depositional environment. The paleoenvironmental record registers, in great detail, the infilling of an oxbow lake, terrestrialization, and the return to stream channel deposition. The regional vegetation development at Sokli during MIS 5c, of pioneer birch vegetation being replaced by pine-dominated forest and then mixed boreal forest with spruce, is similar to the conditions reconstructed for the Holocene (last 11 kyr) for the same location.

Early Weichselian MIS 5d stadial climate and environmental conditions (ca 105–115 kyr BP)

In contrast to an earlier reconstruction, suggesting glaciated conditions in the Sokli region during MIS 5d (the Herning Stadial around 110 kyr BP), our study records in great detail the presence of steppe-tundra vegetation and a braided river system demonstrating ice-free conditions with a severe continental climate. Based on macrofossils from aquatic and shore plant taxa, and chironomids, relatively high summer temperatures are inferred (about present-day values) for the period. These air temperatures are in line with the reconstructed presence of conifer and birch trees in the steppe-tundra vegetation. Quantitative climate data from the European mainland for MIS 5d show that the warm summers were accompanied by cold winters and low precipitation values. Steppe-tundra vegetation was widespread in Europe during the cold stages of the Weichselian. Presently, steppe-tundra associations are rare. The co-occurrence of steppe and arctic tundra species are described for north-eastern Siberia and west-central Greenland, close to the Greenland Ice, i.e. areas with severe continental climate conditions and permafrost.

The results presented here, together with those obtained earlier on sediments of early MIS 3 age (ca 50 kyr BP) in the Sokli basin (Helmens 2009), point to an in general significantly less extensive and more variable ice-sheet cover over Fennoscandia during the Early and Middle Weichselian than previous reconstructions based on correlation of stratigraphic fragments. Placing these results into a northern and central European stratigraphic context suggests that changes in sea-ice cover, and related shifts in continentality, were a more distinctive feature of the Early and Middle Weichselian than Fennoscandian glaciation (Helmens 2013).

MIS 5e Eemian Interglacial climate and environmental conditions (ca 115–130 kyr BP)

The 9m-thick lacustrine diatom-gyttja deposit of MIS 5e age in the Sokli basin allowed for an unusually high-temporal resolution reconstruction of environmental and climate conditions for the last period when large parts of the globe experienced a warmer-than-today climate, i.e. during the Eemian Interglacial between ca 115–130 kyr BP. Fossils of aquatic taxa (e.g. diatoms, green algae) combined with biogeochemical data reveal in great detail the infilling of a relatively deep, nutrient-rich lake that was stratified during its initial phase of development. Macrofossil remains are scarce in the lake sediment, reflecting a relatively large open-water body throughout the lake infilling.

Quantitative climate reconstructions based on pollen from terrestrial plant taxa show mean July temperature values reaching 3 °C warmer than the present-day value of +13 °C at Sokli. The reconstructed curve of mean January temperatures steadily increases during the interglacial indicating a shift from a continental to more oceanic climate regime. Unexpectedly, the multi-proxy record reconstructs a distinct phase of cooling and drying (named the Tunturi event) intersecting peak interglacial warmth.

The cooling/drying event, which lasted in the order of 500–1000 years, and during which mean July temperatures dropped ca 2–4 °C, caused the mixed boreal forest with birch, pine, spruce and larch to be temporarily replaced by open sub-arctic birch forest.

Furthermore, sudden drying and cooling is reconstructed in the upper part of the MIS 5e lake deposit at Sokli (Värriö event), following the start of a general trend in reducing summer temperatures. The Värriö and Tunturi climate events show that major climate variability was not restricted to cold glacial periods but also characterized the Eemian Interglacial, at least at high-latitudes.

Contents

1 Introduction 13
1.1 Background 13
1.2 Objectives 17

2 Present environmental setting of the study area 19

3 Holocene environmental and climate reconstructions for northeastern Fennoscandia 23
3.1 Materials and methods 23
3.1.1 Sediment sampling 23
3.1.2 Radiocarbon dating and age model 23
3.1.3 Sediment biogeochemistry 23
3.1.4 Fossil analyses 24
3.1.5 Zonation of proxy diagrams 25
3.1.6 Application of digital elevation model data 25
3.1.7 Quantitative climate reconstructions 25
3.2 Results 27
3.2.1 Glacial-lake reconstruction using digital elevation data 27
3.2.2 Geochemical data 29
3.2.3 Lithology and chronology 31
3.2.4 Biotic data 32
3.2.5 Quantitative climate reconstructions 32
3.3 Holocene lake development 38
3.3.1 Local zone 1 (900–735 cm; prior to 10 570 cal. yrs BP) 38
3.3.2 Local zone 2 (735–700 cm; 10 570–10 200 cal. yrs BP) 39
3.3.3 Local zone 3 (700–490 cm; 10 200–8 630 cal. yrs BP) 40
3.3.4 Local zone 4 (490–290 cm; 8 630–6 290 cal. yrs BP) 41
3.3.5 Local zone 5 (290–120 cm; 6 290–4 300 cal. yrs BP) 41
3.3.6 Local zone 6 (120–0 cm; 4 300 cal. yrs BP-present) 42
3.4 Holocene terrestrial vegetation development 42
3.4.1 Zone I (prior to 10 570 cal. yrs BP) 42
3.4.2 Zone II (10 570–ca 9 200 cal. yrs BP) 42
3.4.3 Zone III (ca 9 200–4 000 cal. yrs BP) 42
3.4.4 Zone IV (ca 4 000 cal. yrs BP-present) 43
3.5 Holocene temperature evolution 43
3.5.1 Pollen-based mean July air temperature ($\boldsymbol{T}_{jul}$) reconstruction 43
3.5.2 Minimum $\boldsymbol{T}_{jul}$ reconstruction using plant indicator taxa 43
3.5.3 Chironomid-based $\boldsymbol{T}_{jul}$ reconstruction 44
3.6 Discussion 45
3.6.1 Environmental conditions at the moment of deglaciation 46
3.6.2 Timing of maximum Holocene summer temperature 47

4 Early Weichselian (MIS 5d and 5c) environmental and climate reconstructions for northeastern Fennoscandia 49
4.1 Materials and methods 49
4.1.1 Stratigraphy and dating 49
4.1.2 Proxy analyses 51
4.1.3 Zonation of proxy diagrams 51
4.1.4 Quantitative climate reconstructions 51
4.2 Results 54
4.2.1 Biotic data 54
4.2.2 Proxy-based climate reconstructions 54
4.3 Depositional environment and local (azonal) vegetation during the cold MIS 5d stadial period (ca 115–105 kyr BP) 58
4.3.1 Local zone I-1 (19.69–18.69 m depth interval) 58
4.3.2 Local zone I-2 (18.69–18.24 m) 58
4.3.3 Local zone I-3 (18.24–16.80 m) 58

4.4 Depositional environment and local (azonal) vegetation during the warm MIS 5c interstadial period (ca 105–90 kyr BP) 59
4.4.1 Local zone II-1 (16.74–15.80 m depth interval) 59
4.4.2 Local zone II-2 (15.65–15.16 m) 60
4.4.3 Local zone II-3 (15.16–14.65 m) 61
4.4.4 Local zone II-4 (14.65–14.42 m) 61
4.4.5 Local zone III-1 (14.42–14.08 m) 61
4.4.6 Local zone III-2 (14.08–13.56 m) 61
4.4.7 Local zone III-3 (13.56–13.40 m) 62
4.5 Regional (zonal) vegetation development during the cold MIS 5d stadial period (ca 115–105 kyr BP) 62
4.6 Regional (zonal) vegetation development during the warm MIS 5c interstadial period (ca 105–90 kyr BP) 63
4.6.1 Sub-zone II-a (16.74–16.02 m depth interval) 63
4.6.2 Sub-zone II-b (16.02–14.95 m) 64
4.6.3 Sub-zone II-c (14.95–14.42 m) 64
4.6.4 Zone III (14.42–13.40 m) 64
4.7 Climate evolution during MIS 5d and 5c 65
4.7.1 Inferences on climate regime based on pollen 65
4.7.2 Chironomid-based $\boldsymbol{T}_{jul}$ reconstruction 65
4.7.3 Minimum $\boldsymbol{T}_{jul}$ reconstruction using plant indicator taxa 69
4.8 Discussion of the MIS 5d and 5c results 69
4.8.1 Environmental and climate conditions during MIS 5d 69
4.8.2 Environmental and climate conditions during MIS 5c 71
4.8.3 Changes in degree of continentality during MIS 5d and 5c 72

5 Eemian Interglacial (MIS 5e) environmental and climate reconstructions for northeastern Fennoscandia 73
5.1 Materials and methods 73
5.1.1 Stratigraphy and dating 73
5.1.2 Proxy analyses 74
5.1.3 Zonation of proxy diagrams 76
5.1.4 Quantitative climate reconstructions 76
5.2 Results 78
5.2.1 Proxy data 78
5.2.2 Pollen-based climate reconstructions 79
5.3 Environmental conditions during the Eemian Interglacial (MIS 5e; ca 130–115 kyr BP) 82
5.3.1 Zone I (28.40–25.17 m depth interval) 82
5.3.2 Zone II (25.17–24.65 m) 82
5.3.3 Zone III (24.65–23.40 m) 82
5.3.4 Zone IV (23.40–22.51 m) 83
5.3.5 Zone V (22.51–17.98 m) 84
5.3.6 Zone VI (17.98–16.00 m) 84
5.3.7 Zone VII (borehole 901) 85
5.4 Climate evolution during the Eemian Interglacial (MIS 5e; ca 130–115 kyr BP) 85
5.4.1 Pollen-based $\boldsymbol{T}_{jul}$ reconstruction 85
5.4.2 Pollen-based $\boldsymbol{T}_{jan}$ reconstruction 86
5.4.3 Inferences on moisture regime 88
5.5 Correlation with European and North Atlantic records 88

6 Conclusions 91

7 Potential future research 97
7.1 Suggestions for future work on the Sokli data of potential interest for SKB 97
7.2 In addition, the unique Sokli sequence is continuing to provide externally funded spin-off projects 97

References 99

Appendix 1 115

1 Introduction

1.1 Background

The classic geological reconstructions of environmental conditions, such as vegetation and climate, in Fennoscandia for the Last Interglacial-Glacial cycle (i.e. the Late Pleistocene between ca 130 and 11 kyr ago; Figure 1-1) are largely based on long-distance correlation of poorly-dated and highly-fragmented bio(/pollen)- and litho(/till fabric)-stratigraphic evidence (Andersen and Mangerud 1989, Mangerud 1991, Lundqvist 1992, Donner 1995). Long pollen records from the north-western European mainland have been used as templates against which local and regional bio-stratigraphic schemes were correlated. However, as clearly outlined in Donner (1996), these correlations were fraught with uncertainties, caused by e.g. the long distance of correlation, over an area with a great range of climatic conditions, and truncations of geological beds resulting in incomplete interstadial or interglacial sequences. Additionally, correlations were made on the assumption that Late Pleistocene climate and vegetation gradients over central Europe-Fennoscandia were similar as today or steeper, influenced by the presence of the Fennoscandian Ice Sheet, and that climate conditions were similar or warmer than today only during the Eemian Interglacial (Marine Isotope Stage (MIS) 5e between ca 130–115 kyr ago; Figure 1-1). Furthermore, the Late Pleistocene glacial history of Fennoscandia is mostly based on correlations with the marine oxygen-isotope stratigraphy. Although it is widely acknowledged that the latter record carries a composite signal of e.g. ice volume, ocean water temperature and salinity, the marine oxygen-isotope record is widely used as a proxy for global ice volume changes during the Quaternary (last ca 2.5 Myr) (e.g. Kleman et al. 1997).

Long sediment sequences are rare in Fennoscandia due to repeated glacial erosion by the Fenno-scandian Ice Sheet. Findings of sediments predating the Last Glacial Maximum (LGM; at ca 20 kyr BP) are concentrated in the former ice-divide zone, where low ice-flow velocities and/or frozen-bed conditions have resulted in limited glacial erosion. However, a closer look on the till-covered organic beds preserved in the ice-divide zone over northern Finland shows that these beds generally are only a few decimetres thick and often occur in a secondary position, i.e. the sediments are not found *in situ* but have been truncated and transported by the ice sheet (Hirvas 1991).

An unusually long sedimentary sequence has been found preserved at Sokli in north-eastern Finland (Figure 1-2), i.e. in the near-central area of Fennoscandian glaciations. Although limited erosion in the ice-divide zone most probably has contributed to its preservation, the sediments at Sokli have been protected from glacial erosion also by non-typical topographic bedrock conditions. The sediments are situated in a sheltered position in a steep depression formed in relatively soft, highly-weathered rocks of a Paleozoic magma-intrusion (Sokli Carbonatite Massif). With sediments preserved in their original stratigraphic position, combined with an absolute time-frame obtained through OSL/TL and AMS ^{14}C dating, the long sediment record in the Sokli basin provides a unique possibility for studying Late Quaternary environmental and climate change in northern Fennoscandia.

Following reconnaissance studies (Ilvonen 1973, Helmens et al. 2000, 2007), the Sokli sediment sequence has been subjected to detailed studies over the last decade, mostly with funding provided by SKB. The latter studies not only exploit the *in situ* preservation of geological beds in the Sokli basin, but also the unusual thickness of the beds as well as their fossil-richness, allowing detailed and comprehensive reconstructions of past environmental and climate conditions for the last ca 130 kyr. A multi-proxy approach is being applied, i.e. a large variety of fossil remains and sediment characte-ristics are analyzed, and their results are integrated. Furthermore, climate parameters are quantified using novel methods. The studies are conducted by an international team of researchers specialized in e.g. the analysis of pollen, macrofossils, chironomids (aquatic insects) and diatoms, biogeochemical elements, as well as different climate reconstruction methods. Collaboration during the execution of the studies presented in this report is summarized in Table 1-1.

In a first part of the Sokli studies, Helmens (2009) presented the results of a multi-proxy analysis on sediments of early MIS 3 age (ca 50 kyr BP; Tulppio Interstadial Figure 1-1E) in the Sokli basin. In contrast to earlier reconstructions that inferred glaciation over large parts of Fennoscandia during this time-interval (e.g. Donner 1995), the results presented in Helmens (2009) not only indicates ice-free conditions, but also present-day summer temperatures. Vegetation seems to have been remarkably

similar in composition to modern, low-arctic tundra in the continental sector of northern Fennoscandia. The early MIS 3 sediments are interpreted to have been deposited in an ice-marginal environment (Helmens 2009).

The present report focuses on sediments of the MIS 5e, 5d and 5c periods (Nuorti Interglacial, Savukoski 1 Stadial and Sokli I, respectively, in Figure 1-1E) as well as the Holocene. MIS 5e is the warmest period of the Late Pleistocene (Eemian Interglacial between ca 130–115 kyr BP in Figure 1-1D). MIS 5c represents one of the warm intervals of the Early Weichselian (Brørup Interstadial; ca 105–90 kyr BP). It follows the cold MIS 5d (Herning Stadial; ca 115–105 kyr BP). As will be shown in this report, environmental and climate conditions during MIS 5d-c were distinctly different compared to those reconstructed in earlier studies based on the long-distance correlation of stratigraphic fragments found east of the Scandinavian mountains in Sweden and Finland (e.g. Lundqvist 1992, Donner 1995). The Eemian study provides an exceptionally high time-resolution climate record and unexpectedly shows warm interglacial conditions being intersected by two pronounced cold/dry events (Tunturi and Värriö events). The study on the Holocene (last 11 kyr) sediments was executed with the goal to obtain a reference section for the older sediments preserved in the Sokli basin.

The present report summarizes the results published in a series of scientific papers listed in Table 1-2. The latter includes the PhD thesis by Shyhrete Shala on the Holocene environmental and climate record from Loitsana Lake (Shala 2014). A brief summary of our results for MIS 5d-c and MIS 3 at Sokli, combined with data from earlier reconnaissance studies at Sokli (Helmens et al. 2000, 2007), has been placed in a European stratigraphic context in Helmens (2013). The time-interval represented in the long Sokli sedimentary sequence, which is currently under detailed study (i.e. MIS 5a, the Early Weichselian Odderade Interstadial or Sokli II), is also highlighted in Figure 1-1.

Table 1-1. International collaboration during the execution of studies presented in this report.

Stockholm University (Departments of Physical Geography and Geological Sciences; Sweden):
Dr. Krister Jansson (GIS), Dr. Malin Kylander (XRF core scanning and data analysis), Dr. Ludvig Löwemark[1] (XRF core scanning and data analysis), PhD-student MSc Anna Plikk (subsampling, biogeochemical and diatom analyses), Dr. Jan Risberg (diatom identification), PhD-student Dr. Shyhrete Shala (subsampling, ^{14}C dating, biogeochemical, diatom and macrofossil analyses).
[1] Present address: Department of Geosciences, National Taiwan University, Taiwan.
Umeå University (Department of Ecology and Environmental Science; Sweden):
MSc María Fernández-Fernández[2] (FTIRS-BSi analysis).
[2] Present address: Instituto de Investigaciones Agrobiológicas de Galicia, Spain.
University of Helsinki (Departments of Geosciences and Geography, and Environmental Sciences, and Ecosystems and Environment Research Programme; Finland):
Dr. Niina Kuosmanen[3] (pollen analysis), Prof. Dr. Miska Luoto (actuo-ecology), Dr. Tomi Luoto (chironomid analysis and quantitative climate reconstructions), Dr. J. Sakari Salonen (pollen analysis and quantitative climate reconstructions), Dr. Minna Väliranta (macrofossil identification and analysis, and quantitative climate reconstructions), Dr. Jan Weckström (diatom data interpretation and quantitative climate and pH reconstructions).
[3] Present address: Department of Forest Ecology, Czech University of Life Sciences, Czech Republic.
University of Bergen (Department of Earth Science; Norway):
Dr. Jo Brendryen (comparison with N Atlantic marine data).
Birkbeck University of London (School of Geography; U.K.):
Dr. Stefan Engels (chironomid analysis and quantitative climate reconstructions).
VU University Amsterdam (Department of Earth Sciences, The Netherlands):
Prof. Dr. Hans Renssen (data-model comparison).

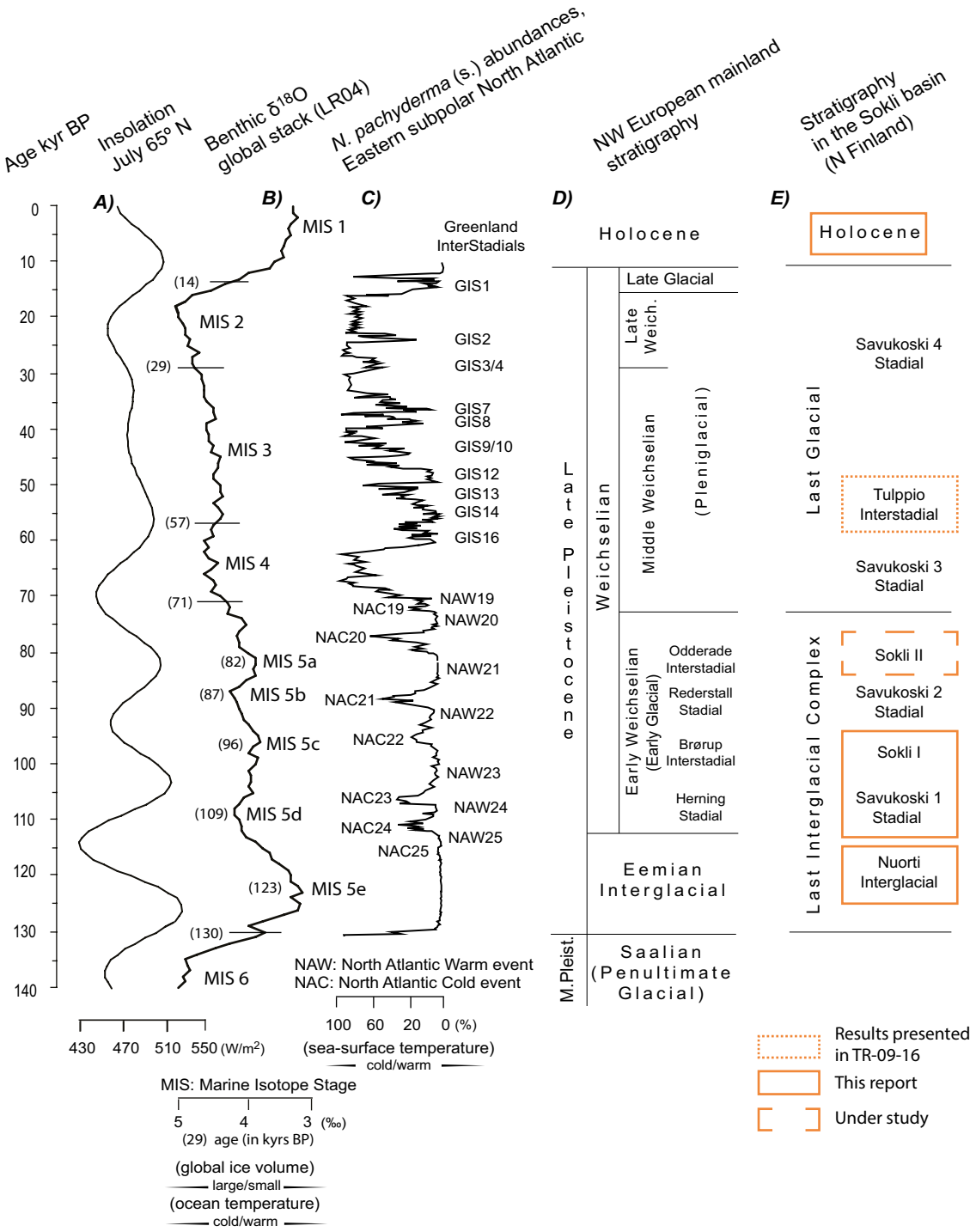

Figure 1-1. ***A*** *Variations in summer insolation at high northern latitudes (Berger and Loutre 1991), i.e. a major driver in orbital-scale climate changes during the Quaternary.* ***B-E*** *Late Quaternary stratigraphies in marine sediments (**B**, globally; Lisiecki and Raymo 2005; **C**, eastern subpolar North Atlantic; McManus et al. 1994, Bond et al. 1993) and terrestrial sediments (**D**, NW European mainland; **E**, Sokli basin in N Finland; Helmens 2014). Greenland Interstadials (GIS) are according to Johnsen et al. (1992) and Dansgaard et al. (1993). Adapted from Helmens (2014). Sediment intervals studied at Sokli are highlighted.*

Table 1-2. Publications on the Holocene and MIS 5e, 5d and 5c deposits in the Sokli basin, based on the present study.

Helmens K F, Katrantsiotis C, Salonen S J, Shala S, Bos J A A, Engels S, Kuosmanen N, Luoto T P, Väliranta M, Luoto M, Ojala A, Risberg J, Weckström J, 2018. Warm summers and rich biotic communities during N-Hemisphere deglaciation. Global and Planetary Change 167, 61–73.
Salonen S J, Helmens K F, Kuosmanen N, Väliranta M, Brendryen J, Goring S, Korpela M, Kylander M, Philip A, Plikk A, Renssen H, Luoto M, 2018. Abrupt high-latitude climate events and decoupled seasonal trends during the Eemian Interglacial. Nature Communications 9. doi:10.1038/s41467-018-05314-1.
Kylander M, Plikk A, Rydberg J, Löwemark L, Salonen S J, Fernández-Fernández M, Helmens K F, 2018. Sediment Geochemistry of the Eemian Sequence at Sokli, NE Finland: New insights from XRF core scanning data into boreal lake ontogeny during the Eemian (Marine Isotope Stage 5e) at Sokli, northeast Finland. Quaternary Research 89, 352–364.
Shala S, Helmens K F, Luoto T P, Salonen J S, Väliranta M, Weckström J, 2017. Comparison of quantitative Holocene temperature reconstructions using multiple proxies from a northern boreal lake. The Holocene 27, 1745–1755.
Plikk A, Helmens K F, Fernández-Fernández M, Kylander M, Löwemark L, Risberg J, Salonen J S, Väliranta M, Weckström J, 2016. Development of an Eemian (MIS 5e) Interglacial paleolake at Sokli (N Finland) inferred using multiple proxies. Palaeogeography, Palaeoecology, Palaeoclimatology 463, 11–26.
Helmens K F, Salonen J S, Plikk A, Engels S, Väliranta M, Kylander M, Brendryen J, Renssen H, 2015. Major cooling intersecting peak Eemian Interglacial warmth in Northern Europe. Quaternary Science Reviews, short communication 122, 293–299.
Väliranta M, Salonen J S, Heikkilä M, Amon L, Birks H H, Helmens K F, Klimaschewski A, Kuhry P, Kultti S, Poska A, Shala S, Veski S, 2015. Plant macrofossil evidence for an early onset of the Holocene summer thermal maximum in Northern Europe. Nature Communications 6. doi:10.1038/ncomms7809.
Helmens K F, 2014. The Last Interglacial-Glacial cycle (MIS 5-2) re-examined based on long proxy records from central and northern Europe. Quaternary Science Reviews 86, 115–143.
Shala S, Helmens K F, Luoto T P, Väliranta M, Weckström J, Salonen J S, Kuhry P, 2014b. Evaluating environmental drivers of Holocene changes in water chemistry and aquatic biota composition at Lake Loitsana, NE Finland. Journal of Paleolimnology 52, 311–329.
Shala S, Helmens K F, Jansson K, Kylander M E, Risberg J, Löwemark L, 2014a. Paleoenvironmental record of glacial lake evolution during the early Holocene at Sokli, NE Finland. Boreas 43, 362–376.
Shala S, 2014. Paleoenvironmental changes in the northern Boreal zone of Finland based on lake sediment analyses: local versus regional drivers. PhD thesis, Stockholm University.
Engels S, Self A E, Luoto T P, Brooks S J, Helmens K F, 2014. A comparison of three Eurasian chironomid-climate calibration datasets on a W-E continentality gradient and the implications for quantitative temperature reconstructions. Journal of Paleolimnology 51, 529–547.
Helmens K F, 2013. The Last Interglacial-Glacial cycle (MIS 5-2) re-examined based on long proxy records from central and northern Europe. SKB TR-13-02, Svensk Kärnbränslehantering AB.
Salonen S J, Helmens K F, Seppä H, Birks H J B, 2013. Pollen-based paleoclimate reconstructions over long glacial-interglacial timescales: methodological tests based on the Holocene and MIS 5d-c deposits of Sokli, northern Finland. Journal of Quaternary Science 28, 271–282.
Helmens K F, Väliranta M, Engels S, Shala S, 2012. Large shifts in vegetation and climate during the Early Weichselian (MIS 5d-c) inferred from multi-proxy evidence at Sokli (northern Finland). Quaternary Science Reviews 41, 22–38.
Engels S, Helmens K F, Väliranta M, Brooks J, Birks H J B, 2010. Early Weichselian (MIS-5d and 5c) temperatures and environmental changes in northern Fennoscandia as recorded by chironomids and macroremains at Sokli, northeast Finland. Boreas 39, 689–704.

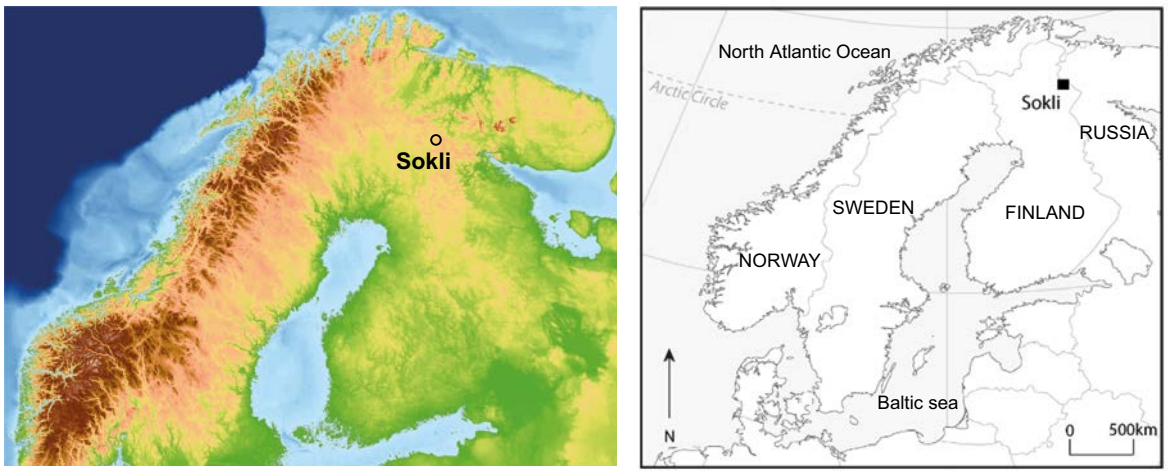

Figure 1-2. *Location of the study site Sokli (lat. 67°48'N, long. 29°18'E, elevation 220 m a.s.l.) in north-eastern Finland, in the relatively flat Precambrian Shield region of north-eastern Fennoscandia.*

Väliranta M, Birks H H, Helmens K F, Engels S, Piirainen M, 2009. Early Weichselian interstadial (MIS 5c) summer temperatures were higher than today in northern Fennoscandia. Quaternary Science Reviews, rapid communications 28, 777–782.

1.2 Objectives

The objectives for the present study are to:

1) Obtain a Holocene reference section for the study of the Late Quaternary sediment sequence preserved in the Sokli basin.
2) Reconstruct in great detail the environmental and climate conditions at the moment of the last deglaciation in the early-Holocene.
3) Determine the timing of maximum Holocene summer warming in north-eastern Fennoscandia.
4) Reconstruct in great detail the environmental and climate conditions at Sokli in the Early Weichselian during MIS 5d-c.
5) To reconstruct in great detail the environmental and climate conditions at Sokli during the Eemian Interglacial (MIS 5e).

2 Present environmental setting of the study area

The deserted mining hamlet of Sokli is situated in north-eastern Finland close to the Russian border. A patterned fen (Sokliaapa) borders a meandering rivulet (Soklioja) just northwest of the hamlet (Figure 2-1).

It is in a small sedimentary basin (ca 2 km^2), which underlies the central part of the Sokliaapa (at lat. 67°48'N, long. 29°18'E; surface elevation ca 220 m a.s.l.), that a thick sedimentary sequence has been preserved reaching back to the Late Saalian or MIS 6 (Figure 1-1) (Ilvonen 1973, Helmens et al. 2000, 2007). The basin is formed in strongly weathered rocks of a Paleozoic carbonate-rich magma intrusion (Sokli Carbonatite Massif in Figure 2-1C). The Sokli Massif has a diameter of ca 7 km and is enriched in the elements phosphorus, niobium, iron, sulphur and calcium (Vartiainen 1980). The surrounding bedrock is crystalline Precambrian Shield. Open water of the Loitsana Lake is found in the south-western part of the Sokliaapa, ca 1 km from the sedimentary basin. The location of boreholes Sokli B-series, 2010/4 and 901 in the sedimentary basin mentioned above, the Loitsana Lake core, and core ×1 just south of Loitsana, all five cores which are subjects of the present study, are shown in Figure 2-1.

The Soklioja rivulet flows into the Nuortti River which drains into the Barents Sea. The highest peaks (ca 500 m a.s.l.) in the Nuortti drainage basin, at some 20 km SE of Sokli (Värriötunturi in Figure 2-1B), reach just above the altitudinal tree-line and are covered with tundra vegetation. Zonal vegetation at Sokli consists of northern boreal forest with *Betula* (*Betula pubescens* and *B. pendula*; birch), *Pinus sylvestris* (pine) and *Picea abies* (spruce) as the dominant tree species. Mires of the aapa-type (i.e. a patterned fen) with *Sphagnum* spp., *Rubus chamaemorus*, Ericales (e.g. *Vaccinium* spp., *Andromeda polifolia*, *Empetrum nigrum*), *Betula nana, Salix* spp. and *Carex* spp. are extensively present in the region (note that only the Sokliaapa is indicated in Figure 2-1C). The present climate is classified as cold boreal, with a mean July air temperature of +13 °C and a mean February air temperature of –14 °C. The mean annual precipitation is between 500 and 550 mm (Figure 2-1D).

The northern limits of spruce and pine are situated ca 100 and 150 km north of Sokli, respectively. Sub-arctic birch forest stretches north of the pine limit. The vegetation of the tundra region beyond the forest limit, i.e. at higher elevations and along the Barents Sea coast, is mainly dwarf-shrub tundra dominated by dwarf birch (*Betula nana*) and Ericales. The northern limits of temperate trees (e.g. *Alnus glutinosa*; alder) are situated hundred to several hundreds of kilometres south of the Sokli site.

Loitsana Lake is situated in a former meltwater channel associated with a northwest-southeast oriented esker chain (Figure 2-1C). Esker ridges situated to the northeast, northwest and southwest of the lake consist of sorted sands inferred to have been deposited during the last deglaciation (Perttunen and Vartiainen 1992). The lake area covers 0.09 km^2, the water depth is 1–2 m, and the water pH is around 7.4 with an alkalinity of 1.90 mmol l^{-1}. The P_{tot} and N_{tot} are 120 and 520 µg l^{-1}, respectively, the watercolor is < 10 mg Pt l^{-1} and the turbidity 2.7 FNU (Finnish Environmental Institute 2010). Water chemistry was measured in April 2008 at a water temperature of +0.3 °C. It is, however, likely that the present water chemistry of Loitsana Lake is influenced by mining just north of the lake. The lake is currently fed by groundwater inflow from the closest esker and limited surficial input particularly from a small stream in the north-western corner of the lake. The Loitsana Lake drains into the Soklioja rivulet. Photos illustrating the present environmental setting of the study area are given in Figures 2-2 and 2-3.

Figure 2-1C further highlights the maximum possible extent of the early-Holocene glacial lake (240 m a.s.l.), and its extent following a partial drainage of the lake (220 m a.s.l.), according to Shala (2014).

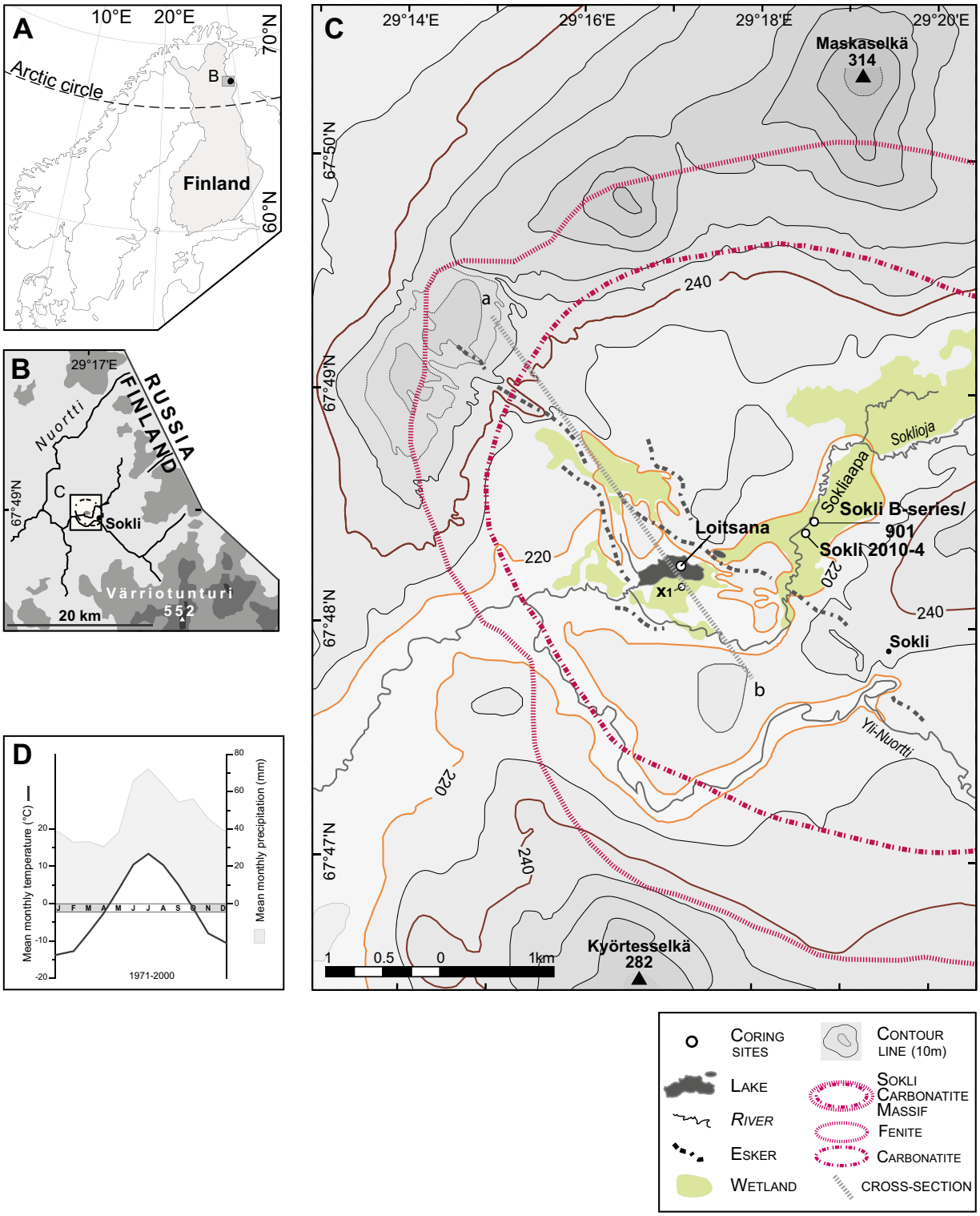

Figure 2-1. *Location map showing **A** the location of the study area in north-eastern Fennoscandia; **B** the regional setting; **C** location of the Sokliaapa fen and Loitsana Lake, coring sites, esker ridges (modified from Johansson 1995), and western limit of the Sokli Carbonatite Massif; and **D** climatogram including mean monthly precipitation and air temperature values for the period 1971–2000 at Savukoski (67°17'N, 28°10'E, 193 m a.s.l.). Climate data were obtained from the Finnish Meteorological Institute. The maximum possible extent of the early-Holocene glacial lake (240 m a.s.l.), and the extent following a partial drainage of the glacial lake (220 m a.s.l.), are highlighted by brown respectively orange contour lines. Adapted from Shala (2014).*

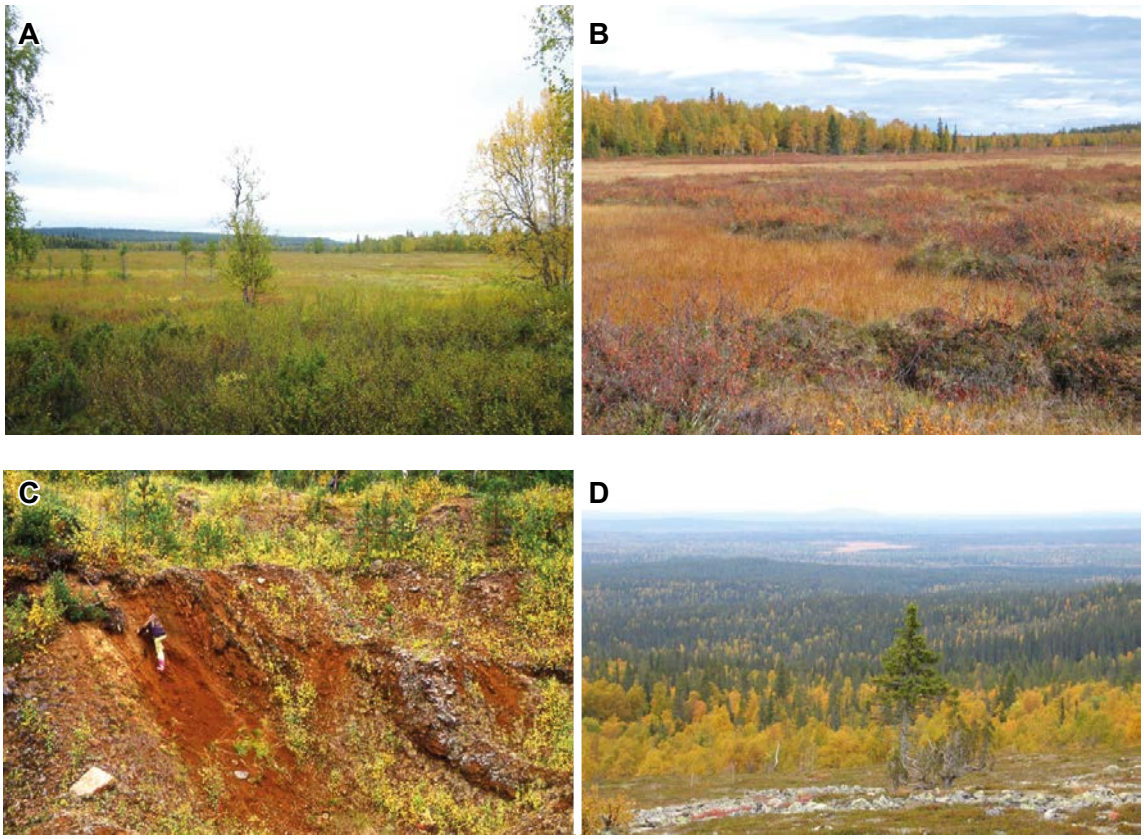

Figure 2-2. *__A__ and __B__ show the Sokliaapa patterned fen; __C__ strongly weathered rocks of the Sokli Massif; and __D__ regional view to northwest from the Värriötunturi (see Figure 2-1B).*

Figure 2-3. ***A*** *view to the west over Loitsana Lake;* ***B*** *the Loitsana Lake outlet;* ***C*** *and* ***D*** *views towards northern and southern lake shores;* ***E*** *the Soklioja rivulet; and* ***F*** *exposure in sandy esker 1 km to the south-west of Loitsana Lake (see Figure 2-1C).*

3 Holocene environmental and climate reconstructions for northeastern Fennoscandia

3.1 Materials and methods

3.1.1 Sediment sampling

Nine metres of lacustrine sediment were collected with a Russian peat corer from the ice-covered Loitsana Lake in spring 2008. The core was mostly subsampled with a 1 cm resolution. Analyses were performed at intervals of 3–20 cm, in the upper unit consisting of organic-rich sediments (735–0 cm), and with 5 cm resolution at 5–10 cm intervals, in the underlying minerogenic sediments (900–735 cm). Additionally, coring was performed in the wetland just south of Loitsana Lake (site x1 in Figure 2-1). Coring was performed by Karin Helmens, Päivi Kaislahti Tillman, Martin Margold, Jan Risberg, Shyhrete Shala and Liselott Wilin (Stockholm University), and Minna Väliranta (University of Helsinki). Subsampling was done by Shyhrete Shala.

3.1.2 Radiocarbon dating and age model

Ten radiocarbon datings on the Loitsana Lake sequence, and one dating at site ×1, were performed by accelerator mass spectrometry (AMS) on plant macrofossil remains at the Poznan Radiocarbon Laboratory, Poland (Table 3-1). The dates were calibrated and an age-depth model was calculated in the R 2.12.2 software (R Development Core Team 2011), using the CLAM package (Blaauw 2010) and the IntCal09 calibration curve (Reimer et al. 2009, Bronk Ramsey 2009). The plant macrofossils were hand-picked, and the age model was constructed, by Shyhrete Shala.

3.1.3 Sediment biogeochemistry

X-ray fluorescence core scanning

Elemental peak areas in the lower part of the sediment succession (ca 900–600 cm) were analyzed with a XRF core scanner at the Department of Geological Sciences, Stockholm University. The cores were scanned at 2 mm resolution using a molybdenum-tube (voltage 30 kV, current 45 mA) and 30 s measuring time (cf. Croudace et al. 2006). Peak areas for each step were normalized by the total number of counts (kcps) for that step in order to remove various instrumental effects. The Compton and Rayleigh scattering ratio (i.e. incoherent (inc) and coherent (coh) scattering), generally linked to changes in organic matter content (e.g. Guyard et al. 2007, Löwemark et al. 2011), is here employed as a complement to loss-on-ignition measurements (see below). Furthermore, the use of elemental ratios (in particular normalization with titanium (Ti)) has been proven effective in revealing patterns that are undetectable in single elemental profiles due to the dilution effect of, for example, carbonates and organic matter (Kylander et al. 2011, Löwemark et al. 2011) is also applied in this study.

To handle the large data set obtained through the XRF core-scanning, and detect potential correlations between different elemental profiles, a principal components analysis (PCA) was made using JMP 9.0.0 software (correlation mode, varimax rotation). As the original data was normalized, and the data set became subsequently “closed”, all elemental profiles were log-transformed prior to analysis. This was done in order to avoid the closure effect of compositional data (e.g. Aitchison 1982). The XRF core-scanning and first analysis of data were performed by Malin Kylander and Ludvig Löwemark (Stockholm University). Data handling and final interpretation were made by Shyhrete Shala.

Table 3-1. Results of radiocarbon dating on the Loitsana Lake sediment sequence, and a basal peat sample (Poz-47403) from site x1 (Figure 2-1). Weighted averages are based on all age-depth model derived ages and the applied model. * Rejected dates.

Lab no.	Depth (cm)	^{14}C age (year BP)	cal. age (year BP) (68.2 %)	(95.4 %)	Weighted avg. age (cal. year BP)	Material
Poz-45930	29	1630±35	1565–1419	1606–1414	1426	*Salix herbacea* leaf
Poz-40495	130–128	8340±50	9432–9302	9480–9144	*	*Betula seed*, Cyperaceae and unidentified epidermal remains
Poz-45928	180	4530±40	5305–5063	5313–5047	5188	*Betula* leaf remains
Poz-40496	347	6020±40	6906–6796	6959–6748	6871	Small twig
Poz-40497	508	7960±60	8978–8725	8997–8636	8811	*Betula* leaf remains
Poz-40498	603–600	8450±70	9529–9430	9542–9303	9440	*Betula* seeds and leaf remains
Poz-38945	664–662	8630±130	9885–9487	10152–9428	9792	*Betula* seeds
Poz-35511	734	9410±50	10697–10581	10756–10511	10560	*Betula* seeds
Poz-43852	760–755	9370±110	10743–10414	11069–10259	10731	*Betula* seeds
Poz-38946	765–760	10080±70	11810–11406	11973–11332	*	*Betula* seeds and leaf fragments, unidentified epidermal remains
Poz-47403	241	5740±40	6627–6486	6650–6440		*Betula* seeds, catkin scale and leaf remains

Loss-on-ignition and C/N measurements

In order to measure the organic and inorganic carbon content of the sediment, loss-on-ignition (LOI) was performed at 550 °C for four hours, respectively 950 °C for five hours, on samples of generally similar size (ca 1 cm^3) following Heiri et al. (2001).

Freeze-dried sediment samples were ground and the material weighed for C/N-analysis. To account for carbonates in the sediment, material was also taken from all samples for organic carbon (C_{org}) analysis. The weighed material was treated with HCL (10 %) and dried over night before analysis. Concentrations were measured through combustion in a Carlo Erba NC2500 Elemental Analyzer at the Stable Isotope Laboratory at the Department of Geological Sciences, Stockholm University. The analyses were performed by Shyhrete Shala.

3.1.4 Fossil analyses

Siliceous microfossils

Diatoms were extracted from the sediment following Battarbee (1986). Organic matter was oxidized in H_2O_2 on a water bath at ca 100 °C and carbonates were removed by 10 % HCl (no visible reaction). Clay particles were decanted from 100 ml beakers in two hour intervals. Sand grains were removed after five seconds of sedimentation. The residue was mounted in Naphrax® and analyzed under a light microscope with X1000 magnification using immersion oil. Flora used for species identification and information on ecological preferences are presented in Helmens et al. (2009). Percentage values of phytoliths and chrysophyte cysts were calculated based on the total sum of diatoms and other siliceous microfossils; these data have previously been shown to provide valuable information on e.g. catchment erosion (Piperno 2001, Helmens et al. 2009). The phytoliths were identified as pooid morphotypes, i.e. having originated from grasses (Carter 2007). A minimum of 500 diatom valves were identified from each sample with the exception of samples at 900–700 cm depth where diatom abundance was low. The total of identified diatom valves varied from 64–246 between 700–795 cm depth; below 795 cm, only single valves were identified.

The pH history of Loitsana Lake was reconstructed using modern diatom-water pH calibration data sets consisting of 109 surface-sediment diatom assemblages and corresponding pH measurements (Korhola et al. 1999). The 2-component weighted average partial least squares (WA-PLS) model is robust for the pH reconstruction ($r^2 = 0.68$, RMSEP = 0.31).

The siliceous microfossil analysis was performed by Shyhrete Shala and the pH reconstruction by Jan Weckström (University of Helsinki).

Chironomids

Chironomids were extracted from the sediment following standard instructions described in Brooks et al. (2007). The sediment samples were sieved using a 100µm mesh and chironomid head capsules were handpicked from the residue with a fine forceps under a stereo-microscope. The chironomids were identified using a light microscope with X400 magnification. A minimum of 50 head capsules was identified from each sample. The nomenclature follows Brooks et al. (2007). The chironomid analysis was performed by Tomi Luoto (University of Helsinki).

Pollen, spores and non-pollen palynomorphs (NPP's)

Samples were prepared using KOH, HF and acetolysis treatments (Fægri and Iversen 1989). Pollen, spore and NPP percentages were calculated on the basis of the Total Sum of terrestrial pollen and spores. The counting sum per sample was ca 500 for most samples, but with lower counts of ca 250 used for some samples with low pollen densities. The palynological analysis was performed by Sakari Salonen (University of Helsinki).

Macrofossils

Macrofossil analysis was performed following methods of Birks (2007). The volume of samples was measured through water displacement and used to convert counts to concentrations. Sample size ranges from 5 to ca 30 cm^3 but is mainly 10–15 cm^3. Samples were washed in a fine jet of water through a 100µm sieve. The residue was analyzed in a Petri-dish under a stereo-microscope and light microscope with X20 magnification. The plant nomenclature follows Mossberg and Stenberg (2003). The macrofossil analysis was performed by Shyhrete Shala.

3.1.5 Zonation of proxy diagrams

The minimum number of significant zones in all individual stratigraphical data sequences (except the terrestrial plant record) was estimated using the broken-stick model (Bennett 1996). The individual zonation for each data sequence was then used to visually construct a common zonation. All numerical analyses were carried out in the statistical environment R 2.12.2 (R Development Core Team 2011), using the additional packages Rioja (Juggins 2009) and Vegan (Oksanen et al. 2011). Numerical zonation was done using the chclust() function (method = "coniss") of Rioja and the data was transformed using the decostand() function (method = "hellinger") of Vegan. Zonation of the terrestrial plant diagram is based on visual examination of the data. The zonation was performed by Shyhrete Shala.

3.1.6 Application of digital elevation model data

A digital elevation model (DEM) obtained from the National Land Survey of Finland (license no. MYY/ 223/06) was employed to refine the reconstructions made by Johansson (1995) of the later stages of the Sokli Ice Lake. The DEM has a spatial resolution of 25 m and a vertical resolution of approximately 1 m. The ice flow direction, used to guide the reconstruction of the retreating ice-margin, was in this study inferred from the pattern of eskers in the area (Johansson 1995; see also Figure 2-1). As the area invoked in the glacial-lake reconstruction is relatively small (ca 30×30 km), possible errors generated due to non-uniform isostasy are considered to be insignificant (cf. Jansson 2003). Also, no consideration was taken to the influence of local topography on the shape of the ice-margin. The elevations presented here are modern values. The DEM-based reconstructions were performed by Krister Jansson (Stockholm University).

3.1.7 Quantitative climate reconstructions

Plant indicator species

Minimum mean July air temperature (T_{jul}) reconstructions were made based on the findings of wetland, aquatic and shore plant indicator taxa (mostly identified in the macrofossil analysis) and their current northern limits (see e.g. Iversen 1954, Kolstrup 1979, Väliranta et al. 2009). Plant indicator species need a certain minimum T_{jul} in order to flower and reproduce. Present-day minimum T_{jul} values of these taxa are inferred from current species distribution maps (Lampinen and Lahti 2013) and mean

July air temperatures calculated from daily measurements (for the period 1961–2000) by the Finnish Meteorological Institute (Venäläinen et al. 2005). A summary of plant indicator taxa and their present-day temperature minima are given in Table 3-2.

Table 3-2. Minimum modern mean July air temperatures (T_{jul}) for plant indicator taxa as indicated by Lampinen and Lahti (2007) and Venäläinen et al. (2005). 1 = narrow-leaved *Potamogeton* taxa such as *P. filiformis*.

Taxon	Min. T_{jul} (˚C)
Nymphaeaceae	(+10–) +12
Potamogeton spp.[1]	+13
Callitriche cophocarpa	+13
Glyceria lithuanica	+15
Typha	+15

Calibration sets

T_{jul} reconstructions based on pollen and chironomids were performed using the transfer function approach (e.g. Birks 2003). Basic information about the two different calibration sets, which are used in this study, is summarized in Table 3-3.

The "central" calibration set (henceforth, c-set) used in the pollen-based T_{jul} reconstruction consists of 218 samples with 127 taxa (further details in Salonen et al. 2013). The calibration sites (i.e. lakes) are spread out along a latitudinal gradient from the Arctic Ocean coast to Lithuania and cover a T_{jul} gradient of 9.0–17.3 °C.

A new and enhanced c-set for Finland is used for the chironomid-based T_{jul} reconstruction. The chironomid-T_{jul} c-set combines the previous temperature calibration sets from the altitudinal gradient in NW Finnish Lapland (Nyman et al. 2005) and the latitudinal gradient in Finland (Luoto 2009), providing a temperature gradient of 7.9–17.1 °C. This combined c-set has 139 calibration sites and includes 117 taxa (Luoto et al. 2014).

Numerical methods

Pollen-based T_{jul} was reconstructed using a two-component weighted averaging-partial least squares regression (WA-PLS; ter Braak and Juggins 1993) calibration model (Table 3-3). Leave-one-out cross-validation (Birks 1995) was used to calculate model performance statistics. In addition to the cross-validated performance metrics, we estimated standard errors of prediction (eSEPs) for each fossil sample using random re-sampling of the calibration data (bootstrapping, 1000 iterations).

Table 3-3. Summary of calibration-set data, applied regression methods and model performance statistics for the different proxies. Two-component WA-PLS models were applied. RMSEP = root mean square error of prediction.

Proxy	Pollen	Chironomids
Number of lakes in the calibration set	218	139
Number of taxa in original calibration set	127	117
Temperature range (°C)	+9.0–17.3	+7.9–17.1
Regression method	WA-PLS	WA-PLS
Cross-validation approach	Leave-one-out	Leave-one-out
R2	0.884	0.880
Average bias (°C)	–0.018	0.005
Maximum bias (°C)	1.248	1.088
RMSEP (°C)	0.831	0.839

The chironomid-based T_{jul} reconstructions were performed using a two-component WA-PLS model, with model performance statistics calculated using leave-one-out cross-validation. Random re-sampling (999 iterations with bootstrapped c-sets) was used to calculate eSEPs for the downcore reconstruction.

The modern analogue technique (MAT; Overpeck et al. 1985, Birks 1998) was used to assess the reliability of the reconstructions by examining the compositional fit between fossil samples and their closest modern analogues in the calibration-sets. Qualitative estimates of the fit are made by comparing down-core distances to closest modern analogues to the distances found with the most-recent fossil samples, using increasing values as an indication of a worsening fit.

The climate reconstructions were performed by Minna Väliranta (macrofossils), Sakari Salonen (pollen), Tomi Luoto (chironomids) and Shyhrete Shala.

3.2 Results

3.2.1 Glacial-lake reconstruction using digital elevation data

In northern Finland, the extent of glacial lakes formed in front of the retreating ice-margin of the Fennoscandian Ice Sheet during the last deglaciation has been reconstructed in detail by Johansson (1995, 2007) using geomorphologic (glacial lake shorelines, outlet channels) and topographic data, in combination with the distribution of coarse-grained outwash and more fine-grained glacio-lacustrine sediment. Although glacial lakes covered extensive areas in northern Finland during the early-Holocene (Figure 3-1), most of the lakes were rather small and restricted to the deepest parts of valleys. The Sokli Ice Lake in north-eastern Finland was one of the glacial lakes reconstructed by Johansson (1995), and was defined as a relatively shallow glacial lake with several metres thick bottom sediments.

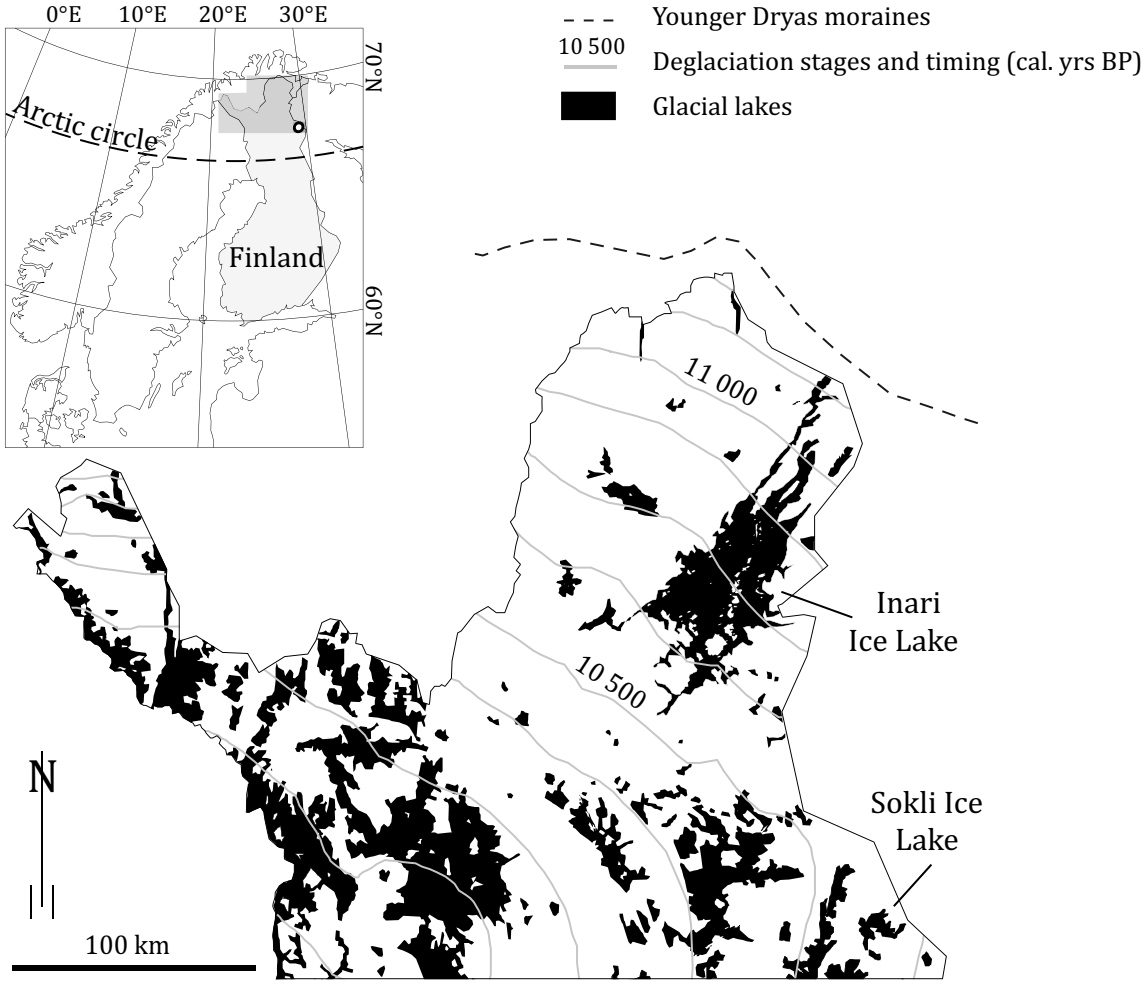

Figure 3-1. *The extent of glacial lakes in northern Finland during the Late Pleistocene – Holocene transition, as well as deglaciation pattern and chronology, according to Johansson (2007). Location of Sokli and Inari Ice Lakes is indicated. Modified from Shala et al. (2014b).*

The Sokli Ice Lake developed as meltwater was trapped between the retreating ice-margin of the Fennoscandian Ice Sheet in the northwest and higher terrain to the southeast (i.e. the Värriötunturi mountain, Figure 2-1B). The Loitsana Lake area became part of the Sokli Ice Lake during the final stages of the latter (Johansson 1995). Our DEM-based reconstruction of the retreating ice-margin near Loitsana and associated glacial-lake stages is presented in Figure 3-2.

During Stages 1 and 2 (Figure 3-2), the level of the glacial lake was controlled by the col at the head of the Törmäoja canyon, which has an elevation of 240 m a.s.l. The glacial lake reached its maximum extension during Stage 2, that is, before the deglaciation of the Nuortti River canyon. As the Nuortti River canyon was gradually deglaciated, the subsequent drainage of the glacial lake led to a lowering in water level by some 20 m (Stage 3). Eventually, the ice-sheet margin retreated beyond the Nuortti River drainage basin and lake sedimentation initiated in Loitsana Lake proper (Stage 4).

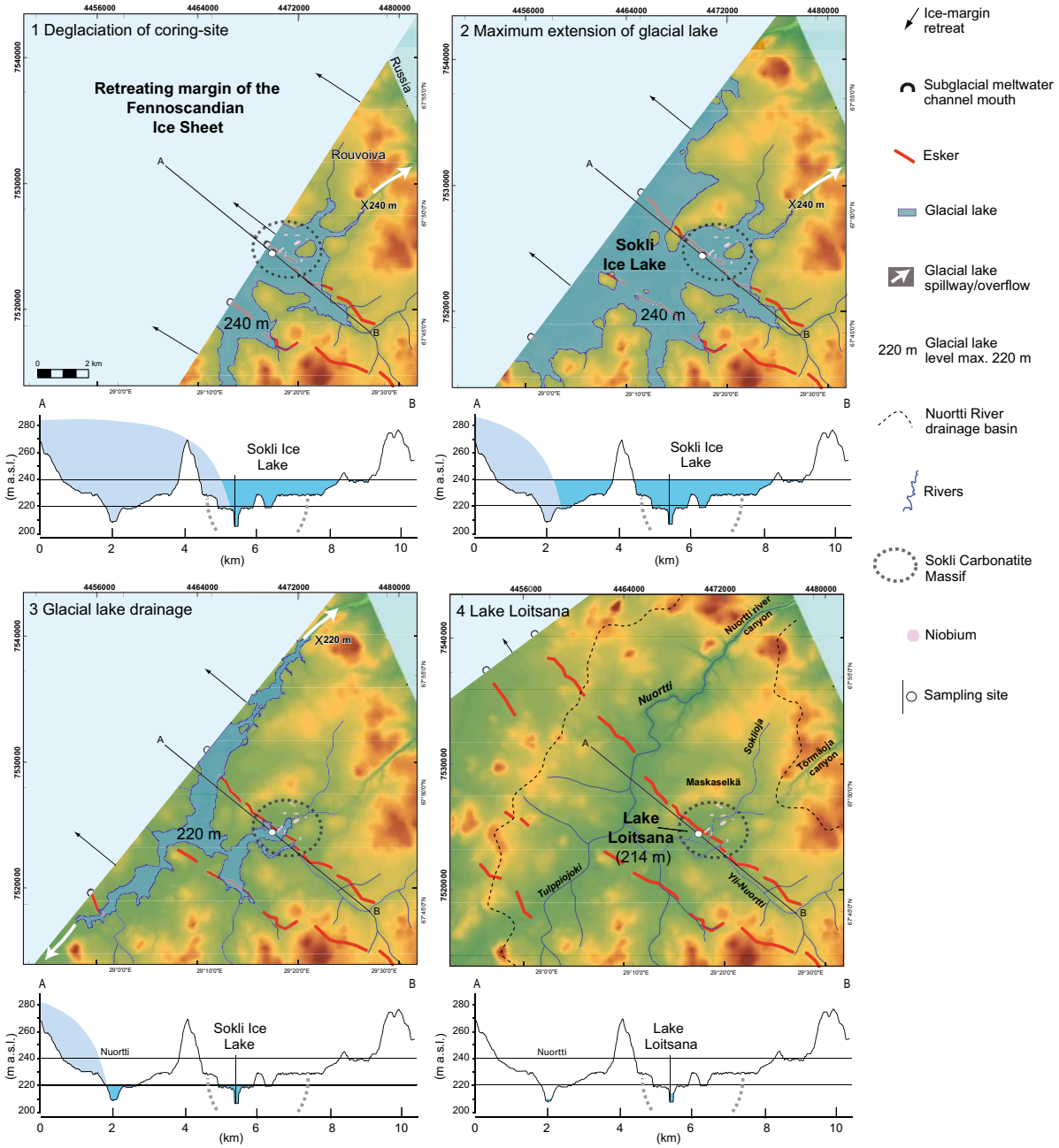

Figure 3-2. *DEM-based reconstruction of glacial-lake evolution at Loitsana during the last deglaciation and development into Loitsana Lake. Three time-slices (Stages 1-3) show the maximum possible extent and depth of the Sokli Ice Lake in the Loitsana area with the ice-margin of the Fennoscandian Ice Sheet positioned at different distances from the coring site. Stage 4 shows Loitsana Lake without influence from the Fennoscandian Ice Sheet. Modified from Shala et al. (2014b).*

3.2.2 Geochemical data

Elemental data obtained through XRF core-scanning has so far not been employed to a great extent in Quaternary environmental reconstructions and as such their potential is not fully explored. Here, we use XRF-based data for the lower two metres of sediment cored in Loitsana Lake (depth interval 900–695 cm) in order to detect catchment changes, through studying variations in the influence of the local bedrock geochemistry within the Loitsana Lake drainage area (Sokli Carbonatite Massif) versus the regional bedrock geochemistry within the glacial-lake drainage area (Precambrian crystalline rocks). Furthermore, geochemical data linked to variations in detrital input of different grain-sizes are explored.

Elements employed for this purpose include Ca, K, Nb, Rb, Si, Sr, S, Ti, Zr and the inc/coh ratio (Figure 3-3). PCA applied on all elements suggests that two factors are representative for the main variations in the geochemical record (Figure 3-3; Table 3-4). The majority of the elements (Ca, K, Rb, Si, Sr, Ti and Zr) as well as the inc/coh ratio are closely related to Factor 1, a process that accounts for more than 70 % of the variability and appears to be distinct in the lower part of the studied sediment succession, that is, in sandy and silty sediments; it generally diminishes in strength above 770 cm. Factor 2, accountable for ca 17 % of the total variability, is mainly coupled to Ca, Nb and S. It is distinct in the lower part (900–795 cm) as well as the uppermost part of the analyzed sequence (i.e. in organic bearing sediment; 735–695 cm).

Factor 1 appears to primarily reflect changes in grain-size related to influx of minerogenic sediment. Sediment geochemistry and particularly the elements Ti, K, Rb, Si, Sr and Zr are recurrently linked to minerogenic input and associated grain-size variations (Koinig et al. 2003, Kylander et al. 2011, Vasskog et al. 2012). Si is generally associated with sand-size fractions of minerogenic input (Kylander et al. 2011), although a biological source is also possible. High values of Si/Ti in the Loitsana Lake sediments are, however, mainly recorded in units with low abundances of siliceous microfossils, suggesting that most of the Si is not of biological origin. The association of Si to sand is further supported by the distinctive peaks in the Si/Ti ratio coupled to sand layers (Figure 3-3). Sr and Zr have both been found to be enriched in medium–coarse silt fractions (Koinig et al. 2003, Vasskog et al. 2012) and can thus be used to infer influxes of silt into the lake. Elemental ratios of Sr/Ti and Zr/Ti display gradually increasing values associated with the upwards-fining sediment sequence, suggesting that both these elements are primarily reflecting changes in grain-size. However, Sr is also related to carbonate weathering and co-precipitation of $SrCO_3$ with $CaCO_3$ during carbonate saturation is common (Cohen 2003, Kylander et al. 2011). The high correlation of Ca/Ti and Sr/Ti in the uppermost part of the studied sequence therefore could be an indication of in-lake precipitation rather than silt influx.

Table 3-4. The rotated factor loadings, squared loadings and communality of factors that explain the major variability of the analyzed sequence. The proportion of each variable's variance allocated to the different factors is indicated by the squared loadings. Squared loadings in bold denote variables that are strongly correlated (> 0.5 of the variance) to a factor; italic characters denote variables that display some correlation (0.1–0.5 of the variance) to a factor.

Factor	Rotated Factor Loadings		Squared Loadings		Communality
	1	2	1	2	
Ti	0.9834	–0.0002	**0.9671**	0.0000	0.9671
Si	0.9449	0.2022	**0.8928**	0.0409	0.9337
S	0.1726	0.8695	0.0298	**0.7560**	0.7858
K	0.9873	0.0524	**0.9748**	0.0027	0.9776
Ca	0.9002	0.3804	**0.8104**	*0.1447*	0.9552
Rb	0.9453	0.0227	**0.8936**	0.0005	0.8942
Sr	0.9587	0.1168	**0.9191**	0.0136	0.9327
Zr	0.9311	0.0118	**0.8669**	0.0001	0.8671
Nb	0.0028	0.8563	0.0000	**0.7333**	0.7333
inc/coh	–0.9450	–0.2118	**0.8929**	0.0448	0.9378
Variance	7.2476	1.7367			
Percent	72.476	17.367			
Cum %	72.476	89.843			

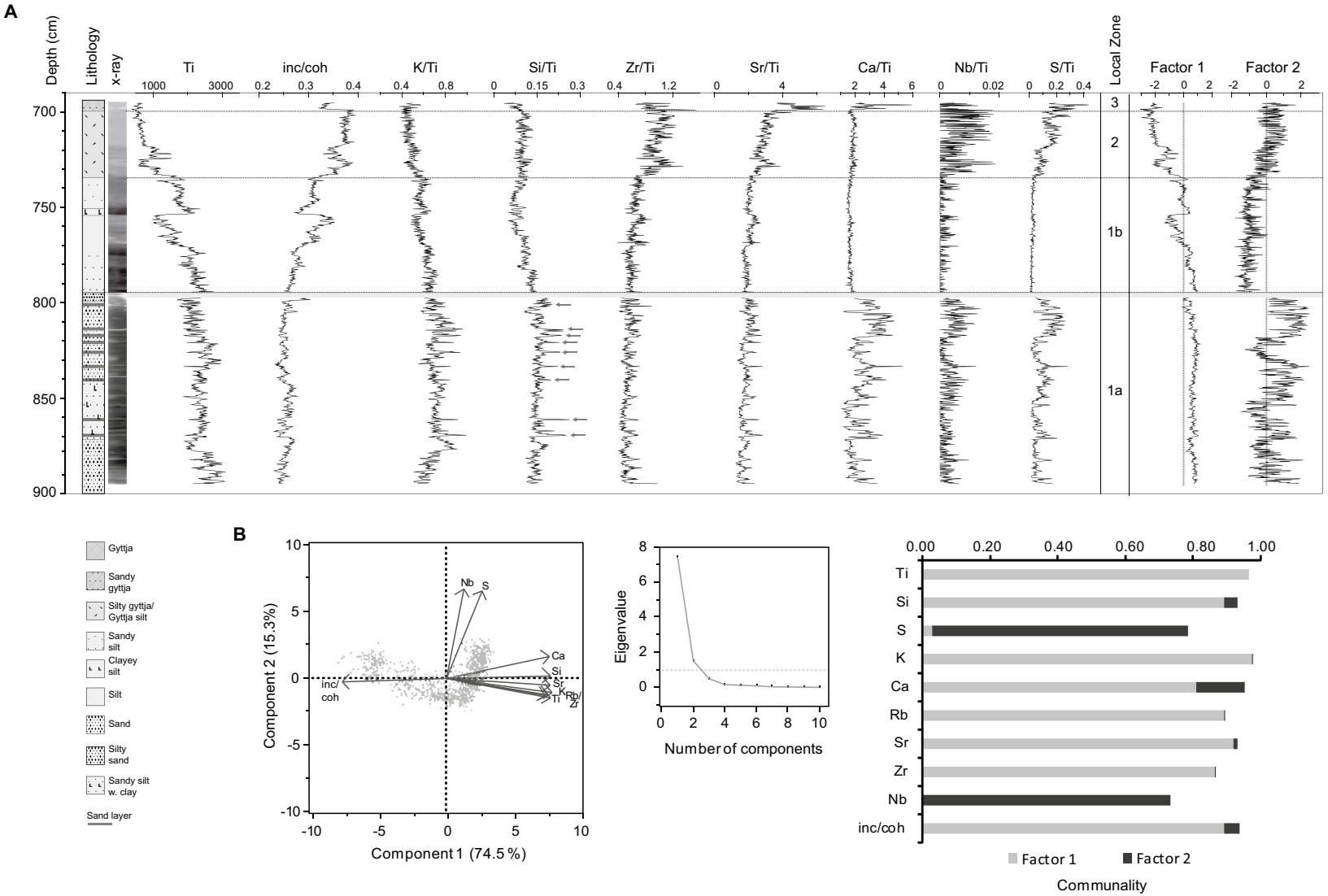

Figure 3-3. ***A*** *Peak areas and elemental ratios of the elements selected for analysis plotted against depth as well as factor-by-depth plot displaying the strength of each factor in the analyzed sediment unit. An X-ray image shows the density of the core (darker → denser). Nine sand layers associated with peaks in the Si/Ti ratio are indicated by arrows.* ***B*** *Principal components analysis plots and communality displaying the major variability and correlations of the analyzed variables. After Shala et al. (2014b).*

The strong association of Factor 2 to elements typical for the Sokli Carbonatite Massif (Nb, S, Ca) suggests that the geochemistry of the local bedrock is also reflected in the geochemistry record of the analyzed sediments. In the organic bearing sediment above 735 cm depth, a deviation from the general trend of these elements is displayed by the Ca/Ti ratio and is attributed to dissolution of Ca through either chemical carbonate weathering or pH changes in the lake (cf. Koinig et al. 2003).

3.2.3 Lithology and chronology

The Loitsana Lake sediment sequence consists of two major lithological units; a lower minerogenic (900–735 cm) and an upper, more organic-rich one (735–0 cm; Figure 3-4). The minerogenic unit consists mainly of upwards fining sands and silts. A transition from the minerogenic to the organic-rich unit at 735–700 cm indicates a gradual change from silt with organic components to silty gyttja. The gyttja in the upper 700 cm shows alternating dark and light-brown layers and intervals with increased sand content at 700–635 cm, 538–535 cm, 377–340 cm and 70–35 cm. Continuous laminations occur from 900 to 538 cm depth but are more distinct above 770 cm and particularly at 575–538 cm.

Two ^{14}C-ages are considered to be too old and are excluded from the age-depth model (Figure 3-4; Table 3-1). We suspect that these samples contained fossil remains of aquatic origin that were contaminated by old carbon as Loitsana is a hard water lake with carbonates in circulation (MacDonald et al. 1991). Sediment accumulation rates range from about 0.2 to 2 mm yr^{-1} but are mainly around 0.8–1 mm yr^{-1} (Figure 3-4). The lowermost sandy sediments (below 760 cm depth) most probably were deposited relatively rapidly, representing a small time-window only. In contrast, the uppermost 180 cm of the Loitsana Lake sequence represents some 5 200 years, indicating a distinctly decreased sediment accumulation rate.

The ^{14}C date obtained at coring site x1 (Figure 2-1) shows that peat deposition replaced limnic sedimentation (gyttja) here at ca 6 560 cal. year BP (Table 3-1).

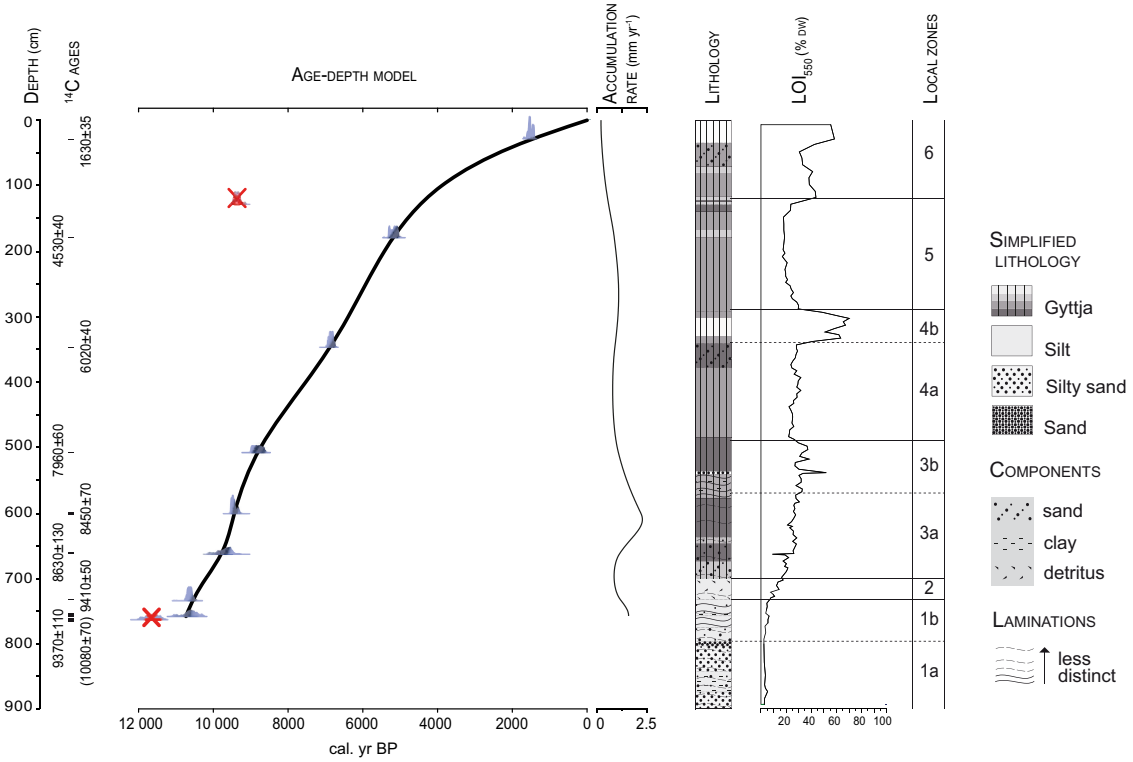

Figure 3-4. *^{14}C-ages, age-depth model (with two rejected dates indicated as outliers), sedimentation rate, lithology and organic content (measured by LOI) for the Holocene Loitsana Lake sequence. Adapted from Shala et al. (2014a).*

3.2.4 Biotic data

Biotic taxa obtained on the Loitsana Lake sequence are presented in Figures 3-5 (compilation of data), 3-6 (selection of diatom taxa), 3-7 (chironomid taxa), 3-8 (other aquatic and wetland taxa) and 3-9 (terrestrial plant taxa). The local zonation (i.e. developments in and close to the lake; local zones 1-6) is applied to the diagrams shown in Figures 3-5 till 3-8, and the regional zonation (i.e. terrestrial vegetation development; zones I-IV) is applied in Figures 3-5 and 3-9. The relation of the local zones 1-6 to the (regional) zones I-IV can be seen in the compilation Figure 3-5; the regional zonation is indicated here to the left and the local zonation to the right. The glacial lake phase at the start of the Loitsana record is highlighted by a blue box in all diagrams. The compilation diagram (Figure 3-5) includes a diatom-based pH reconstruction, as well as species richness curves for both diatoms and chironomids.

Throughout the Holocene, the diatom record (Figure 3-6) is characterized by mass-occurring Fragilariaceae (*Staurosira venter, S. construens, Pseudostaurosira brevistriata, Staurosirella lapponica, S. binodis, Staurosirella pinnata and P. pseudoconstruensas*), which represent more than 90 % of the assemblages. These taxa are generally considered opportunistic and pioneering due to their wide range of ecological preferences and often dominate lakes that have some sort of disturbance (e.g. Lotter et al. 1999, Anderson 2000, Bigler et al. 2003). Their dominance throughout the Loitsana sequence might be related to an alkaline water body and/or disturbances caused by fluvial/minerogenic influx as well as groundwater inflow from the nearby esker.

In Fennoscandia, several plant taxa (including sedges, dwarf birch, Ericales) occur as important elements in both terrestrial (zonal) and wetland (azonal) settings. Pollen of herbs for which a distinct wetland habitat could be inferred (e.g. Cyperaceae), as well as herbs in shore settings (e.g. *Rorippa palustris*) or for which the habitat was undifferentiated (e.g. *Thalictrum*), are given in the lower diagram of Figure 3-9 (“other herbs”). Macrofossils of *Carex* spp., Poaceae, *Salix*, *Betula nana* and Ericales, which can be assumed to have an overall local wetland source, are shown in the aquatic/wetland diagram of Figure 3-8. It should also be stressed that pollen and spores of plants from nearby, local wetland or shore environments (azonal vegetation) are often over-represented in the palynological record and may obscure the signal of the pollen and spore percentage diagram. Therefore, the environmental reconstruction is started with an interpretation of lake phases and azonal vegetation types (Section 3.3) before reconstructing the zonal (regional) vegetation history (Section 3.4).

3.2.5 Quantitative climate reconstructions

Figure 3-10 shows the quantitative T_{jul} reconstructions based on pollen, chironomids and plant indicator taxa according to age. These data are discussed in Section 3.5.

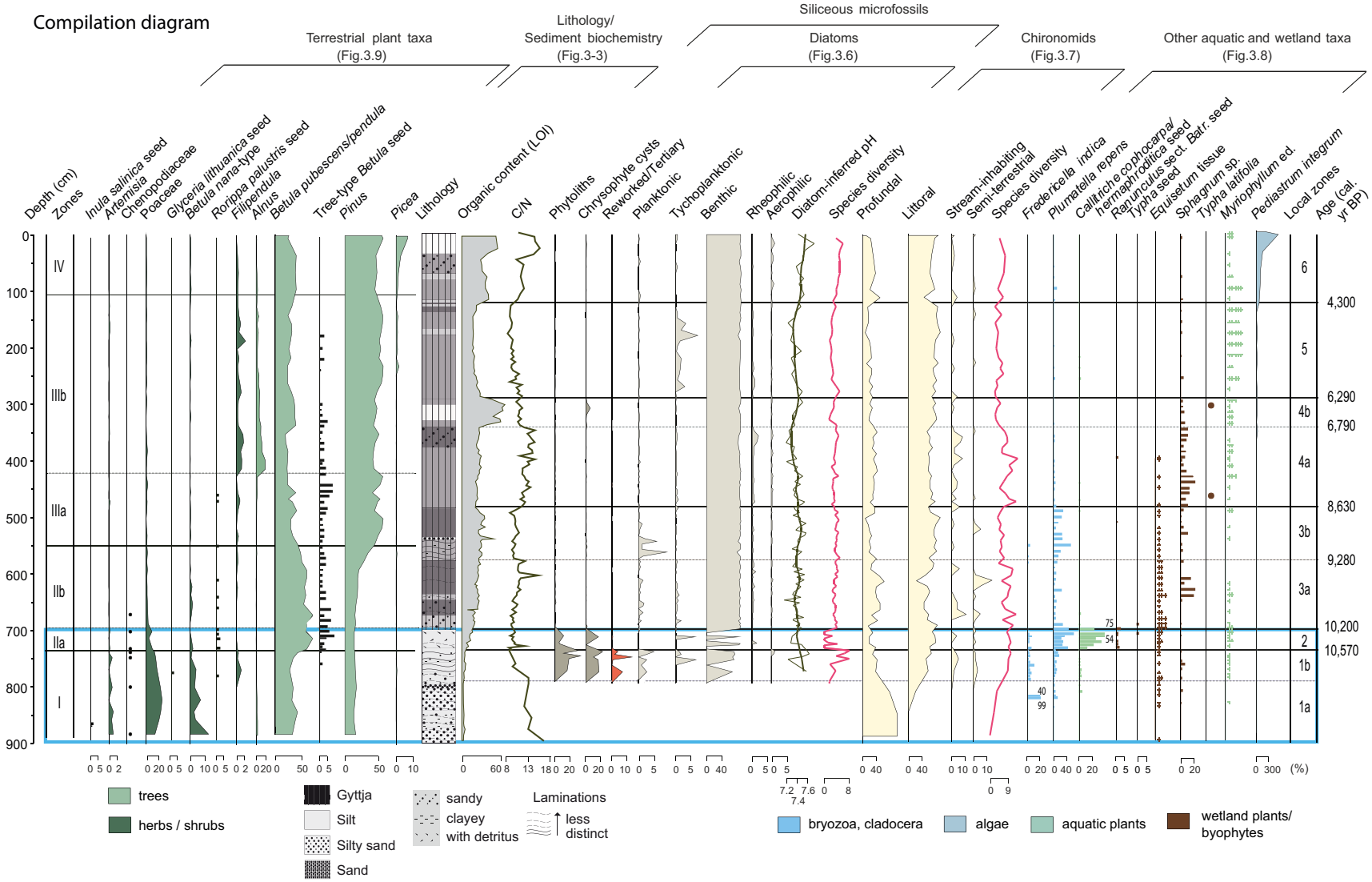

Figure 3-5. *Compilation of proxy data obtained on the 9-m long Holocene lake sediment sequence from Loitsana Lake. In addition to sediment characteristics (lithology, biochemistry), also shown are a selection of fossil remains from both terrestrial and aquatic/wetland plant taxa are shown; groupings of diatoms and chironomids according to living habitat; reworked/Tertiary diatoms, phytoliths and chrysophyte cysts; diatom-based pH reconstruction; and species richness for both diatoms and chironomids. Age estimates for local zone boundaries according to the age-depth model shown in Figure 3-4 are also given. The glacial lake phase at the start of the Loitsana record is highlighted by a blue box. Adapted from Shala (2014).*

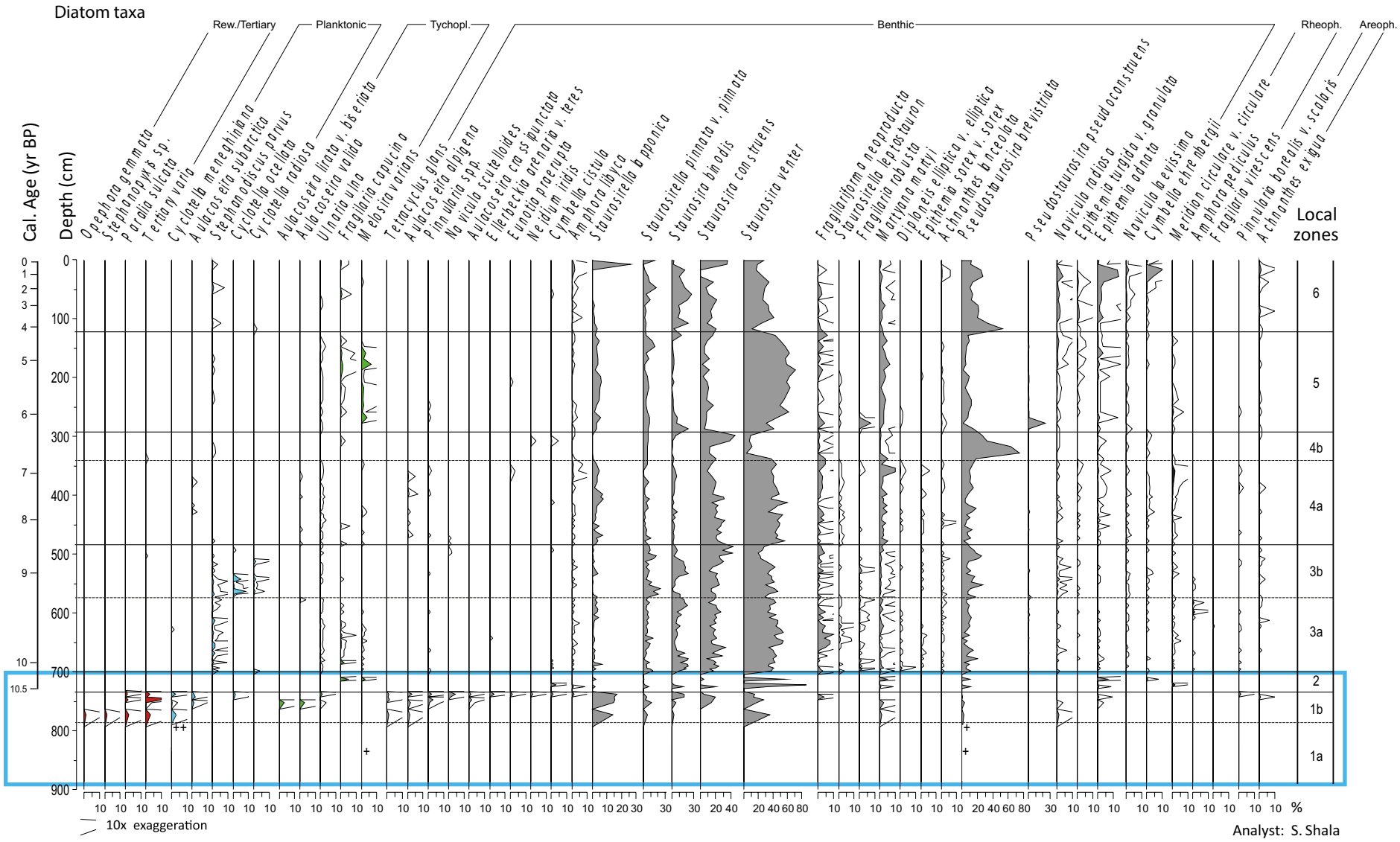

Figure 3-6. *Percentage diagram of diatom taxa which have an abundance of > 1 % in the Loitsana sequence. The taxa are grouped according to living habitat and reworked/ Tertiary taxa. The glacial lake phase at the start of the Loitsana record is highlighted by a blue box. Adapted from Shala et al. (2014a).*

Figure 3-7. *Percentage diagram of chironomid taxa with at least two occurrences of > 2 % abundance in the Loitsana sequence. The glacial lake phase at the start of the Loitsana record is highlighted by a blue box. Adapted from Shala et al. (2014a).*

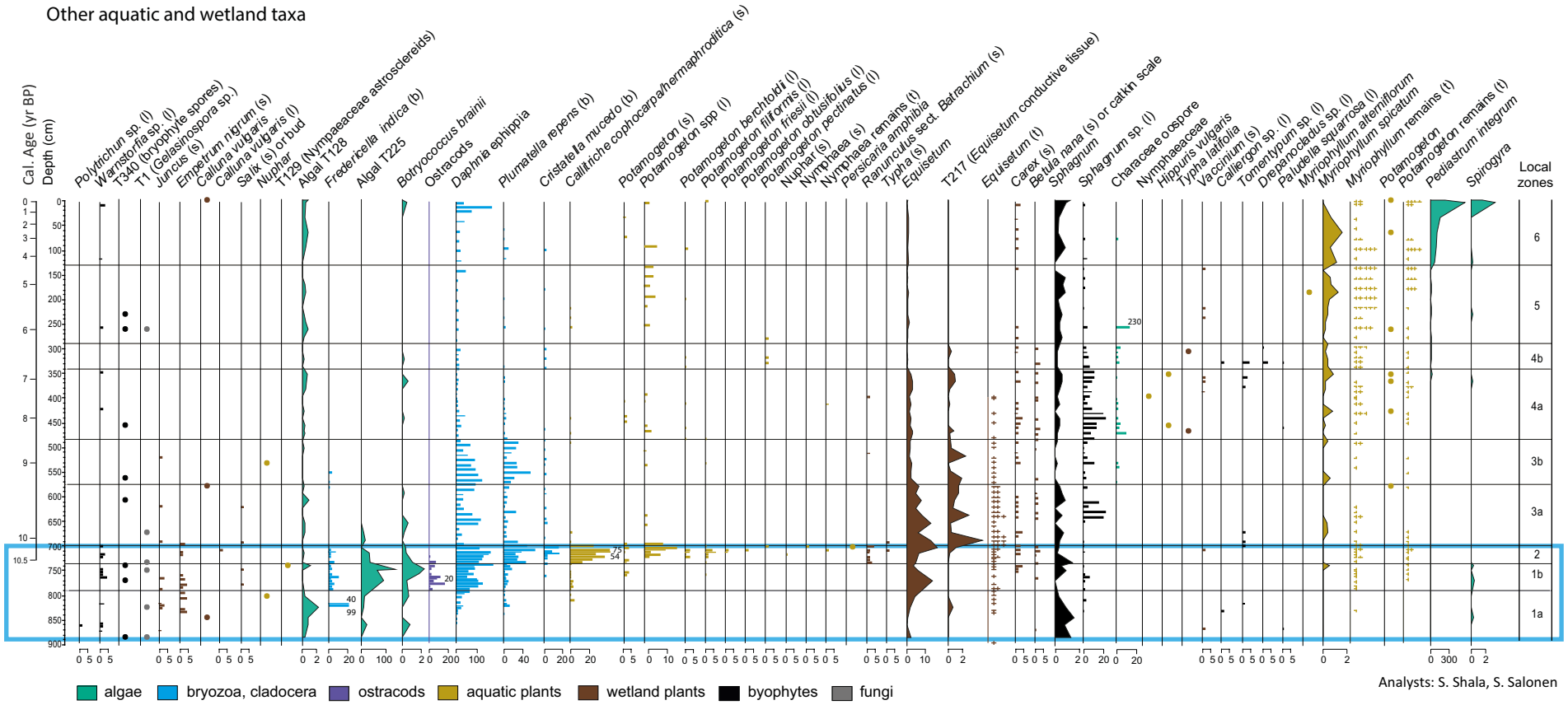

Figure 3-8. *Micro- and macrofossil diagram for aquatics (algae, bryozoa, cladocera, ostracods, aquatic plants) and wetland taxa (bryophytes, fungi, wetland plants) from the Loitsana sequence. Macrofossil results are presented as bars showing concentrations per 10 cm^3 or as relative abundance of tissues and leaf remains, where + = rare (i.e. ≤ 5), ++ = occurring (6-10), +++ = abundant (11-20), ++++ = dominant (21-50), +++++ = the main constituent of the sample. Type of remains are expressed as (b) = bryozoan statoblasts, (l) = leafs, (s) = seeds or (t) = tissue. Microfossils are indicated in percentages where • = < 1 %. The glacial lake phase at the start of the Loitsana record is highlighted by a blue box. Adapted from Shala et al. (2014a).*

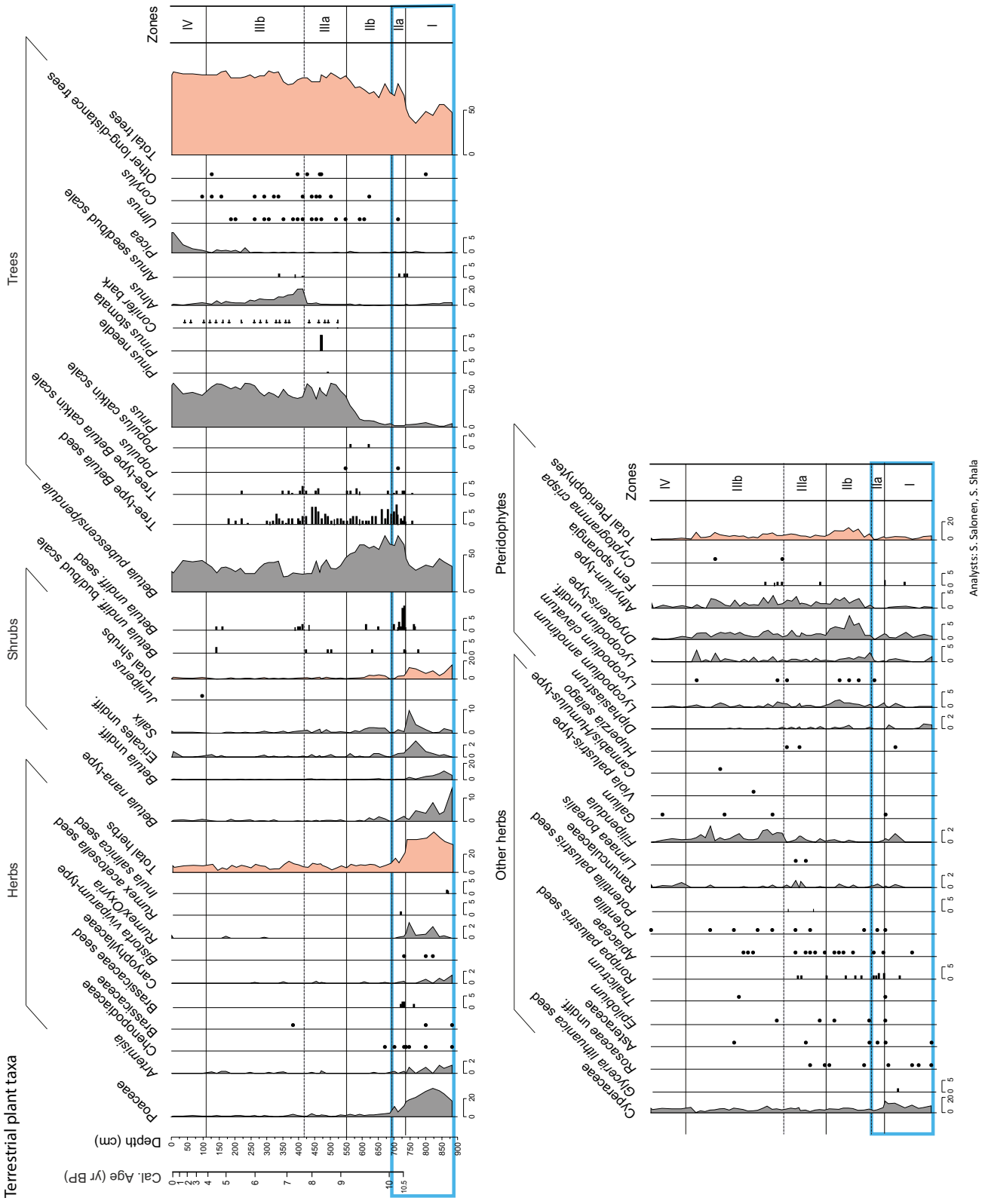

Figure 3-9. *Micro- and macrofossil diagram for terrestrial plants from the Loitsana sequence. For explanation of curves and symbols see Figure 3-8. The glacial lake phase at the start of the Loitsana record is highlighted by a blue box. Adapted from Shala (2014).*

3.3 Holocene lake development

At the start of the Holocene Loitsana record, the combination of the retreating margin of the Fenno-scandian Ice Sheet and the surrounding topography allowed for the formation of a glacial lake that existed at various water depths and surface extensions (local zones 1 and 2). Following the final glacial lake drainage, gyttja started to accumulate in Loitsana Lake proper (transition from local zone 2 to 3). Initially, the lake was fed from the south by the Soklioja riverlet (Figure 2-1), transporting water, sediment and plant fragments from developing wetland to the coring-site (local zones 3 and 4). Fluvial input was temporarily diminished during local sub-zone 3b and a stratified lake water column is registered. Loitsana Lake was an isolated lake, mainly fed by groundwater from the nearby esker chain, during local zones 5 and 6, resulting in progressive sediment infilling at greatly reduced sedimentation rates. The local zones 1-6, which correspond to changes in the local depositional environment, are described in more detail in the following sections.

3.3.1 Local zone 1 (900–735 cm; prior to 10 570 cal. yrs BP)

The sediment and fossil records for local zone 1 show the presence of a relatively large and deep glacial lake in the Sokli/Loitsana basin, surrounded by wetlands with *Empetrum nigrum*, *Calluna vulgaris*, *Juncus*, *Equisetum*, and the bryophytes *Sphagnum* and *Warnstorfia* sp. The timing of deglaciation of the coring-site, which is dated to shortly prior to ca 10 600 cal. yrs BP (Figure 3-5), is in agreement with the early-Holocene deglaciation chronology for northern Finland (Johansson et al. 2011; Figure 3-1). Two local sub-zones (1a and 1b) are distinguished.

Local zone 1a (900–795 cm)

The retreating ice-margin of the Fennoscandian Ice Sheet is interpreted to have been situated near the coring-site during deposition of sediments defined as local zone 1a (900–795 cm; Figures 3-5 till 3-8). This setting corresponds to Stage 1 in the DEM-based glacial lake reconstruction (Figure 3-2). The proximity of the ice-margin to the coring-site, with erosion of local bedrock, is recorded in the input of relatively coarse-grained sandy sediments enriched in elements typical for the Sokli Carbonatite Massif (Ca, S and Nb; Figure 3-3).

The formation of an esker close to the coring-site (Figures 2-1 and 3-2) indicates the proximity of a large input of glacial meltwater and sediment. Turbulent waters in combination with a high influx of sediments, which are typical for proglacial lakes, have been found to significantly decrease primary productivity (Henley et al. 2000) by, for example, creating a shallow photic zone. As diatoms depend on light for their metabolism, this would limit their distribution (Patrick 1977) and explain the very low diatom abundances in local zone 1a (Figure 3-6). Low diatom abundances have also been recorded during times of rapid sedimentation in the Baltic Ice Lake (Kabailiené 1995), Lake Manitoba in Canada (Risberg et al. 1999), and Inari Ice Lake (Figure 3-1; Kujansuu et al. 1998). The disrupted laminations observed in the sediment of local zone 1a further suggest that sedimentation was not associated with quiet-water conditions, most probably due to the close proximity of the ice-margin (Raukas 1994).

The chironomid record of local zone 1a (Figure 3-7) is dominated by *Tanytarsus lugens*-type, i.e. a deep-water taxon (e.g. Engels and Cwynar 2011) associated with cold temperatures and oligotrophic conditions (Brooks et al. 2007), and *Heterotrissocladius maeaeri* which is reported to have dominated the deep waters of the late-glacial Baltic Ice Lake (Luoto et al. 2010).

Local zone 1b (795–735 cm)

The upward-fining sediment of local zone 1b, reflected in the XRF-data by an increase in Sr/Ti and Zr/Ti ratios (silt), and a decreasing Si/Ti ratio (sand), combined with its distinctly laminated character, are indicative of an increasing distance of the ice-margin to the coring-site. The gradually retreating ice-margin of the Fennoscandian Ice Sheet resulted in the formation of a deep and expanding glacial lake and eventually left the coring-site in a confined and relatively sheltered embayment (Stage 2 in the DEM-based glacial lake reconstruction (Figure 3-2)). During this time-interval, the Sokli Massif became submerged in the glacial lake, causing the signal of the massif's elements to become diluted and thus only to be recorded at low intensities.

Rich diatom communities were established dominated by Fragilariaceae, i.e. a group of taxa that are generally considered to be opportunistic and pioneering due to their wide range of ecological preferences. They are often found in lakes that have some sort of disturbance, for example, alpine lakes or, as in this case, recently deglaciated lakes (e.g. Bigler et al. 2003). The presence of heavily silicified planktonic diatoms such as *Aulacoseira subarctica*, *Cyclotella meneghiniana* and *C. ocellata*, which depend on some turbulence to remain in suspension (Reynolds 1993), and the findings of statoblasts from the bryozoan *Fredericella indica*, indicate that some wave action most likely occurred during this time (Økland and Økland 2001). High abundances of pooid grass phytoliths, chrysophyte cysts and reworked/Tertiary diatoms in the sediment reflect prominent shore erosion along the large glacial lake. Lake water conditions appear to have been alkaline with limited organic carbon loading as indicated by the distribution of primarily oligosaprobe – β mesosaprobe diatom taxa such as *Staurosirella binodis*, *Epithemia adnata* and *Navicula scutelloides* (van Dam et al. 1994). The recording of *Tetracyclus glans*, a diatom taxon found to be favored by high Si-content, suggests a relatively high influx and/or availability of nutrients (Michel et al. 2006).

Conditions for aquatic life gradually became more favorable through local zone 1b. This is recorded by distinctly declining C/N values indicating an increase of in-lake productivity. The pioneering planktonic algae *Botryococcus* is increasing registered as well as algal-type 225 (van Geel et al. 1989). The upper part of local zone 1b further shows high percentage values for tychoplanktonic diatom taxa (*Aulacoseira lirata* v. *biseriata* and *A. valida*). The chironomid record shows a sharp decline in *H. maeaeri* and *T. lugens*-type, whereas *Polypedilum nubeculosum*-type (reflecting increased littoral influence and/or warm temperatures) becomes most abundant higher-up in the local zone.

Furthermore, fossil remains of aquatic plants are found (*Myriophyllum, Potamogeton, Callitriche cophocarpa*, Nymphaeaceae), as well as abundant ephippia of the cladoceran *Daphnia* (water flea). Among shore elements, temperate *Glycerina lituanica* is recorded. This grass has a present-day minimum mean July air temperature requirement several degrees higher than the present mean July temperature at Loitsana (see under 3.5). Findings of seeds of tree *Betula* indicate the presence of trees on the surrounding recently deglaciated terrain.

3.3.2 Local zone 2 (735–700 cm; 10 570–10 200 cal. yrs BP)

The progressively retreating ice-margin of the Fennoscandian Ice Sheet eventually reached the Nuortti River canyon. Its subsequent deglaciation allowed for the opening of a spillway and caused a lowering in the glacial lake level by several tens of metres, resulting in a shallower, smaller and less turbulent glacial-lake stage (local zone 2 or Stage 3 in the DEM-based glacial lake reconstruction (Figure 3-2)). Enhanced values of S and Nb are recorded in the sediment of local zone 2, and are expected since the Sokli Carbonatite Massif emerged from the water. According to our age–depth model, local zone 2 lasted around 400 years. According to Johansson (2007), the existence of the even larger Sokli Ice Lake (Figure 3-1) lasted less than 100 years in total. Considering the ca 50–100 year error margins on the radiocarbon dates (Table 3-1), as well as the large spread in calendar ages for this early part of the Holocene (Figure 3-4), a more detailed age estimation for the duration of the glacial lake phases in the Sokli/Loitsana basin, using the ^{14}C dating method, is not possible.

The drop in lake level most probably left the silty glacial lake-shore deposits exposed to erosion, as well as the nearby esker ridges, resulting in a temporarily increased input of fine-grained sediment into the lake. Increased input of silts is reflected in enhanced Sr/Ti and Zr/Ti ratios during local zone 2. This would have resulted in a high amount of suspended sediment in the glacial lake water, which in turn could explain the sharply decreasing diatom species diversity, and low diatom abundances, recorded in this local zone. The diatom assemblage is dominated by benthic *Staurosira venter, s*howing peak values reaching 86 %. This pioneering diatom species has the ability to adapt to rapidly changing environments and tolerates poor light conditions in, for instance, turbid waters (Haworth 1976). Occurrences of other benthic diatom taxa (e.g. *Amphora libyca*, *Cymbella ehrenbergii*, *Epithemia adnata, Melosira varians*) indicate meso-eutrophic lake water conditions with elevated conductivity (Krammer and Lange-Bertalot 1986, 1988, 1991a, b, van Dam et al. 1994).

Moreover, the drop in lake level during local zone 2 placed the glacial lake shore closer to the coring-site (see also Figure 2-1). A closer proximity of shore to coring-site has been shown to significantly increase the amount of macrofossils in lake sediments (Hannon and Gaillard 1997, Väliranta 2006,

Helmens et al. 2009), which is also recorded at the transition from local zone 1 to 2. Macrofossils are found in high abundances in local zone 2 and indicate the presence of diverse aquatic and wetland ecosystems. Aquatic plants included *Callitriche cophocarpa*/*hermaphroditic,* a large variety of, mostly narrow-leaved, *Potamogeton* species (*P. berchtoldii, P. filiformis, P. friesii, P. obtusifolius, P. pectinatus*), *Myriophyllum*, *Nuphar*, *Nymphaea* and *Persicaria amphibia*. Wetlands included, among others, the plants *Ranunculus* sect. *Batrachium*, *Typha*, *Carex* and *Equisetum*. The majority of *Potamogeton* species found in the sediment of local zone 2 thrive in shallow waters and require nutrient-rich lake water conditions. Also *Typha* points to an enhanced tropic status. It is the silts that probably provided the nutrients, allowing rich aquatic and wetland communities to establish.

Plumatella repens and *Cristatella mucedo* and are also well-represented in the macrofossil record, as well as *Daphnia*. The high abundances of resting spores of the bryozoa *P. repens* and *C. mucedo* suggest that pelagic conditions occurred nearby the coring-site, as these bryozoa prefer relatively large water bodies (usually > 2500 m^2, Økland and Økland 2000, Økland et al. 2003). Furthermore, *C. mucedo* prefers more colored water with less wave action than *F. indica* which is recorded more abundantly in local zone 1 (Økland and Økland 2000, 2005). The presence of *Cristatella* (Økland and Økland 2000) and Nymphaeceae (Aalbersberg and Litt 1998) points to a boreal environment rather than a sub-arctic one in this lowermost part of the Loitsana sequence. Like *Glycerina lituanica* (local zone 1), the wetland plant *Typha* currently has considerably more southern distributions in Finland (Lampinen and Lahti 2007).

3.3.3 Local zone 3 (700–490 cm; 10 200–8 630 cal. yrs BP)

Following the final glacial lake drainage, sedimentation at the coring-site continued in the small Loitsana depression (local zone 3 or Stage 4 in the DEM-based glacial lake reconstruction (Figure 3-2)), and gyttja started to accumulate. Organic content of the sediment steadily rises throughout local zone 3, from ca 15 % at the base to ca 35 % near the top. Characteristic are the near continuous registrations of planktonic *Stephanodiscus parvus, Chironomus plumosus*-type*, P. repens*, *Daphnia*, and *Equisetum* fossil remains.

The presence of the (hyper-) eutrophic diatom species *S. parvus*, and the eutrophic chironomid taxon *C. plumosus*-type, indicate a significantly enhanced trophic state. This might be the result of morphometric eutrophication (Hofmann 1998), i.e. a condition created by a reduction in lake water volume. Here, it is probably related to the glacial lake drainage, resulting in the small, relatively shallow Loitsana Lake. Two local sub-zones (3a and 3b) are distinguished.

Local zone 3a (700–570 cm; 10 200–9 280 cal. yrs BP

The diatom abundance and species diversity increase drastically at the transition to local zone 3a. Alkaline water conditions continued to govern, and an increased abundance of diatom taxa with higher saprobity (e.g. *Epithemia sorex, Melosira varians*) indicates slightly enhanced organic-carbon loading (van Dam et al. 1994). Occurrences of rheophilic and aerophilic diatom taxa, as well as stream-inhabiting and semi-terrestrial chironomid taxa, indicate inflow of water into the lake, which is further supported by a sandy lithology and relatively high abundances of *Staurosirella leptostauron,* i.e. a diatom species often found growing attached to sand grains. It is probable that also the macroremains of *Equisetum, Sphagnum, Carex* and *Betula nana* were transported from nearby wetland by flowing water.

The presence of chironomid taxa such as *Cricotopus cylindraceus*-, *Psectrocladius sordidellus*- and *Microtendipes pedellus*-type in local zone 3a suggest high summer temperatures at the study site (Brodersen and Lindegaard 1999, Porinchu and MacDonald 2003).

Local zone 3b (570–490 cm; 9 280–8 630 cal. yrs BP)

Decreasing values for stream-inhabiting and semi-terrestrial chironomid taxa, as well as wetland plant taxa (*Equisetum, Sphagnum, B. nana*), indicate a temporal reduction in flowing water to close to the coring-site during local zone 3b.

The occurrence of distinct sediment laminations in the lower half of local zone 3b suggests that the lake had become stratified with anoxic bottom water conditions. Lake stratification is also suggested by high abundances of the planktonic diatom taxa *Cyclotella ocellata* and *C. radiosa* (Saros et al. 2014). A sharp increase in representation of *P. repens* and *Daphnia* might reflect elevated lake productivity, as supported by low C/N values. High abundances of the mesotrophic chironomid taxon *Cladotanytarsus mancus*-type, and decreasing values for *S. parvus*, suggest a slight reduction in trophic state compared with local zone 3a.

3.3.4 Local zone 4 (490–290 cm; 8 630–6 290 cal. yrs BP)

Characteristic for local zone 4 is the distinct decrease in representation of planktonic diatom taxa, most probably reflecting decreasing lake water depths caused by sediment infilling. A shift in trophic state from meso-/eutrophic in local zone 3b to oligo-/mesotrophic conditions in local zone 4 is recorded by the chironomid assemblage (*Microtendipes pedellus*-type, *Corynocera oliveri*-type*, C. ambigua,*) and low occurrences of eutrophic diatoms. Two local sub-zones (4a and 4b) are distinguished.

Local zone 4a (490–340 cm; 8 630–6 790 cal. yrs BP)

Significant inflow of running water to close to the coring-site is indicated by enhanced values for both rheophilic diatom and stream-inhabiting chironomid taxa as well as macrofossil remains of wetland plants.

The increased representation of the bryophyte *Sphagnum*, and decreasing values for *Equisetum*, most probably point to an advanced stage of wetland development related to progressive terrestrialization of the lake area just south of present-day Loitsana Lake (Figure 2-1). Among wetland plants, also temperate *Typha* is recorded. Furthermore, the aquatic plants *Myriophyllum*, *Potamogeton, Hippuris vulgaris and Nymphaeaceae* are registered.

Local zone 4b (340–290 cm; 6 790–6 290 cal. yrs BP)

Local zone 4b is characterized by an abrupt increase in organic matter to 50–70 %. A sharp increase in organic detritus was noted during macrofossil analysis. It is during this time interval (at 6 627–6 486 cal. yrs BP) that the deposition of gyttja was replaced by accumulation of peat at coring-site x1 directly south of the Loitsana Lake coring-site (Figure 2-1). Relatively high lake water transparency during local zone 4b is suggested by a distinct rise of oligosaprobic *Pseudostaurosira brevistriata* and higher abundances of Characeae oospores. The chironomid taxa *C. ambigua* and *Dicrotendipes pulsus*-type, which are relatively abundant during local zone 5, start their high representation at the base of local zone 4b. Also, C/N starts to decline here.

3.3.5 Local zone 5 (290–120 cm; 6 290–4 300 cal. yrs BP)

Progressive lake infilling is recorded by a distinct representation of tychoplanktonic diatom taxa during local zone 5. Characteristic also is the high representation of aquatic plants (*Myriophyllum*, including *M. spicatum*, and *Potamogeton*). *M. spicatum* is a submerged plant that today grows in nutrient-rich waters (Mossberg and Stenberg 2003). The chironomid taxon *C. ambigua,* which shows high values throughout local zone 5, has a complex ecology (Brodersen and Lindegaard 1999), but has been found to prefer habitats with abundant vegetation (Mothes 1968) and, in this record, seems to be associated with the increasing amounts of *Myriophyllum*.

Macrofossil remains of wetland plants are no longer recorded in large quantities during local zone 5; neither are diatoms or chironomids related to flowing water. Peatland expansion south of Loitsana Lake most probably inhibited further inflow of water from the Soklioja rivulet. With a strong reduction in river influx, sediment accumulation rates in Loitsana Lake significantly declined during local zone 5 (Figure 3-4).

3.3.6 Local zone 6 (120–0 cm; 4 300 cal. yrs BP-present)

Lake infilling continued and is reflected in an increase of aerophilic diatom taxa and the findings of *Carex* macrofossils originating from expanding wetland around the lake. Increasing values of oligosaprobic diatoms (e.g. *P. brevistriata*) and a sharp increase in the algae *Pediastrum integrum* during local zone 6 might reflect a water body with low DOC content. Many *Pediastrum* taxa have a wide ecological span; however, Weckström et al. (2010) found *P. integrum* to have a low DOC optimum. It is probable that, at this point, the lake was mostly groundwater-fed with water from the adjacent esker ridges.

Meso-eutrophic lake water conditions during local zone 6 are suggested by the macrofossil assemblage (*Potamogeton* and *Myriophyllum* remains), diatom taxa (*Cymbella ehrenbergii*, *Epithemia adnata*, *Navicula radiosa*) and chironomid assemblage (*Cladotanytarsus mancus*-type, *Tanytarsus mendax*-type).

3.4 Holocene terrestrial vegetation development

Four zones (I-IV) are distinguished and correspond to changes in the regional vegetation.

3.4.1 Zone I (prior to 10 570 cal. yrs BP)

The pollen assemblage of zone I is dominated by grasses (*Poaceae*; 30 %) and tree birch (*Betula pubescens/pendula*; 40 %) (Figure 3-9). Other herbs that are registered, at low percentage values, include heliophilous (light-demanding) *Artemisia*, Chenopodiaceae, Brassicaceae, Caryophyllaceae, *Polygonum bistorta*-type, and *Rumex/Oxyria*. *Inula salicina,* an "alvar" element (see Section 4.5), is represented in the macrofossil record (Figure 3-9). Among shrubs, dwarf birch (*B. nana*) is well-represented at the base of the zone, and *Salix* at the top.

The vegetation in the Loitsana area during zone 1 was open. Seeds of tree birch, and pollen values of up to 40 % for *B. pubescens/pendula*, indicate the presence of birch trees on the recently deglaciated terrain. Zone 1 corresponds to the deep glacial lake stages (Stages 1 and 2 in Figure 3-2) distinguished at the base of the Loitsana Lake sequence (local zone 1 in Figure 3-5). High abundances of pooid phytoliths in the glacial lake sediment reflect prominent shore erosion. Furthermore, the finding of a seed of *Glycerina lituanica* indicates the local presence (i.e. along the shore) of grasses. Therefore, Poaceae might be over-represented in the pollen assemblages of zone 1, masking a holistic picture of the terrestrial vegetation. Based on this, it cannot be excluded that the deep glacial lake was bordered by open birch forest.

3.4.2 Zone II (10 570–ca 9 200 cal. yrs BP)

The presence of birch forest in the Loitsana/Sokli area is clearly registered during zone II, by pollen percentage values for *B. pubescens/pendula* reaching 70–80 % and high abundances of seeds of tree birch. Light-demanding herbs are still registered, particularly in the pollen assemblage of zone IIa. Ferns (*Athyrium*, *Dryopteris*-type) and lycopods (particularly *Lycopodium annotinum*) are well-represented in zone IIb.

3.4.3 Zone III (ca 9 200–4 000 cal. yrs BP)

The establishment of pine-birch forest is recorded at the base of zone III. The presence of pine trees is not only indicated by high pollen percentage values for *Pinus* (up to 80 %), but also by findings of conifer bark remains in the sediment. Zone III is further characterized by a near continuous registration of long-distance transported pollen of deciduous *Corylus* and *Ulmus.*

The transition from zone IIIa to IIIb, i.e. in the middle part of the Loitsana sequence, corresponds to a distinct increase in pollen of alder (*Alnus*) as well as the herb *Filipendula*. Both plants thrive in moist habitats. On the contrary, the herb *Rorippa palustris*, which is near continuously recorded in the lower half of the Loitsana sequence (Figure 3-5), is a pioneer shore element occurring on nutrient-rich, mineral soils that fall dry in summer. The rise in *Alnus* and *Filipendula* furthermore coincide with a

sudden decrease in macrofossil remains of *Equisetum* and increase in macrofossils of *Myriophyllum*. It is therefore most likely that that the rises in *Alnus* and *Filipendula* pollen percentages at the base of zone IIIb are related to local dynamics (lake/wetland development) allowing the creation of moist habitat suitable for these plants.

3.4.4 Zone IV (ca 4 000 cal. yrs BP-present)

The establishment of boreal forest with spruce (*Picea*) pollen is recorded during zone IV. Percentage values of 27 % for birch, 56 % for pine and 6.7 % for spruce in the uppermost sample are consistent with values recorded in surface lake samples from the Finnish northern boreal forest, with the core top values falling within the range of variation found for the same taxa in the near-most surface samples used in our modern calibration data.

3.5 Holocene temperature evolution

3.5.1 Pollen-based mean July air temperature (T_{jul}) reconstruction

The reconstructed pollen-based T_{jul} (Figure 3-10) shows a distinct increase in the order of ca 3 °C (i.e. from ca +11.5 to +14 °C) in the time interval 9 500 till 7 000 cal. yrs BP, after which it remains at values slightly higher than the current T_{jul} (+13 °C) until present. The compositional distance between each fossil sample and the best-matching calibration sample overall increases with increasing age (Figure 3-10). Cross-validation statistics for the pollen-based calibration model are good (Table 3-3).

The poorest fit between fossil pollen assemblages and modern analogues are recorded at the very base of the lake sequence (zone I). This zone is characterized by high pollen percentage values for both tree birch (*B. pubescens/pendula*) and grasses (Poaceae). High abundances of pooid phytoliths in the sediment, however, point to a local (azonal) presence of grasses, i.e. in shore habitats along the glacial lake, explaining the poor compositional fit between the fossil samples and modern analogues. Similarly, the macrofossil record suggests a local wetland source for the pollen/spores of sedges (Cyperaceae) and *Equisetum* in zone II.

The lakes that form part of the calibration set have been carefully chosen, e.g. avoiding lakes with extensive littoral vegetation, in order to provide pollen assemblages that as best as possible reflect the regional (zonal) vegetation. Since Poaceae, Cyperaceae as well as *Equisetum* are common in surface samples from lakes situated in the tundra, the reconstructed T_{jul} for zones 1 and 2 can be expected to under-estimate the true T_{jul} at Loitsana during this earliest part of the Holocene (i.e. prior to ca 9 000 cal. yrs BP).

Although the compositional fit overall decreases from the base of zone 3 upwards, a relatively poor fit is recorded around ca 7 500 cal. yrs BP. This poor fit observed in the mid-Holocene appears to be associated to high *Alnus* pollen percentage values. Since *Alnus* has a preference for moist habitats (Mossberg and Stenberg 2003), which creation at Loitsana might have been driven purely by local factors (see Section 3.4), *Alnus* is most probably over-represented in the mid-Holocene samples, explaining the poor compositional fit between fossil and analogue samples.

The near +14 °C T_{jul} reconstructed between ca 8 000 and 4 000 cal. yrs BP are most probably driven by the occurrences of pollen from deciduous trees (e.g. *Ulmus*, *Corylus*), occupying more northern locations than their presently distribution in southern Finland.

3.5.2 Minimum T_{jul} reconstruction using plant indicator taxa

A variety of mostly aquatic and wetland plant taxa has been used to estimate minimum T_{jul} (Figure 3-10) including Nymphaeaceae (+12 °C); narrow-leaved *Potamogeton* spp. and *Callitriche cophocarpa* (+13 °C); and *Typha* and *Glyceria lithuanica* (+15 °C; Table 3-2). These so-called plant indicator species/taxa require a specific minimum T_{jul} in order to flower and reproduce (e.g. Iversen 1954, Kolstrup 1979). Fossil remains of Nymphaeaceae and *Typha* were encountered both in the microfossil and macrofossil analysis. Narrow-leaved *Potamogeton, C. cophocarpa* and *G. lithuanica* were identified by their macrofossils.

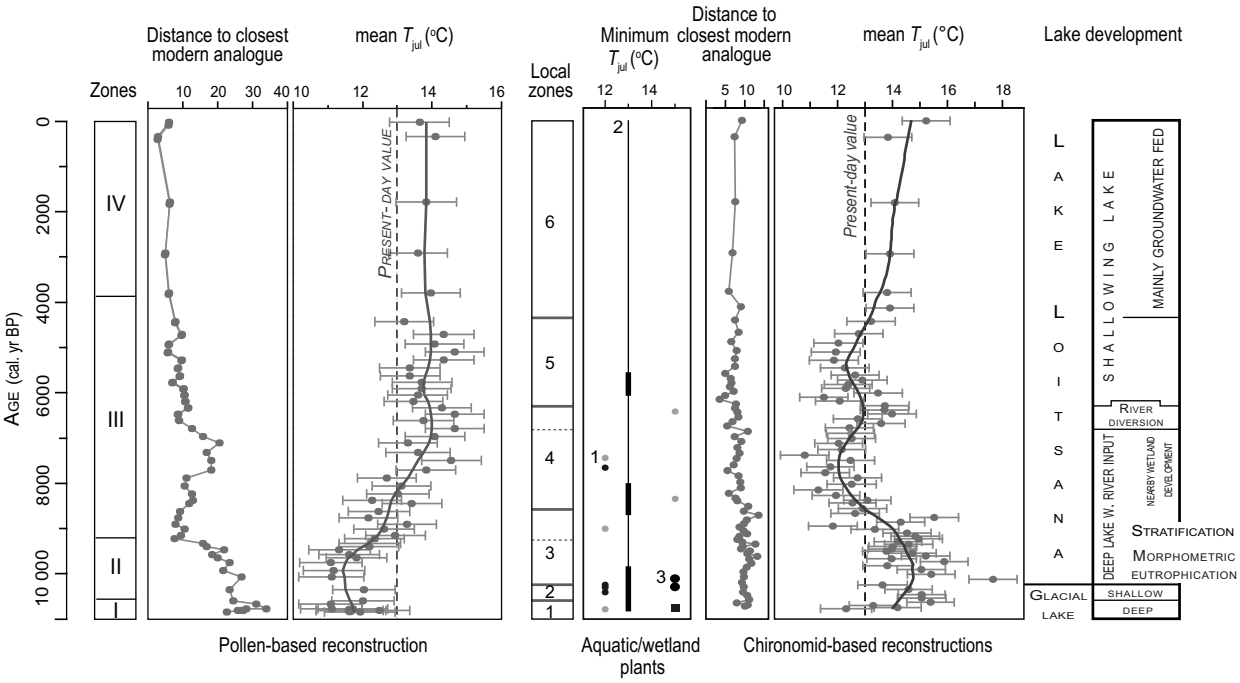

Figure 3-10. *Pollen- and chironomid-based T_{jul} reconstructions using the transfer function approach (with LOESS smoother, span 0.25, one robustifying iteration), and distances to closest modern analogues, and min. T_{jul} based on plant indicator species from the Loitsana sequence, indicated according to age. The plant indicator taxa used to infer min. T_{jul} are 1 = Nymphaeaceae (+12 °C), 2 = narrow-leaved Potamogeton spp and Callitriche cophocarpa (+13 °C), and 3 = Glyceria lithuanica and Typha (+15 °C). Macrofossil remains are given in black whereas grey color represents microfossil occurrences. The relative abundance is indicated with different line thickness; thin line = occurring, medium line = moderate, thick line = abundant. A summary of Holocene lake development at Loitsana is indicated at the right side of the figure. Adapted from Shala (2014).*

Macrofossils (e.g. seeds) can be taken as evidence for the local presence of the plant taxa, i.e. in or relatively close to the paleo-lake. Findings of macrofossil remains in lake sediments, however, are strongly influenced by taphonomic factors, such as distance to the shore, water depth and inflow of streaming water to close to the coring-site. Therefore, the absence of e.g. seeds in a sample cannot be used to infer absence of plants in the contemporary vegetation. Although pollen can have been transported over long distances by wind, pollen dispersal of aquatic and wetland plants is generally considered to be restricted and, for instance, *Typha latifolia* has been found to have a highly localized dispersal (Birks and Birks 2000, Ahee 2013). We can therefore assume that the plant indicator taxa used in this study were locally present, i.e. in or along Loitsana Lake, and, when encountered in a sample, provide an estimate of min. T_{jul}.

Min. T_{jul} of +15 °C is inferred, based on the presence of *Typha* and *G. lithuanica*, right from the start of the Loitsana record till ca 6 000 cal. yrs BP (Figure 3-10). T_{jul} values of minimum +10–13 °C, in about the same time interval, are indicated by the aquatic plants Nymphaeaceae, narrow-leaved *Potamogeton* spp. and *C. cophocarpa*.

3.5.3 Chironomid-based T_{jul} reconstruction

The reconstructed chironomid-based T_{jul} (Figure 3-10) rapidly increases from around +12 to ca +15 °C in the earliest part of the Holocene, and remains high (i.e. above present-day values) till about 9 000 cal. yrs BP. Below present-day T_{jul} is reconstructed between ca 9 000–5 000 cal. yrs BP, interrupted by a brief time interval (around 6 500 cal. yrs BP) during which the current T_{jul} at +13 °C is approached. T_{jul} increases to slightly higher than-today values in the uppermost part of the sequence (after ca 5 000 cal. yrs BP). The squared-chord distance of each fossil sample to the closest modern analogue is generally small, though there appears to be a tendency to a somewhat decreasing fit with increasing age (Figure 3-10). Cross-validation statistics suggest that the model is robust (Table 3-3).

The low T_{jul} reconstructed at the very base of the sequence appears to be related to the cold- and deep-water taxa *Heterotrissocladius maeaeri* and *Tanytarsus lugens*-type, which dominated the early part of the deep glacial lake phase (Stage 1 in Figure 3-2; local zone 1a in Figures 3-5 and 3-7) at Loitsana. The low water temperature was most probably decoupled from air temperature, causing an under-estimation of the true T_{jul} at Loitsana during this earliest part of the Holocene.

High T_{jul} values, which are already recorded near the end of local zone 1, rise further during local zone 2 (shallow glacial lake phase), and peak during the earliest part of gyttja deposition in Loitsana Lake proper (local zone 3). Chironomid taxa that appear to drive the high T_{jul} in this part of the Loitsana sequence also have a preference for nutrient-rich (*Polypedilum nubeculosum*-, *Cricotopus cylindraceus*-, *Psectrocladius sordidellus*-types) and shallow lake/littoral conditions (*P. nubeculosum*-type). However, since *P. nubeculosum*-type is also recorded in local zone 1a (i.e. the deep glacial lake phase), and is still registered during local zone 3b (i.e. where decreasing values for the eutrophic diatom species *Stephanodiscus parvus*, and increasing values for the meso-oligotrophic chironomid taxa *Cladotanytarsus mancus*- and *Corynocera oliveri*-type, indicate a decrease in trophic state), it is possible that at least *P. nubeculosum*-type responded to high July air temperatures at the site.

The low T_{jul} values (< +13 °C) reconstructed for local zones 4 and 5 (between ca 9 000–5 000 cal. yrs BP) appear to be driven by high occurrences of *Corynocera ambigua* and *C. oliveri*-type. The former has the third lowest WA-optima of all dominating taxa in the c-set and the latter has the lowest optima with a value of +10.6 ±1.4 °C (see Shala 2014). *C. ambigua*, however, is known to have a complex ecology (Brodersen and Lindegaard 1999) and appears, in the Loitsana record, to be favored by macrophyte density (*Myriophyllum*). Though generally considered a cold indicator, the stenotherm *C. oliveri*-type has also been found in warmer lakes (Palmer et al. 2002), as well as in lakes with high DOC concentrations (Gajewski et al. 2005, Medeiros and Quinlan 2011), and might be driven here by high DOC values (local zone 4a).

The most recent rise in T_{jul} values, from ca 500 cal. yrs BP and onward, appears to be driven by increased abundances of warm-indicating *Cladotanytarsus mancus*- and *Tanytarsus mendax*-types (Eggermont and Heiri 2012), which, however, also have a preference for shallow waters and nutrient-rich conditions (Brooks et al. 2007, Luoto 2011). It is possible that these taxa responded to the advanced stage of shallowing (/infilling) of the lake.

3.6 Discussion

The multi-proxy analysis of the Loitsana Lake sequence from north-eastern Finland has allowed us to trace in great detail changes in environmental and climate conditions for a site in the present northern boreal zone of Fennoscandia during the Holocene (last ca 11 kyr). The use of multiple proxies has resulted in comprehensive environmental reconstructions and has reduced uncertainties that are inherently related with the analysis of single proxies. Also, it has facilitated discrimination between local factors (i.e. acting at the catchment level), or site-specific factors (e.g. nearby wetland expansion), from regional factors (climate) driving the proxies. Furthermore, the study by Shala (2014) shows that proxy response might be highly individualistic, making the use of multi-proxy analysis even more important.

Comprehensive understandings of the various environmental factors controlling Holocene lake development and fossil assemblages also provide a more reliable basis for preparing and evaluating paleo-climate reconstructions. The reliability of quantitative climate reconstructions prepared with proxy-based transfer functions is increasingly debated (Anderson 2000, Birks et al. 2010, Juggins 2013) and, while it is generally acknowledged that the identification of local events and the separation of driving agents is essential for the evaluation of proxy-based climate reconstructions (Velle et al. 2005, 2010, 2012), detailed reconstructions of lake histories, to explicitly evaluate the influence of such local effects and complex environmental drivers on the proxy records, are few and far-between.

The Loitsana Lake sequence records a shallowing lake with four local events that had major impact on the Holocene sedimentation dynamics, water chemistry and the composition of biotic assemblages. These events are 1) the evolution of the latter phase of the Sokli Ice Lake prior to ca 10 200 cal. yrs BP; 2) the drainage of the glacial lake and initiation of Loitsana Lake; 3) changes in fluvial input due to nearby, progressive wetland expansion (terrestrialization); and 4) continuous infilling of the lake

which eventually resulted in a shallow and groundwater-fed lake after ca 4 300 cal. yrs BP. Although lake development was complex, a combination of events as recognized at Loitsana can be expected to have influenced the Holocene development of many lakes in the formerly glaciated boreal zone of northern Europe.

3.6.1 Environmental conditions at the moment of deglaciation

Although the extent of glacial lakes impounded between the retreating margin of the Fennoscandian Ice Sheet and the surrounding higher topography during the early-Holocene has been mapped in great detail for northern Finland (Johansson 1995, 2007), few glacial lake sediment sequences from this region have been the subject to detailed studies. Whereas glacial-lake histories have been reconstructed in detail for different parts of the world using geomorphologic evidence (e.g. Alexandersson 2002, Jansson 2003, Murton et al. 2010, Margold et al. 2011), combined with sedimentological analysis (e.g. Etienne et al. 2006), relatively few glacial lake sediment successions have been subjected to detailed multi-proxy analysis, that is, a combination of sedimentological, macro- and microfossil and biogeochemical analysis. Lake Inari (Figure 2-1) is, to our knowledge, one of the few sites in northern Finland where early-Holocene glacial lake sediments have been studied in some detail (Kujansuu et al. 1998).

The scarcity of proxy analysis on glacial lake sediments in general is most probably due to their general sparse fossil content (with often broken/degraded fossil remains), making the analysis particularly time-consuming, and the difficulty of recovering the minerogenic sediment with a conventional Russian peat corer. As such, environmental conditions right at the moment of deglaciation remain largely unstudied. The last deglaciation in major part of Fennoscandia took place during the early-Holocene, i.e. when the Fennoscandia Ice Sheet can be expected to have been in disequilibrium with the warming climate and meltwater was excessively available for glacial lake formation.

The combination of the retreating margin of the Fennoscandian Ice Sheet and the surrounding topography in the Loitsana area allowed for the formation of a glacial lake (i.e. a latter phase of the Sokli Ice Lake; Johansson 1995) that existed at various water depths and surface extensions. The retreating ice-margin eventually left the coring-site in a confined and relatively sheltered embayment, which was additionally fed by water draining unglaciated terrain, allowing the establishment of rich aquatic ecosystems. The unexpected richness of the fossil assemblages in the glacial lake sediment is, in the first place, most probably due to the nutrients provided to the lake through glacial erosion of newly exposed bedrock.

The aquatic ecosystem responded quickly to the changing environmental conditions. Diatom abundance, as well as diatom and chironomid species richness, initially increased with increasing distance between the ice-margin and the coring-site. The aquatic ecosystem became enriched with the bryozoan *Fredericella indica* and the pioneering algae *Botryococcus braunii*, and by water plants including *Myriophyllum, Potamogeton, Callitriche cophocarpa* and *Nuphar*.

Particularly rich aquatic and wetland ecosystems are recorded during the final, smaller and shallower glacial lake phase. In addition to the aquatic plants mentioned above, fossil remains of a large variety of *Potamogeton* species (*P. berchtoldii, P. filiformis, P. friesii, P. obtusifolius, P. pectinatus*), and of Nymphaea and Persicaria amphibia, were found in the sediment. Wetlands included, among others, *Ranunculus* sect. *Batrachium* and warm-demanding *Typha*. The bryozoa *Plumatella repens* and (boreal) *Cristatella mucedo* are also well-represented in the fossil record, as is the cladoceran *Daphnia* (water flea). In contrast, turbid water conditions (with high amounts of silts in suspension) in the shallow glacial lake resulted in sharply declining diatom abundances and a diatom assemblage temporarily dominated by pioneering *Staurosira venter.*

The distinct plant successions recorded in the glacial lake sediment at Loitsana, as well as the presence of seeds of tree birch ^{14}C-dated to the early-Holocene, indicate that the fossil content occurs *in situ*, and is not the result of re-deposition (i.e. reworking from older sediments) as often assumed for the fossil remains encountered in glacial lake sediments. The seeds of tree birch point to the presence of birch trees on the surrounding recently deglaciated land. *Betula* ssp. are pioneer taxa and, the advantage of rapid reproductive rate, abundant production of wind-dispersed fruits, fast growth rate and young reproductive-maturity age, makes birch a fast immigrant (Birks 1986). It is probable that tree birch quickly advanced over the newly-deglaciated terrain in front of the retreating margin of the Fennoscandian Ice Sheet. Rapid spread of trees following deglaciation was most probably also

facilitated by the northern location of glacial plant refugia. The existence of boreal tree populations in northerly small pockets of environmentally favorable conditions, in some cases close to the edge of the LGM ice-sheets, has been recently suggested based on evidence from pollen, plant macrofossils, macrofossil charcoal assemblages and ancient DNA (Willis and van Andel 2004, Kullman 2002, 2006, Paus et al. 2011, Väliranta et al. 2011, Parducci et al. 2012).

A detailed paleo-ecological study on sediments deposited in one of the glacial lakes that formed in front of the retreating margin of the Laurentide Ice Sheet in North America, i.e. early-Holocene glacial Lake Hunt in southern Manitoba, also reports rapid colonization by emergent and aquatic vegetation on the recently-drained, nutrient-rich proglacial lake surfaces, generating a viable resource base for the ice-marginal, so-called "Folsom" hunter-gathers (Boyd et al. 2003). Similarly, macrofossil remains of spruce (*Picea*) and *Populus* indicate the presence of trees on the surrounding, recently deglaciated terrain, and a peak in pollen of the wetland plant *Typha latifolia* reflects substantial postglacial warming. Moreover, the glacial Lake Hunt fossil record shows high frequencies of Type 225 algal microfossils (van Geel et al. 1989). The latter are interpreted to represent algal mats, stranded following seasonal drawdown (Harris and Marshall 1963 in Boyd et al. 2003). The auto-ecology of algal Type 225 is still poorly understood. The type is also well-represented in the glacial lake sediment at Loitsana; it occurs here associated with e.g. high percentage values of pooid grass phytoliths and reworked Tertiary diatoms, reflecting prominent shore erosion.

Great similarities in lithology and fossil content between the early-Holocene glacial lake phase at Loitsana and sediments dated to early MIS 3 in the Sokli basin further support the interpretation of the latter sediments as being of glacio-lacustrine origin (Helmens 2009, Helmens et al. 2009).

3.6.2 Timing of maximum Holocene summer temperature

While our T_{jul} reconstruction for the Holocene based on pollen of terrestrial plant taxa follows the classical trend of gradually increasing early-Holocene mean July air temperatures in Fennoscandia, with a mid-Holocene maximum July warming between ca 8 000 and 4 000 cal. yrs BP (e.g. Seppä et al. 2009), plant macrofossils of telmatic vegetation (aquatics, wetland, shore habitats) encountered in the Loitsana Lake sequence point to an early onset of high T_{jul}, i.e. in the early-Holocene prior to ca 10 000 cal. yrs BP. The macrofossil assemblage, including Nymphaeaceae, a large variety of narrow-leaved *Potamogeton* spp., *Callitriche cophocarpa*, *Typha* and *Glyceria lithuanica,* indicates T_{jul} in the order of at least +12–15 °C between ca 10 500 and 6 000 cal. yrs BP, compared to the present-day T_{jul} at Loitsana Lake of +13 °C.

The use of a multi-proxy approach allows us to validate the pollen-based T_{jul} reconstruction at Loitsana Lake against the detailed environmental record. This shows that the low early-Holocene T_{jul} values depicted in the pollen-based temperature reconstruction are most probably driven by local (site-specific) conditions and not by the regional climate. The multi-proxy data set shows that the high pollen/spore percentage values for e.g. Poaceae and *Equisetum* during the-early Holocene are most probably due to the presence of these plants in local shore or wetland habitats, causing these plants to be over-represented in the palynological record. Since Poaceae and *Equisetum* have low temperature optima in the calibration set used for the temperature reconstruction, the pollen-/spore-based T_{jul} values reconstructed for the early-Holocene can be expected to under-estimate the true mean July air temperatures at that time.

Similarly, the Holocene chironomid (aquatic insect) - based T_{jul} reconstruction at Loitsana Lake is at least partly influenced by factors other than regional climate. For instance, the low T_{jul} values (< +13 °C) reconstructed for the mid-Holocene are in part driven by high percentage values for *Corynocera ambigua*. *C. ambigua* has a low temperature optimum in the chironomid calibration set; however, *C. ambigua* is known to have a complex ecology (Brodersen and Lindegaard 1999) and appears, in the Loitsana record, to be favored by macrophyte density (*Myriophyllum*).
The early-Holocene chironomid assemblage, including *Polypedilum nubeculosum*-, *Cricotopus cylindraceus*- and *Psectrocladius sordidellus*-types, suggests warm summers, similar as recorded in the macrofossil-based T_{jul} reconstruction. However, these chironomid taxa might also be favored by eutrophic conditions during this time, making the inference of warm summers during the early-Holocene, based on the chironomid record only, uncertain.

Early-Holocene summer warming suggested by chironomids and aquatic/wetland plant macrofossils, and low T_{jul} suggested by pollen-based models, has been observed at several locations in Fennoscandia (Väliranta et al. 2011, 2015, Luoto et al. 2014, Paus 2013) and north-western European Russia (Jones et al. 2011, Salonen et al. 2011; Figure 3-11). In central Norway, chironomid-based reconstructions show an early-Holocene warming, with T_{jul} higher than present-day values, some time prior to 9 000 cal. yrs BP; the presence of pine megafossils dated to 9 500–9 700 cal. yrs BP further support an early-Holocene summer warming in central Norway (Paus et al. 2011). Furthermore, chironomid and diatom records, and megafossils, from northern Sweden show maximum July warming in the early-Holocene (Kullman 1999, Bigler et al. 2003). The low early-Holocene pollen-inferred T_{jul} values are probably driven by local factors as well as a relatively slow response of trees (particularly tree populations), compared to aquatic/wetland taxa (which e.g. do not depend on soil formation), to climate warming (e.g. Väliranta et al. 2015). The latter paper notes that "simulations from paleo-climate models are frequently validated against pollen-inferred temperatures; if early-Holocene summer temperatures really were higher than those reconstructed from pollen data, paleo-climate models will have to be re-assessed and validated against the new paleoclimate scenario".

The Holocene summer temperatures, reconstructed by aquatic/wetland taxa at the sites mentioned above, follow the gradually decreasing orbitally-forced June insolation at 60 °N since 11 cal. kyr BP (Figure 3-11). Milankovitch forcing of early-Holocene warm summers has earlier been proposed by Ritchie et al. (1983) based on fossils remains of e.g. *Typha* dated to 6 000–11 800 yrs BP (and clustering at ca 10 000 yrs BP) at 12 high-latitude sites in northern Canada. During the early-Holocene, December insolation at 60 °N was approximately 5 W/m^2 (ca 28 %) lower than present-day (Berger and Loutre 1991; Figure 3-11). The increased seasonality of the insolation (summer 10 % higher, winter 28 % lower), as well as the chironomid-inferred continentality-index (Figure 3-11), point to a more continental climate regime, with warm summer and cold winter, during the early-Holocene than at present.

The close comparison between the early-Holocene T_{jul} reconstructed at Loitsana and other sites in e.g. northern Europe shows that the effect of the local carbonate-rich bedrock at Sokli on paleo-temperature reconstructions is neglectable.

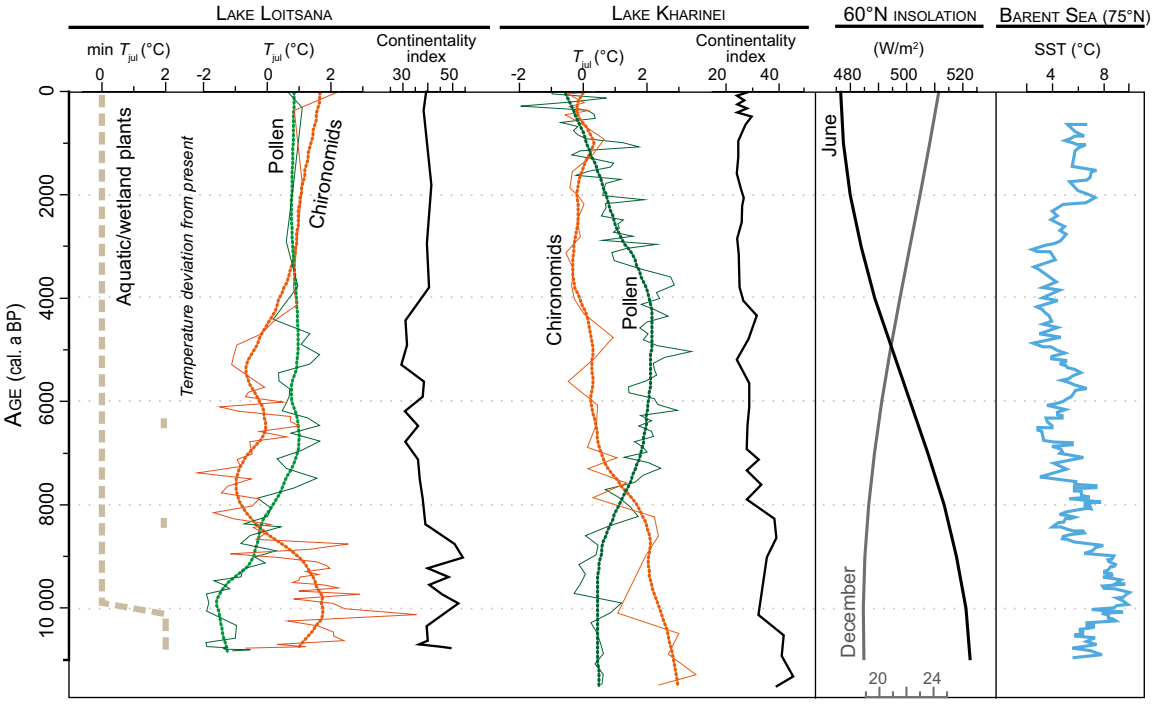

Figure 3-11. *Holocene T_{jul} reconstructions for Loitsana (this report) compared to pollen- and chironomid-based T_{jul} reconstructions at Lake Kharinei (north-west Russia; Jones et al. 2011, Salonen et al. 2011); 60 °N summer and winter insolation (Berger and Loutre 1991); and Barents Sea sea-surface temperatures (SST; 75 °N) (Hald et al. 2007). Chironomid-inferred continentality index for both Lakes Loitsana (Engels et al. 2014) and Kharinei (Jones et al. 2011) are also shown. From Shala (2014).*

4 Early Weichselian (MIS 5d and 5c) environmental and climate reconstructions for northeastern Fennoscandia

4.1 Materials and methods

4.1.1 Stratigraphy and dating

Our studies were conducted on the Sokli B-series borehole, representing the most complete sediment recovery from the central part of the Sokli basin (Helmens et al. 2007, Helmens 2009). The borehole location is indicated in Figure 2-1 and a simplified lithological log with inferred depositional environments is given to the left in Figure 4-1.

The Sokli B-series borehole is dated by means of optically stimulated luminescence (OSL) and AMS ^{14}C dating. The chronology and correlation with the marine isotope stratigraphy (Figure 1-1) are discussed in detail in Helmens et al. (2007), Alexanderson et al. (2008) and Helmens and Engels (2010). We here provide a brief description of the Sokli sedimentary sequence focusing on the early part of the Late Quaternary record preserved in the basin.

The sediments which are the topic of this study occur at depths of ca 13.5–20 m below the present surface of the Sokliaapa patterned fen. They include a ca two-metre-thick, highly compacted sandy gyttja deposit, which is overlain by sand and gravel layers and underlain by ca two metres of silty to sandy sediment. The upper sands have yielded OSL ages on quartz of 94 ± 16 and 94 ± 19 kyr in the B-series borehole (Figure 4-1), and infrared stimulated luminescence (IRSL) and thermoluminescence (TL) ages on feldspar of 111 ± 18 and 110 ± 20 kyr, respectively, in parallel core Sokli-900 (Helmens et al. 2000).

More recent coring (parallel borehole Sokli-2010/1; Helmens, unpublished data) has shown that the gravelly sediment at the base of our studied sediment sequence, at depths of around 19 m, continues throughout a one-metre gap in the B-series recovery. The gravels are underlain by diatom gyttja similar to the sequence at the B-series borehole site (Figure 4-1). The diatom gyttja deposit reaches a thickness of nine metres in the recently recovered Sokli-2010/4 core (Helmens, unpublished data). The diatom gyttja deposit is here underlain by at least three metres of laminated glacial lake sediment. The diatom gyttja deposit, with its characteristic yellowish brown color, stretches as a marker horizon through the Sokli basin near the base of the unconsolidated sediment infill (Ilvonen 1973, Helmens et al. 2000). Sands underlying the horizon have been dated by IRSL and TL dating on feldspar at 178 ± 29 kyr BP respectively 150 ± 29 kyr BP (borehole Sokli-902; Helmens et al. 2000).

The diatom gyttja deposit has been correlated with the Eemian Interglacial (MIS 5e) based on its pollen record (Ilvonen 1973, Forsström 1990) combined with the bracketing IRSL/TL feldspar chronology of ca 110 and 150–180 kyr BP discussed above (Helmens et al. 2000). The seven metres of minerogenic and organic sediment on top of the diatom gyttja bed, with the OSL dates on quartz of ca 94 kyr BP, are correlated to MIS 5d-c (Helmens et al. 2007). The OSL dating on the Sokli B-series borehole has shown that the earlier obtained feldspar luminescence dates slightly overestimate the depositional ages, probably due to incomplete bleaching (Alexanderson et al. 2008).

The upper part of the Sokli sedimentary record consists of glacial till and glacio-fluvial gravels, which in the central basin are interlayered with two more sorted, fine-grained lacustrine sediment sequences (Figure 4-1). These ice-free intervals are dated to MIS 5a and early MIS 3, whereas glaciation of the Sokli basin is dated to MIS 5b, MIS 4 and late MIS 3-2 (Helmens et al. 2007, Alexanderson et al. 2008, Helmens and Engels 2010).

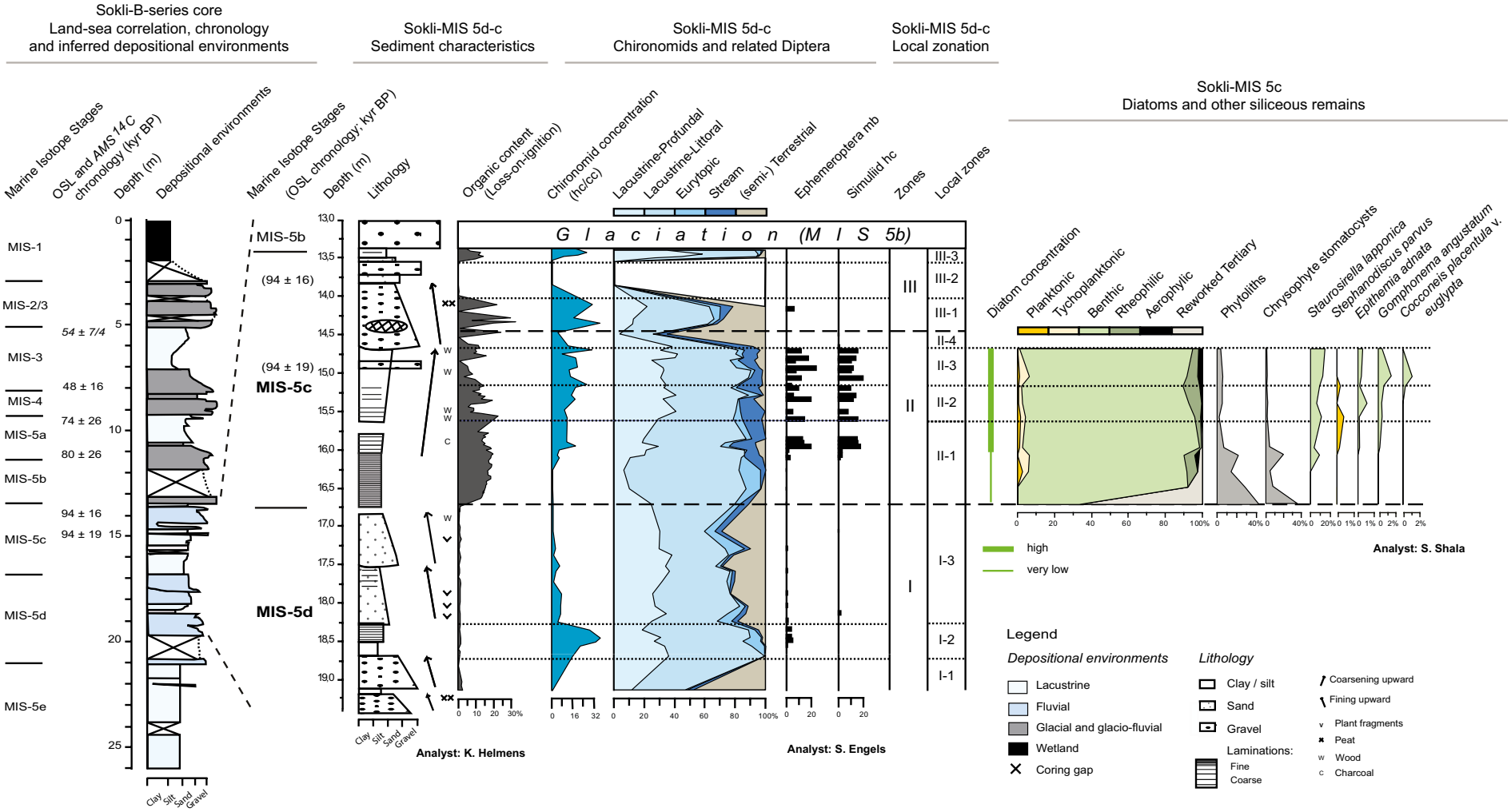

Figure 4-1. *Selection of data on sediment characteristics, chironomids and related Diptera, and siliceous microfossils obtained from the sediments of MIS 5d-c age in the Sokli B-series borehole. Simplified lithology with inferred depositional environments, OSL and ^{14}C chronology, and land-sea correlation is given to the left. Chironomid and diatom taxa are grouped in the figure according to preferred habitats; mass-occurring benthic diatom taxa Staurosira construens and S. venter were excluded in order to illustrate more clearly the different recorded living habitats. Phytoliths and chrysophyte stomatocysts are given as percentage abundances of the total sum of diatoms plus other siliceous microfossils. From Helmens et al. (2012) with permission from Quaternary Science Reviews.*

4.1.2 Proxy analyses

The palynological and siliceous microfossil analyses conducted on the Sokli MIS 5d-c deposit are similar to the analyses applied on the sediments of early MIS 3 age in the Sokli basin (Helmens 2009) and follow the methods described in Bos et al. (2009) and Helmens et al. (2009). The analysis of macrofossils is described in Väliranta et al. (2009) and of chironomids and other insect remains in Engels et al. (2010). The latter paper also describes the measurements of loss-on-ignition (LOI).

The different fossil analyses were generally conducted on the same sample intervals. Sample resolution is ca 15–20 cm in minerogenic sediment and ca 5 cm in gyttja. Because chironomid concentrations were low in parts of the sediment sequence, several samples were amalgamated (see Engels et al. 2010). The analysis of siliceous microfossils focuses on the gyttja deposit in depth interval ca 16.75–14.65 m, at a sample resolution of ca 20 cm.

Percentages of all plant microfossils (pollen, spores, algae, fungi) were calculated based on the sum of terrestrial plant taxa (trees, shrubs, dwarf shrubs, herbs and Pteridophytes), which varied between ca 250–500. *Equisetum* was removed from the Total Sum since the fossil record clearly points to its local (azonal) presence. Because of mass occurrences of specific diatom genera, the total sum of diatom valves counted per sample is in general high (ca 750–1 500), with the exception of the four lowermost samples from finely laminated gyttja (depth interval ca 16.8–16.0 m) where counts of only 5–105 valves per sample were reached. Counts of macrofossils are based on 5–15 cm^3 sediment samples with the smaller samples from gyttja and the larger ones (10–15 cm^3) from minerogenic sediment. Chironomid count sums ranged between 49 and 367 head capsules (hcs) per (amalgamated) sample.

The pollen analysis was performed by Karin Helmens and Jonas Bergman (Stockholm University); macrofossil analysis by Minna Väliranta (University of Helsinki); diatom analysis by Shyhrete Shala (Stockholm University); and chironomid analysis by Stefan Engels (Birkbeck University of London).

4.1.3 Zonation of proxy diagrams

Zonation of the chironomid stratigraphy was obtained by using the optimal sum-of-squares partitioning method (Birks and Gordon 1985) using ZONE (Lotter and Juggins 1991), where the number of significant zones was assessed by a broken stick model (Bennett 1996) using BSTICK (Birks and Line, unpublished program). Zonation of the other diagrams is based on visual examination of the entire multi-proxy data set with focus on the pollen and macrofossil evidence.

4.1.4 Quantitative climate reconstructions

Plant indicator species

The minimum T_{jul} reconstruction is based on the plant indicator method (after e.g. Iversen 1954). This method uses the modern geographical limits of the distribution of a given plant taxon to estimate the minimum temperature needed for this taxon to flower and reproduce. We used the species distribution maps of Lampinen and Lahti (2007) to define the current area of distribution of several indicator species in Finland, and compared these distributions with calculated mean July temperature data (1961–2000) based on daily measurements by the Finnish Meteorological Institute (Venäläinen et al. 2005). Table 4-1 lists the indicator taxa together with the minimum required temperatures. The modern distribution of a selection of plant indicator species encountered in the MIS 5d-c deposit, and present temperature sums, are given in Figure 4-2. The climate reconstruction was performed by Minna Väliranta (University of Helsinki).

Calibration set and numerical methods

Mean July air temperatures were reconstructed using a chironomid-temperature calibration data set from Norway and Svalbard (Brooks and Birks 2001, 2004, and personal communication). The calibration set contains a total of 157 lakes, and 4 outliers were omitted from the final model after screening the data set. The calibration set includes 140 chironomid taxa and spans a mean July air temperature gradient from +3.5 to +16.0 °C. A 3-component weighted-averaging partial least squares (WA-PLS) model was selected as the model with the strongest predictive power, which was tested using leave-one-out cross validation (jack-knifing; Birks 1995). Bootstrap cross-validation

(1000 cycles) was used to obtain sample-specific error estimates (eSEBs) for the individual fossil samples. The chironomid-based climate-inference model has a RMSEP of 1.01 °C, an r^2_{jack} of 0.91 and a maximum bias of 1.05 °C, and is identical to the model used to reconstruct MIS 3 paleo-temperatures for Sokli (Engels et al. 2008a).

Table 4-1. Minimum modern mean July air temperatures (T_{jul}) for plant and animal indicator taxa as indicated by Lampinen and Lahti (2007) and Aalbersberg and Litt (1998), except for C. mucedo after Økland and Økland (2001).

Taxon	Minimum T_{jul} (°C)
Potentilla palustris	+8
Menyanthes trifoliate	+8
Cristatella mucedo	+10
Betula (tree-type)	+10
Nymphaeaceae (*Nuphar* and *Nymphaea*)	+10–12
Potamogeton spp.	+12
Pinus sylvestris	+12
Callitriche cophocarpa	+12
Callitriche hermaphroditica	+12
Crassula aquatica	+14
Elatine triandra	+15
Ranunculus sceleratus	+15
Bidens tripartita	+15
Rhyncospora alba	+15
Typha	+15
Glyceria lithuanica	+15
Najas tenuissima	+16

The chironomid taxon richness (TR) was calculated for all the fossil samples using rarefaction analysis. This method simulates a random selection without replacement, and estimates the taxon richness for all samples using the smallest count size recorded in the entire sequence of samples. In our case, this smallest sample contained 49 identified headcapsules, and the TR was determined for all 47 (amalgamated) fossil samples using RAREPOLL (Birks and Line 1992).

A range of methods are used to test the representation of both the individual chironomid taxa encountered in the fossil data set as well as the representation of the entire fossil assemblages in the Norwegian calibration set. The percentage abundance of the identified fossil chironomids that are absent from the Norwegian calibration data set is calculated, as well as the percentage of fossil chironomids that are rare in the modern data. A taxon is considered to be rare in the modern data when it has a Hill's N_2 (Hill 1973) below 5 in the calibration data set. Brooks and Birks (2001) state that the temperature optima of taxa with a $N_2 > 5$ in the modern data are likely to be reliably estimated, whereas taxa with $N_2 \leq 5$ are rare in the modern data, and the optima for these taxa are probably poorly estimated. Following the modern analogue technique described in Birks et al. (1990), the cut-levels of the 2nd and 5th percentile of all squared χ^2-distances in the modern calibration data were determined and used to define "no close" and "no good" analogues when comparing the distance between an individual fossil assemblage and the most similar assemblage in the modern data set. A canonical correspondence analysis (CCA) (ter Braak 1986) with July air temperature as the only constraining parameter was performed with the fossil samples added passively in the analysis. The residual distances of the fossil samples to the first CCA-axis were compared with the residual distances of all the modern samples to the first CCA-axis. When fossil samples showed a residual distance larger than the 90th and 95th percentile of the residual distances of all the modern samples, they were identified as samples with a "poor fit" and a "very poor fit" with temperature, respectively (after e.g. Birks et al. 1990, Heiri et al. 2003). In all our analyses except for the rarefaction analysis, the chironomid abundance data are square-root transformed.

The climate reconstruction was performed by Stefan Engels (Birkbeck University of London).

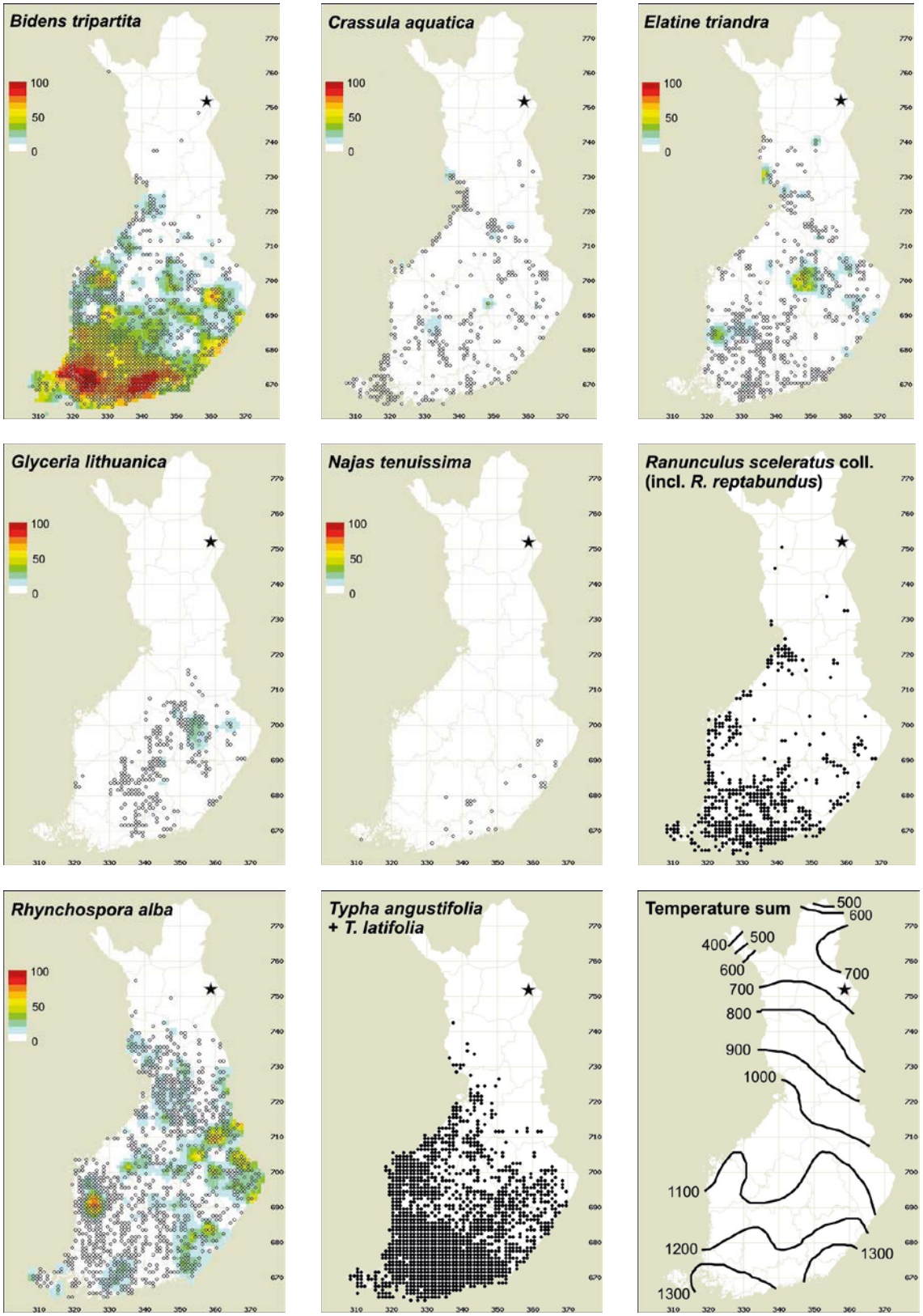

Figure 4-2. *Modern distributions of selected plant species in Finland and present temperature sums. The location of the Sokli study site is indicated by a star *. Species records are marked with grey circles and species groups with black dots. The colored scale gives an estimated frequency (%) of the species per one km². Lower right: effective daily temperature sums in Finland in day-degree (d.d.) units (re-drawn from Helminen 1988). Grids follow the Finnish National Grid system. From Väliranta et al. (2009) with permission from Quaternary Science Reviews.*

4.2 Results

4.2.1 Biotic data

Sediment characteristics (lithology and LOI) and a selection of chironomid, other insect, and siliceous microfossil data are given in Figure 4-1. Chironomid and diatom taxa are grouped in the figure according to preferred habitat. We acknowledge that the classification of diatom taxa according to living habitat should be considered as an approximation only since the search of ecological preferences in the literature may give contradictory information or be vague. Nevertheless, the multi-proxy record obtained on the early MIS 3 deposit in the Sokli basin, that also included groupings of diatoms according to living habitat, has given coherent environmental reconstructions (see Helmens et al. 2009 and references therein). Likewise, many of the encountered chironomid taxa are typical inhabitants of profundal environments in temperate and sub-arctic regions, but occur in littoral habitats in arctic regions. For these taxa, we assume a temperate to sub-arctic environment at the Sokli site in order to be able to classify them into a single category. The figure additionally shows the occurrences of phytoliths and chrysophyte stomatocysts (as percentage abundances of the total sum of diatoms plus other siliceous microfossils) and a selection of diatom taxa mentioned in the text. The full diatom diagram is provided in Appendix 1.

All plant microfossil remains and macrofossils of plants and zoological taxa (excluding insects) encountered in the Sokli sediments of MIS 5d-c age are given in Figures 4-3 and 4-4. Figure 4-3 combines micro- and macrofossil remains of taxa that occur in aquatic and wetland environments, and Figure 4-4 combines fossil remains of terrestrial plant taxa. Figure 4-3 additionally shows remains of lemming and soil fungi. Similar as for the Holocene Loitsana record (see Section 3.2.4), pollen of herbs for which a distinct wetland habitat could be inferred (e.g. Cyperaceae), as well as herbs in shore settings (e.g. *Rorippa palustris*) or for which the habitat was undifferentiated (e.g. *Thalictrum*), are given in the lower diagram of Figure 4-4 (“other herbs”). Macrofossils of *Carex* spp., Poaceae, *Salix*, *Betula nana* and Ericales, which can be assumed to have an overall local wetland source, are shown in the aquatic/wetland diagram of Figure 4-3.

The main zonation in zones (zones I-III in Figures 4-3 and 4.4) and sub-zones (II-a till -c; Figure 4-4) follows the zonal vegetation development. The local zones (I-1 till -3, II-1 till -4, and III-1 till -3 in Figure 4-3) describe the contemporary depositional history and associated azonal vegetation types. The zonations are summarized in Figure 4-5 A. The latter figure (Figure 4-5 B) also gives schematic representations of reconstructed environmental conditions for a selection of time-windows.

4.2.2 Proxy-based climate reconstructions

The chironomid diagram (Figure 4-6) is discussed together with the chironomid-based climate reconstruction (Figure 4-7) under Section 4.7.

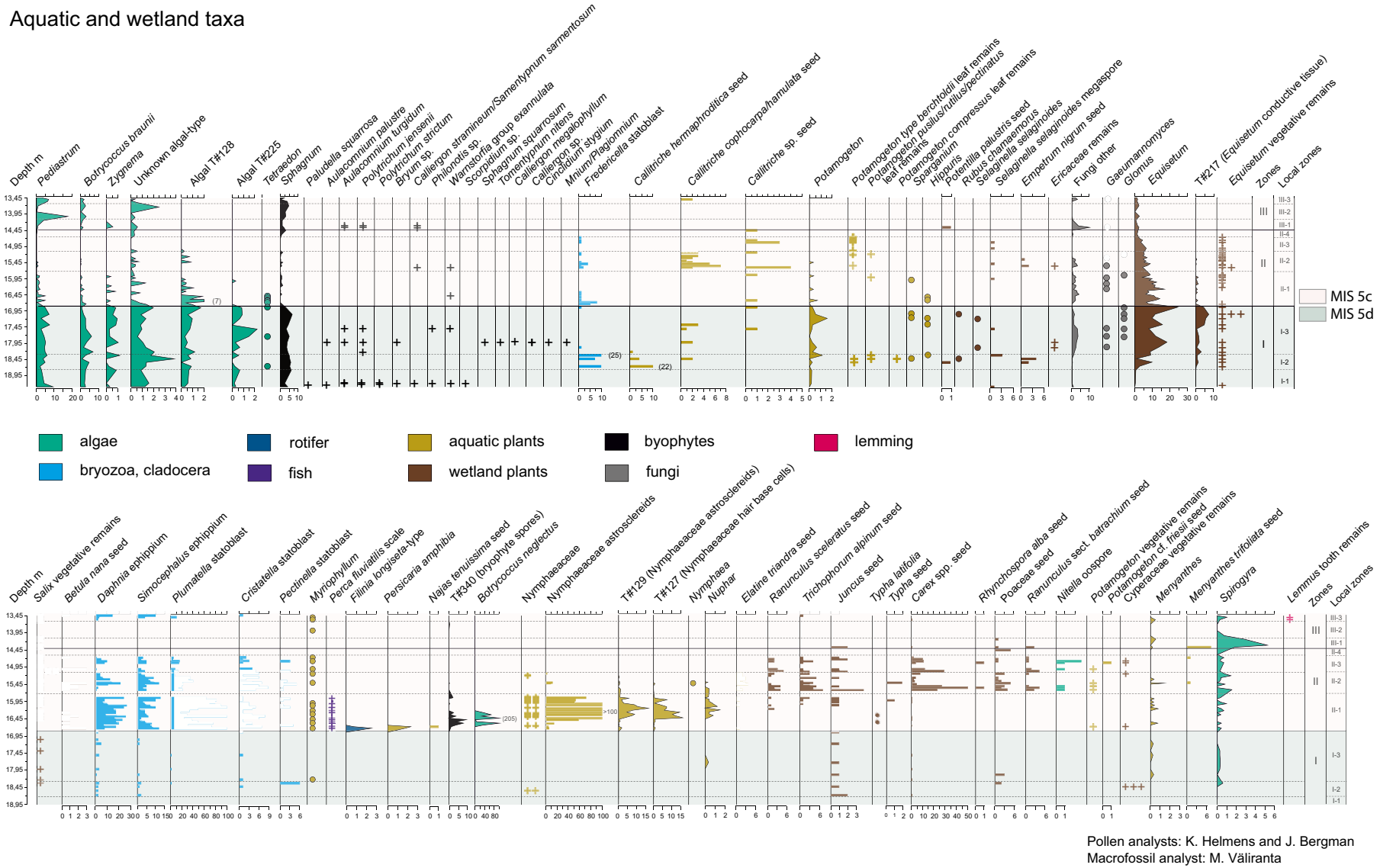

Pollen analysts: K. Helmens and J. Bergman
Macrofossil analyst: M. Väliranta

Figure 4-3. *Micro- and macrofossil diagram for aquatics and wetland taxa from the MIS 5d-c deposit in the Sokli B-series borehole. Also shown are tooth remains of lemming and spores of the soil fungus Glomus. Macrofossil remains are expressed as concentrations (amounts/5–15 cm^3) and drawn as histograms or as present (+) or high abundances (+++). Percentages of microfossils are calculated as percentages of Total Sum of terrestrial pollen and spores; dots show single samples with percentage values < 1 %. From Helmens et al. (2012).*

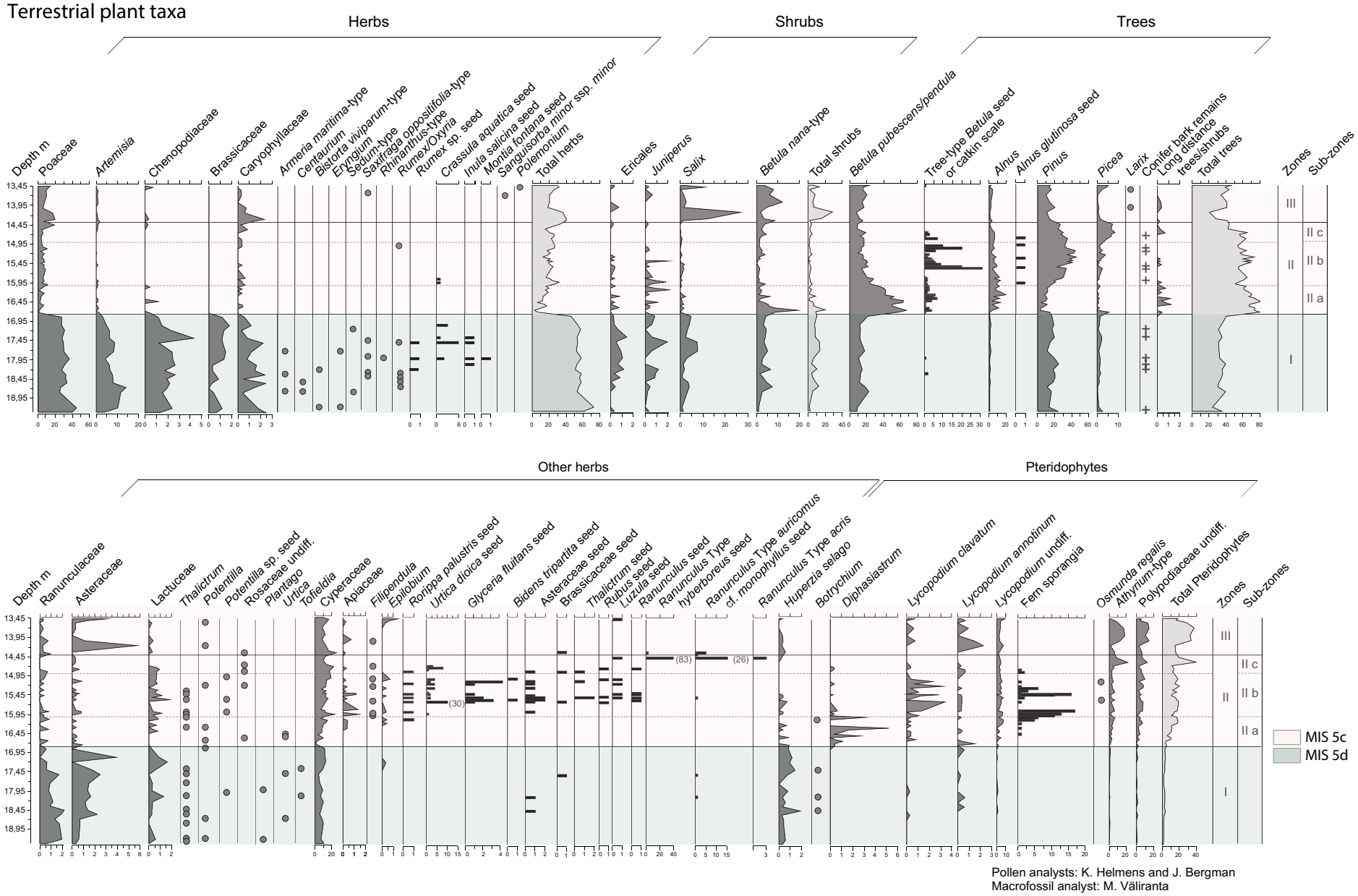

Figure 4-4. *Micro- and macrofossil diagram for terrestrial plant taxa from the MIS 5d-c deposit in the Sokli B-series borehole. For explanation of curves and symbols see Figure 4-3. From Helmens et al. (2012).*

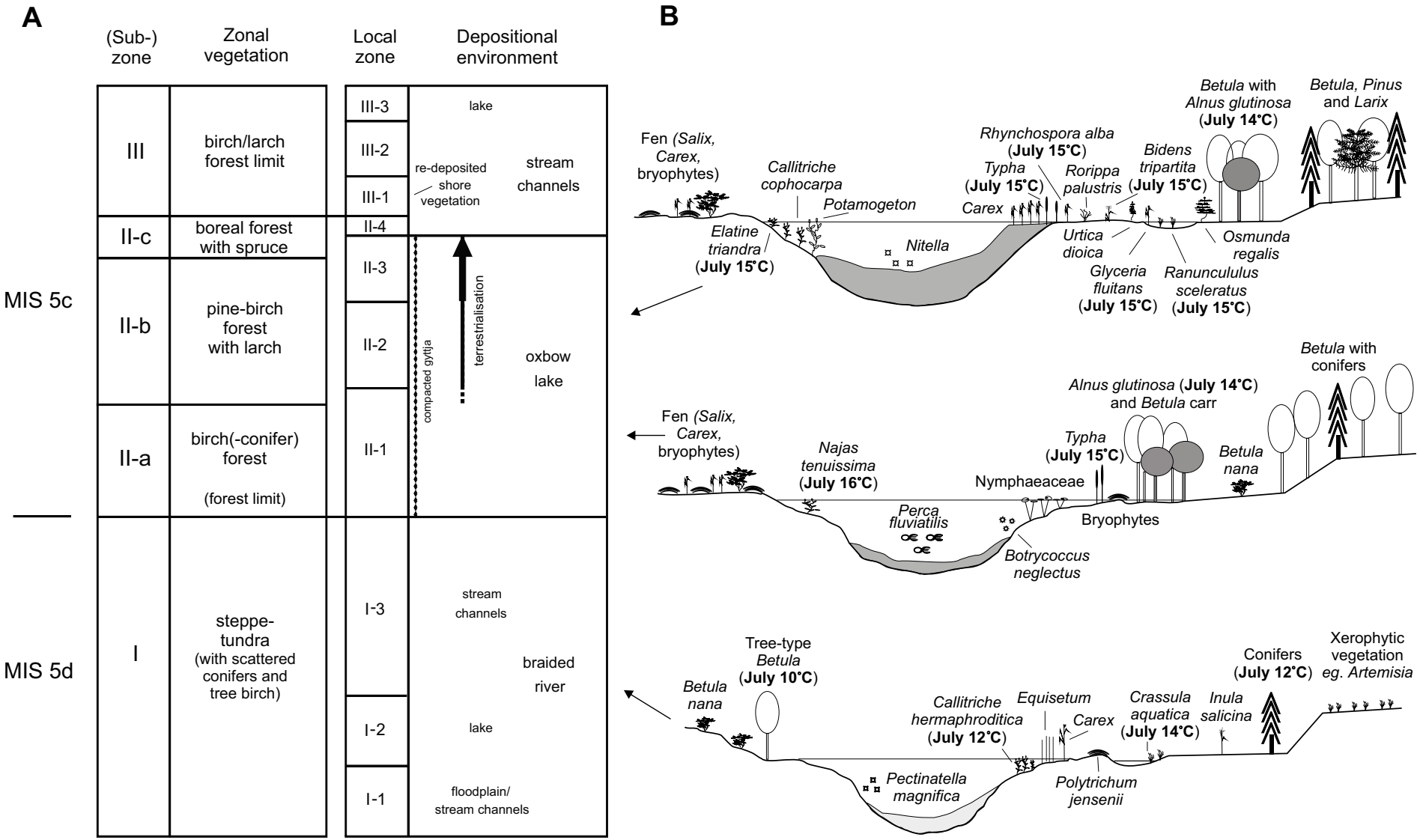

Figure 4-5. ***A*** *shows a summary of the zonation applied to the sediments of MIS 5d-c age in the Sokli B-series borehole, and* ***B*** *gives schematic cross-sections that show paleo-environmental conditions in the Sokli basin for a selection of time-slices during MIS 5d-c; minimum mean July temperatures based on plant indicator species are shown in* ***B*** *in-between brackets (present-day mean July temperature at Sokli is +13 °C). From Helmens et al. (2012) with permission from Quaternary Science Reviews.*

4.3 Depositional environment and local (azonal) vegetation during the cold MIS 5d stadial period (ca 115–105 kyr BP)

Spores of a variety of algae (*Pediastrum*, *Botryococcus braunii*, *Zygnema*, *Spirogyra*, *Tetraedon*, and algal types Type 128 and Type 225 (van Geel et al. 1983, 1989); Figure 4-3) indicate an aquatic depositional environment for the lower three metres of silty to gravelly sediment of MIS 5d age (depth interval 19.69–16.80 m in Figure 4-1). Spores of *Sphagnum* are also recorded continuously and in relatively high percentages and reflect the presence of nutrient-poor wetlands or peaty soils in the Sokli basin. The sediment shows a series of upward fining sequences and is most probably for major part deposited in a fluvial environment. The records of spores of *Zygnema* and *Spirogyra* (if produced locally) indicate at times the presence of stagnant water at the coring-site, and a distinct phase with lacustrine sedimentation is recorded around 18.50 m depth. As will be discussed below, the multi-proxy record suggests a dynamic depositional environment, with frequent changes in the position of water courses, indicating that the river most likely followed a braided pattern. The braided river system indicates a high sediment load and/or low precipitation values. Three local zones are distinguished (see also Figure 4-5).

4.3.1 Local zone I-1 (19.69–18.69 m depth interval)

The coarse sediments in the lowermost part of the fluvial deposit include two sequences of gravel grading into silt or fine sand (Figure 4-1) and are interpreted as representing changes from a stream channel to floodplain environment. The floodplain sediments contain well-preserved remains of a variety of mosses. The bryophyte assemblage (Figure 4-3), including for instance *Aulacomnium turgidum*, *Polytrichum jensenii*, *P. strictum*, *Warnstorfia* group *exannulata* and *Scorpidium* spp., indicates a nearby minerotrophic fen and an environment with wet depressions influenced by (seasonal) flooding (Ulvinen et al. 2002). The chironomid assemblage reflects the shallow water to (semi-) terrestrial conditions on the floodplain as well (Figure 4-1). Ranunculaceae and Asteraceae are relatively well-represented among the pollen taxa (Figure 4-4, lower diagram) and, like during local zones II-4 and III-1 (see below), these herbs most probably bordered the stream channels.

4.3.2 Local zone I-2 (18.69–18.24 m)

Local zone I-2 corresponds to a 50 cm thick silty sediment layer in which the high abundance of chironomids living in the profundal or littoral zone of lakes indicates a lacustrine origin. Some gravel is found in the lower part of the silt layer, whereas the upper part is finely laminated showing grain sizes from clayey silt to sand and some thin organic lamina. Both the lithology and the presence of Ephemeroptera mandibles indicate a regular input of water into the former lake and sedimentation most probably took place in an abandoned stream channel. Despite the low LOI (2–4 %; Figure 4-1), the sediment contains a rich fossil assemblage. Statoblasts of the bryozoa *Fredericella* and *Pectinatella* are well-represented and vegetative remains of *Equisetum* indicate its continuous presence in the littoral zone of the lake. Aquatic plants included a variety of species of *Callitriche* (*C. hermafroditica* and *C. cophocarpa/hamulata*) and *Potamogeton (P.* Type *berghtoldii, P. pusilus/rutilus/pectinatus* and *P. compressus*) as well as *Sparganium*, *Hippuris* and Nymphaeaceae. The macrofossil record in the upper laminated sediment registers an encroaching wetland zone with *Juncus*, Poaceae, Cyperaceae*, Potentilla palustris*, *Selaginella selaginoides* and *Empetrum nigrum*; in addition, pollen of the wetland plant *Rubus chamaemorus* are registered. Presently, scattered occurrences of the bryozoan *Pectinatella* are reported only from southern locations on the European mainland (Wood and Okamura 2005).

4.3.3 Local zone I-3 (18.24–16.80 m)

The coring-site became part of the active river system again during local zone I-3. Two stream channel deposits occur in depth interval 18.24–16.80 m. Conditions within the channels, however, were less energetic than during deposition of the gravels in local zone I-1 and likely included prolonged phases of standing water, particularly during deposition of the lower stream channel deposit. The sands of the latter deposit show macroscopic plant fragments, probably of *Equisetum*, and are interlayered near the top with thin, brownish silty beds. The fossil record shows the local presence of wetland vegetation, with *Equisetum*, *Juncus*, *Carex* spp., Poaceae and *S. selaginoides*, and of the aquatic plants *C. cophocarpa/hamulata*, *Potamogeton*, *Myriophyllum*, *Nuphar* and *Menyanthes*. The presence of local stands of *Carex* is not only indicated by macrofossils (seeds) but also by hyphopodia of

Gaeumannomyces (Type 126, Pals et al. 1980), which is a fungus that is parasitic on *Carex* spp. (van Geel et al. 1983). Other recorded fungal remains indicate the local presence of wetland as well (van Geel 2001). The palynomorph Type 225 shows relatively high percentage values; this algal type has been recorded under open water conditions and ephemeral pool phases (van Geel et al. 1989). The lower stream channel deposit also contains a rich bryophyte assemblage with *P. jensenii*, *Sphagnum squarrosum*, *W.* group *exannulata*, *Tomentypnum nitens* and *A. turgidum* reflecting an environment influenced by surface water flow and flooding (Ulvinen et al. 2002).

The upper stream channel deposit is more coarse-grained and consists of coarse sand fining upward into silty sand. Conductive tissue (Type 217, van Geel et al. 1989) accompanies spores and stem fragments of *Equisetum* in the fossil record indicating the abundance of *Equisetum* in the channel. Similarly, *Juncus* is represented as are the aquatic plants *Potamogeton*, *Sparganium*, *Hippuris* and *Menyanthes*. Chironomid concentrations in the sediment are low.

It is possible that the terrestrial herbs *Rumex*, *Crassula aquatica*, *Inula salinica*, *Montia fontana* and *Ranunculus* Type *auricomus* cf. *monophyllus* directly bordered the stream channels or that their macrofossils were transported from the adjacent floodplain to the channels during phases of flooding. Similarly, chironomids living in (semi-) terrestrial habitats are relatively well-represented in the fossil record of local zone I-3. The fluvial sediment further contains fossil remains of stream-inhabiting chironomids and of *Glomus*. The spores of the soil fungus *Glomus* were most probably transported from the catchment by the flowing water as well (van Geel et al. 1989).

4.4 Depositional environment and local (azonal) vegetation during the warm MIS 5c interstadial period (ca 105–90 kyr BP)

The highly variable local conditions at and near the coring-site during MIS 5c have resulted in the identification of seven local zones (II-1, -2, -3, -4; III-1, -2, -3; see also Figure 4-5).

The sediment of local zones II-1 till -3, in depth interval 16.74–14.65 m, consists of a two metre thick silty gyttja deposit (LOI at ca 20 %) that becomes increasingly interlayered with sand, wood and some gravel in its upper part (LOI from 25 % to < 5 %). The gyttja deposit is highly compacted and its original thickness might have been significantly more. As will be discussed below, the gyttja was most likely deposited in an oxbow lake of a meandering river that remained flooded during the entire process of infilling. The active river returned to the coring-site during the following local zones II-4 and III-1 and -2 (mostly gravelly sediment between 14.65–13.56 m depth). After a brief interval with lacustrine deposition (sandy gyttja of local zone III-3), the Sokli basin became glaciated (glacial till bed of MIS 5b age in Figure 4-1).

The diatom record from the gyttja deposit in local zones II-1 till -3 is dominated by *Staurosira* spp. (ca 50–60 %) and *Staurosirella* spp. (ca 10–20 %; Supplement). These taxa are common in alkaline waters and are tolerant of a broad range of ecological parameters as well as rapid shifts in environmental conditions (Weckström and Korhola 2001, Schmidt et al. 2004).

4.4.1 Local zone II-1 (16.74–15.80 m depth interval)

The gyttja in local zone II-1 contains high abundances of statoblasts of bryozoa (*Plumatella*, *Cristatella, Pectinatella*) and ephippia of cladocera (*Daphnia*, *Simocephalus*) (Figure 4-3). Fossil scales of perch (*Perca fluviatilis*) and high counts/percentages of fossil remains of Nymphaeaceae are confined to the zone. Although open water is recorded at the coring-site, the nearby-presence of shallow water or wetland is indicated by spores, conductive tissue (Type 217) and stem fragments of *Equisetum*; pollen of Cyperaceae (Figure 4-4, lower diagram), hyphopodia of *Gaeumannomyces* and seeds of *Carex* spp.; as well as fungal remains. The lake in which the gyttja was deposited most probably occupied an abandoned stream channel bordered by wetland (see also below). Today, the Sokli basin is drained by the meandering rivulet Soklioja (Figure 2-1) which is flanked by mire vegetation of the Sokli aapa; a *Carex-Salix* rich fen surrounded by a *Carex-Betula nana* moderate-rich fen border the rivulet. Macrofossils of *Betula nana* and *Salix* are present in the gyttja and the plants probably formed important elements in the local mire vegetation at the time of local zones II-1 to II-3 as well. *Myriophyllum* is abundantly found in the present Soklioja and pollen of this aquatic plant is recorded throughout the gyttja deposit of zone II.

The lowermost samples from the gyttja are characterized by pollen of *Persicaria amphibia* and seeds of *Najas tenuissima*. *N. tenuissima* thrives on soft mud in water less than 1.5 m deep; it is presently very rare with scarce occurrences in southern Finland and Japan. The aquatic plant *Persicaria amphibia* is found today along the major water courses in Fennoscandia. In oxbow lakes, the species can tolerate the relatively high level of disturbance associated with flooding during the early phases of infilling of the lakes (Westhoff et al. 1981). Nymphaeaceae are well-represented in the fossil record both by macrofossils (astrosclereids; Type 129 in the pollen samples, Pals et al. 1980) and base cells of Nymphaeaceae hairs (Type 127). These cells are common in lake sediments where *Nuphar* and/or *Nymphaea* played a role in the local vegetation (Pals et al. 1980) and are considered to be a better indicator of the local presence of *Nymphaea* than pollen of the entomophilous taxa of Nymphaeaceae (Ralska-Jasiewiczowa et al. 1992). Few pollen grains of *Nuphar* and *Nymphaea* are present in the gyttja. Compared to *Persicaria amphibia*, the water lily *Nymphaea alba* favors more moderate levels of disturbance which occur when increasing sediment infill in an oxbow lake decreases the strength of water flow during flooding (Westhoff et al. 1981).

Both alder and birch are well-represented in the pollen record, and particularly during local zone II-2 also in the macrofossil record, and it is likely that both trees were present in a marshy forest along the abandoned stream channel forming a *Betula-Alnus* carr. Conditions under a birch-alder carr are acid (pH < 5) and oligotrophic as plant remains are washed away during flooding (Jansen et al. 2000). Similar conditions (pH 5–7, oligotrophic) are favored by *Perca fluviatilis* (Hokanson 1977). The damp local conditions could explain the high percentages of bryophyte spores (Type 340, van Geel et al. 1989) and remains of the aquatic moss *W.* group *exannulata*. *Botryococcus neglectus* is also well-represented in the microfossil record of local zone II-1; this alga occurs in relatively small, oligotrophic and mesotrophic water bodies (Jankovská and Komárek 2000).

The gyttja of local zone II-1 is rhythmically interlayered with very thin silt laminae. The low concentrations of fossil remains of both chironomids and diatoms in the sediment are striking. It is possible that the remains were washed away during flooding. The siliceous microfossil record consists mostly of phytoliths, chrysophyte stomatocysts and Tertiary diatoms. The Tertiary diatoms are re-deposited from till in the catchment; their robust structure allows for multiple phases of re-working (e.g. Helmens et al. 2009 and references therein).

Chironomid and diatom concentrations increase sharply in the uppermost part of local zone II-1. It is also here that we see the start of a near continuous representation of black flies (Simuliidae) and stream-inhabiting chironomids and diatoms. Additionally, both the gyttja and the silt laminae are thicker here. Black flies are inhabitants of streams and rivers, however, their fossil remains are rarely found in fluvial sediments. It is only when stream flow diminishes (such as upon entering a lake) that remains of black flies preserve (Klink 1989). Probably stream flow through the abandoned channel had further diminished in the uppermost part of local zone II-1 and, instead of an “erosive regime”, sediment was now being deposited during flooding. The sediment accumulation allowed for the start of terrestrialization of the oxbow lake. The latter is recorded by a peak for tychoplanktonic diatoms followed by the start of macrofossil records for several wetland plants including *Ranunculus sceleratus*, *Trichophorum alpinum* and *Juncus.* The aquatic plant *Elatine triandra* and the shore taxa *Rorippa palustris* also appear in the uppermost part of local zone II-1. High abundances of fern sporangia here suggest the presence of ferns along the shore as well.

4.4.2 Local zone II-2 (15.65–15.16 m)

The presence of an extended littoral zone in the oxbow lake is indicated by high abundances of *Carex* spp. seeds and of macrofossil remains of other wetland elements in local zone II-2. Open water, however, still prevailed at the coring-site as indicated by the presence of e.g. benthic diatoms and chironomids living in the profundal of lakes, bryozoa, cladocera and the macro-algae *Nitella*. Moreover, a diverse aquatic plant assemblage is recorded with *P. berchtoldii*, *P. pusilus/rutilus/pectinatus*, *C. cophocarpa/hamulata*, *E. triandra*, *R.* sect. *batrachium*, *Menyanthes trifoliata*, Nymphaeacea and *Myriophyllum*. Wetland vegetation consisted of Cyperaceae (*Carex* spp., *Trichophorum alpinum*, *Rhynchospora alba*), *Juncus*, Poaceae, *Typha* spp., *R. sceleratus*, *S. selaginoides*, *E. nigrum,* and the mosses *W.* group *exannulata* and *Calliergon stramineum/Samentypnum sarmentosum*. *C. cophocarpa/hamulaa* and *E. triandra* suggest mesotrophic water quality (Heino and Toivonen 2008). This trophic state is further indicated by the occurrence of meso-eutrophic diatom species such as *Stephanodiscus parvus* and *Epithemia adnata* (Fairchild and Lowe 1984, van Dam et al. 1994).

Shore elements included the tall herbs *Filipendula*, *Epilobium*, *R. palustris*, *Urtica dioica*, *Glyceria fluitans* and *Bidens tripartita*, as well as ferns and alder. *R. palustris* and the grass *G. fruitans* are pioneer shore elements occurring on nutrient-rich, mineral soils that fall dry in summer. *B. tripartita* favors nitrogen-rich moist habitats which occur where fresh organic material accumulates and decomposes (Jansen et al. 2000); the presence of nitrogen-rich habitats is also indicated by *R. sceleratus*. Macrofossils of Asteraceae*,* Brassicaceae*, Thalictrum*, *Rubus* and the Juncaceae *Luzula* were additionally found in the gyttja suggesting their presence in the local shore/wetland vegetation as well. The gyttja in local zone II-2 becomes increasingly sandier and is intercalated with wood. The sandy lithology and wood fragments, the large abundances of taxa characteristic of flowing water, and the presence of species such as *R. palustris*, *G. fluitans* and *B. tripartita,* indicate that the active stream channel stayed in the vicinity of the oxbow lake and that the coring-site remained periodically flooded.

4.4.3 Local zone II-3 (15.16–14.65 m)

The sediment in local zone II-3 consists of sandy gyttja interlayered with wood, sand and some gravel, reflecting a still further diminished strength of water flow through the channel. Open water still prevailed at the coring-site, but high numbers of *Carex* spp. seeds and vegetative remains of Cyperaceae, as well as the registration of aerophilic diatoms, indicate an advanced stage of terrestrialization of the oxbow lake. *C. cophocarpa/hamulata*, *E. triandra*, *G. fluitans* and *B. tripartita*, which were all well-represented during local zone II-2, are absent from the fossil record. Apart from *Nitella* and *Spirogyra*, no other algae (such as *Pediastrum*, *Botryococcus*, *Zygnema*) are recorded; *Sphagnum* spores are absent as well. Nutrients concentrations most probably had further increased which is also suggested by the presence of the aquatic plant *Potamogeton* cf. *friesii* (syn. *mucronatus*) which favors shallow, eutrophic water conditions. The ongoing infilling of the lake and further increase in nutrient availability are also indicated by the elevated abundance of *Staurosirella lapponica* and *Gomphonema angustatum* as well as the occurrence of *Cocconeis placentula* var. *euglypta*, a taxon with an affinity for bryophyte substratum (Selby and Brown 2007, Filippi et al. 2011).

4.4.4 Local zone II-4 (14.65–14.42 m)

The sediment of local zone II-4 consists of fluvial sand and gravel and shows that, after a prolonged phase with lacustrine sedimentation, the coring-site became part of the active river system again. The macrofossil record is poor in taxa and consists of fossil remains from shore elements including *Ranunculus* Type *hyperboreus*, *R*. Type *auricomus* cf. *monophyllum and R*. Type *acris*, and grasses. The chironomid assemblage is also dominated by taxa living in (semi-) terrestrial habitats. Peak spore percentage values for the fern *Athyrium* (20 %) suggest it presence along the river as well. Spores of *Sphagnum* are recorded again.

4.4.5 Local zone III-1 (14.42–14.08 m)

Local zone III-1 is represented by slabs of peaty sediment (LOI to 30 %) that occur intercalated in sands and gravels (LOI approaching 0 %). The fossil record indicates that the organic-rich intercalations represent wetland and shore vegetation that was locally eroded and re-deposited together with the coarse-grained stream channel sediment. The peaty slabs contain macro-remains of mosses (*P. jensenii, C. stramineum/S. sarmentosum*, *A. turgidum*), wetland plants (*Carex* spp.*,* Poaceae, *Juncus*, *P. palustris*), shore taxa (*R.* Type *hyperboreus*, *R*. Type *auricomus* cf. *monophyllum*, Brassicaceae) and of aquatic plants (*M. trifoliata*, *R.* sect. *batrachium*). *M. trifoliata* shows peak values in local zone III-1; this plant is an early colonizer of new habitats and can be regarded as a pioneer in the hydroseral succession (Hewett 1964). Peak pollen percentage values for *Salix*, Asteraceae and Caryophyllaceae, as well as the algae *Spirogyra* and fungi, suggest their local presence as well. Many of the chironomid taxa in local zone III-1 are associated with aquatic macrophytes (Engels et al. 2010).

4.4.6 Local zone III-2 (14.08–13.56 m)

The sediment consists of layers of sand to coarse gravel that are barren of chironomids and macro-remains. The fluvial sediment contains pollen of *Myriophyllum*, *Menyanthes* and *Potentilla* and spores of *B. braunii* and *Sphagnum*. Peak values are recorded for the algae *Pediastrum* and the fern *Athyrium*.

4.4.7 Local zone III-3 (13.56–13.40 m)

A 15 cm thick gyttja layer, interlayered with sand, some gravel and wood, is found on top of the stream channel deposits of local zones II-4 till III-2. The gyttja has a LOI of ca 15 % and contains macrofossils of *Daphnia*, *Simocephalus*, *C. cophocarpa/hamulata*, *Carex* spp., *T. alpinum* and *Luzula*.

4.5 Regional (zonal) vegetation development during the cold MIS 5d stadial period (ca 115–105 kyr BP)

The terrestrial pollen spectra of zone I (19.69–16.80 m depth interval; Figures 4-4 and 4-5) are characterized by high percentages of non-arboreal pollen taxa (NAP to ca 60 %) representing a combination of steppe and tundra elements. Relatively high pollen values for *Artemisia* and Chenopodiaceae (up to 8–14 % and 2–4 %, respectively), together with a high representation of grasses (Poaceae to 30–45 %), suggest the presence of dry, steppe-like vegetation in the Sokli area. Presently, the herbs *Artemisia* and Chenopodiaceae are common elements in the steppe and steppe-like vegetation of central and NE Eurasia (Shahgedanova 2008). Poaceae are a main constituent of the N Eurasian tundra, but high pollen percentage values are primarily reported from modern pollen samples in the steppes (Tarasov et al. 1998). The shrub *Betula nana* (dwarf birch) is represented in the pollen spectra of zone I as well (values to 7 %), and like other recorded plants such as sedges (Cyperaceae), is a typical element of the present-day NW and north-central Eurasian low-arctic shrub tundra (Shahgedanova and Kuznetsov 2008). NAP further includes a variety of heliophilous (light-demanding) herbs (Brassicaceae, Caryophyllaceae, *Armeria maritima, Centaurium, Bistorta viviparum*, *Sedum*), the arctic-alpine herb species *Saxifraga oppositifolia*, and the (dwarf) shrubs *Juniperus*, *Salix* and Ericales. Lycopodiaceae (lycopods) and Polypodiaceae (ferns) are represented by low spore percentages only, mostly those of *Huperzia selago.*

The macrofossil record indicates that the open herb-dominated vegetation, however, was not tree-less. Well-preserved bark tissue of conifer trees, either pine or spruce, as well as seeds of tree-type birch were found in the sediment. These trees were probably present in scattered occurrences in favorable spots. The regional vegetation in the Sokli area seems to have been rather similar throughout zone I. It might have been most open during the earliest part (depth interval 19.69–18.64 m) as suggested by relatively high pollen percentage values for grasses and *Artemisia* and generally low values for (dwarf) shrubs.

Steppe-tundra vegetation was widespread in central Europe during the cold stages of the Weichselian (see e.g. Granoszewski 2003). Presently, steppe-tundra associations are rare. The co-occurrence of steppe and arctic-alpine species are described for the Chukotka Peninsula in NE Siberia (Yurtsev 1981 in Zlotin 2008) and for west-central Greenland close to the Greenland Ice Sheet (Böcher 1954 in Pennington 1980). Steppe-like vegetation in arid NE Eurasia ("cold steppes") is not confined to the Siberian Arctic. As examples, cryoarid steppes and steppified meadows dominated by grasses and xerophilous species are characteristic of the larch forest biome in Sakha-Yakutia, central Siberia, and steppe communities are described for the basins of the great Siberian rivers such as the Lena (Tishkov 2008). Notably, xerophilous plant species are absent from the N European - W Siberian provinces (Shahgedanova and Kuznetsov 2008).

Precipitation values are low in E Siberia and west-central Greenland. A thin snow cover combined here with low winter temperatures has formed a permafrost layer of several hundred metres thickness (Tumel 2008, Claesson Liljedahl et al. 2016). The steppe communities form in response to local controls, especially moisture availability, with steppe plants occupying dry local habitats; disturbances and sandy substrates furthermore support their presence (e.g. Kienast et al. 2008). In west-central Greenland, steppe communities dominated by grasses, *Artemisia* and sedges occur on south-facing slopes where the active layer dries out in summer; on wind-exposed slopes and ridges characterized by a discontinuous plant cover with much unstabilized mineral soil; and on sand and loess. Their presence contrasts markedly with the low shrub tundra background dominated by *B. nana* and *Ledum palustre* (Böcher 1954) which occur on relatively moist, north-facing slopes. In this mosaic of steppe and tundra, *Artemisia* pollen percentages ranging from 1 to 40 % are recorded (Pennington 1980). The highest values occur in terrestrial moss polsters from the steppe vegetation itself and relatively low percentage values (2–7 %) in surface lake samples in which pollen of dwarf birch is over-represented with values of up to 70 %. Pollen values of over 50 % for *Artemisia*, Chenopodiaceae and Poaceae

are recorded in surface pollen data along the Lena River (Tarasov et al. 1998). In contrast, *Artemisia* is represented by a few percentages only in surface lake samples from the N European Russian tundra (Paus 2000, Salonen et al. 2011).

It is possible that the local sandy floodplain within the Sokli basin during MIS 5d provided suitable habitats for some of the recorded xerophilous herbs. Chenopodiaceae and Brassicaceae, for instance, flourish well on freshly deposited mineral-rich river sediment (Hoek 1997). Some macrofossil remains of grasses indicate their presence in the azonal (wetland) vegetation as well (Figure 4-3), however, the high pollen percentage values for Poaceae during zone I most probably are related to their presence in the zonal steppe-like vegetation. Notably, the recorded herbaceous taxa *Armeria maritima* and *Centaurium* are halophytes (salt-tolerant) and presently occur in Fennoscandia in mostly southern, coastal areas. Their presence in the fossil record of zone I may indicate soils with high salt concentrations as nowadays found in continental Eurasia (Tishkov 2008). The herb *Inula salicina* occurs today in the so-called alvar vegetation on the limestone island of Öland in the south Baltic Sea. The flora of the open alvar landscape (which is extensive on Öland but also occurs on Gotland) is adapted to tolerate dryness, strong wind, thin snow cover, frost and flooding, i.e. conditions that can also be expected to have occurred in the steppe-tundra environment at Sokli during MIS 5d. Several of the herbs of the alvar are considered glacial relicts (Berglund et al. 1996).

4.6 Regional (zonal) vegetation development during the warm MIS 5c interstadial period (ca 105–90 kyr BP)

Two zones are distinguished for MIS 5c, in which zone II represents forested conditions at Sokli and zone III indicates a return to more open vegetation (see also Figure 4-5).

In contrast to zone I in which pollen assemblages indicate the former presence of herb-dominated vegetation types in the Sokli area, the pollen spectra of zone II (depth interval 16.74–14.42 m in Figure 4-4) show forested conditions. Pollen of thermophilous trees and shrubs (*Quercus*, *Ulmus*, *Fraxinus*, *Carpinus*, *Tilia*, *Corylus*) reach low percentage values only and are considered as long-distance transported. Zone II includes three sub-zones (II-a, -b, -c) that relate to different phases in forest development. A return to more open vegetation is registered in zone III (depth interval 14.42–13.40 m).

4.6.1 Sub-zone II-a (16.74–16.02 m depth interval)

Pollen of tree birch (*Betula pubescens/pendula*) dominate in sub-zone II-a, with values reaching ca 40–65 % of the Total Sum of terrestrial pollen and spores (Figure 4-4). In addition, alder (*Alnus*) shows relatively high values (to 13–20 %). Conifer trees are represented by low pollen percentages only (< 15 %), with the exception of the lowermost sample in which pine (*Pinus*) is represented by 14 % and spruce (*Picea*) by 6 %. The shrub *Juniperus* reaches values up to 2 %. Lycopodiaceae and Polypodiaceae show the start of rising trends that continue through sub-zones II-a and II-b (lycopods) and II-a till II-c (polypods). Herbs that attain high percentage values in zone I (Poaceae, *Artemisia*, Chenopodiaceae, Brassicaceae) are absent in sub-zone II-a, or represented by low values only.

The dominance of tree *Betula* pollen suggests the presence of sub-arctic birch forest in the Sokli area. The relatively high values for *Pinus* and *Picea* at the base of the sub-zone are probably related to the open character of the birch forest allowing long-distance transported pollen to significantly contribute to the sum (e.g. Aario 1940, Prentice 1978, Hicks 1994). *B. nana* is also well-represented in the basal samples (20 %) and, although a local source from wetland vegetation cannot be ruled out, the high pollen percentages of dwarf birch might reflect the openness of the forest vegetation as well, particularly at the start of sub-zone II-a. *B. nana* is presently an important element in the birch tree-line ecotone in Fennoscandia.

It cannot be excluded that either pine or spruce formed part of the forest vegetation at Sokli during sub-zone II-a (as they might have been during zone I). It is likely that the dominance of *Betula* and *Alnus* pollen in sub-zone II-a is in part due to the local presence of a birch-alder carr along the abandoned stream channel. The over-representation of locally derived pollen might obscure the holistic view of the zonal vegetation composition. Macrofossils of conifer trees were not found in the sediment, but abundances of macrofossils of non-aquatic taxa, including tree-type *Betula*, are relatively low in sub-zone II-a, most probably because macro-remains were transported away as a consequence of flooding.

4.6.2 Sub-zone II-b (16.02–14.95 m)

In sub-zone II-b, pollen percentages of *Pinus* increase to ca 45 %, tree *Betula* pollen decrease to 15 %, and *Picea* is represented by 2 %. Comparison with recent pollen deposition in lakes in Finland (Prentice 1978, Seppä et al. 2004) suggests the presence of pine-birch forest in the Sokli area. *Alnus* is represented by seeds and, especially in the lower part of the sub-zone, by still relatively high pollen percentages (to ca 8–12 %). Counts of fern sporangia are also particularly high in the lower part of sub-zone II-b and, like alder, were probably present in the marshy forest bordering the stream channel.

The wingless seeds of alder found in the gyttja are probably those of *Alnus glutinosa*. Seeds of *Alnus incana* have small wings. Since the more fragile wings of tree birch were found attached to their fruit bodies and were well-preserved in the sediment, it is unlikely that the sturdier wings of *A. incana* had completely eroded away. We therefore suggest that the encountered *Alnus* seeds originated from *A. glutinosa* rather than from *A. incana*. *A. glutinosa* thrives in moist, nutrient-rich, swampy habitats and our paleo-botanical record, with for instance *Carex*, ferns and *U. dioica*, suggests that such conditions prevailed. The current northern limit of *A. glutinosa* is some 400 km south of Sokli. Although pollen of larch was not encountered during the analysis, single counts of *Larix* pollen have been made in the corresponding part of the MIS 5c gyttja in parallel borehole Sokli-900 (Helmens et al. 2000, 2007). Since *Larix* is generally very poorly represented in the fossil record, these single counts strongly suggest the presence of larch trees in the pine-birch forest in the Sokli area.

Whereas in sub-zone II-a, lycopods were mostly represented by spores of *Diphasiastrum*, sub-zone II-b shows relatively high spore percentages of *Lycopodium clavatum*. Similar values for *Diphasiastrum* are reported in pollen samples from surface lake sediments in the present-day birch forest, and similar values for *L. clavatum* are found in modern pollen samples from both the birch and pine-birch forests (Seppä et al. 2004). Sub-zone II-b additionally includes single spores identified as those of the thermophilous fern *Osmunda regalis*. *O. regalis* presently has a rare occurrence on shaded, moist soil along lakes and rivers in southernmost Fennoscandia.

4.6.3 Sub-zone II-c (14.95–14.42 m)

Picea pollen percentages increase to 5–8 %, especially at the expense of *Pinus*. Pollen values of tree *Betula* remain at around 15 %. Values of ca 10 % of *Picea* pollen are recorded in surface lake sediments from the present-day northern boreal forest in Finland where spruce forms an important element in the forest vegetation (Seppä et al. 2004). When taking into account that sedges and ferns from local wetland/shore vegetation contribute to the total sum of sub-zone II-c, with values of up to 20 % each, the pollen values of *Picea* in sub-zone II-c can be interpreted as evidence for the presence of boreal forest in the Sokli area.

4.6.4 Zone III (14.42–13.40 m)

Pinus pollen percentages continue to decrease to values of ca 15 %. *Picea* is represented by low percentage values only (< 1 %), except in the uppermost part of the zone where *Picea* increases to 5 %. Tree *Betula* reaches about 20 % and pollen of *Larix* is present as well. One seed of tree-type birch was found. Zone III is further characterized by pollen of *B. nana* (10 %), *Poaceae* (10 %) and of Cyperaceae (10–15 %); high spore percentages for both lycopods and polypods; the representation of several heliophilous herbs including *S. oppositifolia*, *Sanguisorba minor* ssp. *minor* and *Polemonium*; and tooth remains of lemming.

The fossil record suggests the presence of open, sub-arctic birch/larch forest limit vegetation in the Sokli area. *S. minor* has been reported as typical for the early part of the Late Glacial in The Netherlands (Hoek 1997). The species nowadays occurs sporadically on dry calcareous soils in southernmost Fennoscandia; it is an element in the alvar vegetation. *Lycopodium annotium* is relatively well-represented in zone III; similar spore percentages are recorded in surface lake samples from the birch tree-line ecotone in N Fennoscandia (Seppä et al. 2004). At the base of zone III, peak percentage values for several herbs (Asteraceae, Caryophyllaceae, Poaceae, Cyperaceae) and shrubs (*Salix*) are attributed to local sources along the stream channel.

4.7 Climate evolution during MIS 5d and 5c

4.7.1 Inferences on climate regime based on pollen

A pollen-based mean July air temperate reconstruction (T_{jul}) for MIS 5d-c at Sokli has been presented in Salonen et al. (2013). However, the poor compositional fit between fossil and calibration samples resulted in an unreliable summer temperature reconstruction as discussed below.

By far the largest distance between fossil and calibration samples was found with the MIS 5d assemblages, with typical north-eastern Eurasian glacial features (high Gramineae and *Artemisia* values, relatively little arboreal pollen). A close currently existing vegetation analogue is found in strong continental E Siberia, i.e. a climate regime not covered by our transfer functions.

A reliable T_{jul} reconstruction for MIS 5c is hampered by the large contribution of wetland and shore elements (e.g. Cyperacea, ferns) to the Pollen Sum. In our calibration data set, the selection of the sampling sites has been carefully controlled to restrict the amount of local pollen, with samples generally from central parts of lakes ca. 10–50 ha in area and with limited littoral vegetation (Salonen et al. 2012). However, during MIS 5c the depositional environment of our fossil data set does not meet these criteria, with fossil samples from sediments deposited in a fluvial setting (small oxbow lake and stream-channel deposits).

Although T_{jul} for MIS 5d-c could not be quantitatively reconstructed in detail using the palynological record, the sediment sequence for MIS 5d (indicating a braided river system) combined with the fossil pollen assemblages (recording the co-occurrence of steppe and tundra plants) point to a severe continental climate regime. Climate in the present-day areas with steppe-tundra vegetation is strong continental with large differences between summer and winter temperatures and low precipitation values. In E Siberia, mean January temperatures and annual precipitation values are as low as ca. – 40 °C and 200 mm, respectively (Shahgedanova 2008). A high sediment load (to be expected in a landscape with open herb-dominated vegetation) and/or low precipitation values explains the presence of a braided river system in the Sokli basin during MIS 5d.

The vegetation development that is recorded for MIS 5c, i.e. the replacement of pioneer birch vegetation by pine-dominated forest and then mixed boreal forest with spruce, greatly resembles the vegetation development during the present interglacial (Holocene) at Sokli (see session 3.4; see also Sorsa 1965, Hyvärinen et al. 1998). The additional presence of larch in the boreal forest during MIS 5c might, however, point to a more continental climate regime than at present. The present range of larch starts ca 500 km E of Sokli, where with increasing continentality *Larix sibirica* becomes an important component of the Russian northern taiga and the vegetation near the arctic and alpine forest limits. Furthermore, in a detrended correspondence analysis (DCA) ordination, the MIS 5c fossil pollen samples show a better fit with west Russian calibration samples compared to the local, Fennoscandian calibration set (Salonen et al. 2013).

Larix is generally very poorly represented in the fossil record. Its pollen is known to have short-distance dispersal from the pollen-producing tree, poor preservation (Gunin et al. 1999, MacDonald et al. 2000) and indistinct morphological features. Remarkably, only single larch pollen grains have been encountered in modern lake samples from the boreal forest and forest tundra in north-western Russia where larch is an important component in the zonal vegetation (S. Salonen, pers. comm.). Thus, the absence of pollen of *Larix* in the braided river deposit of MIS 5d does not exclude its presence at Sokli at this time. In eastern Siberia, open larch forest with steppe communities and thickets of birch and pine stretches south of the steppe-tundra, where larch has a high resistance to extremely low temperatures and effects of permafrost changes (Tishkov 2008).

4.7.2 Chironomid-based T_{jul} reconstruction

The chironomid record obtained on the MIS 5d-c sediments (Figure 4-6) has been used in detail to reconstruct mean July air temperatures (T_{jul}) (Figure 4-7A). We here use the zonation as in Engels et al. (2010).

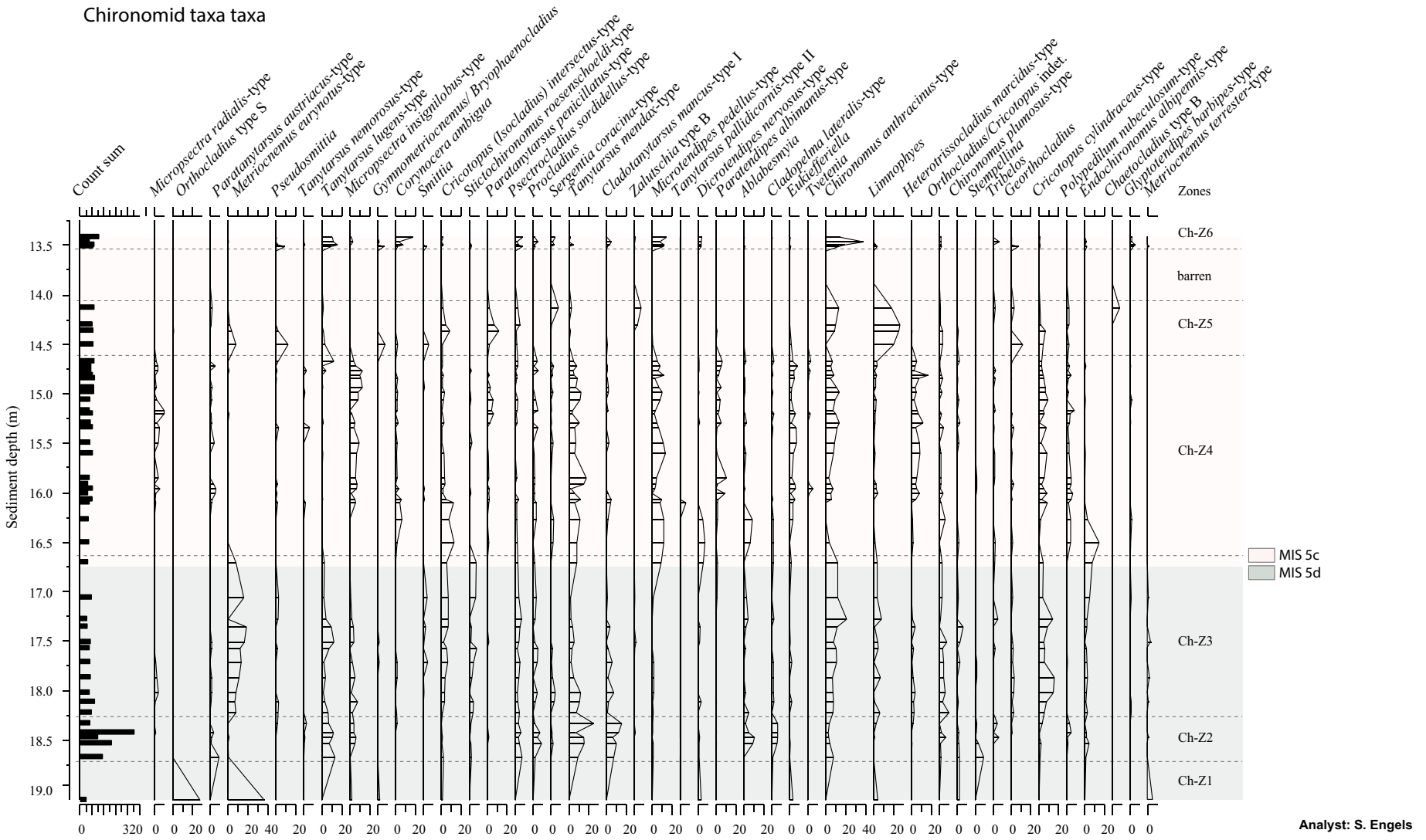

Figure 4-6. *Percentage diagram of the major chironomid taxa (i.e. with abundances of ≥ 5 % for at least one sample) from the MIS 5d-c deposit in the Sokli B-series borehole. The chironomid taxa are ordered according to weighted average (WA) optima in the Norwegian calibration set, with taxa with the lowest optima plotted to the left. The three right-most taxa are not present in the calibration set. Adapted from Engels et al. (2010).*

Of the 103 chironomid taxa that are identified in the MIS 5d-c sediment record, 13 are not represented in the modern calibration set. Most of these taxa only have single occurrences (e.g. *Stilocladius*, *Symposiocladius*; not presented in Figure 4-6) in the fossil record, but three taxa occur in higher percentages (i.e. *Chaetocladius*-type B, *Glyptotendipes barbipes*- and *Metriocnemus terrester*-types). On average 98 % of the identified chironomid remains of the fossil samples are used in the reconstruction (range: 89–100 %). Fourteen taxa have a Hill's $N_2 < 5$ (Figure 4-7C), and are here defined as not being well-represented in the Norwegian calibration set. *Stempellina* has an abundance of 3.0–8.4 % in the lower samples of zone Ch-Z2, and has a Hill's N_2 of 4.6. *Stempellinella* is a warm stenothermic taxon (Brooks et al. 2007) and it occurs in parts of the record where inferred temperatures are high. *Georthocladius* and *Gymnometriocnemus/ Bryophaenocladius* are present in high percentages in the lowermost sample of zone Ch-Z5, and both taxa are not well-represented in the modern calibration set either (Hill's $N_2 = 1.0$ and 2.8, respectively). The depositional environment during the formation of this sample was interpreted as (semi-) terrestrial or very shallow lacustrine, while the calibration set only includes purely lacustrine environments. The temperature inference for this sample might be influenced by the poor representation of 15 % of the fossil assemblage in the calibration set as well as the differences in the environment between the fossil site and the modern lakes incorporated in the calibration set.

Figure 4-7D shows that no fossil sample has a close analogue in the modern data, and only the lowermost sample scores as a "no good" analogue. However, all dominant taxa of the fossil record are well-represented in the Norwegian calibration set, and although the relative abundances of the fossil samples are not well-reflected in the Norwegian calibration set, WA-PLS models can perform relatively well in poor analogue situations (Birks 1998). Only two samples in the fossil record had a very poor fit with temperature if added passively in a CCA with July air temperature as the only constraining variable (Figure 4-7E) and besides these two samples, no samples show a poor fit with temperature. The lowermost sample of zone Ch-Z5 shows a very poor fit to temperature, and has been discussed above as probably being deposited in a (semi-) terrestrial or very shallow lacustrine environment.

Metriocnemus eurynotus-type and *Orthocladius*-type S are the dominant chironomid taxa in the lowermost part of the MIS 5d record (zone Ch-Z1 (19.30–18.69 m) in Figure 4-6). Both taxa rank amongst the most cold-adapted taxa in the Norwegian calibration set, where *Orthocladius*-type S is currently common on Svalbard and is known to occur frequently in lacustrine deposits dated to the Younger Dryas in Norway (Brooks et al. 2007). However, although *M. eurynotus*-type is associated with cold temperatures in the Norwegian calibration set, it is also known to occur in temperate regions such as North Carolina (Epler 2001). Some of the other taxa that occur in lower abundances (0–5 %) in this part of the sequence (e.g. *Micropsectra insignilobus*-type) can be considered as typical cool-temperate to sub-arctic taxa (e.g. Brooks and Birks 2001). The chironomid-inferred temperature record shows a reconstructed mean July air temperature (T_{jul}) of +6.6 °C (Fig 4-7A). However, the chironomid assemblage shows a very poor fit to temperature (Figure 4-7E) and the reconstructed depositional environment (shallow water body on a former floodplain) is not well-represented in the Norwegian calibration set, even though this sample shows a closer modern analogue than the other samples in the sequence (Figure 4-7D). Therefore, the quantitative temperature inference should be treated with caution.

Starting from 18.69 m (zones Ch-Z2 and -Z3), there is a marked increase in the concentration of chironomids (Figure 4-1). Many of the abundant chironomid taxa indicate an environment with temperate conditions (e.g. *Ablabesmyia*, *Cladotanytarsus mancus*-type I*, Cladopelma lateralis*-type), although a few cold-stenothermic taxa such as *Paratanytarsus austriacus*-type are present. At 18.24 m, *Metriocnemus eurynotus*-type, a taxon that is able to tolerate cold climate conditions, returns to the chironomid fauna. However, taxa indicative of intermediate to warm environments are also present in this part of the record (e.g. *Cricotopus cylindraceus*-type, and *C. (Isocladius) intersectus*-type). The chironomid-fauna of zone Ch-Z3 (16.60–18.24 m) might indicate a slight decrease in temperature when compared to Ch-Z2 (18.24–18.69 m); T_{jul} during Ch-Z2 reaches +12–13 °C, and during Ch-Z3 is around +12 °C.

The lakes were probably situated on a floodplain during zones Ch-Z1 till -Z3 (MIS 5d), and this might have influenced the chironomid-based temperature estimates. Engels et al. (2008b) studied 13 floodplain lakes from N Finland and compared the modern chironomid fauna of these lakes to 20 lakes that are isolated from riverine influence. Their results show that in their study area there was no major difference between temperature-inferences derived from chironomid-assemblages from floodplain lakes when compared to lakes that are un-affected by running water. The authors state that floodplain

lakes provide suitable alternatives for chironomid-based climate reconstructions when other records are unavailable. This suggests that the samples from Ch-Z2 and -Z3 might be used to infer quantitatively past July air temperatures from the chironomid assemblages.

Endochironomus albipennis-type, *Ablabesmyia*- and *Dicrotendipes nervosus*-type are abundant in the lowermost samples of zone Ch-Z4 (16.60–14.66 m), and these taxa are characteristic of high July air temperatures in the Norwegian calibration set. Increasing temperatures can be seen in the chironomid-inferred temperature record already at 16.75 m (i.e. at the transition from MIS 5d to 5c), with a sharp increase of T_{jul} to above +15 °C at 16.60 m. After the peak-temperatures inferred at 16.60 m, the reconstruction shows a gradual decline to temperatures of ca +11 °C reached in the uppermost part of the MIS 5c record.

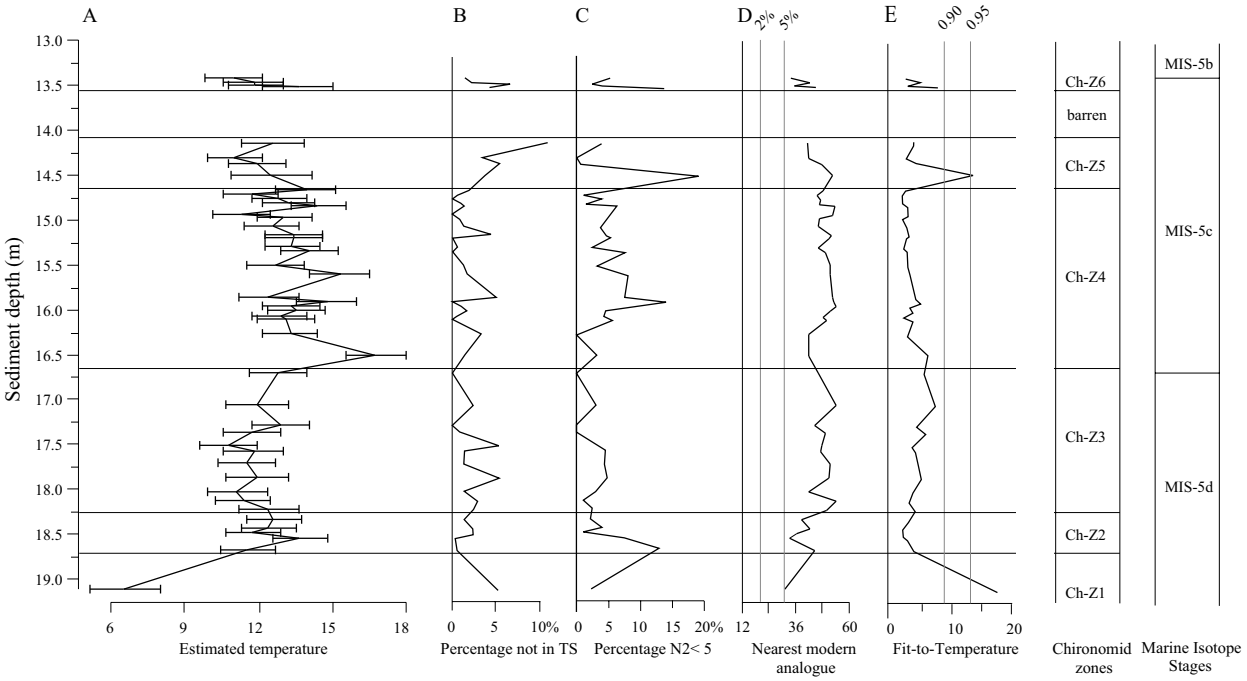

Figure 4-7. ***A*** *Chironomid-inferred mean July air temperatures (°C) together with sample-specific estimated standard errors (eSEPs) as estimated through bootstrapping (1000 cycles);* ***B*** *percentage of identified fossil chironomid head capsules not present in the Norwegian calibration set;* ***C*** *the percentage of identified fossil chironomid head capsules that are rare in the Norwegian calibration set as defined by a Hill's $N_2 < 5$;* ***D*** *nearest modern analogues in the Norwegian calibration set (squared χ2-distance), the vertical lines indicate the 2nd and 5th percentile of all squared χ2-distances in the Norwegian calibration set and are defined here as "no close" and "no good" analogues respectively (after Birks et al. 1990);* ***E*** *goodness-of-fit of the fossil samples to temperature, the vertical lines indicate the 90th and 95th percentile in residual distances of the modern samples to the first axis in a constrained CCA, and are defined here as a "poor" and "very poor" fit respectively (e.g. Birks et al. 1990, Heiri et al. 2003). Adapted from Engels et al. (2010).*

4.7.3 Minimum T_{jul} reconstruction using plant indicator taxa

With the initiation of the gyttja layer at ca 16.75 m depth (start of MIS 5c), the species diversity relieved by macrofossils significantly increases when compared to the underlying minerogenic sediments (MIS 5d) which contained very few macroscopic plant remains. Most of the plant fossils were intact and well-preserved and thus are unlikely to be re-deposited interglacial material. Furthermore, the local environmental conditions reconstructed based on the thick gyttja deposit of MIS 5c age, i.e. a relatively small oxbow lake that remained flowed during the entire process of infilling, are very different from those inferred from the diatom gyttja marker horizon of Eemian Interglacial (MIS 5e) age in the Sokli basin. The latter was deposited in a relatively large lake bordered by a fringe of wetland vegetation (Helmens et al. 2000, Plikk et al. 2016). Our results therefore strongly support earlier conclusions made by Helmens et al. (2000, 2007) that the organic layers in the Sokli sequence represent individual and successive environmental developments and are not the result of re-deposition of older sediment as has been earlier suggested by Forsström (1990).

A minimum T_{jul} reconstruction for MIS 5d-c based on plant indicator species is given in Figure 4-8 (B). When a sample contained several indicator species, the species that requires the highest minimum July temperature was used in the figure to infer a minimum temperature value. Not all samples contained such indicator species. Accordingly, the reconstruction (curve) is not contiguous.

High T_{jul} values of up to at least +12–14 °C (compared to the present-day value of ca +13 °C) are indicated by the botanical macrofossil record for MIS 5d. These high summer temperatures are in line with the presence of conifer and birch trees in the steppe-tundra vegetation, as inferred based on findings of tree-type *Betula* seeds and conifer bark remains (session 4-5), and can be expected under strong continental climate conditions.

The macrofossil assemblages encountered in the MIS 5c deposit, with the representation of e.g. Nymphaeaceae (Aalbersberg and Litt 1998), *Cristatella* (Økland and Økland 2000) and perch fish (*Perca fluviatilis*; Hokanson 1977), indicate that the environment at Sokli during MIS 5c was boreal. Many of the species, including *Najas tenuissima*, *Elatine triandra*, *Ranunculus sceleratus*, *Typha* spp., *Crassula aquatica*, *Glyceria lithuanica*, *Rhynchospora alba* and *Bidens tripartita,* currently have considerably more southern distributions in Finland (Figure 4-2) and worldwide (e.g. Hultén and Fries 1986). For example, the northernmost occurrences of *E. triandra* and *N. tenuissima* in Finland today are, respectively, ca 150 and 580 km south of Sokli (Lampinen and Lahti 2007). None of the key species in Figure 4-2 grows as far north as Sokli today, even though suitable habitats such as wet, nutrient-rich fens and lake shores are available. The MIS 5c macrofossils record rich plant assemblages related to an overall fluvial depositional environment (Figure 4-5) and reconstruct min. T_{jul} values of +15–16 °C (Figure 4-8B).

4.8 Discussion of the MIS 5d and 5c results

According to the marine oxygen isotope stratigraphy, MIS 5d and MIS 5c lasted in the order of ca 10 kyr each (Figure 1-1). MIS 5d roughly corresponds in time to the cold Herning Stadial in the northwest European mainland stratigraphy and Savukoski 1 in the stratigraphy at Sokli (N Finland). MIS 5c roughly corresponds to the warm Brørup Interstadial and Sokli I, respectively (Figure 1-1).

The extensive multi-proxy data set obtained on the Sokli sediments has allowed us to reconstruct in great detail environmental and climate conditions for MIS 5d-c (Figure 4-8). These reconstructions, and their implications for the climate and glaciation history of the Early Weichselian, are discussed below.

4.8.1 Environmental and climate conditions during MIS 5d

MIS 5d (Savukoski 1) at Sokli was characterized by steppe (with e.g. Poaceae, *Artemisia*, Chenopodiaceae) - tundra vegetation (*Betula nana*) with scattered conifers and tree birch, and a braided river system, suggesting a strong continental climate regime (Figure 4-8) with short warm summers, long cold winters and low precipitation values. Herbaceous taxa such as *Armeria maritima* and *Centaurium* may indicate soils with high salt concentrations. The herb *Inula salicina* is also recorded and is a typical "alvar" element. Its presence in the terrestrial vegetation during MIS 5d may reflect the extreme conditions, such as dryness, strong wind, thin snow cover, frost and flooding, that characterize the present-day environment of the alvar vegetation.

In general, our chironomid-inferred T_{jul} values for MIS 5d are slightly lower than those estimated by plant indicator species (Figure 4-8). The high T_{jul} values of up to at least +12–14 °C (compared to the present-day value of ca +13 °C) indicated by the botanical macrofossil record for MIS 5d are in line with the presence of conifer and birch trees in the steppe-tundra vegetation, and conform to strong continental climate conditions. The difference between the T_{jul} values based on the plant and chironomid records might be related to the choice of the geographic source area of the modern chironomid-temperature calibration set. The application of a transfer function based on calibration data from Siberia, instead of Norway-Svalbard, has produced July temperatures more in line with the macrofossil-inferred values (A. Self, pers. comm.). This can be explained by the fact that the same chironomid taxa require higher July temperatures under more continental conditions as a result of e.g. shorter summer duration (Self et al. 2011). The choice of transfer functions in paleo-climatological reconstructions, using the Sokli studies as an example, is discussed in more detail in Engels et al. (2014).

Steppe-tundra vegetation was widespread in Europe during the cold stages of the Weichselian (see e.g. Granoszewski 2003). Presently, steppe-tundra associations are rare. The co-occurrence of steppe and arctic-alpine species are described for the Chukotka Peninsula in NE Siberia (Yurtsev 1981 in Zlotin 2008) and for west-central Greenland close to the Greenland Ice Sheet (Böcher 1954 in Pennington 1980).

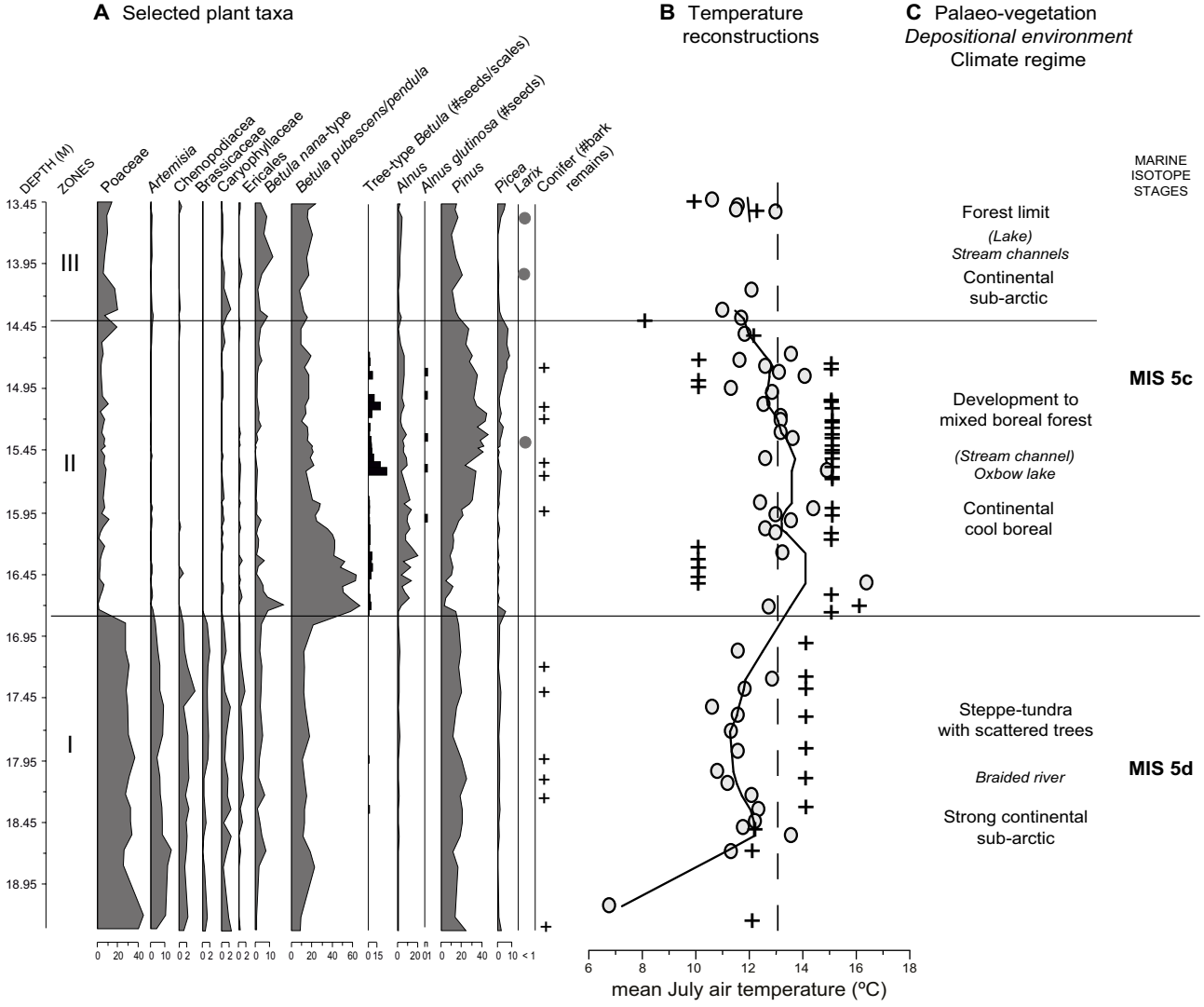

Figure 4-8. *A shows a selection of terrestrial pollen and plant macrofossil data from the MIS 5d-c deposit at Sokli;* ***B*** *gives quantitative estimates of T_{jul} based on chironomids and minimum T_{jul} inferred from plant indicator species; and* ***C*** *summarizes inferred paleo-environmental conditions. The present-day T_{jul} of +13 °C is indicated by a hatched line for reference. The chironomid-inferred temperatures values are given with a locally weighted scatterplot smoother (LOWESS, span = 0.20; Cleveland 1979) applied to the reconstructed values; maximum bias is 1.05 °C. From Helmens et al. (2012) with permission from Quaternary Science Reviews.*

Although studies on Early Weichselian sediments are relatively numerous in central Europe, only few studies have provided quantitative paleo-climate data. Climate parameters have been reconstructed quantitatively based on fossil plant data of MIS 5d age at Gröbern in central Germany (Kühl et al. 2007) and at several sites in the northern Alpine foreland (Klotz et al. 2004), and towards the far east at Lake Baikal in central Russia (Tarasov et al. 2005).

Kühl et al. (2007) employed a multivariate probabilistic approach to pollen and plant macrofossils to reconstruct temperature and precipitation changes. This approach involves taxon-specific probability density functions (pdf's) that describe the plant-climate relation of individual species. Their reconstruction shows a major drop in mean January temperature of up to 20 °C for the transition from MIS 5e (Eemian Interglacial; Figure 1-1) to MIS 5d. July temperatures remained high enough (i.e. around +15 °C) to support boreal trees. The study concludes that a decrease in precipitation (although difficult to reconstruct) in combination with lowering in January temperatures most probably were major factors driving vegetation changes during the Eemian/Early Weichselian transition in central Germany (Kühl et al. 2007).

Klotz et al. (2004) combined two different climate reconstruction methods, a modern analogue technique and a mutual climate range approach, on high-resolution pollen records from the northern Alpine foreland. A distinct climate evolution is reconstructed across cold MIS 5d that included, at first, an intensification of continentality as the mean temperatures of the coldest month (MTC) fell to an average minimum of ca –15 °C, and the mean temperatures of the warmest month (MTW) remained stable or even increased. Following an intra-stadial amelioration, which is mostly documented by a rise in winter temperatures, another reduction in winter temperatures with mostly stable or decreasing summer temperatures is observed. Most severe conditions during the earliest part of MIS 5d seem also to be recorded at the Oerel site in north Germany (Behre 1989) and at Sokli (north Finland) by the deposition of sterile fluviatile sands and gravels.

Using an extensive surface pollen data set from northern Eurasia, and combining reconstructed pollen-based biomes (main vegetation types) with current climate data, Tarasov et al. (2005) infer cool and very dry continental conditions for MIS 5d at Lake Baikal, with MTC and MTW in the ranges of ca –29 °C and ca +15 °C, respectively, and annual precipitation at ca 250 mm.

Additionally, coleoptera data, periglacial structures and paleo-botanical evidence from various sites on the northern European mainland and in the U.K. have suggested a severe continental climate regime with low winter temperatures and low precipitation values for MIS 5d (summarized in Aalbersberg and Litt 1998).

It should be stressed that the climate reconstruction methods that have been employed to infer quantitatively paleo-climate values are based on present-day plant/insect-climate relationships. The basic assumption throughout is methodological uniformitarianism (Birks and Birks 1980, Birks 2003), namely that modern-day observations and relationships can be used as a model or analogue for past conditions and, more specifically, that fossil taxa – climate relationships have not changed with time, at least in the Late Quaternary (see further Birks and Seppä 2004). Working on time-scales of 100 000 years, however, these relationships might not have been always valid in the past due to non-analogue climates and/or vegetation types. Furthermore, detailed reconstructions of the climate parameters are further hampered by a possible influence of grazing by large herbivores on the former extensive presence of steppe plant communities during the Weichselian stadials (e.g. Guthrie 1982).

4.8.2 Environmental and climate conditions during MIS 5c

Prolonged sedimentation in an oxbow lake, terrestrialization, and return to stream channel deposition is recorded in great detail at Sokli for MIS 5c (Sokli I). The most compelling result of our study is the similarity in forest development between MIS 5c and the Eemian (MIS 5e) (see Section 5.3) and Holocene Interglacials at Sokli (see under 3.4). All three time-slices show the replacement of pioneer birch vegetation by pine-dominated forest and then mixed boreal forest with spruce (Figure 4-8). Earlier reconstructions based on correlation of poorly-dated bio-stratigraphic fragments from Fennoscandia with the European mainland pollen sequence had suggested the presence of tundra vegetation at Sokli during MIS 5c. Furthermore, according to these studies, sub-arctic birch woodland occupied areas presently covered by mixed boreal forest south of Sokli, with the location of the conifer (pine) tree-limit being situated in the present temperate southern boreal zone in south Fennoscandia (Donner 1995 and references therein).

Our chironomid-inferred T_{jul} values for MIS 5c are generally a few degrees lower compared to those estimated by plant indicator species. The latter reconstruct minimum T_{jul} values of +15–16 °C (Figure 4-8). It is possible that the former suffer from the so-called "edge-effect"; since the inferred-temperature values are close to one of the edges of the temperature gradient of the modern calibration set (i.e. +16 °C), the chironomid-inferred T_{jul} might therefore under-estimate the true paleo-temperatures. The low macrofossil-based minimum T_{jul} values for the early part of the MIS 5c forested phase most probably reflect the overall scarcity of macrofossil remains in the sediment during this early infilling of the oxbow lake.

The higher-than-present summer temperatures reconstructed at Sokli during MIS 5c, the presence of larch, as well as the relatively good fit between the MIS 5c fossil pollen samples and the west Russian calibration samples (Salonen et al. 2013), suggest a higher degree of continentality during MIS 5c compared to the Holocene. The present range of larch starts ca 500 km E of Sokli, where, with increasing continentality, *Larix sibirica* becomes an important component of the Russian northern taiga and the vegetation near the arctic and alpine forest limits. *Larix* fossil remains are absent from the Holocene record at Sokli and from Finland overall.

A stronger continentality during MIS 5c, compared to MIS 5e and the Holocene, is also indicated by the fossil record from the European mainland. It is factors related to increased continentality, including low winter temperatures, low precipitation values, thin snow cover, frost, and a shorter growing season, that probably caused the absence of temperate trees in central Europe during MIS 5c, except for the W part of France (Helmens 2014 and references therein). By applying the mutual climatic range (MCR) method to fossil Coleoptera from the Oerel site in north Germany, Behre et al. (2005) have reconstructed continental conditions for MIS 5c with temperatures of the warmest month in the range of ca +16–19 °C and the coldest month at ca –8 to –14 °C. Similar temperature values (July temperatures of ca +17 °C and January temperatures in the range of ca –10 to –15 °C) are inferred in central Germany at Gröbern (Kühl et al. 2007). Aalbersberg and Litt (1998) reconstruct mean January temperatures of ca –13 °C for MIS 5c based on the simultaneous occurrence of *Calluna vulgaris* and *Larix* in the fossil records from several central European sites. Similar as noted under Section 4.8.1, however, the climate reconstructions might be hampered by non-analogue paleo-climates and/or -vegetation types as well as grazing by large herbivores.

Our T_{jul} values reconstructed for MIS 5c at Sokli are remarkably similar to those reconstructed for Germany by Behre et al. (2005) and Kühl et al. (2007) and suggest weaker N-S summer temperature gradient over N Europe during MIS 5c than at present. The reasons for the lower temperature gradient during MIS 5c are possibly contemporary orbital forcing, with several feedback mechanisms amplifying the primary effects of orbitally induced insolation, as discussed in Väliranta et al. (2009) and Engels et al. (2010). Fossil data from Greenland indicate that July temperatures during MIS 5c were more than 4 °C higher than today (Bennike and Böcher 1992). In contrast, Guiter et al. (2003) have suggested a steep climate gradient during the Early Weichselian warm intervals, with a low intensity of warming at high European latitudes due to a weakening of the Gulfstream, a lower sea level and a cold Norwegian sea.

4.8.3 Changes in degree of continentality during MIS 5d and 5c

Despite the very different zonal vegetation types that have been reconstructed for MIS 5d and MIS 5c in Europe, summer temperatures during this time period (ca 115 to 95 kyr BP) remained largely unchanged. Differences in climate between MIS 5d and 5c were mostly in terms of winter temperatures with lowest winter temperature values during MIS 5d. The role of seasonality in the climate shifts of the Weichselian in the N Atlantic region, with winter-time cooling and drying during cold stadial episodes, is explored in detail by Denton et al. (2005). The latter paper mentions as most likely source of this winter-climate leverage, the spread of sea-ice over the N Atlantic Ocean in response to a shutdown (or reduction in strength) of the AMOC (Atlantic Meridional Overturning Circulation) (Rahmstorf 2002). Denton et al. (2005) note that when the N Atlantic Ocean is ice-covered, the expanse of the N Hemisphere from northwest Greenland to eastern Asia is essentially continental and hence susceptible to large winter-time temperature changes.

5 Eemian Interglacial (MIS 5e) environmental and climate reconstructions for northeastern Fennoscandia

5.1 Materials and methods

5.1.1 Stratigraphy and dating

The present study was conducted on a new borehole, Sokli 2010/4, that was cored by percussion drilling (Figure 5-1) at a site located between borehole Sokli B-series from the central part of the Sokli basin and boreholes 901 and 902 from the basin´s margin (Helmens et al. 2000, 2007). In addition, several samples from core 901 were re-analyzed for pollen (Helmens et al. 2000). The latter core records the final birch phase that is missing (truncated) at the site of borehole Sokli 2010/4. The borehole location is indicated in Figure 2-1 and a simplified lithological log is given to the left in Figure 5-2.

The Eemian diatom gyttja is found between 16 and 25 m below the surface at the Sokli 2010/4 core location. The Sokli basin has been glaciated several times since the Eemian, probably compressing the Eemian lake deposit. As such, its original thickness might have been greater than the nine metres recorded.

Figure 5-1. *Drilling of the Sokli 2010/4 borehole by the Geological Survey of Finland. A core slice of the Eemian diatom gyttja sediment is shown in the foreground.*

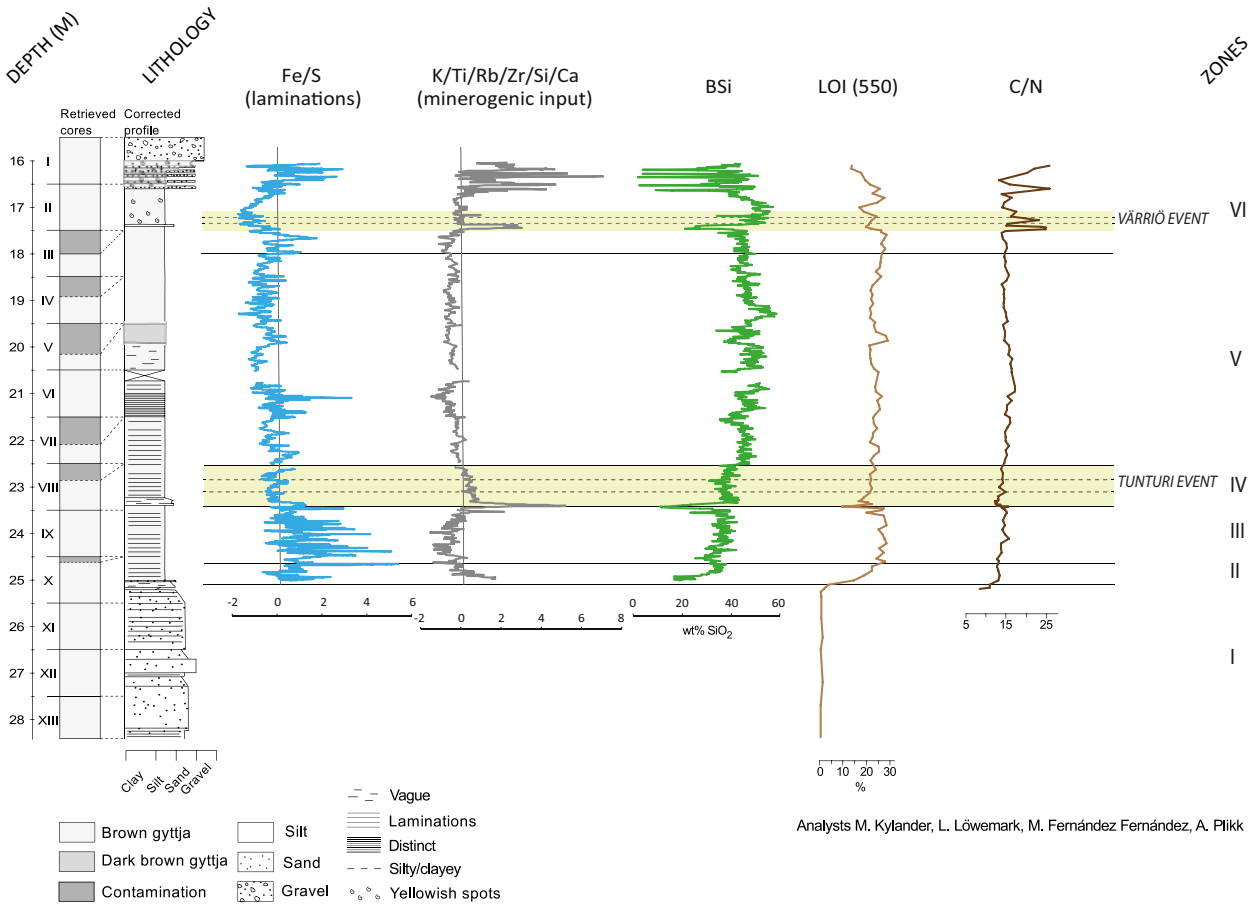

Figure 5-2. *Sediment characteristics obtained from the sediments of Eemian age in the Sokli 2010/4 borehole.*

The Eemian diatom gyttja deposit at Sokli occurs as a marker horizon near the base of the Sokli sequence. Its interglacial pollen content was first noted by Ilvonen (1973), who correlated it with the Eemian Interglacial. Stratigraphic studies of the overlying Weichselian sediment sequence, and absolute dating control, have supported the Eemian age assignment (Helmens et al. 2000, 2007). The diatom gyttja has been bracketed by TL and IRSL dating to > ca 110 and < ca 150–180 kyr (Helmens et al. 2000), and by OSL dating on quartz (using SAR dose protocol) to > ca 95 kyr (Helmens et al. 2007, Alexanderson et al. 2008). The Eemian at Sokli has been defined as the Nuortti Interglacial (Helmens 2014; Figure 1-1).

5.1.2 Proxy analyses

Subsampling

The flow-through coring device that was used during the percussion drilling allowed contamination (sand and gravel) to enter the 1 m long and 5 cm thick PVC sampling tubes before reaching the Eemian diatom gyttja bed. The diatom gyttja had to push out this contamination, which caused compression of the diatom gyttja to various degrees. The contact between the diatom gyttja and the contamination was usually sharp, and the contamination was easily removed in the laboratory. The compressed core sections are shown along-side the lithological column in Figure 5-2. In total 12 m of sediment was recovered, including 9 m of Eemian diatom gyttja and 3 m of underlying minerogenic sediment. The core sections were split lengthwise, lithologically described and scanned by XRF before subsampling. The core halves from the diatom gyttja were subsampled into 50 respectively 100 separate samples, originally corresponding to 2 and 1 cm sediment intervals. The minerogenic sediment was subsampled at lower resolution. The subsampling was carried out by Anna Plikk (Stockholm University).

Biogeochemical analyses

The diatom gyttja was scanned using an Itrax XRF Core Scanner. The XRF analyses were performed using a molybdenum tube set at 30 kV and 45 mA with a step size of 2.5 mm and a dwell time of 60 s (Croudace et al. 2006). Based on analytical performance (counting statistics), reliable data was acquired for Si, S, K, Ca, Ti, Mn, Fe, Rb, Sr and Zr. All data were normalized to the (incoherent+coherent) scattering to remove various instrumental effects and then smoothed using a 5-point running mean to capture the main shifts. Elemental correlations were made in order to quantify the strength of association between pairs of elements in the dataset. The XRF scanning was carried out by Ludvig Löwemark and the interpretation of data was made by Malin Kylander (Stockholm University).

Biogenic silica (BSi) concentration was quantified by the use of Fourier-transform infrared spectroscopy (FTIRS) (Rosén et al. 2010). 900 subsamples from the gyttja were analyzed by diffuse reflectance FTIRS using a VERTEX 70 FTIR spectrometer (Bruker Optics). The top of the underlying minerogenic sediment was also analyzed. All spectra were pretreated to minimize the spectral variation not related to the sample properties. OPUS 5.5 (Bruker Optics Inc.) and SIMCA-P+ 12.0 (Umetrics) were used for the visualization and pretreatment of the FTIR spectra. An independent calibration model for BSi was chosen for the Sokli data (Meyer-Jacob et al. 2014). Thirty samples were selected for conventional BSi measurements and used for validation of the model. The correlation between FTIRS-inferred and wet-chemical measured BSi concentrations using this model has a square correlation (R2) of 0.95 and a root-mean-square error of prediction (RMSEP) of 4.8 wt%. The BSi analysis was performed by María Fernández-Fernández (Umeå University).

Loss-on-ignition (LOI) and carbon/nitrogen (C/N) analyses were performed at 10 cm intervals in the diatom gyttja sequence, except for the depth intervals 23.49–23.20 m and 17.52–17.28 m which were analyzed at 2–4 cm intervals. Additionally, the minerogenic sediment was sampled for LOI at 30–70 cm interval. Samples for LOI were prepared and analyzed following Heiri et al. (2001). Using ca 1 cm^3 of sediment, organic and carbonate content was calculated after combustion at 550 °C for 4 hours and at 950 °C for 2 hours. Total organic carbon (TOC) and total nitrogen (TN) content were measured with a Carlo Erba NC2500 Elemental Analyzer. Inorganic carbon was removed with HCl (10 %). The C/N molar ratio was calculated and used as an indication for the origin of organic matter (Meyers and Teranes 2001). These analyses were performed by Anna Plikk.

Siliceous microfossil analysis

Samples were prepared at 10 cm intervals from the diatom gyttja, except for the depth intervals 23.49–23.20 m and 17.52–17.28 m where 2–5 cm intervals were used. The samples were processed using standard techniques (Battarbee et al. 2003). The residue was mounted in Naphrax® and analyzed using oil immersion optics at ×1000 magnification. In total, 100 samples were analyzed with a minimum counting sum of 400 diatom valves. From the minerogenic sediment, six samples were analyzed, but diatoms were rare. Diatom identification was mainly based on Krammer and Lange-Bertalot (1991a, b, 2008a, b, 2010a, b) and an updated taxonomic nomenclature (AlgaeBase, Guiry and Guiry 2016) was used. An environmental scanning electron microscope (ESEM) was used to clarify the taxonomy of certain taxa. Percentages were counted from the sum of all diatoms. Chrysophyte cysts and phytoliths were counted as well and percentages were calculated from the sum of all siliceous microfossils. The analysis was performed by Anna Plikk.

Pollen/spores, non-pollen palynomorph (NPP), and stomata analyses

Samples were prepared from 1 cm^3 subsamples, using KOH, sieving (212 µm mesh), Na-pyrophosphate, acetolysis, and finally a bromoform heavy-liquid treatment to remove silicate. *Eucalyptus* markers were added to estimate absolute microfossil concentrations. The residual was mounted in glycerol and counted using a light microscope. A mean of 401 (min = 220.5, max = 526) terrestrial pollen and spore grains were counted from each sample. In addition to pollen and spores, conifer stomata (Sweeney 2004) and various NPP's (Komárek and Jankovská 2001, van Geel 2001) were counted. Percentages for pollen, spores and NPP's were calculated based on the Total Sum which consists of the sum of all terrestrial pollen and spores. A total of 217 samples were counted, mostly at 4 or 6 cm intervals, and at 2 cm interval in sections with rapid species turnover, providing a generally sub-centennial resolution across the Eemian. The minerogenic sediment at the base of the diatom gyttja deposit was analyzed at lower resolution. The analyses were performed by Sakari Salonen and Niina Kuosmanen (University of Helsinki).

Macrofossil analysis

Sediment subsamples of ca 5 cm^3 were prepared at 20 cm intervals in the diatom gyttja sequence, except for depth intervals 23.49–23.20 m and 17.52–17.28 m, which were subsampled at 5 cm interval. The sediment was sieved using a 100 µm mesh under running water and the residue was examined using stereo and high-magnification light microscopes. The analysis was performed by Minna Väliranta (University of Helsinki).

5.1.3 Zonation of proxy diagrams

A zonation of the terrestrial pollen and spore diagram was performed using a multivariate regression tree (MRT; De'ath 2002), with fossil assemblages as the multivariate response and core depth as the sole predictor (see also Simpson and Birks 2012). The size of the MRT was selected by cross-validation, using the smallest tree within one standard error of the best tree. The MRT was implemented using the R package MVPART (version 1.6-1; Therneau and Atkinson 2013). This zonation was applied to all proxy data and was performed by Sakari Salonen (University of Helsinki).

5.1.4 Quantitative climate reconstructions

We synthesized a new pollen-climate calibration data-set based on the European Modern Pollen Database (EMPD; Davis et al. 2013). We selected all EMPD lake samples but excluded samples from semi-arid and dry-summer climates, to focus the pollen–climate modelling on taxa which are likely components in the northern European vegetation during the Eemian Interglacial. The final dataset includes 807 lakes (Figure 5-3). The EMPD species data for the selected samples were synthesized into 73 terrestrial pollen and spore types. Climate data for the pollen samples were extracted from CRU CL v. 2.0 climate grids (New et al. 2002) with the RASTER library (Hijmans 2014), using bilinear interpolation based on four closest grid cells and lapse-rate corrected (6.4 °C/km) based on the difference between site elevation and grid cell elevation. A full description of this calibration dataset is given in Salonen et al. (2014).

Eemian paleo-climate reconstructions were prepared for mean July temperature (T_{jul}) and mean January temperature (T_{jan}). These variables were chosen due to their ecological influence on vegetation and their low correlation (r = 0.27) in the calibration data which facilitates the modelling of the independent effects of each variable (cf. Juggins 2013). Partial CCA (pCCA; implemented in VEGAN version 2.2-0 (Oksanen et al. 2014)) was used to test the independent effect of T_{jul} and T_{jan} in the calibration data, using either T_{jul} or T_{jan}, and in addition a second ecologically significant variable, annual water balance, as covariables. The pCCA was significant (p = 0.001) for both T_{jul} and T_{jan}.

Six different calibration methods were used to create pollen–climate models: weighted averaging (WA; Birks et al. 1990) and weighted averaging-partial least squares (WA-PLS; ter Braak and Juggins 1993) regression, maximum likelihood response surfaces (MLRC; Birks et al. 1990), the modern analogue technique (MAT; Overpeck et al. 1985), and two machine-learning approaches based on regression tree ensembles, the random forest (RF; Breiman 2001) and the boosted regression tree (BRT; De'ath 2007). The reconstruction algorithms were implemented in R (version 3.0.3; R Development Core Team 2014) using the packages GBM (version 2.1; Ridgeway 2013), RANDOMFOREST (version 4.6-10; Liaw and Wiener 2002), and RIOJA (version 0.8-7; Juggins 2012). Further details about the calibration models are presented in Table 5-1.

Reconstruction errors, estimated by 10-fold cross-validations, are in the range of 1.1–2.1 °C for T_{jul} and 1.8–3.4 °C for T_{jan}, depending on model (Table 5-1). Although the model performance was assessed by cross-validation, there is a possible further error component due to fossil samples lacking good modern analogues in the calibration data. The problem of non-analogue samples in paleo-reconstruction is acknowledged in literature (Jackson and Williams 2004), however, the sensitivity of individual reconstruction algorithms remains poorly understood. Some recent studies using simulated non-analogue fossil data have suggested that regression-tree ensemble models (here, RF and BRT) may be more robust in non-analogue conditions compared to classical methods such as WA, WA-PLS, and MAT (Juggins et al. 2015, Goring et al. 2015). Due to these challenges in model evaluation, we use all six methods as they all showed acceptable performance in cross-validations. To estimate the likelihood of non-analogue errors, we estimated the compositional distance to closest analogue in the modern pollen data. To assess the Eemian analogue distances, we also calculated the mean analogue distance for

late-Holocene samples from Loitsana Lake (Salonen et al. 2013). As a further validation step, we test the statistical significance of the paleo-climate reconstructions using the Telford and Birks (2011) test (implemented with PALAEOSIG version 1.1-2; Telford 2013). This test uses redundancy analysis to assess whether the paleo-reconstruction explains more fossil data variation compared to reconstructions of 999 random variables.

The climate reconstructions were carried out by Sakari Salonen (University of Helsinki).

Table 5-1. Summary of model performances.

Climate parameter	Method	Model parameters	RMSEP	Max. Bias	Reconstruction significance
T_{jul}	WA	Monotonic deshrinking, tolerance downweighting	1.68	6.88	-
T_{jul}	WAPLS	2 components	1.80	6.46	-
T_{jul}	MLRC	Default	2.05	5.22	-
T_{jul}	MAT	Weighted mean of 5 analogues, sq. chord distance	1.12	8.27	p = 0.001
T_{jul}	BRT	LR = 0.025, MT = 3000, TC = 4, BF = 0.5	1.15	3.31	-
T_{jul}	RF	n.trees = 100	1.25	7.63	-
T_{jan}	WA	Monotonic deshrinking, tolerance downweighting	3.13	13.26	-
T_{jan}	WAPLS	3 components	3.19	9.77	-
T_{jan}	MLRC	Default	3.44	5.97	-
T_{jan}	MAT	Weighted mean of 5 analogues, sq. chord distance	1.79	3.20	p = 0.456 (entire core), p = 0.011 (zones V–VI)
T_{jan}	BRT	LR = 0.025, MT = 3000, TC = 4, BF = 0.5	1.99	5.01	-
T_{jan}	RF	n.trees = 100	2.17	8.32	-

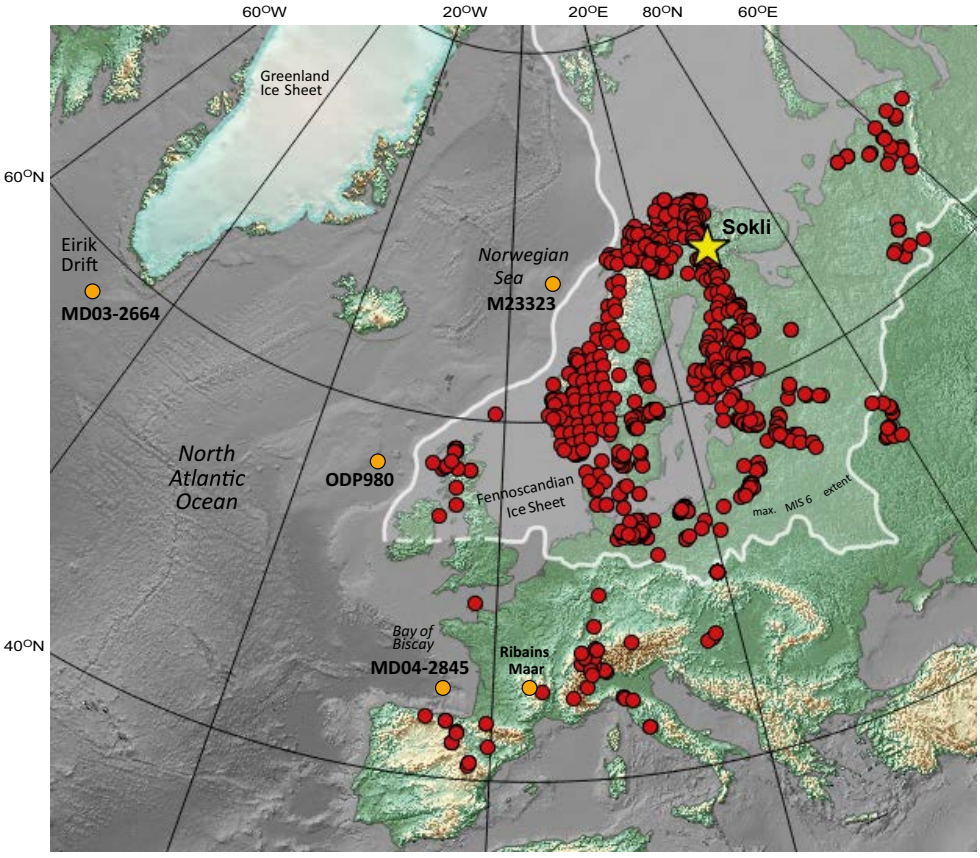

Figure 5-3. *Map of pollen calibration sites used in the present study on Eemian climate reconstruction. Also indicated are sites mentioned in the text.*

5.2 Results

5.2.1 Proxy data

The analyzed sequence consists of 3 m of sandy and silty sediment overlain by 9 m of yellowish brown diatom gyttja (Figure 5-2). Two intervals with siltier sediment are found in the lower (23.40–23.24 m) respectively upper (17.50–17.32 m) part of the diatom gyttja. The lower part of the gyttja is laminated. Laminations, however, are less visible in those core sections which were severely compressed during coring (Figure 5-2). A series of sand and gravel layers occur intercalated in the uppermost part of the diatom gyttja (16.5–16.0 m) which is then capped by a thick gravel layer of MIS 5d age.

The correlation matrix of the XRF-elemental profiles yielded two main groups of elements with a correlation of 0.5 or better (Table 5-2). The elements K, Ti, Rb and Zr, and to a lesser extent Si and Ca, belong to the first group. These elements all have in common their conservative nature being transported detritally into lakes, hosted in minerals such as rutile, feldspars, zircon, calcite and various silicates. This group is thus interpreted to represent minerogenic input to the lake, which is further confirmed by the close relation to variations in the LOI/BSi profiles and lithology (Figure 5-2).

Sulfur and Fe form the second group with high correlation in the XRF data. Increased values are recorded in the lower laminated portion of the diatom gyttja sequence (25.00–20.73 m), and between ca 18.30 and 17.40 m (Figure 5-2). Sulfate laminations have been observed in the latter interval in borehole 901 (Helmens et al. 2000). Plikk et al. (2016) suggest that S and Fe are linked to the laminations. Laminations consisting of iron hydroxide and iron sulfide precipitates can form and be preserved in high latitude lakes that are dimictic and sufficiently productive or receive a sufficient amount of allochthonous organic material for anoxia to develop in the hypolimnion during the stagnation periods (Renberg 1981, Gälman et al. 2009). Intervals where these elements are elevated thus imply oxygen deficient conditions in the hypolimnion.

FTIRS-inferred BSi concentration shows a sharp increase at the base of the diatom gyttja sequence (near 0 to ca 30 %; Figure 5-2). An overall increasing trend to 50 % is seen until ca 21.0 m depth. The values then remain more or less stable. Relatively low BSi values are associated with minerogenic input (upper sandy/gravelly intercalations and the two silt intercalations).

Organic content, as measured by LOI, increases rapidly around the transition from minerogenic sediment to diatom gyttja (Figure 5-2), then remains relatively stable at values of ca 20–25 %. Distinct decreases in LOI are found in the silt intercalations and the upper sandy/gravelly intercalations.

The C/N ratio varies around 15 throughout the diatom gyttja sequence, suggesting an equally large input of terrestrial and aquatic organic matter (Figure 5-2). In general, aquatic plants and algae typically have C/N ratios below 10, while terrestrial plants typically have C/N ratios above 20 (Meyers and Teranes 2001). Rising values in the lower half of the diatom gyttja (up to 21.0 m), from ca 12 to ca 18, most probably reflects an increasing contribution of terrestrial material. C/N is high (ca 25) in the upper silt intercalation, and in the upper sandy/gravelly intercalations.

The siliceous microfossil analysis shows that the major part of the BSi content consists of diatoms. Phytoliths are rare and the abundance of chrysophyte cysts, although slightly enhanced in the lowermost part of the diatom gyttja, is low. The sediments are generally rich in well-preserved diatoms, apart from the lowest 3 m of minerogenic sediments, which contain only a few diatom valves, and the uppermost 0.5 m, which contain a number of broken valves. Many species of Fragilariaceae (including the revised genera) are preserved in their colonial form, as chains. In total, 196 diatom taxa were enumerated, but only a few species make up the majority of the assemblage in a sample and are shown, together with other aquatic taxa, in Figure 5-5. The siliceous microfossil diagram, with a large selection of taxa, is seen in Plikk et al. (2016, Figure 3). The lowest and uppermost parts of the diatom gyttja sequence are dominated by periphytic taxa, mainly small Fragilariaceae (e.g. *Staurosirella pinnata*, *Staurosira venter*, and *S. construens*). Throughout the main part of the sequence, however, planktonic diatoms are nearly equally abundant to, or dominate over, benthic diatoms. The planktonic assemblages are characterized by small *Stephanodiscus* spp. (*S. medius* and *S. minutulus*) and *Aulacoseira* spp. (*A. subarctica* and *A. ambigua*). The assemblages generally reflect circumneutral to slightly alkaline, meso-eutrophic conditions within the lake.

A selection of pollen, spores and stomata of terrestrial plants are given in Figure 5-4. Seven pollen zones (I-VII) are distinguished; zone VII corresponds with the final birch phase reconstructed in core 901 (see Section 5.1.1). In contrast to the Holocene and MIS 5d-c sediments in the Sokli basin, in which fossil assemblages representing wetland and/or shore habitats are nearly continuously recorded, these taxa show a limited occurrence in the Eemian diatom gyttja sequence. On the other hand, assemblages of aquatic taxa are rich and show large turn-overs, and these have been the basis for distinguishing a series of Eemian lake phases; the latter are described in great detail in Plikk et al. (2016). The lake phases appear to be mostly driven by changes in climate or climate-induced changes in regional vegetation (Plikk et al. 2016). As such, we here integrate the terrestrial and aquatic assemblages and interpret the Eemian environmental record at Sokli according to the zonation in terrestrial vegetation (zones I-VII). A selection of aquatic biota (including diatoms) is given in Figure 5-5, with inferred lake level changes to the far right. Aquatic plants include *Myriophyllum spicatum*-type in the lower part of the diatom gyttja sequence, while *Potamogeton* and Nymphaeaceae become more common in the upper part. The NPP assemblage is dominated by taxa of the green algae *Pediastrum* and *Tetraëdron minimum*. Six taxa of *Pediastrum* were distinguished, but *P. boryanum* and *P. boryanum* var. *pseudoglabrum* are the most dominant. *Pediastrum* concentrations overall increase, particularly above 21.0 m, reaching values of over 16 000 colonies/cm^3 (Plikk et al. 2016). The latter increase might explain the general decrease in C/N values in the upper part of the diatom gyttja deposit (Figure 5-2). Other aquatic taxa that are registered include the green algae *Botryococcus braunii*, algal Type HdV-225 (van Geel et al. 1989) and *Spirogyra* spp. Note that the diagram of Figure 5-5 additionally shows several wetland elements (e.g. *Sphagnum*, *Equisetum*, Fungi).

Macrofossils of aquatic and wetland plants, as well as of terrestrial taxa, are generally scarce, suggesting a relatively long distance between the coring-site and the lake shore throughout the lake's history. The morphology of the Sokli basin and the thickness of the Eemian deposit suggest that the Sokli Eemian paleo-lake reached a dimension of maximal ca 500 × 500 m and was relatively deep (ca 10–15m).

Table 5-2. Correlation matrices (r values) for the geochemical data from the Sokli Eemian diatom gyttja sequence. Bold figures indicate r values ≥ 0.5.

	S	K	Ca	Ti	Mn	Fe	Zn	Rb	Sr	Zr
Si	0.22	**0.68**	0.43	**0.59**	–0.01	0.17	0.14	**0.62**	0.01	0.31
S		0.26	**0.63**	0.26	0.28	**0.73**	0.38	0.13	–0.13	–0.13
K			**0.60**	**0.93**	0.17	0.43	0.24	**0.86**	0.01	**0.61**
Ca				**0.60**	0.24	0.42	0.32	0.47	0.26	0.30
Ti					0.18	0.48	0.27	**0.82**	0.05	**0.67**
Mn						0.42	**0.62**	0.20	–0.24	–0.15
Fe							**0.54**	0.34	–0.44	0.03
Zn								0.31	–0.22	–0.09
Rb									–0.03	**0.57**
Sr										0.23

5.2.2 Pollen-based climate reconstructions

The pollen-based climate reconstruction (Figure 5-6) are discussed in Section 5.4.

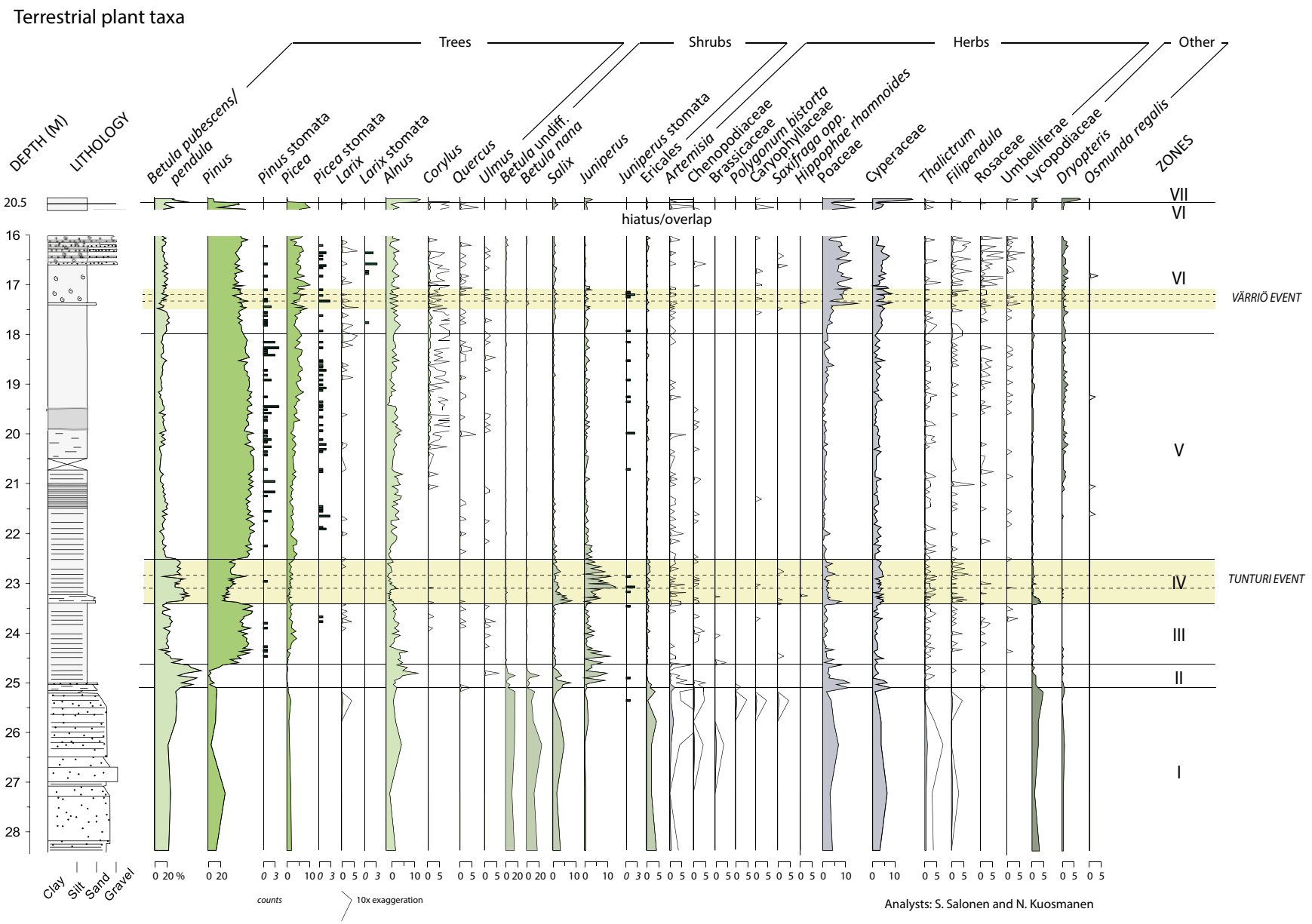

Figure 5-4. *A selection of pollen, spores and stomata from terrestrial plants encountered in the Sokli Eemian sequence.*

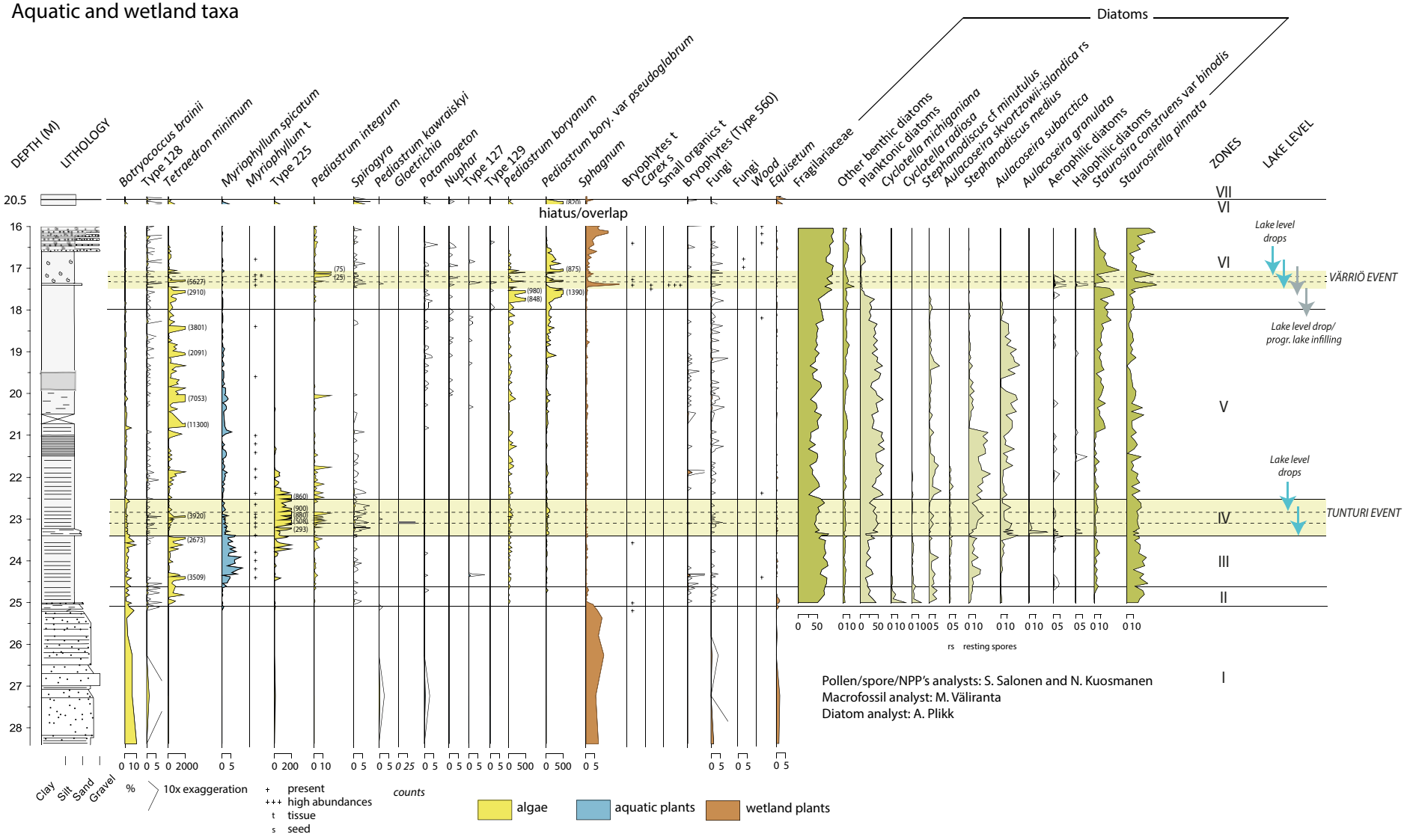

Figure 5-5. *A selection of aquatic biota (including diatoms) and wetland plants encountered in the fossil record from the Sokli Eemian sequence. Inferred lake level changes are indicated to the far right.*

5.3 Environmental conditions during the Eemian Interglacial (MIS 5e; ca 130–115 kyr BP)

5.3.1 Zone I (28.40–25.17 m depth interval)

The pollen composition of zone I with percentage values of up to 65 % for *Betula* (including *B. pubescens/pendula* (tree birch) and *B. nana* (dwarf birch); Figure 5-4) indicates the presence of pioneering birch vegetation in the Sokli area. Other plants that are recorded are dwarf shrubs (Ericales), lycopods (e.g. *Diphasiastrum*) and a variety of heliophilous (light-demanding) herbs including *Artemisia*, Caryophyllaceae, Brassicaceae, Chenopodiaceae, *Polygonum bistorta*-type and *Saxifraga oppositifolia*-type. Additionally, *Larix* is represented in the pollen record. Pollen of larch is known to have short-distance dispersal from the pollen-producing tree, poor preservation (Gunin et al. 1999, MacDonald et al. 2000) and rather indistinct morphological features. As such, even very low percentage values for *Larix* in the pollen record can be used to infer the local presence of larch trees.

The sediment that was deposited during zone I consists of sands grading into laminated silty and clayey sediment. A similar deposit is found at the base of the Holocene lake sequence and is interpreted as having a glacio-lacustrine origin (Shala et al. 2014a, b). Fossil remains are scarce in this relatively coarse-grained minerogenic sediment. The microfossil record reveals the wetland taxa *Sphagnum* and *Equisetum* and the pioneering alga *Botryococcus braunii*. *Pediastrum kawraiskyi* shows a rare occurrence (Figure 5-5). The latter alga has been recorded from nutrient-poor, oligotrophic waters of large lakes during cold phases of the Pleistocene and the late-glacial (Jankovská and Komárek 2000).

5.3.2 Zone II (25.17–24.65 m)

Pollen of *B. pubescens/pendula* dominate the pollen assemblage of zone II and indicate the presence of sub-arctic birch forest. The open character of the forest allowed pollen of the shrub *Juniperus* to significantly contribute to the sum, showing values up to ca 10 %.

The early part of zone II is recorded in a silt layer. *Sphagnum* is still well-represented in the pollen/spore record, and *Equisetum*, *Salix* (also macrofossils present), sedges (Cyperaceae) and grasses (Poaceae) show increased percentage values, most probably reflecting an extended wetland zone. Silts deposited under relatively shallow water conditions also cap the silty/clayey glacial lake sediment of early-Holocene age and are interpreted to represent a phase of partial drainage of the Sokli Ice Lake (see local zone 2 in Section 3.3.2).

The initiation of deposition of diatom gyttja within the Sokli depression is recorded during the latter part of zone II. Pollen of *Alnus* reach percentage values of 10–15 % reflecting its presence in a distinct moist habitat bordering the Sokli paleo-lake; planktonic *Tetraëdron minimum* becomes well-established in the lake.

At the base of the diatom gyttja deposit, minerogenic input sharply decreases, and the organic content of the sediment (measured by LOI) rapidly increases (Figure 5-2), most probably due to stabilization of the catchment through soil formation. LOI reaches 25 % similar as measured in the sediment of a typical modern sub-arctic lake in northern Fennoscandian (Korhola and Weckström 2004). The BSi content of the sediment is initially low, possibly due to turbidity caused by the enhanced influx of sediment into the lake, but then sharply increases to nearly 40 % reflecting a productive lake. The diatom assemblage is characterized by high percentage values of the planktonic taxa *Cyclotella michiganiana* (reaching 20 %) and *C. radiosa* (15 %). These are oligo-mesotrophic diatoms, favored by deep, warm waters and stable summer stratification (Stoermer 1993, Wolin 1996, Whitlock et al. 2012). The presence of a stratified lake with a regularly anoxic hypolimnion is supported by the preservation of laminations in the sediment (indicating low levels of bioturbation) and high Fe/S values.

5.3.3 Zone III (24.65–23.40 m)

Pollen assemblages during zone III depict a period of dynamic forest development in which open pine-dominated forest (*Pinus* pollen reaching almost 80 %) with *Juniperus* is replaced by mixed boreal forest with *Picea* (stomata present) and then *Larix*. In concordance with the forest dynamics, distinct changes in the lake environment are recorded. Initially (during the pine-dominated forest phase), *Alnus* and *T. minimum* are still well-represented in the micro fossil record. These taxa decline at the transition

to mixed boreal forest, while pollen of *Myriophyllum spicatum*-type sharply increase to values of 10 %, indicating the development of a distinct littoral zone along the lake. *M. spicatum*-type (including *M. verticillatum* and *M. sibiricum*) is a submerged aquatic plant that can grow in water depths varying from ca 1 to 5 m (Hannon and Gaillard 1997). It presently has a high occurrence in sheltered waters of eutrophic lakes. Increased nutrient availability is also indicated by relatively high percentage values for the planktonic diatom taxon *Stephanodiscus medius*. Soil development likely resulted in external nutrient load to the lake due to enhanced weathering (Fritz and Anderson 2013).

The level of minerogenic input into the lake increases as larch expands, probably due to a more open character of the forest. Furthermore, changes in the representation of several aquatic taxa suggest a drop in nutrient levels and transition to a colder climate. The algae *T. minimum* and *B. braunii* increase again in percentage values, while eutrophic *S. medius*, *S. minutulus* and *M. spicatum*-type decrease. Characteristic is the sudden increase of both the alga *Pediastrum integrum* and algal type T.225 (van Geel et al. 1989). *P. integrum* is associated with cold, oligotrophic waters of lakes and swamps (Komárek and Jankovská 2001, Sarmaja-Korjonen et al. 2006, Weckström et al. 2010). T.225 remains unidentified. In the Sokli sequence, it is encountered in minerogenic sediment deposited under glacial lake phases (see local zone Ib in Section 3.3.1) and in braided stream channels (see local zone I-3 in Section 4.3.3), suggesting dynamic conditions. Van Geel et al. (1989) found this possible algal type associated with open water and ephemeral pool phases.

5.3.4 Zone IV (23.40–22.51 m)

Zone IV corresponds with the Tunturi cooling event defined in Helmens et al. (2015). The pollen-based climate reconstruction (see Section 5.4), as well as T_{jul} inferred from chironomids (Helmens et al. 2015), show a drop in mean July air temperature in the order of 2–4 °C; the cooling was abrupt and had a step-wise recovery.

In the pollen record, the Tunturi cooling event is manifested by a sudden increase of *B. pubescens/pendula* pollen to values of 50 %, and increased representations of *Juniperus* and lycopods, indicating the replacement of boreal forest by sub-arctic open birch-pine forest. Pollen of *Pinus* slightly increase at the expense of *B. pubescens/pendula* pollen during the first recovery phase, after which birch pollen again increase to ca 40 %. *Juniperus* is particularly well-represented during the recovery phase. This shrub is known to be frost-susceptible and prefers a winter snow-cover (Iversen 1954, Lauber et al. 1998). Its decreased values during the cooling peaks suggest relatively dry climatic conditions. Additionally, *Alnus* shows low pollen percentage values during zone IV suggesting a reduction in its moist habitat.

The start of the Tunturi event is marked by a peak in minerogenic influx into the lake, and levels remain above average throughout the event, probably indicating enhanced catchment erosion. The latter is also suggested by the presence of *Juniperus* and *Hippophaë rhamnoides*, plants that can tolerate an unstable soil cover. The climate deterioration during the Tunturi event (and its impact on vegetation and levels of soil erosion) had a major impact on the aquatic ecosystem as well. Percentage values for the planktonic and heavily silicified diatom taxon *Aulacoseira subarctica* sharply increase, particularly during the first cold peak, reflecting increased Si-input to the lake. Also, the increases in *A. subarctica* suggest high levels of wind-driven turbulence (in order for this diatom taxon to remain in suspension), which can be related to the more open character of the vegetation. Furthermore, during the first cold peak, *Pediastrum kawraiskyi* returns in the fossil record, while peak values are recorded for heavily silicified, eutrophic *Aulacoseira granulata* and for colonies of the cyanobacteria *Gloeotrichia*, the latter most probably reflecting an unbalance of the P/N ratio in the lake water due to sediment influx. These changes in the aquatic environment during the Tunturi event resemble changes observed during late-glacial/Holocene cooling events, e.g. the Younger Dryas or the Little Ice Age, where similar increases in high nutrient species (e.g. *A. granulata* and *Gloeotrichia*) and minerogenic input are recorded (Björck et al. 2000, Rioual et al. 2007, Cvetkoska et al. 2014, Pędziszewska et al. 2015, Zawiska et al. 2015).

Whereas the algae *T. minimum*, *P. integrum* and *T.225*, as well as *Spirogyra*, are well-represented during the Tunturi event, values drop during the cold peaks (particularly the first cooling), probably due to turbid water conditions. The macro-alga *Spirogyra* is characteristic of shallow, meso-eutrophic freshwaters (van Geel and Grenfell 1996) and suggests reduced lake levels during the Tunturi event. A drop in lake level and extension in the wetland zone (particularly during the first cooling peak) is

further suggested by increased pollen values of Cyperaceae and *Salix* (also macrofossil present) and occurrences of aerophilic and halophilic diatoms. A reduction in the thermal summer stratification of the lake water (as suggested by the geochemical record) could be related to the decreased lake levels and/or increased wind stress.

5.3.5 Zone V (22.51–17.98 m)

Mixed boreal forest with spruce and larch returned to the Sokli area following the Tunturi cooling event. Characteristic for zone V are the overall increasing pollen percentage values for *Picea* reaching ca 20 % in the uppermost part of the zone. In comparison, *Picea* pollen attain some 10 % in late-Holocene lake records from the northern boreal zone in north-eastern Fennoscandia (see zone IV in Section 3.4.4). Pollen of *Pinus* reach maximum values of nearly 80 % in depth interval 20.75–20.25 m, after which values start an overall decline to ca 60 %. Simultaneously as *Pinus* pollen start to decrease, pollen of *Corylus* become near continuously recorded; the percentage values suggest the local presence of hazel at Sokli. The pollen of *Quercus* and *Ulmus* can be considered as long-distance transported.

Pollen percentage values of *Alnus* and *M. spicatum*-type are low in the early part of zone V (below 21.50 m), and values for the algae *T. minimum* and *P. integrum*, and algal-type T.225, are still relatively high, suggesting some level of continuation of/recovering from the environmental conditions provoked by the Tunturi cooling event.

The diatom *Stephanodiscus medius* attains peak values in depth interval 21.50–20.85 m. High Fe/S values in combination with the distinctly laminated character of the sediment here indicate strongly oxygen-deficient conditions in the hypolimnion. The dominance of planktonic *S. medius* may be attributed to strong internal P-loading resulting from pronounced summer stratification in combination with prolonged autumn mixing. Low values of *T. minimum* in the sediment of depth interval 21.50–21.00 m (similar as during the middle part of zone III) possibly reflect a lower competitive ability of this alga under nutrient-rich (high P) conditions.

A most pronounced change in the lake ecosystem is recorded at 20.85 m depth. *S. medius* is abruptly replaced by *A. subarctica* as the dominant planktonic diatom taxa, while the representation of the alga *T. minimum* overall increases. The change coincides with the disappearance of distinct laminae in the sediment and a lowering in Fe/S values, suggesting a break-up of lake stratification and a change to a Si-dominated trophic regime. The reason for the break-up of lake stratification can be progressive lake infilling (a sudden extension in the littoral zone is suggested by an increased representation of benthic *Staurosira construens* var. *binodis*) and/or climate. In this upper part of zone V, ferns become continuously recorded (possibly as a result of the extended littoral zone) and the emergent aquatic plant *Nuphar* is represented in the fossil record.

5.3.6 Zone VI (17.98–16.00 m)

Boreal forest with spruce and larch continues to be present in the Sokli area during zone VI. Pollen of *Pinus* overall continue to decline to ca 50 %, to slightly increase again at ca 16.25 m depth. *Picea* pollen fluctuate between values of 20 and 40 %. Furthermore, pollen of Cyperaceae is higher during zone VI compared to zone V, and also pollen of Poaceae increase, particularly from 17.40 m onwards.

The lower part of zone VI (and uppermost part of zone V) (depth interval ca 18.20–17.40 m) shows step-wise increases in percentage values for *S. construens* var. *binodis* accompanied by strongly reducing percentages of planktonic diatoms. During the second step (at 17.70 m depth), also the alga *Pediastrum boryanum* (including *P. boryanum* var. *pseudoglabrum*) strongly increases. *S. construens* var. *binodis* and *P. boryanum* var. *pseudoglabrum* are taxa that are associated with shallow, macrophyte-rich, eutrophic environments (Bradbury and Winter 1976, Cronberg 1982). These changes in fossil assemblages, combined with increasing LOI values, reflect a now shallow (and further shallowing) and highly productive, infilling lake. Cyperaceae increase in pollen percentages during the first step, and *Salix* pollen during the second step, most probably reflecting extensions in the wetland zone along the lake (*Carex* macrofossil present). The preservation of laminations in the sediment as observed at a similar stratigraphic level in parallel core 901, and enhanced Fe/S values (present study), suggest prolonged anoxia.

Between depths 17.40–17.05 m, distinct shifts are recorded in the aquatic and wetland proxies. This drying and cooling event (Helmens et al. 2015, Plikk et al. 2016) is defined the "Värriö event" (Salonen et al. 2018). Most severe conditions are recorded at the beginning of the event. Here, peak values for *Sphagnum* (20 %), macrofossil findings of bryophytes and *Carex*, and abundant organic tissue, are accompanied by peak values for the littoral diatom taxon *Staurosira pinnata*, the presence of the shallow-water alga *Spirogyra*, as well as aerophilic and halophilic diatoms, indicating an abrupt drop in lake level. Also *P. kawraiskyi* and *H. rhamnoides* return to the fossil record (see Tunturi event, zone IV). A large input of minerogenic matter into the lake coincides with sharply reducing values for the algae *P. boryanum* and *T. minimum*, most probably due to increased levels of turbidity of the lake water. Furthermore, a slight increase in *Pinus* pollen coincides with reductions in pollen of both *Picea and B. pubescens/pendula*. Following a recovery phase (during which e.g. *P. integrum* is recorded), a second drop in lake level is registered as well as another, slight expansion of pine at the cost of spruce and birch; macrofossils of macro-algae *Chara* and *Nitella* suggest enhanced Ca-levels in the lake water.

The upper part of zone VI shows the return of peak values for the littoral diatom taxa *S. construens* var. *binodis* followed by *S. pinnata*. The former occurs attached to macrophytes; the latter to sediment particles and its occurrence coincides with peaks in minerogenic matter (during the Värriö event) and layers of sandy sediment intercalated in the uppermost part of the diatom gyttja deposit. Furthermore, strongly increasing spore percentage values for *Sphagnum* reflects a large extension in the wetland zone. It is possible that also high values for grasses are related to extended wetland zone. Following the first lake level drop during the Värriö event, the diatom gyttja becomes marked with light yellowish spots. Similar features have been interpreted as a sign of desiccation caused by subaerial exposure or bottom freezing (Björck et al. 2000), and could indicate that the lake at periods experienced very low water levels.

5.3.7 Zone VII (borehole 901)

The replacement of boreal forest by sub-arctic birch forest is recorded during zone VII.

5.4 Climate evolution during the Eemian Interglacial (MIS 5e; ca 130–115 kyr BP)

For much of the Eemian diatom gyttja sequence (particularly from the boreal forest phase in zone III to the start of the Värriö event in zone VI), the analogue distances are low (Figure 5–6C), being similar as during the late-Holocene (0–4 cal. kyrs BP) at Sokli (Salonen et al. 2013), suggesting that good modern pollen analogues are found and that relatively robust climatic reconstruction should thus be possible. The closeness of the modern analogues likely results from both analogous climate and similar depositional environment (relatively small lakes of ca 0.3 km^2 with limited wetland zones) between the Eemian and the calibration pollen samples.

5.4.1 Pollen-based T_{jul} reconstruction

The pollen-based mean July air temperature (T_{jul}) reconstruction is highly consistent between the six different reconstruction methods used, with similar long-term Eemian climate trends reconstructed with all methods (Figure 5-6A). Most notable between-method differences are found in pollen zones I, II and VII, where the fossil pollen samples have relatively poor analogues in the modern calibration data.

T_{jul} increases from ca +12 to +14 °C during the birch forest phase of zone II. However, in northern Fennoscandian records, elevated early-Holocene summer temperatures indicated by the aquatic ecosystem have been found to pre-date the rise in pollen-inferred T_{jul} and related to high summer insolation (Luoto et al. 2014, Väliranta et al. 2015; see Section 3.6.2). Also, our Eemian record, with high occurrences for the diatoms *Cyclotella michiganiana* and *C. radiosa* (pointing to a stable summer stratification of the lake), might indicate that early-Eemian T_{jul} was higher than reconstructed based on the pollen record. One reason for this discrepancy might be a delayed response of terrestrial vegetation compared to aquatic communities to warming, due to slow soil forming processes.

T_{jul} values up to ca 2 °C higher than the present-day value of ca +13 °C at Sokli are inferred for the boreal forest phase in zone III. This interval can be defined as the first climate optimum. Subsequently, both the pollen-based T_{jul} reconstruction, and T_{jul} inferred using chironomids (Helmens et al. 2015), indicate a decrease of 2–4 °C during the Tunturi event, with maximum cooling at the onset of the event.

Following the Tunturi event, T_{jul} increases to ca +16 °C recording the second climate optimum. The fossil pollen assemblages of zone V are remarkably similar to those presently encountered in surface samples from lakes located in the boreal zone south of Sokli (Figure 5-6D). T_{jul} starts a gradual but continuous decline at a depth of ca 20 m (and particularly from the base of zone VI onwards) in concordance with declining *Pinus* pollen percentage values (Figure 5-4). T_{jul} sharply decreases in the late birch forest phase (zone VII).

A sharp decrease in T_{jul} is reconstructed at the start of the Värriö event. Some caution, however, should be taken in estimating the precise T_{jul} lowering here based on the pollen/spore record. For comparison with N American pollen calibration sets, *Sphagnum* spores have been included in our calibration set; this moss has a distinct occurrence in the boreal forest zone of N America However, when reconstructing temperature changes within the boreal zone, as is the case in our study, *Sphagnum* merely reflects the presence of local moist habitats. *Sphagnum* reaches 20 % in the lower part of the Värriö event; we have re-run the climate reconstruction by taking *Sphagnum* out of the sum and this only slightly changed the reconstructed T_{jul} value.

5.4.2 Pollen-based T_{jan} reconstruction

From a methodological standpoint, we note that reconstructions from fossil data of so-called secondary variables, with a comparatively small ecological effect, have been a contentious issue in recent literature (e.g. Juggins 2013, Telford and Birks 2005, 2009, 2011). Such secondary variables are commonly correlated with the primary variable in the used calibration data. Using reconstructions from simulated fossil data, Juggins (2013) and Rehfeld et al. (2016) showed that these calibration-data correlations may induce spurious reflections of the past variability of the primary variable in the reconstruction for the secondary variable.

In the present work, these challenges are particularly relevant for the presented T_{jan} reconstruction, as analyses of northern European surface pollen data (Salonen et al. 2012, 2014) show summer temperature to be the dominant influence on pollen variation. However, literature on northern European modern vegetation (Sykes et al. 1996, Skov and Svenning 2004, Seppä et al. 2015) and surface pollen datasets (Salonen et al. 2012) suggest a signal of winter temperature in a subset of taxa or pollen types, and thus an ecological case for T_{jan} reconstruction exists. The relative contribution to the T_{jul} model is distributed between a variety of taxa, while the T_{jan} model is more selective in the use of taxa and includes the well-understood winter indicators *Corylus* and *Quercus* (Sykes et al. 1996, Salonen et al. 2012, Seppä et al. 2015) among the three most important predictors. Thus the T_{jul} and T_{jan} models show a degree of independence, likely aided by the low correlation ($r = 0.27$) between T_{jul} and T_{jan} in the calibration data (cf. Juggins 2013, Rehfeld et al. 2016). Also, the first-order trends in the reconstructions are opposite (falling T_{jul}, rising T_{jan} during the Eemian; Figure 5-6A, B) and thus the trend in T_{jan} is unlikely to be driven by the weak positive correlation in the calibration data.

Crucially, the first-order trend of increasing T_{jan} that we reconstruct during our Eemian record is supported by independent data from diatoms. Dominance of small Fragilariaceae in the lower part of the diatom gyttja deposit (Figure 5-5) suggests a continental climate regime with prolonged periods of lake ice-cover (Lotter and Bigler 2000). Extension in the mixing periods is recorded by the diatom assemblages following the Tunturi event (Plikk et al. 2016), suggesting a change to a more oceanic climate regime (with warmer winters).

However, due to the comparatively weak signal of T_{jan} in northern European pollen data, the T_{jan} reconstruction should be interpreted with caution, and here we regard the shift towards warmer winters as the salient feature.

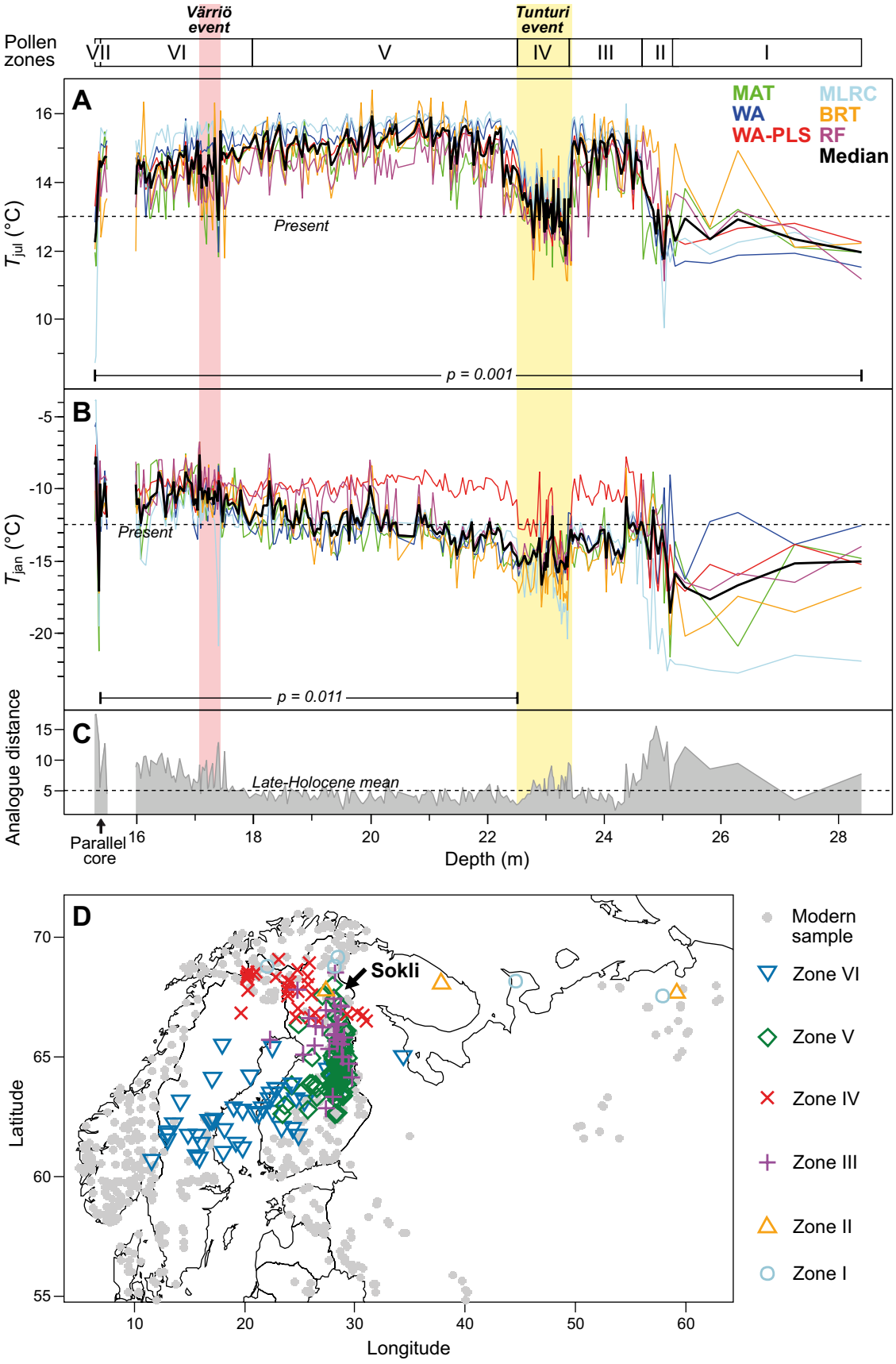

Figure 5-6. *Pollen-based climate reconstructions for the Eemian at Sokli. Fossil pollen assemblages are compared with modern pollen assemblages encountered in the calibration-set lakes in* ***D****.*

5.4.3 Inferences on moisture regime

Our multi-proxy evidence from the Eemian diatom gyttja deposit shows, in addition to changes in temperature, distinct changes in moisture regime. This is most obvious during the Tunturi and Värriö events where abrupt lake level falls are reconstructed in concordance with lowerings in T_{jul} (Figure 5-4).

5.5 Correlation with European and North Atlantic records

Comparison of Eemian records from Europe and the North Atlantic Ocean is hampered by the scarcity of independent, absolute chronologies.

To compare the Sokli sequence with regional paleo-climate data-sets and climate forcing time series (Figure 5-7), we assign a tentative absolute timescale to the Sokli Eemian sequence. First, we assume rapid deglaciation following Saalian glaciation due to high summer insolation in the high northern latitudes, reaching peak values early in the Last Interglacial at ca 127 kyr BP (Figures 1-1, 5-7J). This is supported by global sea-level data (Figure 5-7G) which suggest a global sea level close to the Eemian maximum and above present-day values by ca 129–126 kyr BP. We then assume the base of the Eemian Interglacial at Sokli to have the same age as the beginning of the Central European Eemian Interglacial, in line with Tzedakis (2003), who proposed that the base of Eemian pollen sequences has roughly the same age across a wide latitudinal range in Europe, similar as the Holocene. An age of ca 127 kyr for the base of the Eemian in central and southern Europe is generally been used based on e.g. stalagmite data from the Austrian Alps (Holzkämper et al. 2004), and this age is supported by preliminary U/Th datings of a stalagmite obtained from a central Swedish cave (personal communication N. Frank, Institute of Environmental Physics, Heidelberg, Germany)). Stalagmite data from the Austrian Alps indicate that Eemian warmth came to a halt at ca 115 kyr BP (Spötl et al. 2002) and we use this age for the end of the Eemian at Sokli. A total length of ca 11–12 kyr for the Eemian Interglacial is also inferred from annually laminated diatomite sections in Germany (Turner 2002). Furthermore, based on the rather uniform sediment type at Sokli (diatom gyttja), we assume a constant sedimentation rate between 127–115 kyr BP (Figure 5-7A, B).

The overall declining mean July air temperatures (T_{jul}) during the Eemian reconstructed at Sokli (Figure 5-7B) are also reflected by pollen and macrofossil data from central Europe (Figure 5-7C, D; Zagwijn 1996, Kühl et al. 2007), and follow the general decreasing trend in high-latitude June insolation (Figure 5-7J). The opposite trend, i.e. the overall increasing T_{jan} at Sokli, follows the increase in high-latitude December insolation (Figure 5-7I). Moreover, benthic $\delta^{13}C$ data from the North Atlantic Ocean (Figure 5-7E) suggest an increasingly vigorous AMOC during the Eemian (Galaasen et al. 2014) which would explain the change towards a more maritime climate regime at Sokli during the later half of the Eemian.

The Tunturi cooling detected in the high-resolution Sokli Eemian sequence at ca 125 kyr BP is matched by a major decline in sea-surface temperatures (SST), accompanied by reducing North Atlantic Deepwater Formation (NADW), recorded in marine core MD03-2664 (Figure 5-3) from the high sediment-accumulation rate site on the Eirik Drift at this time (Figure 5-7F, E; Irvalı et al. 2012, Galaasen et al. 2014). Moreover, a major cooling event intersecting peak Eemian warmth has recently been recorded in great detail in the very high-resolution core M23323 (Figure 5-3) from the Norwegian Sea (Bauch et al. 2011). The cooling event recorded in the latter marine core has approximately the same temperature decrease, structure, and duration as reconstructed at Sokli. Furthermore, a spike in ice-rafted-debris (IRD) suggests that widespread expansions of winter sea-ice cover accompanied the surface cooling of the Norwegian Sea (Bauch et al. 2011). The latter might explain the dry climate reconstructed at Sokli during the Tunturi event. The cooling in the Norwegian Sea record, and the start of the Eemian here, have been dated several thousands of years later than at Sokli and at the Eirik Drift (Bauch et al. 2011); it should be noted, however, that uncertainties in marine chronologies can result in age differences of up to 3–5 kyrs between marine records (Govin et al. 2015).

Major cooling interrupting Eemian warmth is not reported from European paleo-climate archives (see e.g. Figure 5-7C, D). In line with this, Eemian climate stability has previously been suggested based on proxy evidence from lake sediments in the Ribains Maar in France (Rioual et al. 2001; Figure 5-3).

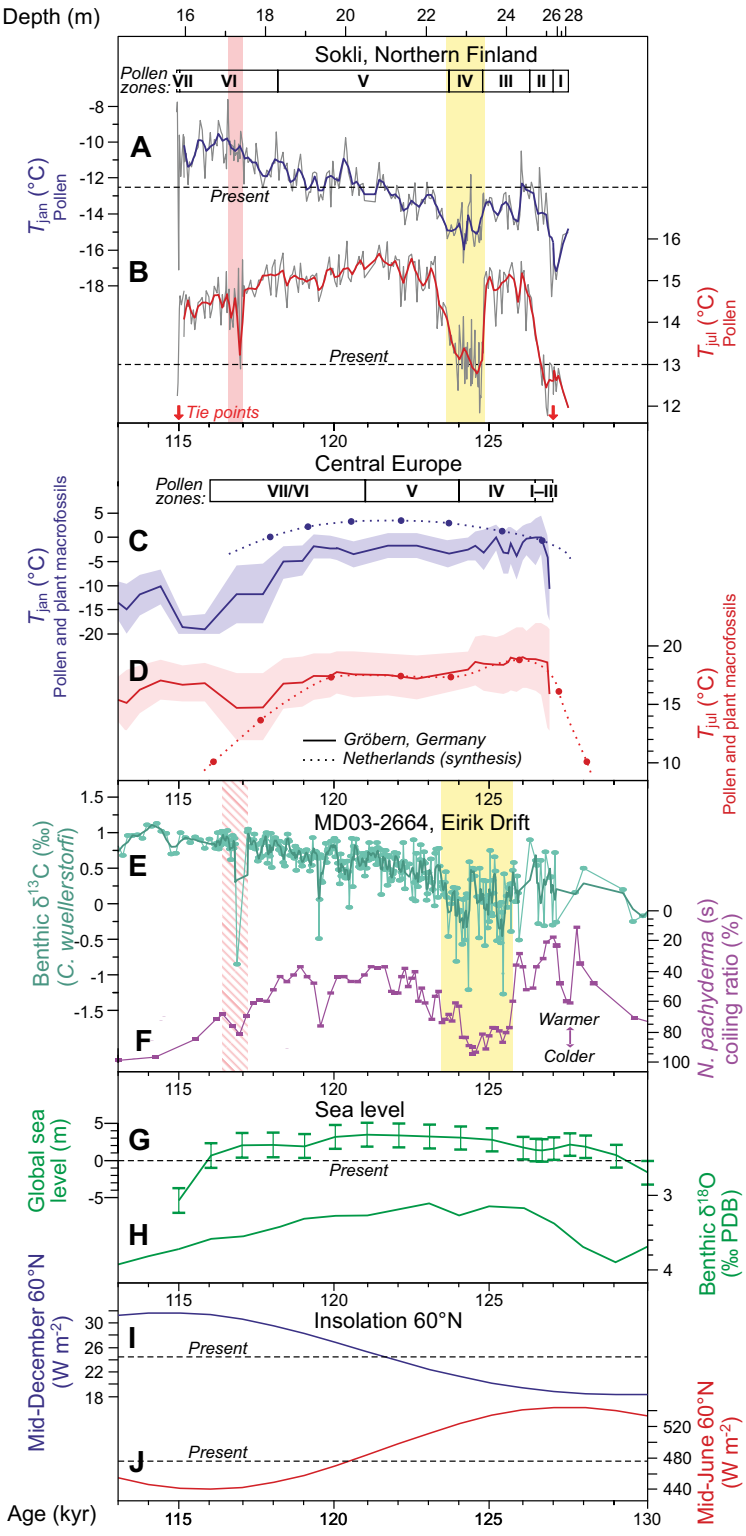

Figure 5-7. *Comparison of Sokli (**A, B**; present study), central European (**C, D**; Zagwijn 1996, Kühl et al. 2007) and North Atlantic Ocean (Eirik Drift; **E, F**; adapted from Irvalı et al. 2012, and Galaasen et al. 2014) Eemian Interglacial records. The yellow box highlights the Tunturi cooling event at Sokli and a major cooling event, and reduction in NADW, of similar age reconstructed at the Eirik Drift. The red box highlights the Värriö cooling event. The glacio-lacustrine sediment in the lowermost part of the Sokli record (below depth 25 m) is considered to represent a relatively short time window of rapid sediment accumulation. Also indicated are **G**, global sea-level during the Eemian (Dutton and Lambeck 2012, Masson-Delmotte et al. 2013); **H**, the benthic global stack with Marine Isotope Stages (MIS; Lisiecki and Raymo 2005); and **I/J**, insolation values from Berger and Loutre (1991). The time-scale of the Sokli record (**A/B**) is based on stalagmite evidence from the Alps (Spötl et al. 2002; end of Eemian Interglacial warmth) and preliminary U/Th-dated stalagmite data from central Sweden for the start of the Eemian in Fennoscandia (personal communication N. Frank, Institute of Environmental Physics, Heidelberg, Germany).*

New analysis at a considerably higher resolution, however, allowed the identification of several cold events of various amplitudes (Rioual et al. 2007); the climate changes at Ribains Maar are characterized as minor or subdued although quantification is lacking. It is possible that the vegetation-based proxies are more sensitive in northern Finland due to the location close to a major ecotone (tree-line), and thus while central Europe also underwent cooling no distinct imprint was left in the proxy records. Alternatively, major cooling event might have been mostly restricted to the high-latitude North Atlantic region as earlier suggested based on marine data (Cortijo et al. 1994, Fronval et al. 1998). The latter explanation is supported by the recently obtained mid-latitude Atlantic (ODP 980) (Govin et al. 2012) and Bay of Biscay (MD04-2845) (Sánchez Goñi et al. 2012) marine records (Figure 5-3) which suggest only minor (<1 °C) SST fluctuations during the Eemian. Recently, the long-term Eemian climate evolution has been simulated with several general circulation models, using orbital and greenhouse gas forcings (Bakker et al. 2013). These simulations do not indicate any major cooling event in the North Atlantic region, suggesting that other forcings are required to explain such a climatic anomaly.

It is possible that the younger Värriö cooling/drying event distinguished at Sokli corresponds to the ca 500 yrs long, cold and dry “late-Eemian aridity pulse”, recorded as a period of increased dust deposition in paleo-limnological studies from the Eifel in Germany (Sirocko et al. 2005, Seelos and Sirocko 2007). This event has been related to a southward shift of the North Atlantic drift at ca 118 kyrs BP, as a response to lowering of insolation (Sirocko et al. 2005), and correlated to cold event C26 at the beginning of global sea level drop in marine records from the North Atlantic (Sirocko et al. 2005, Seelos and Sirocko 2007).

6 Conclusions

The conclusions that can be drawn based on the present study are given below. Also briefly summarized are conclusions based on the early MIS 3 deposit in the Sokli basin (Helmens 2009) and preliminary conclusions for the MIS 5a deposit at Sokli (interpretation and publication of results are still ongoing). Figure 6-1 provides a first attempt to schematically show environmental and climate conditions in north-eastern Fennoscandia during the last ca 130 kyr based on our studies at Sokli (A). For comparison, B in Figure 6-1 shows conditions according to earlier reconstructions using long-distance correlation of highly fragmented stratigraphic evidence from Fennoscandia.

The Holocene Interglacial (last 11 kyr)

1) The analysis of multiple proxies on the 9 m-thick lacustrine deposit that accumulated in Loitsana Lake (Sokli basin, northeastern Finland) during the Holocene has revealed a complex lake development, including i) an initial phase of glacial lake evolution; ii) marked changes in fluvial input due to nearby, progressive wetland expansion (terrestrialization); iii) lake infilling; and iv) groundwater flow from a nearby esker chain. A combination of events, as recognized at Loitsana, can be expected to have influenced the Holocene development of many lakes in the formerly glaciated boreal zone of northern Europe.

2) Surprisingly rich biotic communities are reconstructed during the initial early-Holocene glacial lake stages. With the ice margin of the Fennoscandian Ice Sheet within a distance of 10 km from the coring-site, fossils reflect rich ecosystems both in the glacial lake and along its shores and surrounding birch forests on recently deglaciated land. Rich biota during deglaciation developed due to high nutrient levels (resulting from erosion of fresh bedrock and sediment) and warm summers.

3) Higher mean July temperatures (T_{jul}) than the present-day value of ca +13 °C at Sokli are inferred for the early-Holocene based on chironomids and macrofossil remains of aquatic and wetland taxa. T_{jul} during the early-Holocene was in the order of at least +12–15 °C.

4) During deglaciation, aquatic/wetland taxa responded quickly to enhanced, orbitally-induced early-Holocene summer insolation and reflect boreal conditions; the terrestrial vegetation responded with delay, probably due to slow soil formation processes, and was sub-arctic in origin.

5) The Holocene climate evolution as reconstructed based on the Loitsana Lake sequence is similar to recently inferred climate developments at other sites in Fennoscandia and indicate that the effect of the local carbonate-rich bedrock at Sokli on paleo-temperature reconstructions is neglectable.

The Middle Weichselian early MIS 3 Interstadial (ca 50 kyr ago)

6) According to earlier reconstructions, which were based on the long-distance correlation of highly fragmented stratigraphic evidence, Sokli was glaciated throughout MIS 4-2 (ca 70–10 kyr BP). The accumulation of lake sediments in the Sokli basin dated to ca 50 kyr BP, however, demonstrate ice-free conditions in what was the near-central area of Fennoscandia Weichselian glaciation.

7) Evidence from multiple proxies analyzed in the early MIS 3 sediment reconstructs warm summers (about present-day T_{jul} of +13 °C) and low-arctic shrub tundra vegetation remarkably similar in composition to the current vegetation in northernmost Fennoscandia. Warm summers were most probably driven by higher-than-today summer insolation.

8) The similarity in lithology and fossil content between the early MIS 3 and early-Holocene sediments in the Sokli basin supports the inferred glacio-lacustrine depositional environment for the early MIS 3 sediments.

The Early Weichselian MIS 5a Odderade Interstadial (ca 85–80 kyr ago)

9) A first integration of multi-proxy data most recently obtained on the sediments of MIS 5a age in the Sokli basin shows, following deglaciation of a MIS 5b ice sheet, the development of shrub tundra

vegetation to sub-arctic birch forest and then pine-dominated forest with larch. Aquatic and wetland taxa indicate minimum T_{jul} in the order of +12 to +15 °C. Additionally, the infilling of a relatively shallow lake can be traced in detail based on the fossil data.

The Early Weichselian MIS 5c Brørup Interstadial (ca 105–90 kyr ago)

10) A development towards a mixed boreal forest, similar in character to the present-day regional vegetation at Sokli, is inferred for the MIS 5c interstadial, based on our multi-proxy record from the Sokli basin. This is in sharp contrast to the cold tundra conditions at Sokli during MIS 5c (and MIS 5a), and sub-arctic birch woodland in areas presently covered by mixed boreal forest south of Sokli, reconstructed in previous studies based on the fragmented stratigraphic record for Fennoscandia.

11) Exceptionally rich plant macrofossil assemblages, associated with an overall fluvial depositional environment, indicate minimum T_{jul} values of +15–16 °C during MIS 5c. The warm summers during MIS 5c (similar as during early MIS 3 and MIS 5a) were most probably driven by higher-than-today summer insolation.

12) The fossil assemblages encountered in the MIS 5c sediment further record in great detail the infilling of an oxbow lake, terrestrialization, and the subsequent return to stream channel deposition.

The Early Weichselian MIS 5d Herning Stadial (ca 115–105 kyr ago)

13) In contrast to earlier reconstructed glaciation of Sokli during MIS 5d, we reconstruct a braided river environment; high T_{jul} values of up to at least +12–14 °C; and steppe-tundra vegetation with the local presence of birch trees and conifers.

14) The braided river pattern, the steppe-tundra vegetation, and the relatively high T_{jul}, indicate that the climate regime was most probably strongly continental with short warm summers and long cold winters. Present-day analogs for steppe-tundra vegetation are found in north-eastern Siberia and west-central Greenland, i.e. areas with a dry, strong continental climate and underlain by deep permafrost. Steppe vegetation is found here on south-facing slopes where the thin active layer dries out in summer; in contrast, the active layer remains moist on north-facing slopes, which are covered by tundra vegetation. Steppe-tundra vegetation was widespread in Europe during cold stages of the Weichselian.

The Eemian MIS 5e Interglacial (ca 130–115 kyr ago)

15) A vegetation development of pioneer birch forest followed by pine-dominate forest and then mixed boreal forest with spruce, similar as during the Holocene and MIS 5a, is reconstructed based on our study of a 9 m-thick lacustrine, diatom-gyttja deposit dated to MIS 5e (Eemian Interglacial) in the Sokli basin. *Larix* was present at Sokli during MIS 5e, 5c and 5a, but *Larix* pollen have not been encountered in Holocene lake deposits in Fennoscandia.

16) The pollen-based climate reconstructions show T_{jul} increasing to ca +16 °C and T_{jan} to ca –10 °C. The combined T_{jul} and T_{jan} reconstructions show a shift towards a maritime climate regime about half-way through the sequence; here, T_{jul} decreases in parallel to decreasing summer insolation, whereas T_{jan} increases in line with increasing winter insolation.

17) Our high-resolution multi-proxy record shows that the general trends in summer and winter temperatures, as forced by high-latitude insolation, were abruptly interrupted by two centennial/millennial-scale climate events. During the early-Eemian, so-called "Tunturi-event", T_{jul} dropped by ca 2–4 °C compared to earliest Eemian summer temperatures, causing the mixed boreal forest with birch, pine, spruce and larch to be temporarily replaced by open sub-arctic birch forest rich in juniper. In addition, cooling was accompanied by drying (inferred as lake level drops). The late-Eemian, so-called "Värriö-event" was also characterized by drying and cooling. Both events started abruptly and had a step-wise recovery.

18) Our results show the potential of major climate instability on the northern European continent in a warm climate. Similar cooling events as reconstructed at Sokli during the Eemian Interglacial have recently been recorded at high sediment accumulation sites in the Norwegian Sea and at the Eirik Drift

(south of Greenland). The cooling here occurs associated with reductions in North Atlantic Deepwater Formation. These results show that major climate variability was not restricted to cold glacial periods but also characterized the warm Eemian Interglacial, at least at high-latitudes.

19) Fossils of aquatic taxa combined with biogeochemical data reveal in great detail the infilling of a relatively deep, nutrient-rich, warm lake in the Sokli basin during the Eemian. The lake was stratified during its initial phase of development. Macrofossil remains are scarce in the lake sediment reflecting a relatively large open-water body throughout the lake infilling.

Summary of the last ca 130 kyr at Sokli

20) The fossil remains found in the deposits that were laid down in the Sokli basin during ice-free intervals over the last 130 kyr show, for most time-windows, successive developments in both vegetation (e.g. pioneer birch vegetation being replaced by pine-dominated forest and then mixed boreal forest with spruce) and depositional environments (e.g. lake infilling). Additionally, each deposit has unique aquatic/wetland fossil assemblages related to overall different local depositional environments (e.g. lake versus river). This, together with the general pattern of infilling of the Sokli basin over the last 130 kyr (see under point 21), shows that the deposits that make up the 30 m thick sediment infill in the Sokli basin occur *in situ*, i.e. there are not the result of re-deposition of older sediment/fossil remains.

21) The infilling of the Sokli basin (following glaciation dated to MIS 6, the Saalian) started around 130 kyr ago with sediment accumulation in a relatively deep and large lake (MIS 5e). As the lake was filled-in with diatom gyttja, a fluvial environment prevailed during MIS 5d (characterized by a braided river pattern) and 5c (infilling of oxbow lake). The area was glaciated again during MIS 5b starting at ca 90 kyr ago; the weight of the ice sheet can be expected to have compressed the basin infill, allowing for renewed lacustrine sedimentation during ice-free MIS 5a (although in a smaller and shallower lake than during MIS 5e). Subsequent glaciation during MIS 4 was once-more followed by deglaciation and glacial lake sedimentation during early MIS 3 around 50 kyr ago. As the early MIS 3 glacial lake drained, it is possible that sedimentation in the Sokli basin came to a halt due to infilling; alternatively, non-glacial/glacial sediment did accumulate during late MIS 3 but was eroded during the last phase of glaciation (MIS 2). Recent studies in both northern Finland and Sweden have revealed that ice-free conditions (with birch-dominated vegetation) in the central area of Fennoscandian glaciation might have lasted (possible interrupted by glaciation) through major part of MIS 3 to ca 35 kyr ago (Mäkinen 2005), Wohlfarth 2010), Sarala and Eskola 2011, Väliranta et al. 2012, Sarala et al. 2016; see also Helmens 2014). Finally, the Holocene lacustrine sediments in the Sokli basin were laid down in Loitsana Lake which occupies a deep depression forming part of an esker chain.

22) In contrast to earlier reconstructions which were based on the long-distance correlation of highly fragmented stratigraphic evidence from Fennoscandia, our studies on the long Sokli sequence from northern Finland reveal a highly dynamic Fennoscandian Ice Sheet, with less-extensive ice-cover, both in time and space, during the Weichselian glacial (ca 115–11 kyr BP). Additionally, biota responded quickly to increases in high-latitude summer insolation as seen by the reconstruction of forest at Sokli for MIS 5e, 5c, 5a and the Holocene. MIS 5, as a whole, was mostly warm and is defined in the Sokli stratigraphy as the Last Interglacial complex (ca 130–70 kyr BP; Helmens 2014). During the cold MIS 5d, severe continental climate conditions are recorded. The Last Glacial (ca 70–10 kyr BP; Helmens 2014) was characterized by at least two extended intervals of glaciation (MIS 4 and 2). Sokli was deglaciated in early MIS 3 when present-day T_{jul} values are reconstructed. Furthermore, our studies on the Eemian (MIS 5e) lake deposit in the Sokli basin show that abrupt, centennial/millennial-scale climate variability was not restricted to the Last Glacial (particularly MIS 3; Helmens 2014 and references herein). Our study reveals major climate instability during the Eemian, i.e. the last period of global warming when large parts of our planet experienced a warmer-than-today climate.

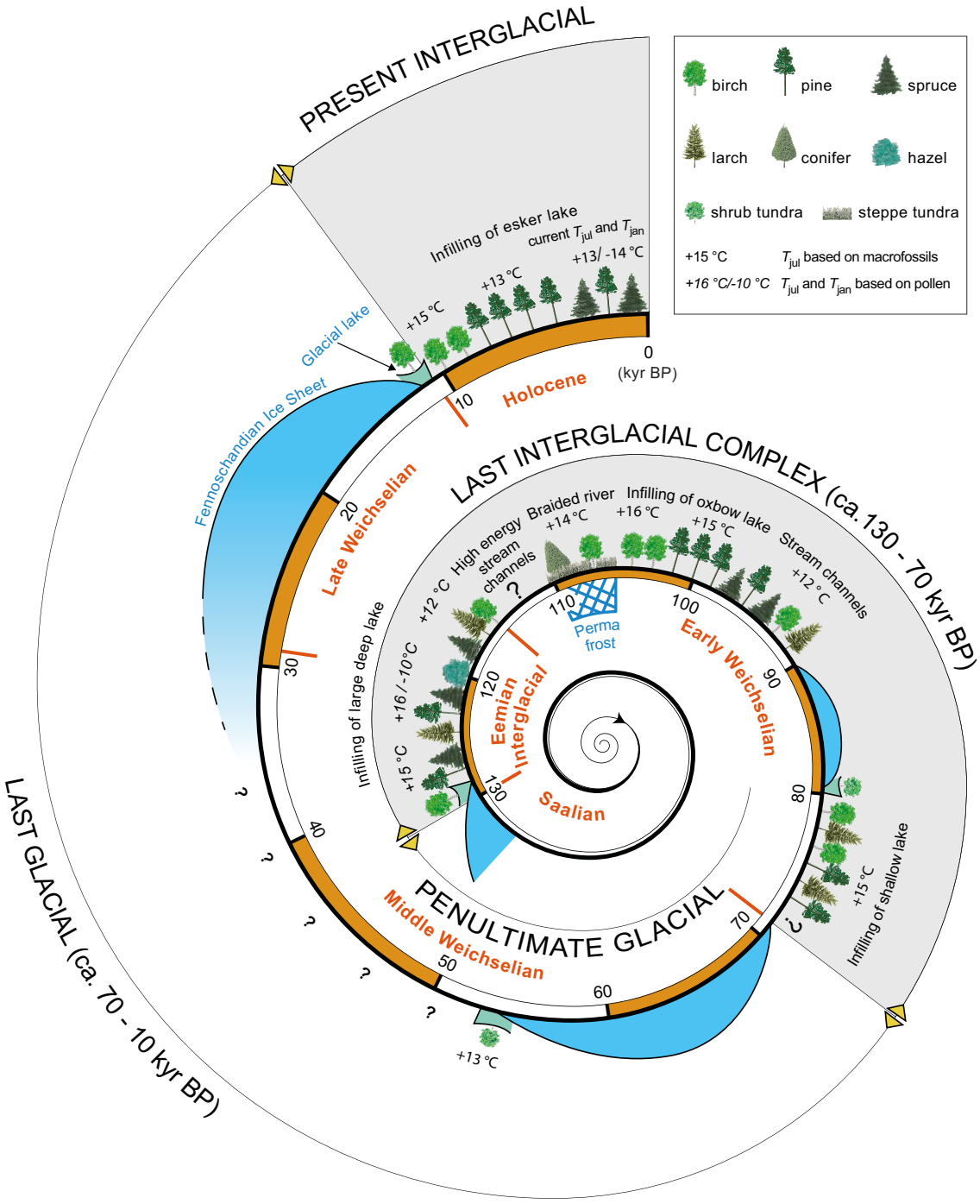

Figure 6-1A. *Environmental and climate conditions at Sokli during the Last Interglacial-Glacial cycle and the present Holocene Interglacial (last ca 130 kyr) based on the present study: a first integration.*

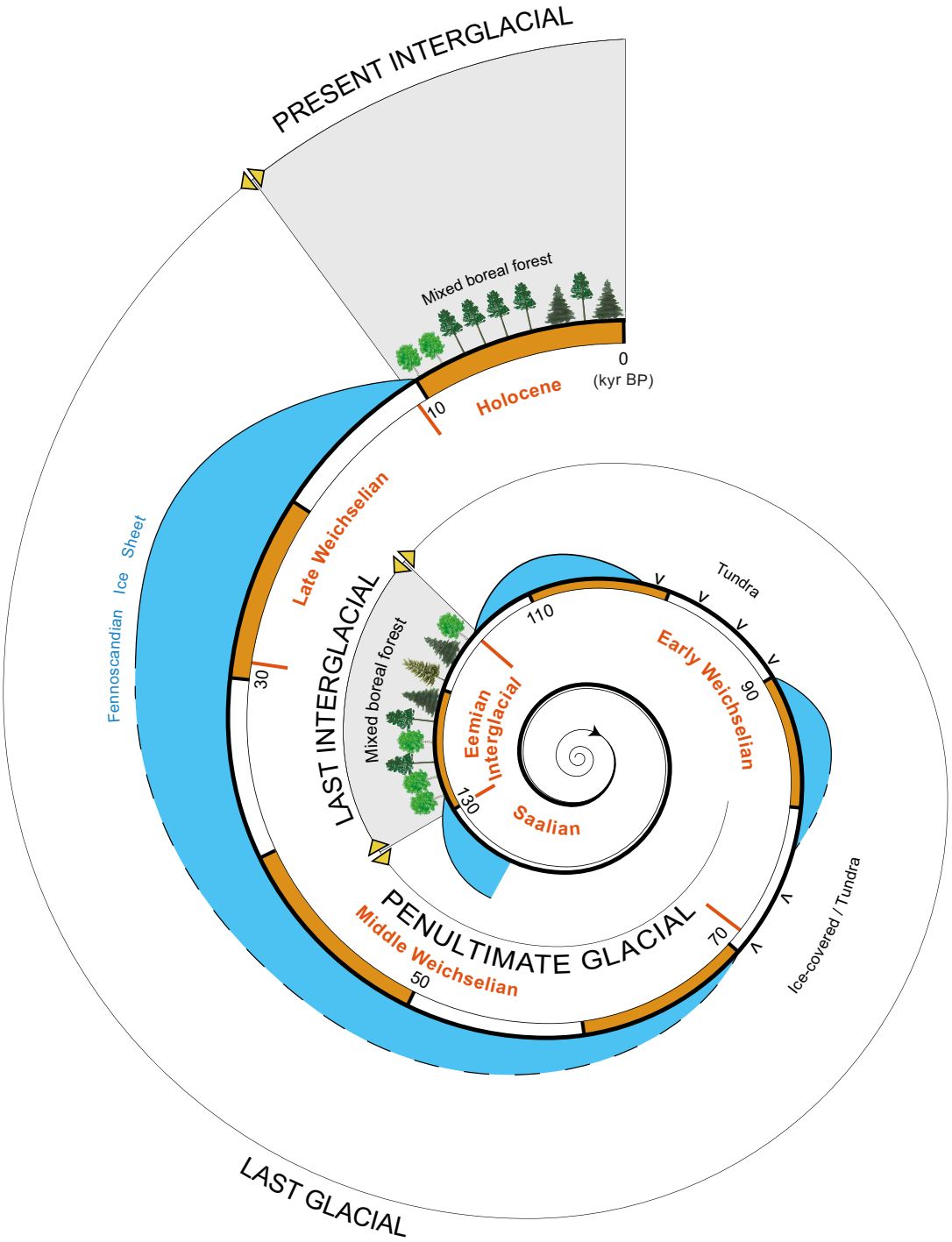

Figure 6-1B. *Previous reconstruction of environmental and climate conditions in north-eastern Fennoscandia during the Last Interglacial-Glacial cycle and the present Holocene Interglacial (last ca 130 kyr) based on long-distance correlation of fragmented stratigraphic evidence (e.g. Lundqvist 1992, Donner 1995).*

7 Potential future research

7.1 Suggestions for future work on the Sokli data of potential interest for SKB

- *Integration of multi-proxy data from the MIS 5a deposit in the Sokli basin*

A full interpretation and integration of multi-proxy data is needed for the most recently studied MIS 5a deposit in the Sokli basin. This will allow a detailed reconstruction of the depositional environment, and related azonal vegetation types, as well as changes in regional vegetation and climate for MIS 5a, similar as has been made based on the early MIS 3, MIS 5d-c, MIS 5e and Holocene deposits at Sokli.

This work is presently funded by SKB and will be finished the end of 2019.

- *Sokli data synthesis*

With the finalization of the MIS 5a project at Sokli, the foundation will be laid for *the final stage of the Sokli studies* focusing on full data synthesis.

In this synthesis, the multi-proxy data-sets obtained on the individual interstadial, stadial and interglacial deposits represented in the Sokli sedimentary sequence will be compared. Quantitative climate reconstructions will be performed using the most suitable fossil-climate calibration dataset and pollen sum, and newest state-of-the-art statistical methods (e.g. machine-learning techniques). In the course of the Sokli studies (2007–2017), new calibration datasets have become available and statistical methods have been significantly improved. Also, the choice of calibration set for the climate reconstructions has been explored, with the geographical footprint of the calibration samples, statistical performance of the transfer functions and length of the calibration-set gradient influencing the quantitatively reconstructed climate parameters (Salonen et al. 2013, Engels et al. 2014, Plikk et al. 2019). Furthermore, our detailed reconstructions of azonal (local) vegetation types will allow a reevaluation of the pollen sum to be used in calculating the pollen percentages.

With all proxy data from the entire Sokli sequence soon available, the stage is set for a full and consistent paleoenvironmental reconstruction for the Last Glacial-Interglacial cycle. Importantly, results from this data synthesis should be published in a single volume such as a book. This will allow bringing together more than a decade of detailed work at Sokli, it will present climate reconstructions based on a coherent and most up-to-date approach, and provide invaluable knowledge on the Late Quaternary history and climate of Fennoscandia.

7.2 In addition, the unique Sokli sequence is continuing to provide externally funded spin-off projects

- *Data-model and land-sea comparisons*

Detailed data-model and land-sea comparisons will contribute to the understanding of forcing mechanisms behind the observed Late Quaternary environmental and climate changes in Fennoscandia.

Presently, a study financed by the Finnish Academy (to Dr. Sakari Salonen; 2017–2020) focuses on MIS 5 climate modeling and land-sea comparisons. The project intends to use a coupled ocean-atmosphere global climate model (in collaboration with climate model specialists) and a comprehensive spatio-temporal synthesis of MIS 5 paleo-climate data including from the North Atlantic Ocean (in collaboration with Prof. María Sánchez-Goñi, Bordeaux University, France) to explore e.g. climate gradients over Europe during the MIS 5 warm stages (MIS 5a, 5c and 5e). Our results from Sokli now allow these gradients to be modeled and validated by proxy data from high latitude Europe.

Climate modeling should also be executed to explore forcing and amplifying mechanisms behind the cold events found to intersect warm Eemian (MIS 5e) Interglacial climate conditions at Sokli (*Tunturi and Värriö events*). This climate instability has important ramifications from a societal and policy perspective concerning future projected global warming. For this purpose, collaboration is being sought within the Bolin Centre of Climate Research at Stockholm University.

Acknowledgments

The data on the MIS 5e-5d-5c and Holocene deposits at Sokli presented in this report would not have been produced, interpreted and integrated without the help of the following persons whom I wish to thank for their great dedication and enthusiasm (placed according to institute/alphabetical order): Peter Kuhry, Malin Kylander, Krister Jansson, Anna Plikk, Jan Risberg, Shyhrete Shala (Stockholm University, Sweden); María Fernández-Fernández (Umeå University, Sweden); Miska Luoto, Tomi Luoto, Sakari Salonen, Heikki Seppä, Minna Väliranta, Jan Weckström (University of Helsinki, Finland); Stefan Engels (Birkbeck University of London, UK); Steven Brooks, Angela Self (Natural History Museum, UK); Hillary Birks, John Birks, Jo Brendryen (University of Bergen, Norway); Hans Renssen (VU University Amsterdam, The Netherlands); Niina Kuosmanen (Czech University of Life Sciences, Czech Republic); and Ludwig Löwemark (National Taiwan University).

Jens-Ove Näslund (SKB) is acknowledged for discussions and support throughout this project. The main part of the study was funded by SKB, Sweden. Additional funding has been received from Posiva, Finland; Bolin Centre of Climate Research (Stockholm University); Academy of Finland; Carl Mannerfelt Foundation; Swedish Society for Anthropology and Geography; INTIMATE COST Action; BioCold and NEPAL projects (Nordforsk); Gerard De Geer Fund; Margit Althin's Foundation; K&A Wallenberg Foundation; Stiftelsen Längmanska Kulturfonden; L&E Kinanders Stiftelse; and Lagrelius Fund, for which we are grateful. The report manuscript was scientifically reviewed by Normunds Stivrins (University of Latvia) and Christian Bigler (Umeå University). Jimmy Galle (LAJ Illustration) and Anders Lindblom (SKB) drew the summary figures in the Conclusion chapter.

References

SKB's (Svensk Kärnbränslehantering AB) publications can be found at www.skb.com/publications.

Aalbersberg G, Litt T, 1998. Multiproxy climate reconstructions for the Eemian and early Weichselian. Journal of Quaternary Science 13, 367–190.

Aario L, 1940. Waldgrenzen und subrezenten Pollenspektren in Petsamo Lappland. Annales Academiae Scientiarum Fennicae A. LIV. 8.

Ahee J, 2013. The spatial dynamics of wind pollination in broadleaf cattail (*Typha latifolia*): a new method to infer spatial patterns of pollen dispersal. MSc thesis. Trent University, Canada.

Aitchison J, 1982. The statistical analysis of compositional data. Journal of the Royal Statistical Society, Series B (Methodological) 44, 139–177.

Alexandersson H, 2002. Glacial geology and paleo-ice dynamics of two ice-sheet margins, Taymyr Peninsula, Siberia and Jameson Land, East Greenland. PhD thesis. Lund University, Sweden. (LUNDQUA Thesis 48)

Alexanderson H, Eskola K O, Helmens K F, 2008. Optical dating of a Late Quaternary sediment sequence from northern Finland. Geochronometria 32, 51–59.

Andersen B G, Mangerud J, 1989. The last interglacial-glacial cycle in Fennoscandia. Quaternary International 3–4, 21–29.

Anderson N J, 2000. Diatoms, temperature and climatic change. European Journal of Phycology 35, 307–314.

Bakker P, Stone E J, Charbit S, Gröger M, Krebs-Kanzow U, Ritz S P, Varma V, Khon V, Lunt D J, Mikolajewicz U, Prange M, Renssen H, Schneider B, Schulz M, 2013. Last interglacial temperature evolution – a model inter-comparison. Climate of the Past 9, 605–619.

Battarbee R W, 1986. Diatom analysis. In Berglund B E (ed). Handbook of Holocene palaeoecology and palaeohydrology. Chichester: Wiley, 527–570.

Battarbee R W, Jones V J, Flower R J, Cameron N G, Bennion H, Carvalho L, Juggins S, 2003. Diatoms. In Smol J P, Birks H J B, Last W M (eds). Tracking environmental change using lake sediments. Vol 3. Terrestrial, algal and siliceous indicators. Dordrecht: Kluwer Academic, 155–202.

Bauch H A, Kandiano E S, Helmke J, Andersen J, Rosell-Mele A, Erlenkeuser H, 2011. Climatic bisection of the last interglacial warm period in the Polar North Atlantic. Quaternary Science Reviews 30, 1813–1818.

Behre K E, 1989. Biostratigraphy of the last glacial period in Europe. Quaternary Science Reviews 8, 25–44.

Behre K E, Hölzer A, Lemdahl G, 2005. Botanical macro-remains and insects from the Eemian and Weichselian site of Oerel (northwest Germany) and their evidence for the history of climate. Vegetation History and Archaeobotany 14, 31–53.

Bennett K D, 1996. Determination of the number of zones in a biostratigraphical sequence. New Phytologist 132, 155–170.

Bennike O, Böcher J, 1992. Early Weichselian interstadial land biotas at Thule, Northwest Greenland. Boreas 21, 111–117.

Berger A, Loutre M F, 1991. Insolation values for the climate of the last 10 million years. Quaternary Science Reviews 10, 297–317.

Berglund B E, Björse G, Liljegren R, 1996. From the Ice Age to the present day. In Gustafsson L, Ahlén I (eds). Geography of plants and animals. National Atlas of Sweden, 14–24.

Bigler C, Grahn E, Larocque I, Jeziorski A, Hall R, 2003. Holocene environmental change at Lake Njulla (999 m a.s.l.), northern Sweden: a comparison with four small nearby lakes along an altitudinal gradient. Journal of Paleolimnology 29, 13–29.

Birks H H, 2007. Plant macrofossil introduction. In Elias S A (ed). Encyclopedia of Quaternary science. Oxford: Elsevier, 2266–2288.

Birks H H, Birks H J B, 2000. Future uses of pollen analysis must include plant macrofossils. Journal of Biogeography 27, 31–35.

Birks H J B, 1986. Late-Quaternary biotic changes in terrestrial and lacustrine environments, with particular reference to north-western Europe. In Berglund B E (ed). Handbook of Holocene palaeoecology and palaeohydrology. Chichester: Wiley, 3–65.

Birks H J B, 1995. Quantitative paleoenvironmental reconstructions. In Maddy D, Brew J S (eds). Statistical modelling of Quaternary science data. Cambridge: Quaternary Research Association. (Technical guide 5)

Birks H J B, 1998. Numerical tools in paleolimnology: progress, potentialities and problems. Journal of Paleolimnology 20, 307–332.

Birks H J B, 2003. Quantitative paleoenvironmental reconstructions from Holocene biological data. In Mackay A, Battarbee R W, Birks H J B, Oldfield F (eds). Global change in the Holocene. London: Arnold, 107–123.

Birks H J B, Birks H H (eds), 1980. Quaternary palaeoecology. London: Arnold.

Birks H J B, Gordon A D (eds), 1985. Numerical methods in Quaternary pollen analysis. London: Academic Press.

Birks H J B, Line M J, 1992. The use of rarefaction analysis for estimating palynological richness from Quaternary pollen-analytical data. The Holocene 2, 1–10.

Birks H J B, Seppä H, 2004. Pollen-based reconstructions of late-Quaternary climate in Europe – progress, problems, and pitfalls. Acta Palaeobotanica 44, 317–334.

Birks H J B, Line J M, Juggins S, Stevenson A C, ter Braak C J F, 1990. Diatoms and pH reconstruction. Philosophical Transactions of the Royal Society of London, Series B 327, 263–278.

Birks H J B, Heiri O, Seppä H, Bjune A E, 2010. Strengths and weaknesses of quantitative climate reconstructions based on late-Quaternary biological proxies. Open Ecology Journal 3, 68–110.

Björck S, Noe-Nygaard N, Wolin J, Houmark-Nielsen M, Hansen H, Snowball I, 2000. Eemian Lake development, hydrology and climate: a multi-stratigraphic study of the Hollerup site in Denmark. Quaternary Science Reviews 19, 509–536.

Blaauw M, 2010. Methods and code for "classical" age-modelling of radiocarbon sequences. Quaternary Geochronology 5, 512–518.

Bond G, Broecker W, Johnsen S, Mc Manus J, Labeyrie L, Jouzel J, Bonani G, 1993. Correlations between climate records from North Atlantic sediments and Greenland ice. Nature 365, 143–147.

Bos J A A, Helmens K F, Bohncke S J P, Seppä H, Birks H J B, 2009. Flora, vegetation and climate near Sokli, northern Fennoscandia, during Oxygen Isotope Stage 3. Boreas 38, 335–348.

Boyd M, Running G L, Havholm K, 2003. Paleoecology and geochronology of Glacial Lake Hind during the Pleistocene-Holocene transition: a context for Folsom surface finds on the Canadian Prairies. Geoarchaeology: An International Journal 18, 583–607.

Bradbury J P, Winter T C, 1976. Areal distribution and stratigraphy of diatoms in the sediments of Lake Sallie, Minnesota. Ecology 57, 1005–1014.

Breiman L, 2001. Random forests. Machine Learning 45, 5–32.

Brodersen K P, Lindegaard C, 1999. Classification, assessment and trophic reconstruction of Danish lakes using chironomids. Freshwater Biology 42, 143–157.

Bronk Ramsey C, 2009. Bayesian analysis of radiocarbon dates. Radiocarbon 51, 337–360.

Brooks S J, Birks H J B, 2001. Chironomid-inferred air temperatures from Lateglacial and Holocene sites in north-west Europe: progress and problems. Quaternary Science Reviews 20, 1723–1741.

Brooks S J, Birks H J B, 2004. The dynamics of Chironomidae assemblages in response to environmental change during the past 300 years in Spitsbergen. Journal of Paleolimnology 31, 483–498.

Brooks S J, Langdon P G, Heiri O, 2007. The identification and use of palaeoarctic Chironomidae larvae in palaeoecology. London: Quaternary Research Association.

Böcher T W, 1954. Oceanic and continental vegetation complexes in south-west Greenland. Meddelelser om Grønland 148.

Carter J A, 2007. Phytoliths. In Elias S A (ed). Encyclopedia of Quaternary science. Oxford: Elsevier, 2257–2265.

Claesson Liljedahl L, Kontula A, Harper J, Näslund J-O, Selroos J-O, Pitkänen P, Puigdomenech I, Hobbs M, Follin S, Hirschorn S, Jansson P, Kennell L, Marcos N, Ruskeeniemi T, Tullborg E-L, Vidstrand P, 2016. The Greenland Analogue Project: Final report. SKB TR-14-13, Svensk Kärnbränslehantering AB.

Cleveland W S, 1979. Robust locally weighted regression and smoothing scatterplots. Journal of the American Statistical Association 74, 829–836.

Cohen A S, 2003. Paleolimnology: the history and evolution of lake systems. Oxford: Oxford University Press.

Cortijo E, Duplessy J C, Labeyrie L, Leclaire H, Duprat J, van Weering T C E, 1994. Eemian cooling in the Norwegian Sea and North Atlantic ocean preceding continental ice-sheet growth. Nature 372, 446–449.

Cronberg G, 1982. *Pediastrum* and *Scenedesmus* (Chlorococcales) in sediments from lake Växjösjön, Sweden. Archiv für Hydrobiologie Supplementband Algologcial Studies 29, 500–507.

Croudace I W, Rindby A, Rothwell R G, 2006. ITRAX. Description and evaluation of a new multi-function X-ray core scanner. In Rothwell R G (ed). New techniques in sediment core analysis. London: Geological Society of London, 51–63.

Cvetkoska A, Levkov Z, Reed J M, Wagner B, 2014. Late Glacial to Holocene climate change and human impact in the Mediterranean: the last ca 17 ka diatom record of Lake Prespa (Macedonia/Albania/Greece). Palaeogeography, Palaeoclimatology, Palaeoecology 406, 22–32.

Dansgaard W, Johnsen S J, Clausen H B, Dahl-Jensen D, Gundestrup N S, Hammer C U, Hvidberg C S, Steffensen J P, Sveinbjörnsdottir A E, Jouzel J, Bond G, 1993. Evidence for general instability of past climate from a 250-kyr ice-core record. Nature 364, 218–220.

Davis B A S, Zanon M, Collins P, Mauri A, Bakker J, Barboni D, Barthelmes A, Beaudouin C, Birks H J B, Bjune A E, Bozilova E, Bradshaw R H W, Brayshay B A, Brewer S, Brugiapaglia E, Bunting J, Connor S E, de Beaulieu J L, Edwards K J, Ejarque A, Fall P, Florenzano A, Fyfe R, Galop D, Giardini M, Giesecke T, Grant M J, Guiot J, Jahns S, Jankovska V, Juggins S, Kahrmann M, Karpińska-Kołaczek M, Kołaczek P, Kühl N, Kuneš P, Lapteva E G, Leroy S A G, Leydet J, Lopéz Sáez J A, Masi A, Matthias I, Mazier F, Meltsov V, Mercuri A M, Miras Y, Mitchell F J G, Morris J L, Naughton F, Nielsen A B, Novenko E, Odgaard B, Ortu E, Overballe-Petersen M V, Pardoe H S, Peglar S M, Pidek I A, Sadori L, Seppä H, Severova E, Shaw H, Święta-Musznicka J, Theuerkauf M, Tonkov S, Veski S, van der Knaap P W O, van Leeuwen J F N, Woodbridge J, Zimny M, Kaplan J O, 2013. The European Modern Pollen Database (EMPD) project. Vegetation History and Archaeobotany 22, 521–530.

De'ath G, 2007. Boosted trees for ecological modeling and prediction. Ecology 88, 243–251.

Denton G H, Alley R B, Comer G C, Broecker W S, 2005. The role of seasonality in abrupt climate change. Quaternary Science Reviews 24, 1159–1182.

Donner J, 1995. The Quaternary history of Scandinavia. Cambridge: Cambridge University Press. (World and Regional Geology 7)

Donner J, 1996. The Early and Middle Weichselian interstadials in the central area of the Scandinavian glaciations. Quaternary Science Reviews 15, 471–479.

Dutton A, Lambeck K, 2012. Ice volume and sea level during the Last Interglacial. Science 337, 216–219.

Eggermont H, Heiri O, 2012. The chironomid-temperature relationship: expression in nature and paleoenvironmental implications. Biological Reviews 87, 430–456.

Engels S, Cwynar L C, 2011. Changes in fossil chironomid remains along a depth gradient: evidence for common faunal thresholds within lakes. Hydrobiologia 665, 15–38.

Engels S, Bohncke S J P, Heiri O, Nyman M, 2008a. Intraregional variability in chironomid-inferred temperature estimates and the influence of river inundations on lacustrine chironomid assemblages. Journal of Paleolimnology 40, 129–142.

Engels S, Bohncke S J P, Bos J A A, Brooks S J, Heiri O, Helmens K F, 2008b. Chironomid-based palaeotemperature estimates for northeast Finland during Oxygen Isotope Stage 3. Journal of Paleolimnology 40, 49–61.

Engels S, Helmens K F, Väliranta M, Brooks J, Birks H J B, 2010. Early Weichselian (MIS-5d and 5c) temperatures and environmental changes in northern Fennoscandia as recorded by chironomids and macroremains at Sokli, northeast Finland. Boreas 39, 689–704.

Engels S, Self A E, Luoto T P, Brooks S J, Helmens K F, 2014. A comparison of three Eurasian chironomid–climate calibration datasets on a W–E continentality gradient and the implications for quantitative temperature reconstructions. Journal of Paleolimnology 51, 529–547.

Epler J H, 2001. Identification manual for the larval Chironomidae (Diptera) of North and South Carolina. North Carolina Department of Environmental and Natural Resources, Raleigh, NC, and St Johns River Water Management District, Palatka, FL.

Etienne J L, Jansson K N, Glasser N F, Hambrey M J, Davies J R, Waters R A, Wilby P R, 2006. Paleoenvironmental reconstruction of an ice-contact glacial lake succession: an example from the Late Pleistocene of southwest Wales, UK. Quaternary Science Reviews 25, 739–762.

Faegri K, Iversen J, 1989. Textbook of pollen analysis. Chichester: Wiley.

Fairchild G W, Lowe R L, 1984. Artificial substrates which release nutrients: effects on periphyton and invertebrate succession. Hydrobiologia 114, 29–37.

Filippi M L, Piliposian G, Marziali L, Angeli N, Lencioni V, Cantonati M, 2011. Is it possible to study paleoenvironmental changes in Alpine spring habitats? Few examples from the south-eastern Alps (NE Italy). Journal of Limnology 70, 155–167.

Finnish Environmental Institute, 2010. Environmental data obtained from the Environmental Information System (HERTTA) data base at the Finnish Environment Institute. Vattenkvalité, resultatblad 8.2.2010.

Forsström L, 1990. Occurrence of larch (*Larix*) in Fennoscandia during the Eemian interglacial and the Brørup interstadial according to pollen analytical data. Boreas 19, 241–248.

Fritz S C, Anderson N J, 2013. The relative influences of climate and catchment processes on Holocene lake development in glaciated regions. Journal of Paleolimnology 49, 349–362.

Fronval T, Jansen E, Haflidason H, Sejrup H P, 1998. Variability in surface and deep water conditions in the Nordic seas during the last interglacial period. Quaternary Science Reviews 17, 963–985.

Gajewski K, Bouchard G, Wilson S E, Kurek J, Cwynar L C. 2005. Distribution of Chironomidae (Insecta: Diptera) head capsules in recent sediments of Canadian Arctic lakes. Hydrobiologia 549, 131–143.

Galaasen E V, Ninnemann U S, Irvalı N, Kleiven H K F, Rosenthal Y, Kissel C, Hodell D A, 2014. Rapid reductions in North Atlantic deep water during the peak of the last interglacial period. Science 343, 1129–1132.

Goring S, Salonen J S, Luoto M, Williams J, 2015. Non-analogues in paleoecological reconstruction: model behaviour and implications. In Dy J G, Emile-Geay J, Lakshmanan V, Liu Y (eds). Proceedings of the Fifth International Workshop on Climate Informatics: CI 2015, Boulder, Colorado, 24–25 September 2015.

Govin A, Braconnot P, Capron E, Cortijo E, Duplessy J-C, Jansen E, Labeyrie L, Landais A, Marti O, Michel E, Mosquet E, Risebrobakken B, Swingedouw D, Waelbroeck C, 2012. Persistent influence of ice sheet melting on high northern latitude climate during the early Last Interglacial. Climate of the Past 8, 483–507.

Govin A, Capron E, Tzedakis P C, Verheyden S, Ghaleb B, Hillaire-Marcel C, St-Onge G, Stoner J S, Bassinot F, Bazin L, Blunier T, Combourieu-Nebout N, El Ouahabi A, Genty D, Gersonde R, Jimenez-Amat P, Landais A, Martrat B, Masson-Delmotte V, Parrenin F, Seidenkrantz M-S, Veres D, Waelbroeck C, Zahn R, 2015. Sequence of events from the onset to the demise of the Last Interglacial: evaluating strengths and limitations of chronologies used in climatic archives. Quaternary Science Reviews 129, 1–36.

Granoszewski W, 2003. Late Pleistocene vegetation history and climatic changes at Horoszki Duże, Eastern Poland: a paleobotanical study. Acta Palaeobotanica, Supplement 4, 3–95.

Guiry M D, Guiry G M, 2016. AlgaeBase. World-wide electronic publication, National University of Ireland, Galway. Available at: http://www.algaebase.org

Guiter F, Andrieu-Ponel V, de Beaulieu J-L, Cheddadi R, Calvez M, Ponel P, Reille M, Keller T, Goeury C, 2003. The last climatic cycles in Western Europe: a comparison between long continuous lacustrine sequences from France and other terrestrial records. Quaternary International 111, 59–74.

Gunin P D, Vostokova E A, Dorofeyuk N I, Tarasov P E, Black C C, 1999. Vegetation dynamics of Mongolia. Dordrecht: Springer. (Geobotany 26)

Guthrie R D, 1982. Mammals of the mammoth steppe as palaeoenvironmental indicators. In Hopkins D M, Matthews Jr. J H, Schweger C, Young S B (eds). Palaeoecology of Beringia. New York: Academic Press, 307–326.

Guyard H, Chapron E, St-Onge G, Anselmetti F-S, Arnaud F, Magand O, Francus P, Mélières M-A, 2007. High-altitude varve records of abrupt environmental changes and mining activity over last 4000 years in the Western French Alps (Lake Bramant, Grandes Rousses Massif). Quaternary Science Reviews 26, 2644–2660.

Gälman V, Rydberg J, Shchukarev A, Sjöberg S, Martínez-Cortizas A, Bindler R, Renberg I, 2009. The role of iron and sulfur in the visual appearance of lake sediment varves. Journal of Paleolimnology 42, 141–153.

Hald M, Andersson C, Ebbesen H, Jansen E, Klitgaard-Kristensenc D, Risebrobakken B, Salomonsen G R, Sarnthein M, Sejrup H P, Telford R J, 2007. Variations in temperature and extent of Atlantic Water in the northern North Atlantic during the Holocene. Quaternary Science Reviews 26, 3423–3440.

Hannon G, Gaillard M-J, 1997. The plant macrofossil record of past lake-level changes. Journal of Paleolimnology 18, 15–28.

Harris S W, Marshall W H, 1963. Ecology of water-level manipulations on a northern marsh. Ecology 44, 331–343.

Haworth E, 1976. Two Late-Glacial (Late Devensian) diatom assemblage profiles from northern Scotland. New Phycologist 77, 227–256.

Heino J, Toivonen H, 2008. Aquatic plant biodiversity at high latitudes: patterns of richness and rarity in Finnish freshwater macrophytes. Boreal Environment Research 13, 1–14.

Heiri O, Lotter A F, Lemcke G, 2001. Loss on ignition as a method for estimating organic and carbonate content in sediments: reproducibility and comparability of results. Journal of Paleolimnology 25, 101–110.

Heiri O, Lotter A F, Hausmann S, Kienast F, 2003. A chironomid-based Holocene summer air temperature reconstruction from the Swiss Alps. The Holocene 13, 477–484.

Helmens K F, 2009. Climate, vegetation and lake development at Sokli (northern Finland) during early MIS 3 at ~ 50 kyr: revising earlier concepts on climate, glacial and vegetation dynamics in Fennoscandia during the Weichselian. SKB TR-09-16, Svensk Kärnbränslehantering AB.

Helmens K F, 2013. The Last Interglacial-Glacial cycle (MIS 5-2) re-examined based on long proxy records from central and northern Europe. SKB TR-13-02, Svensk Kärnbränslehantering AB.

Helmens K F, 2014. The Last Interglacial-Glacial cycle (MIS 5-2) re-examined based on long proxy records from central and northern Europe. Quaternary Science Reviews 86, 115–143.

Helmens K F, Engels S, 2010. Ice-free conditions in eastern Fennoscandia during early Marine Isotope Stage 3: lacustrine records. Boreas 39, 399–409.

Helmens K F, Räsänen M E, Johansson P, Jungner H, Korjonen K, 2000. The Last Interglacial-Glacial cycle in NE Fennoscandia: a nearly continuous record from Sokli (Finnish Lapland). Quaternary Science Reviews 19, 1605–1623.

Helmens K F, Johansson P W, Räsänen M E, Alexanderson H, Eskola K O, 2007. Ice-free intervals continuing into Marine Isotope Stage 3 at Sokli in the central area of the Fennoscandian glaciations. Bulletin of the Geological Society of Finland 79, 17–39.

Helmens K F, Risberg J, Jansson K N, Weckström J, Berntsson A, Kaislahti Tillman P, Johansson P W, Wastegård S, 2009. Early MIS 3 glacial lake evolution, ice-marginal retreat pattern and climate at Sokli (northeastern Fennoscandia). Quaternary Science Reviews 28, 1880–1894.

Helmens K F, Väliranta M, Engels S, Shala S, 2012. Large shifts in vegetation and climate during the Early Weichselian (MIS 5d-c) inferred from multi-proxy evidence at Sokli (northern Finland). Quaternary Science Reviews 41, 22–38.

Helmens K F, Salonen J S, Plikk A, Engels S, Väliranta M, Kylander M, Brendryen J, Renssen H, 2015. Major cooling intersecting peak Eemian Interglacial warmth in Northern Europe. Quaternary Science Reviews, short communication 122, 293–299.

Helmens K F, Katrantsiotis C, Salonen S J, Shala S, Bos J A A, Engels S, Kuosmanen N, Luoto T P, Väliranta M, Luoto M, Ojala A, Risberg J, Weckström J, 2018. Warm summers and rich biotic communities during N-Hemisphere deglaciation. Global and Planetary Change 167, 61–73.

Helminen, V A, 1988. Temperature. In Atlas of Finland. Folio 131. Climate. Helsinki: Maanmittaushallitus.

Henley W E, Patterson M A, Neves R J, Lemly D A, 2000. Effects of sedimentation and turbidity on lotic food webs: a concise review for natural resource managers. Reviews in Fisheries Science 8, 125–193.

Hewett D G, 1964. The biological flora of the British Isles – Menyanthes trifoliate L. Journal of Ecology 52, 723–735.

Hicks S, 1994. Present and past pollen records of Lapland forests. Review of Palaeobotany and Palynology 82, 17–35.

Hijmans R J, 2014. raster: Geographic data analysis and modeling. R package version 2.2-31. Available at: http://CRAN.R-project.org/package=raster

Hill M O, 1973. Diversity and evenness: a unifying notation and its consequences. Ecology 54, 427–432.

Hirvas H, 1991. Pleistocene stratigraphy of Finnish Lapland. Helsinki: Geological Survey of Finland. (Bulletin 354)

Hoek W Z, 1997. Atlas to palaeogeography of lateglacial vegetations. Utrecht: Royal Dutch Geographical Society. (Nederlandse Geografische Studies 231)

Hofmann W, 1998. Cladocerans and chironomids as indicators of lake level changes in north temperate lakes. Journal of Paleolimnology 19, 55–62.

Hokanson K E F, 1977. Temperature requirements of some percids and adaptations to the seasonal temperature cycle. Journal of the Fisheries Research Board of Canada 34, 1524–1550.

Holzkämper S, Mangini A, Spötl, C, Mudelsee M, 2004. Timing and progression of the Last Interglacial derived from a high alpine stalagmite. Geophysical Research Letters 31, L07201. doi:10.1029/2003GL019112

Hultén E, Fries M, 1986. Atlas of North European vascular plants north of the Tropic of Cancer I–III. Königstein: Koeltz Scientific Books.

Hyvärinen H, Martma T, Punning J-M, 1998. Stable isotope and pollen stratigraphy of a Holocene lake marl section from NE Finland. Boreas 19, 17–24.

Ilvonen E, 1973. Eem-kerrostuma Savukosken Soklilla. Geologi 25, 81–84. (In Finnish.)

Irvalı N, Ninnemann U S, Galaasen E V, Rosenthal Y, Kroon D, Oppo D W, Kleiven H F, Darling K F, Kissel C, 2012. Rapid switches in subpolar North Atlantic hydrography and climate during the Last Interglacial (MIS 5e). Paleoceanography and Paleoclimatology 27. doi:10.1029/2011PA002244

Iversen J, 1954. The late-glacial flora of Denmark and its relation to climate and soil. Danmarks Geologiske Undersøgelse II 80, 87–119.

Jackson S T, Williams J W, 2004. Modern analogs in Quaternary paleoecology: here today, gone yesterday, gone tomorrow? Annual Review of Earth and Planetary Sciences 32, 495–537.

Jankovská V, Komárek J, 2000. Indicative value of *Pediastrum* and other coccal green algae in paleoecology. Folia Geobotanica 35, 59–82.

Jansen A J M, Schaminée J H J, Schipper P C, Schouten M G C, 2000. Plantengemeenschappen van waterrijke gebieden. In Weeda E J, Schaminée J H J, van Duuren L (eds). Atlas van plantengemeenschappen in Nederland. Deel 1. Wateren, moerassen en natte heiden. Utrecht: KNNV, 34–75.

Jansson K N, 2003. Early Holocene glacial lakes and ice marginal retreat pattern in Labrador/Ungava, Canada. Palaeogeography, Palaeoclimatology, Palaeoecology 193, 437–501.

Johansson P, 1995. The deglaciation in the eastern part of the Weichselian ice divide in Finnish Lapland. Helsinki: Geological Survey of Finland. (Bulletin 383)

Johansson P, 2007. Late Weichselian deglaciation in Finnish Lapland. In Johansson P, Sarala P (eds). Applied Quaternary research in the central part of glaciated terrain. Espoo: Geological Survey of Finland. (Special paper 46), 47–54.

Johansson P, Lunkka P J, Sarala P, 2011. The glaciation of Finland. In Ehlers J, Gibbard P L, Hughes P D (eds). Quaternary glaciations – Extent and chronology: a closer look. Oxford: Elsevier. (Developments in Quaternary Science 15), 105–116.

Johnsen S J, Clausen H B, Dansgaard W, Fuhrer K, Gundestrup N, Hammer C U, Iversen P, Jouzel J, Stauffer B, Steffensen J P, 1992. Irregular glacial interstadials recorded in a new Greenland ice core. Nature 359, 311–313.

Jones V J, Solovieva N, Self A E, McGowan S, Rosén P, Salonen J S, Seppä H, Väliranta M, Parrott E, Brooks S J, 2011. The influence of Holocene tree-line advance and retreat on an arctic lake ecosystem: a multi-proxy study from Kharinei Lake, North Eastern European Russia. Journal of Paleolimnology 46, 123–137.

Juggins S, 2009. Rioja: Analysis of Quaternary Science Data, R package version 0.5-6. Available at: http://cran.r-project.org/package=rioja. Newcastle: University of Newcastle.

Juggins S, 2012. rioja: Analysis of Quaternary Science Data, R package version 0.8-7. Available at: http://cran.r-project.org/package=rioja. Newcastle: University of Newcastle.

Juggins S, 2013. Quantitative reconstructions in paleolimnology: new paradigm or sick science? Quaternary Science Reviews 64, 20–32.

Juggins S, Simpson G L, Telford R J, 2015. Taxon selection using statistical learning techniques to improve transfer function prediction. The Holocene 25, 130–136.

Kabailiené M, 1995. The Baltic Ice Lake and Yoldia sea stages, based on data from diatom analysis in the central, south-eastern and eastern Baltic. Quaternary International 27, 69–72.

Kienast F, Tarasov P, Schirrmeister L, Grosse G, Andreev A A, 2008. Continental climate in the East Siberian Arctic during the last interglacial: implications from paleobotanical records. Global and Planetary Change 60, 535–562.

Kleman J, Hättestrand C, Borgström I, Stroeven A P, 1997. Fennoscandian paleoglaciology reconstructed using a glacial geological inversion model. Journal of Glaciology 43, 283–299.

Klink A, 1989. The lower Rhine: paleoecological analysis. In Petts G E (eds). Historical change of large alluvial rivers: western Europe. Chichester: Wiley, 183–201.

Klotz S, Müller U, Mosbrugger V, de Beaulieu J-L, Reille M, 2004. Eemian to early Würmian climate dynamics: history and pattern of changes in Central Europe. Palaeogeography, Palaeoclimatology, Palaeoecology 211, 107–126.

Koinig K A, Shotyk W, Lotter A F, Ohlendorf C, Sturm M, 2003. 9000 years of geochemical evolution of lithogenic major and trace elements in the sediment of an alpine lake – the role of climate, vegetation and land-use history. Journal of Paleolimnology 30, 307–320.

Kolstrup E, 1979. Herbs as July temperature indicators for parts of the pleniglacial and late-glacial in the Netherlands. Geologie en Mijnbouw 58, 377–380.

Komárek J, Jankovská V, 2001. Review of the green algal genus *Pediastrum*: implication for pollen-analytical research. Berlin: Cramer. (Bibliotheka Phycologica 108)

Korhola A, Weckström J, 2004. Paleolimnological studies in Arctic Fennoscandia and the Kola Peninsula (Russia). In Pienitz R, Douglas M S V, Smol J P (eds). Long-term environmental change in Arctic and Antarctic lakes. Dordrecht: Springer, 381–418.

Korhola A, Weckström J, Nyman M, 1999. Predicting the long-term acidification trends in small subarctic lakes using diatoms. Journal of Applied Ecology 36, 1021–1034.

Krammer K, Lange-Bertalot H, 1986. Bacillariophyceae. 1. Teil: Naviculaceae. In Ettl H, Gerloff J, Heynig H, Mollenhauser D (eds). Süßwasserflora von Mitteleuropa. Band 2/1. Stuttgart: Fischer.

Krammer K, Lange-Bertalot H, 1988. Bacillariophyceae. 2. Teil: Bacillariaceae, Epithemiaceae, Surirellaceae. In Ettl H, Gerloff J, Heynig H, Mollenhauser D (eds). Süßwasserflora von Mitteleuropa 2/2. Stuttgart: Fischer.

Krammer K, Lange-Bertalot H, 1991a. Bacillariophyceae. 3. Teil: Centrales, Fragilariaceae, Eunotiaceae. In Ettl H, Gerloff J, Heynig H, Mollenhauser D (eds). Süßwasserflora von Mitteleuropa 2/3. Stuttgart: Fischer.

Krammer K, Lange-Bertalot H, 1991b. Bacillariophyceae. 4. Teil: Achnanthaceae. Kritische Ergänzungen zu Navicula (Lineolate) und Gomphonema. In Ettl H, Gerloff J, Heynig H, Mollenhauser D (eds). Süßwasserflora von Mitteleuropa 2/4. Stuttgart: Fischer.

Krammer K, Lange-Bertalot H, 2008a. Süßwasserflora von Mitteleuropa. Bd 2, Bacillariophyceae, T. 2, Bacillariaceae, Epithemiaceae, Surirellaceae. Heidelberg: Spektrum Akademischer Verlag.

Krammer K, Lange-Bertalot H, 2008b. Süßwasserflora von Mitteleuropa. Bd 2, Bacillariophyceae, T. 3, Centrales, Fragilariaceae, Eunotiaceae. Heidelberg: Spektrum Akademischer Verlag.

Krammer K, Lange-Bertalot H, 2010a. Bacillariophyceae. T. 1, Naviculaceae. A, Text. Heidelberg: Spektrum Akademischer Verlag.

Krammer K, Lange-Bertalot H, 2010b. Bacillariophyceae. T. 1, Naviculaceae. B, Tafeln. Heidelberg: Spektrum Akademischer Verlag.

Kujansuu R, Eriksson B, Grönlund T, 1998. Lake Inarijärvi, northern Finland: sedimentation and late Quaternary evolution. Report of Investigation 143, Geological Survey of Finland.

Kullman L, 1999. Early Holocene tree growth at a high elevation site in the northernmost Scandes of Sweden (Lapland): a paleobiogeographical case study based on megafossil evidence. Geografiska Annaler 81A, 63–74.

Kulmann J, 2002. Boreal tree taxa in the central Scandes during the Lateglacial: implications for Late Quaternary forest history. Journal of Biogeography 29, 1117–1124.

Kulmann J, 2006. Lateglacial trees from arctic coast to alpine tundra: response to Birks et al. 2005 and 2006. Journal of Biogeography 33, 377–378.

Kühl N, Litt T, Schölzel C, Hense A, 2007. Eemian and Early Weichselian temperature and precipitation variability in northern Germany. Quaternary Science Reviews 26, 3311–3317.

Kylander M E, Ampel L, Wohlfarth B, Veres D, 2011. High-resolution X-ray fluorescence core scanning analysis of Les Echets (France) sedimentary sequence: new insights from chemical proxies. Journal of Quaternary Science 26, 109–117.

Kylander M, Plikk A, Rydberg J, Löwemark L, Salonen S J, Fernández-Fernández M, Helmens K F, 2018. Sediment Geochemistry of the Eemian Sequence at Sokli, NE Finland: new insights from XRF core scanning data into boreal lake ontogeny during the Eemian (Marine Isotope Stage 5e) at Sokli, northeast Finland. Quaternary Research 89, 352–364.

Lampinen R, Lahti T, 2007. Kasviatlas 2006. Helsinki: Botanical Museum, Finnish Museum of Natural History. (Digital atlas of vascular plants in Finland.) Available at: http://www.luomus.fi/kasviatlas

Lampinen R, Lahti T, 2013. Kasviatlas 2012. Helsinki: Botanical Museum, Finnish Museum of Natural History. (Digital atlas of vascular plants in Finland.) Available at: http://www.luomus.fi/kasviatlas

Lauber K, Wagner G, Gygax A, Eggenberg S, Michel A, 1998. Flora Helvetica. Bern: Haupt.

Liaw A, Wiener M, 2002. Classification and Regression by randomForest. R News 2/3, 18–22.

Lisiecki L E, Raymo M E, 2005. A Pliocene-Pleistocene stack of 57 globally distributed benthic $\delta^{18}O$ records. Paleoceanography and Paleoclimatology 20, 1–17.

Lotter A F, Juggins S, 1991. POLPROF, TRAN and ZONE: programs for plotting, editing and zoning pollen and diatom data. Inqua-Subcommission for the study of the Holocene, Working Group on Data-Handling Methods. Newsletter 6, 4–6.

Lotter A F, Bigler C, 2000. Do diatoms in the Swiss Alps reflect the length of ice-cover? Aquatic Sciences 62, 125–141.

Lotter A F, Pienitz R, Schmidt R, 1999. Diatoms as indicators of environmental change near arctic and alpine treeline. In Stoermer E F, Smol J P (eds). The diatoms: application to the environmental and earth sciences. Cambridge: Cambridge University Press, 205–226.

Löwemark L, Chen H F, Yang, T N, Kylander M, Yu E F, Hsu Y W, Lee T Q, Song S R, Jarvis S, 2011. Normalizing XRF-scanner data: a cautionary note on the interpretation of high-resolution records from organic-rich lakes. Journal of Asian Earth Sciences 40, 1250–1256.

Lundqvist J, 1992. Glacial stratigraphy in Sweden. In Kauranne K (ed). Glacial stratigraphy, engineering geology and earth construction. Espoo: Geological Survey of Finland. (Special paper 15), 43–59.

Luoto T P, 2009. Subfossil Chironomidae (Insecta: Diptera) along a latitudinal gradient in Finland: development of a new temperature inference model. Journal of Quaternary Science 24, 150–158.

Luoto T P, 2011. The relationship between water quality and chironomid distribution in Finland – A new assemblage-based tool for assessments of long-term nutrient dynamics. Ecological Indicators 11, 255–262.

Luoto T P, Kultti S, Nevalainen L, Sarmaja-Korjonen K, 2010. Temperature and effective moisture variability in southern Finland during the Holocene quantified with midge-based calibration models. Journal of Quaternary Science 25, 1317–1326.

Luoto T P, Kaukolehto M, Weckström J, Korhola A, Väliranta M, 2014. New evidence of warm early-Holocene summers in subarctic Finland based on an enhanced regional chironomid-based temperature calibration model. Quaternary Research 81, 50–62.

MacDonald G M, Beukens R P, Kieser W E, 1991. Radiocarbon dating of limnic sediments: a comparative analysis and discussion. Ecology 72, 1150–1155.

MacDonald G M, Velichko A A, Kremenetski C V, Borisova O K, Goleva A A, Andreev A A, Cwynar L C, Riding R T, Forman S L, Edwards T W D, Aravena R, Hammarlund D, Szeicz J M, Gattaulin V N, 2000. Holocene treeline history and climate change across Northern Eurasia. Quaternary Research 53, 302–311.

Mangerud J, 1991. The Last Interglacial/Glacial cycle in northern Europe. In Shane L C K, Cushing E J (eds). Quaternary Landscapes. Minneapolis: University of Minnesota Press, 38–75.

Margold M, Jansson K N, Stroeven A, Jansen J D, 2011. Glacial lake Vitim, a 3 000 km^3 outburst from Siberia to the Arctic Ocean. Quaternary Research 76, 393–396.

Masson-Delmotte V, Schulz M, 2013. Information from Paleoclimate Archives. In Stocker T F, Qin D, Plattner G-K, Tignor M, Allen S K, Boschung J, Nauels A, Xia Y, Bex V, Midgley P M (eds). Climate Change 2013: The Physical Science Basis, Contribution of Working Group I to the Fifth Assessment Report of the Intergovernmental Panel of Climate Change. Cambridge and New York: Cambridge University Press, 383–464.

McManus J F, Bond G C, Broecker W S, Johnsen S, Labeyrie L, Higgins S, 1994. High-resolution climate records from the North-Atlantic during the Last Interglacial. Nature 371, 326–329.

Medeiros A, Quinlan R, 2011. The distribution of the Chironomidae (Insecta: Diptera) along multiple environmental gradients in lakes and ponds of the eastern Canadian Arctic. Canadian Journal of Fisheries and Aquatic Sciences 68, 1511–1527.

Meyers P A, Teranes J L, 2001. Sediment organic matter. In Last, W M, Smol, J P (eds). Tracking environmental change using lake sediments. Vol 2. Physical and geochemical methods. Dordrecht: Kluwer Academic, 239–269.

Meyer-Jacob C, Vogel H, Boxberg F, Rosén P, Weber M E, Bindler R, 2014. Independent measurement of biogenic silica in sediments by FTIR spectroscopy and PLS regression. Journal of Paleolimnology 52, 245–255.

Michel T J, Saros J E, Interlandi S J, Wolfe A P, 2006. Resource requirements of four freshwater diatom taxa determined by in situ growth bioassays using natural populations from alpine lakes. Hydrobiologia 568, 235–243.

Mossberg B, Stenberg L, 2003. Den nya nordiska floran. Stockholm: Wahlström and Widstrand. (In Swedish.)

Mothes G, 1968. Einige ökologisch interessante Chironomiden aus dem Stechlinseegebiet. Annales Botanici Fennici 5, 92–96.

Murton J B, Bateman M D, Dallimore S R, Teller J T, Yang Z, 2010. Identification of Younger Dryas outburst floodpath from Lake Agassiz to the Arctic Ocean. Nature 464, 740–743.

Mäkinen K, 2005. Dating the Weichselian deposits of southwestern Finnish Lapland. Espoo: Geological Survey of Finland. (Special Paper 40), 67–78.

New M, Lister D, Hulme M, Makin I, 2002. A high-resolution data set of surface climate over global land areas. Climate Research 21, 1–25.

Nyman M, Korhola A, Brooks S J, 2005. The distribution and diversity of Chironomidae (Insecta: Diptera) in western Finnish Lapland, with special emphasis on shallow lakes. Global Ecology and Biogeography 14, 137–153.

Oksanen J, Blanchet F G, Kindt R, Legendre P, Minchin P R, O'Hara R B, Simpson G L, Solymos P, Stevens M H H, Wagner H, 2011. Vegan: Community Ecology Package. R package version 2.0-1. Available at: http://CRAN R-project org/package=vegan

Oksanen J, Blanchet F G, Kindt R, Legendre P, Minchin P R, O'Hara R B, Simpson G L, Solymos P, Stevens M H H, Wagner H, 2014. Vegan: Community Ecology Package. R package version 2.2-0. Available at: http://CRAN R-project org/package=vegan

Overpeck J T, Webb T III, Prentice I C, 1985. Quantitative interpretation of fossil pollen spectra: dissimilarity coefficients and the method of modern analogs. Quaternary Research 23, 87–108.

Økland K A, Økland J, 2000. Freshwater bryozoans (Bryozoa) of Norway: distribution and ecology of *Cristatella mucedo* and *Paludicella articulate*. Hydrobiologia 421, 1–24.

Økland K A, Økland J, 2001. Freshwater bryozoans (Bryozoa) of Norway II: distribution and ecology of two species of *Fredericella*. Hydrobiologia 459, 103–123.

Økland K A, Økland J, 2005. Freshwater bryozoans (Bryozoa) of Norway V: review and comparative discussion of the distribution and ecology of the 10 species recorded. Hydrobiologia 534, 31–55.

Økland K A, Økland J, Geimer G, Massard J A, 2003. Freshwater bryozoans (Bryozoa) of Norway IV: distribution and ecology of four species of *Plumatella* with notes on *Hyalinella punctate*. Hydrobiologia 501, 179–198.

Palmer S, Walker I R, Heinrichs M, Hebda R, Scudder G, 2002. Postglacial midge community change and Holocene paleotemperature reconstructions near treeline, southern British Columbia (Canada). Journal of Paleolimnology 28, 469–490.

Pals J P, van Geel B, Delfos A, 1980. Paleoecological studies in the Klokkeweel bog near Hoogkarspel (prov. of Noord Holland). Review of Palaeobotany and Palynology 30, 371–418.

Parducci L, Jørgensen T, Tollefsrud M M, Elverland E, Alm T, Fontana S L, Bennett K D, Haile J, Matetovici I, Suyama T, Edwards M E, Andersen K, Rasmussen M, Boessenkool S, Coissac E, Brochmann C, Taberlet P, Houmark-Nielsen M, Larsen N K, Orlando L, Gilbert M T P, Kjær K H, Alsos I G, Willerslev E, 2012. Glacial survival of boreal trees in northern Scandinavia. Science 335, 1083–1086.

Patrick R, 1977. Ecology of freshwater diatoms and diatom communities. In Werner D (ed). Biology of diatoms. Oxford: Blackwell Scientific Publications, 284–332. (Botanical Monographs 13)

Paus A, 2000. Interpretative problems and sources of error related to pollen-analytical studies of the Holocene on the Timan ridge, western Pechora Basin, northern Russia. AmS-Skrifter 16, 1–16.

Paus A, 2013. Human impact, soil erosion, and vegetation response lags to climate change: challenges for the mid-Scandinavian pollen-based transfer-function temperature reconstructions. Vegetation History and Archaeobotany 22, 269–284.

Paus A, Velle G, Berge J, 2011. The Lateglacial and early Holocene vegetation and environment in the Dovre mountains, central Norway, as signaled in two Lateglacial nunatak lakes. Quaternary Science Reviews 30, 1780–1796.

Pędziszewska A, Tylmann W, Witak M, Piotrowska N, Maciejewska E, Latałowa M, 2015. Holocene environmental changes reflected by pollen, diatoms, and geochemistry of annually laminated sediments of Lake Suminko in the Kashubian Lake District (N Poland). Review of Palaeobotany and Palynology 216, 55–75.

Pennington W, 1980. Modern pollen samples from west Greenland and the interpretation of pollen data from the British Late-Glacial (Late Devensian). New Phytologist 84, 171–201.

Perttunen M, Vartiainen H, 1992. Glaciofluvial transport of clasts and heavy minerals from the Sokli Carbonatite complex, Finnish Lapland. Espoo: Geological Survey of Finland. (Bulletin 366)

Piperno D R, 2001. Phytoliths. In Smol J P, Birks H J B, Last W M (eds). Tracking environmental change using lake sediments. Vol 3. Terrestrial, alga, and siliceous indicators. Dordrecht: Kluwer Academic, 235–252.

Plikk A, Helmens K F, Fernández-Fernández M, Kylander M, Löwemark L, Risberg J, Salonen J S, Väliranta M, Weckström J, 2016. Development of an Eemian (MIS 5e) Interglacial paleolake at Sokli (N Finland) inferred using multiple proxies. Palaeogeography, Palaeoecology, Palaeoclimatology 463, 11–26.

Plikk A, Engels S, Luoto T P, Nazarova L, Salonen J S, Helmens K F, 2019. Chironomid-based temperature reconstruction for the Eemian Interglacial (MIS 5e) at Sokli, northeast Finland. Journal of Paleolimnology. doi.org/10.1007/s10933-018-00064-y

Porinchu D F, MacDonald G M, 2003. The use and application of freshwater midges (Chironomidae: Insecta: Diptera) in geographical research. Progress in Physical Geography 27, 378–442.

Prentice I C, 1978. Modern pollen spectra from lake sediments in Finland and Finnmark, north Norway. Boreas 7, 131–153.

Rahmstorf S, 2002. Ocean circulation and climate during the past 120 000 years. Nature 419, 207–214.

Ralska-Jasiewiczowa M, van Geel B, Goslar T, Kuc T, 1992. The record of the Late Glacial/ Holocene transition in the varved sediments of lake Gosciaz, central Poland. Sveriges Geologiska Undersökning Ser. Ca 81, 257–268.

Raukas A, 1994. Annually laminated Late-Glacial sediments in the Eastern Baltic countries and the evolution of ice-dammed lakes. In Hicks S, Miller U, Saarnisto M (eds). Laminated Sediments. PACT 41, 45–55.

R Development Core Team, 2011. R: A language and environment for statistical computing. Vienna: R Foundation for Statistical Computing. Available at: https://www.r-project.org/

R Development Core Team, 2014. R: A language and environment for statistical computing. Vienna: R Foundation for Statistical Computing. Available at: https://www.r-project.org/

Rehfeld K, Trachsel M, Telford R J, Laepple T, 2016. Assessing performance and seasonal bias of pollen-based climate reconstructions in a perfect model world. Climate of the Past 12, 2255–2270.

Reimer P J, Baillie M G L, Bard E, Bayliss A, Beck J W, Blackwell P G, Bronk Ramsey C, Buck C E, Burr G S, Edwards R L, Friedrich M, Grootes P M, Guilderson T P, Hajdas I, Heaton T J, Hogg A G, Hughen K A, Kaiser K F, Kromer B, McCormac F G, Manning S W, Reimer R W, Richards D A, Southon J R, Talamo S, Turney C S M, van der Plicht J, Weyhenmeyer C, 2009. IntCal09 and Marine09 radiocarbon age calibration curves, 0–50 000 years cal BP. Radiocarbon 51, 1111–1150.

Renberg I, 1981. Formation, structure and visual appearance of iron-rich, varved lake sediments. Verhandlungen Internationalen Vereinigung für Theoretische und Angewandte Limnologie 21, 94–101.

Reynolds C S, 1993. The ecology of freshwater phytoplankton. Cambridge: Cambridge University Press.

Ridgeway G, 2013. gbm: Generalized boosted regression models. R package, version 2.1. Available at: https://cran.r-project.org/web/packages/gbm/index.html

Rioual P, Andrieu-Ponel V, Rietti-Shati M, Battarbee R W, de Beaulieu J-L, Cheddadi R, Reille M, Svobodova H, Shemesh A, 2001. High-resolution record of climate stability in France during the last interglacial period. Nature 413, 293–296.

Rioual P, Andrieu-Ponel V, de Beaulieu J-L, Reille M, Svobodova H, Battarbee R W, 2007. Diatom responses to limnological and climatic changes at Ribains Maar (French Massif Central) during the Eemian and Early Würm. Quaternary Science Reviews 26, 1557–1609.

Risberg J, Sandgren P, Teller J T, Last W M, 1999. Siliceous microfossils and mineral magnetic characteristics in a sediment core from Lake Manitoba, Canada: a remnant of glacial Lake Agassiz. Canadian Journal of Earth Sciences 36, 1299–1314.

Ritchie J C, Cwynar L C, Spear R W, 1983. Evidence from north-west Canada for an early Holocene Milankovitch thermal maximum. Nature 305, 126–128.

Rosén P, Vogel H, Cunningham L, Reuss N, Conley J, Persson P, 2010. Fourier transform infrared spectroscopy, a new method for rapid determination of total organic and inorganic carbon and biogenic silica concentration in lake sediments. Journal of Paleolimnology 43, 247–259.

Salonen J S, Seppä H, Väliranta M, Jones V J, Self A, Heikkilä M, Kultti S, Yang H, 2011. The Holocene thermal maximum and late-Holocene cooling in the tundra of NE European Russia. Quaternary Research 75, 501–511.

Salonen J S, Seppä H, Luoto M, Bjune A E, Birks H J B, 2012. A North European pollen–climate calibration set: analyzing the climate response of a biological proxy using novel regression tree methods. Quaternary Science Reviews 45, 95–110.

Salonen J S, Helmens K F, Seppä H, Birks H J B, 2013. Pollen-based paleoclimate reconstructions over long glacial-interglacial timescales: methodological tests based on the Holocene and MIS 5d-c deposits of Sokli, northern Finland. Journal of Quaternary Science 28, 271–282.

Salonen J S, Luoto M, Alenius T, Heikkilä M, Seppä H, Telford R J, Birks H J B, 2014. Reconstructing Late-Quaternary climatic parameters of northern Europe from fossil pollen using boosted regression trees: comparison and synthesis with other quantitative reconstruction methods. Quaternary Science Reviews 88, 69–81.

Salonen S J, Helmens K F, Kuosmanen N, Väliranta M, Brendryen J, Goring S, Korpela M, Kylander M, Philip A, Plikk A, Renssen H, Luoto M, 2018. Abrupt high-latitude climate events and decoupled seasonal trends during the Eemian Interglacial. Nature Communications 9. doi:10.1038/s41467-018-05314-1.

Sánchez Goñi M F, Bakker P, Desprat S, Carlson A E, Van Meerbeeck C J, Peyron O, Naughton F, Fletcher W J, Eynaud F, Rossignol L, Renssen H, 2012. European climate optimum and enhanced Greenland melt during the Last Interglacial. Geology 40, 627–630.

Sarala P, Eskola T, 2011. Middle Weichselian interstadial deposit at Petäjäselkä, Northern Finland. E&G Quaternary Science Journal 60, 488–492.

Sarala P, Väliranta M, Eskola T, Vaikutiené G, 2016. First physical evidence for forested environment in the arctic during MIS 3. Scientific Reports 6, 1–9.

Sarmaja-Korjonen K, Seppänen A, Bennike O, 2006. *Pediastrum* algae from the classic late glacial Bølling Sø site, Denmark: response of aquatic biota to climate change. Review of Palaeobotany and Palynology 138, 95–107.

Saros, J E, Strock K E, McCue J, Hogan E, Anderson N J, 2014. Response of *Cyclotella* species to nutrients and incubation depth in Arctic lakes. Journal of Plankton Research 36, 450– 460.

Schmidt R, Kamenik C, Lange-Bertalot H, Klee R, 2004. *Fragilaria* and *Staurosira* (Bacillariophyceae) from sediments surfaces of 40 lakes in the Austrian Alps in relation to environmental variables, and their potential for paleoclimatology. Journal of Limnology 63, 171–189.

Seelos K, Sirocko F, 2007. Abrupt cooling events at the very end of the Last Interglacial. Developments in Quaternary Science 7, 207–222.

Selby K A, Brown A G, 2007. Holocene development and anthropogenic disturbance of a shallow lake system in Central Ireland recorded by diatoms. Journal of Paleolimnology 38, 419–440.

Self A E, Brooks S J, Birks H J B, Nazarova L, Porinchu D, Odland A, Yang H, Jones V J, 2011. The distribution and abundance of chironomids in high-latitude Eurasian lakes with respect to temperature and continentality: development and application of new chironomid-based climate-inference models in northern Russia. Quaternary Science Reviews 30, 1122–1141.

Seppä H, Birks H J B, Odland A, Poska A, Veski S, 2004. A modern pollen-climate calibration set from northern Europe: developing and testing a tool for paleoclimatological reconstructions. Journal of Biogeography 31, 251–267.

Seppä H, Bjune A E, Telford R J, Birks H J B, Veski S, 2009. Last nine-thousand years of temperature variability in Northern Europe. Climate of the Past 5, 523–535.

Seppä H, Schurgers G, Miller P A, Bjune A E, Giesecke T, Kühl N, Renssen H, Salonen J S, 2015. Trees tracking a warmer climate: the Holocene range shift of hazel (*Corylus avellana*) in northern Europe. The Holocene 25, 53–63.

Shahgedanova M, 2008. The physical geography of northern Eurasia. Oxford: Oxford University Press.

Shahgedanova M, Kuznetsov M, 2008. The Arctic Environments. In Shahgedanova M (ed). The Physical Geography of northern Eurasia. Oxford: Oxford University Press, 191–215.

Shala S, 2014. Paleoenvironmental changes in the northern Boreal zone of Finland based on lake sediment analyses: local versus regional drivers. PhD thesis. Stockholm University, Stockholm.

Shala S, Helmens K F, Luoto T P, Väliranta M, Weckström J, Salonen J S, Kuhry P, 2014a. Evaluating environmental drivers of Holocene changes in water chemistry and aquatic biota composition at Lake Loitsana, NE Finland. Journal of Paleolimnology 52, 311–329.

Shala S, Helmens K F, Jansson K, Kylander M E, Risberg J, Löwemark l, 2014b. Paleoenvironmental record of glacial lake evolution during the early Holocene at Sokli, NE Finland. Boreas 43, 362–376.

Shala S, Helmens K F, Luoto T P, Salonen J S, Väliranta M, Weckström J, 2017. Comparison of quantitative Holocene temperature reconstructions using multiple proxies from a northern boreal lake. The Holocene 27, 1745–1755.

Simpson G, Birks H, 2012. Statistical learning in palaeolimnology. In Birks H J B, Lotter A F, Juggins S (eds). Tracking environmental change using lake sediments: data handling and numerical techniques. Dordrecht: Springer, 249–327.

Sirocko F, Seelos K, Schaber K, Rein B, Dreher F, Diehl M, Lehne R, Jäger K, Krbetschek M, Degering D, 2005. A late Eemian aridity pulse in central Europe during the last glacial inception. Nature 436, 833–836.

Skov F, Svenning J-C, 2004. Potential impact of climatic change on the distribution of forest herbs in Europe. Ecography 27, 366–380.

Sorsa P, 1965. Pollenanalytische Untersuchungen zur spätquartären Vegetations- und Klimaentwicklung im östlichen Nordfinnland. Annales Botanici Fennici 2, 300–413.

Spötl C, Mangini A, Frank N, Eichstädter R, Burns S J, 2002. Start of the last interglacial period at 135 ka: evidence from a high Alpine speleothem. Geology 30, 815–818.

Stoermer E, 1993. Evaluating diatom succession: some pecularities of the Great Lakes case. Journal of Paleolimnology 8, 71–83.

Sweeney C, 2004. A key for the identification of stomata of the native conifers of Scandinavia. Review of Palaeobotany and Palynology 128, 281–290.

Sykes M T, Prentice I C, Cramer W, 1996. A bioclimatic model for the potential distributions of north European tree species under present and future climates. Journal of Biogeography 23, 203–233.

Tarasov P E, Webb III T, Andreev A A, Afanas'Eva N B, Berezina N A, Bezusko L G, Blyakharchuk T A, Bolikhovskaya N S, Cheddadi R, Chernavskaya M M, Chernova G M, Dorofeyuk N I, Dirksen V G, Elina G A, Filimonova L V, Glebov F Z, Guiot J, Gunova V S, Harrison S P, Jolly D, Khomutova V I, Kvavadze E V, Osipova I M, Panova N K, Prentice I C, Saarse L, Sevastyanov D V, Volkova V S, Valentina, Zernitskaya P, 1998. Present-day and mid-Holocene biomes reconstructed from pollen and plant macrofossil data from the former Soviet Union and Mongolia. Journal of Biogeography 25, 1029–1053.

Tarasov P, Granoszewski W, Bezrukova E, Brewer S, Nita M, Abzaeva A, Oberhänsli H, 2005. Quantitative reconstruction of the last interglacial vegetation and climate based on the pollen record from Lake Baikal, Russia. Climate Dynamics 25, 625–637.

Telford R J, 2013. palaeoSig: Significance tests of quantitative paleoenvironmental reconstructions. R package, version 1.1-2.

Telford R J, Birks H J B, 2005. The secret assumption of transfer functions: problems with spatial autocorrelation in evaluating model performance. Quaternary Science Reviews 24, 2173–2179.

Telford R J, Birks H J B, 2009. Evaluation of transfer functions in spatially structured environments. Quaternary Science Reviews 28, 1309–1316.

Telford R J, Birks H J B, 2011. A novel method for assessing the statistical significance of quantitative reconstructions inferred from biotic assemblages. Quaternary Science Reviews 30, 1272–1278.

ter Braak C J F, 1986. Canonical correspondence analysis: a new eigenvector method for multivariate direct gradient analysis. Ecology 67, 1167–1179.

ter Braak C J F, Juggins S, 1993. Weighted averaging partial least squares regression (WA-PLS): an improved method for reconstructing environmental variables from species assemblages. Hydrobiologia 269/270, 485–502.

Therneau T M, Atkinson B, 2013. mvpart: Multivariate partitioning. R package version 1.6-1.

Tishkov A, 2008. Boreal forests. In Shahgedanova M (ed). The physical geography of northern Eurasia. Oxford: Oxford University Press, 216–233.

Tumel N, 2008. Permafrost. In Shahgedanova M (ed). The physical geography of northern Eurasia. Oxford: Oxford University Press,149–168.

Turner C, 2002. Problems of the duration of the Eemian Interglacial in Europe north of the Alps. Quaternary Research 58, 45–48.

Tzedakis C, 2003. Timing and duration of Last Interglacial conditions in Europe: a chronicle of a changing chronology. Quaternary Science Reviews 22, 763–768.

Ulvinen T, Syrjänen K, Anttila S (eds), 2002. Suomen sammalet – levinneisyys, ekologia, uhanalaisuus. Suomen ympäristö 560, Finnish Environment Institute. (In Finnish.)

van Dam H, Mertens A, Sinkeldam J, 1994. A coded checklist and ecological indicator values of freshwater diatoms from the Netherlands. Netherlands Journal of Aquatic Ecology 28, 117–133.

van Geel B, 2001. Non-pollen palynomorphs. In Smol J P, Birks, H J B, Last W M (eds). Tracking environmental change using lake sediments. Vol 3. Terrestrial, algal, and siliceous indicators. Dordrecht: Kluwer Academic Publishers.

van Geel B, Grenfell H R, 1996. Spores of Zygnemataceae. In Jansonius J, McGregor D C (eds). Palynology: principles and applications. Dallas: American Association of Stratigraphic Palynologists Foundation, 173–176.

van Geel B, Hallewas D P, Pals J P, 1983. A Late Holocene deposit under the Westfriese dijk near Enkhuizen (Prov.of Noord-Holland, The Netherlands): paleoecological and archaeological aspects. Review of Palaeobotany and Palynology 38, 269–335.

van Geel B, Coope G R, van der Hammen T, 1989. Paleoecology and stratigraphy of the Lateglacial type section at Usselo (The Netherlands). Review of Palaeobotany and Palynology 60, 25–129.

Vartiainen H, 1980. The petrography, mineralogy and petrochemistry of the Sokli carbonatite massif, northern Finland. Espoo: Geological Survey of Finland. (Bulletin 313)

Vasskog K, Paasche Ø, Nesje A, Boyle J F, Birks H J B, 2012. A new approach for reconstructing glacier variability based on lake sediments recording input from more than one glacier. Quaternary Research 77, 192–204.

Velle G, Larsen J, Eide W, Peglar S M, Birks H J B, 2005. Holocene environmental history and climate of Råtåsjøen, a low-alpine lake in south-central Norway. Journal of Paleolimnology 33, 129–153.

Velle G, Brodersen K P, Birks H J B, Willassen E, 2010. Midges as quantitative temperature indicator species: lessons for paleoecology. The Holocene 20, 989–1002.

Velle G, Brodersen K P, Birks H J B, Willassen E, 2012. Inconsistent results should not be overlooked: a reply to Brooks et al. (2012). The Holocene 22, 1501–1508.

Venäläinen A, Tuomenvirta H, Pirinen P, Drebs A, 2005. A basic climate data set 1961–2000 – description and illustrations. Reports 5, Finnish Meteorological Institute.

Väliranta M, 2006. Terrestrial plant macrofossil records; possible indicators of past lake-level fluctuations in north-eastern European Russia and Finnish Lapland? Acta Palaeobotanica 46, 235–243.

Väliranta M, Birks H H, Helmens K F, Engels S, Piirainen M, 2009. Early Weichselian interstadial (MIS 5c) summer temperatures were higher than today in northern Fennoscandia. Quaternary Science Reviews 28, 777–782.

Väliranta M, Weckström J, Siitonen S, Seppä H, Alkio J, Juutinen S, Tuittila E-S, 2011. Holocene aquatic ecosystem change in the boreal vegetation zone of northern Finland. Journal of Paleolimnology 45, 339–352.

Väliranta M, Sarala P, Eskola T, 2012. Uusia todisteita boreaalisista olosuhteista Veikselinterstadiaalin aikana. Geologi 64, 9–14. (In Finnish with English summary.)

Väliranta M, Salonen J S, Heikkilä M, Amon L, Birks H H, Helmens K F, Klimaschewski A, Kuhry P, Kultti S, Poska A, Shala S, Veski S, 2015. Plant macrofossil evidence for an early onset of the Holocene summer thermal maximum in Northern Europe. Nature Communications 6. doi:10.1038/ncomms7809.

Weckström J, Korhola A, 2001. Patterns in the distribution, T composition and diversity of diatom assemblages in relation to ecoclimatic factors in Arctic Lapland. Journal of Biogeography 28, 31–45.

Weckström K, Weckström J, Yliniemi L-M, Korhola A, 2010. The ecology of *Pediastrum* (Chlorophyceae) in subarctic lakes and their potential as paleobioindicators. Journal of Paleolimnology 43, 61–73.

Westhoff V, Bakker P A, van Leeuwen C G, van der Voo E E, 1981. Wilde planten. Deel 2. Het lage land. Deventer: Lange/van Leer.

Whitlock C, Dean W, Fritz S, Stevens L, Stone J, Power M, Rosenbaum J, Pierce K, Bracht-Flyr B, 2012. Holocene seasonal variability inferred from multiple proxy records from Crevice Lake, Yellowstone National Park, USA. Palaeogeography, Palaeoclimatology, Palaeoecology 331, 90–103.

Willis K J, van Andel T H, 2004. Trees or no trees? The environments of central and eastern Europe during the Last Glaciation. Quaternary Science Reviews 23, 2369–2387.

Wohlfarth B, 2010. Ice-free conditions in Sweden during Marine Oxygen Isotope Stage 3? Boreas 39, 377–398.

Wolin J, 1996. Late Holocene lake-level and lake development signals in Lower Herring Lake, Michigan. Journal of Paleolimnology 15, 19–45.

Wood T S, Okamura B, 2005. A new key to the freshwater bryozoans of Britain, Ireland and Continental Europe: with notes on their ecology. (Freshwater Biological Association Scientific Publications 63)

Yurtsev B A, 1981. Reliktovye stepnye kompleksy severo-vostochnoi Azii (The relict steppes of north-eastern Asia). Novosibirsk: The USSR Academy of Science Press.

Zagwijn W H, 1996. An analysis of Eemian climate in Western and Central Europe. Quaternary Science Reviews 15, 451–469.

Zawiska I, Słowiński M, Correa-Metrio A, Obremska M, Luoto T, Nevalainen L, Woszczyk M, Milecka K, 2015. The response of a shallow lake and its catchment to Late Glacial climate changes — A case study from eastern Poland. CATENA 126, 1–10.

Zlotin R, 2008. Biodiversity and Productivity of Ecosystems. In Shahgedanova M (ed). The physical geography of northern Eurasia. Oxford: Oxford University Press, 169–190.

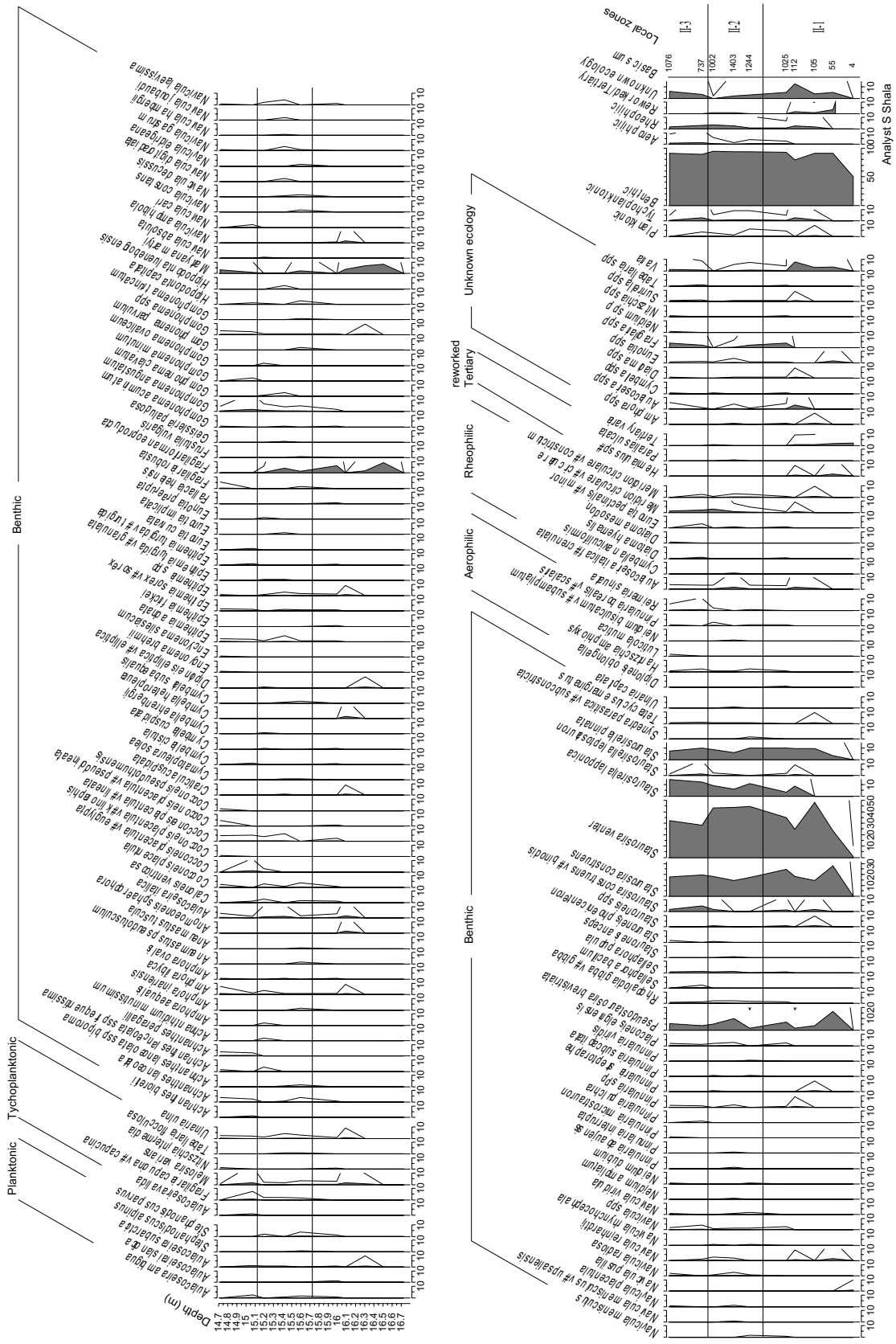

Figure A1-01. *Percentage diagram of diatom taxa in the MIS 5c deposit at Sokli. The solid curves show the actual percentages; the hatched curves show an ×10 exaggeration.*

Arkitektkopia AB, Bromma, 2019

SKB is responsible for managing spent nuclear fuel and radioactive waste produced by the Swedish nuclear power plants such that man and the environment are protected in the near and distant future.

skb.se